



University
of Glasgow

<https://theses.gla.ac.uk/>

Theses Digitisation:

<https://www.gla.ac.uk/myglasgow/research/enlighten/theses/digitisation/>

This is a digitised version of the original print thesis.

Copyright and moral rights for this work are retained by the author

A copy can be downloaded for personal non-commercial research or study, without prior permission or charge

This work cannot be reproduced or quoted extensively from without first obtaining permission in writing from the author

The content must not be changed in any way or sold commercially in any format or medium without the formal permission of the author

When referring to this work, full bibliographic details including the author, title, awarding institution and date of the thesis must be given

Enlighten: Theses

<https://theses.gla.ac.uk/>
research-enlighten@glasgow.ac.uk

THE EFFECT OF TOTAL ACUTE ISCHAEMIA ON THE STRUCTURE AND
FUNCTION OF THE RABBIT RETINA AND THE PATTERN OF POST-ISCHAEMIC RECOVERY

by

Neil F. Johnson, B.Sc., M.Sc.

Thesis submitted in two volumes for the Degree of Doctor
of Philosophy in the Faculty of Medicine, University of
Glasgow.

September, 1976

Temment Institute of Ophthalmology,
Glasgow University and Western
Infirmary,
GLASGOW, G11 6NT.

ProQuest Number: 10646909

All rights reserved

INFORMATION TO ALL USERS

The quality of this reproduction is dependent upon the quality of the copy submitted.

In the unlikely event that the author did not send a complete manuscript and there are missing pages, these will be noted. Also, if material had to be removed, a note will indicate the deletion.



ProQuest 10646909

Published by ProQuest LLC (2017). Copyright of the Dissertation is held by the Author.

All rights reserved.

This work is protected against unauthorized copying under Title 17, United States Code
Microform Edition © ProQuest LLC.

ProQuest LLC.
789 East Eisenhower Parkway
P.O. Box 1346
Ann Arbor, MI 48106 – 1346

Thesis
4566
Copy 2.
Vol. 1.



THE EFFECT OF TOTAL ACUTE ISCHAEMIA ON THE STRUCTURE
AND FUNCTION OF THE RABBIT RETINA AND THE PATTERN OF
POST-ISCHAEMIC RECOVERY

Volume I

List of Contents.

List of Tables and Illustrations	xiii
Acknowledgments	xvii
Summary	xx

VOLUME I:

	<u>Page.</u>
<u>Chapter 1 - Introduction.</u>	2
1-1 Introduction.	3
1-2 The organisation of the retina.	3
1-3 The function of the retina.	4
1-4 The blood supply of the retina.	5
1-5 Background to present study.	6
1-6 Total retinal ischaemia.	7
1-6.1 Structural effects of total ischaemia.	7
1-6.2 Functional effects of total ischaemia.	9
1-7 Partial retinal ischaemia.	10
1-7.1 Structural effects of partial ischaemia.	10
1-7.2 Functional effects of partial ischaemia.	12
 <u>Chapter 2 - Material and Methods.</u>	 15
2-1 Materials.	16
2-2 Methods employed in investigation into pressure-induced ischaemia.	16 ₁₈
2-3 Methods employed in investigation into post-mortem changes in the retina.	19
2-4 Electoretinography.	19
2-5 Tissue preparation for electron microscopy.	21
2-6 Microscopy.	22
2-7 Animal section - pressure-induced ischaemia study.	22
 <u>Chapter 3 - Control observations.</u>	 23
3-1 Introduction.	24
3-2 Light microscopy.	24
3-2.1 The visual streak.	24
3-2.2 The peripheral retina.	26
3-2.3 The horizontal nerve fibre layer.	27
3-3 Electron microscopy.	27
3-3.1 The retinal pigment epithelium.	27
3-3.2 The visual cells and outer plexiform layer.	30
3-3.3 The inner nuclear and inner plexiform layers.	33
3-3.4 The ganglion cell and nerve fibre layers.	35
 <u>Chapter 4 - The effect of total acute ischaemia on the structure of the rabbit retina.</u>	 39
4-1 Introduction.	40
4-2 Light microscopy of the retinal pigment epithelium.	40
4-3 Light microscopy of the neural retina.	41
4-3.1 The outer segments.	41
4-3.2 The inner segments.	42
4-3.3 Macrophages.	42
4-3.4 The outer nuclear layer.	43
4-3.5 The outer plexiform and inner nuclear layers.	43
4-3.6 The inner plexiform and ganglion cell layers.	44
4-4 Electron microscopy - Introduction.	44

4-5	Electron microscopy of the effect of pressure-induced ischaemia on the retinal pigment epithelium.....	45
4-6	Electron microscopy of post-mortem changes in the retinal pigment epithelium.	48
4-7	Electron microscopy of the visual cells.	49
	4-7.1 The outer segments.	50
	4-7.2 The inner segments.	50
	4-7.3 The outer nuclear layer and external limiting membrane. ...	52
4-8	Electron microscopy of the outer plexiform layer.	53
4-9	Electron microscopy of the inner nuclear layer.	54
4-10	Electron microscopy of the inner plexiform layer.	55
4-11	Electron microscopy of the ganglion cells and inner retina.	56
4-12	Electron microscopy of post-mortem changes in tissue maintained at 37°C.	57
4-13	Discussion.	58

<u>Chapter 5 - The structure of the rabbit retina during post-ischaemic recovery.</u>	67
5-1 Introduction.	68
5-2 Light microscopy of the retinal pigment epithelium.	69
5-2.1 15 minutes ischaemia, 60 and 240 minutes recovery.	69
5-2.2 30 minutes ischaemia, 60 minutes recovery.	69
5-2.3 30 minutes ischaemia, 240 minutes recovery.	69
5-2.4 60 minutes ischaemia, 60 minutes recovery.	69
5-2.5 60 minutes ischaemia, 240 minutes recovery.	69
5-2.6 90 minutes ischaemia, 60 and 240 minutes recovery.	69
5-2.7 120 minutes ischaemia, 60 and 240 minutes recovery.	70
5-3 Light microscopy of the outer segments.	70
5-3.1 15 minutes ischaemia, 60 and 240 minutes recovery.	70
5-3.2 30 minutes ischaemia, 60 minutes recovery.	70
5-3.3 30 minutes ischaemia, 240 minutes recovery.	70
5-3.4 60 minutes ischaemia, 60 minutes recovery.	70
5-3.5 60 minutes ischaemia, 240 minutes recovery.	70
5-3.6 90 minutes ischaemia, 60 minutes recovery.	71
5-3.7 90 minutes ischaemia, 240 minutes recovery.	71
5-3.8 120 minutes ischaemia, 60 and 240 minutes recovery.	71
5-4 Light microscopy of the visual cell inner segments.	71
5-4.1 15 minutes ischaemia, 60 and 240 minutes recovery.	71
5-4.2 30 minutes ischaemia, 60 and 240 minutes recovery.	71
5-4.3 60 minutes ischaemia, 60 minutes recovery.	71
5-4.4 60 minutes ischaemia, 240 minutes recovery.	71
5-4.5 90 minutes ischaemia, 60 and 240 minutes recovery.	72
5-4.6 120 minutes ischaemia, 60 and 240 minutes recovery.	72
5-5 Light microscopy of the external limiting membrane and the outer nuclear layer.	72
5-5.1 15 minutes ischaemia, 60 and 240 minutes recovery.	72
5-5.2 30 minutes ischaemia, 60 and 240 minutes recovery.	72
5-5.3 60 minutes ischaemia, 60 minutes recovery.	72
5-5.4 60 minutes ischaemia, 240 minutes recovery.	72
5-5.5 90 minutes ischaemia, 60 minutes recovery.	73
5-5.6 90 minutes ischaemia, 240 minutes recovery.	73
5-5.7 120 minutes ischaemia, 60 and 240 minutes recovery.	73
5-6 Light microscopy of the outer plexiform and inner nuclear layers.	73
5-6.1 15 minutes ischaemia, 60 and 240 minutes recovery.	73
5-6.2 30 minutes ischaemia, 60 and 240 minutes recovery.	74
5-6.3 60 minutes ischaemia, 60 minutes recovery.	74
5-6.4 60 minutes ischaemia, 240 minutes recovery.	74
5-6.5 90 minutes ischaemia, 60 minutes recovery.	74
5-6.6 90 minutes ischaemia, 240 minutes recovery.	74
5-6.7 120 minutes ischaemia, 60 minutes recovery.	75
5-6.8 120 minutes ischaemia, 240 minutes recovery.	75
5-7 Light microscopy of the inner plexiform and ganglion cell layers.	75
5-7.1 15 minutes ischaemia, 60 and 240 minutes recovery.	75
5-7.2 30 minutes ischaemia, 60 and 240 minutes recovery.	75
5-7.3 60 minutes ischaemia, 60 minutes recovery.	75
5-7.4 60 minutes ischaemia, 240 minutes recovery.	76
5-7.5 90 minutes ischaemia, 60 minutes recovery.	76
5-7.6 90 minutes ischaemia, 240 minutes recovery.	76
5-7.7 120 minutes ischaemia, 60 minutes recovery.	76
5-7.8 120 minutes ischaemia, 240 minutes recovery.	76

5-8	Light microscopy of the nerve fibre and myelinated nerve fibre layers.	76
5-9	General retinal organisation.	76
5-10	Electron microscopy - Introduction.	77
5-11	Electron microscopy of the retinal pigment epithelium.	77
5-11.1	15 minutes ischaemia, 60 minutes recovery.	77
5-11.2	15 minutes ischaemia, 240 minutes recovery.	77
5-11.3	30 minutes ischaemia, 60 minutes recovery.	78
5-11.4	30 minutes ischaemia, 240 minutes recovery.	78
5-11.5	60 minutes ischaemia, 60 minutes recovery.	78
5-11.6	60 minutes ischaemia, 240 minutes recovery.	79
5-11.7	90 minutes ischaemia, 60 minutes recovery.	80
5-11.8	90 minutes ischaemia, 240 minutes recovery.	80
5-11.9	120 minutes ischaemia, 60 minutes recovery.	82
5-11.10	120 minutes ischaemia, 240 minutes recovery.	82
5-12	Electron microscopy of the visual cell outer segments.	83
5-12.1	15 minutes ischaemia, 60 minutes recovery.	83
5-12.2	15 minutes ischaemia, 240 minutes recovery.	83
5-12.3	30 minutes ischaemia, 60 minutes recovery.	83
5-12.4	30 minutes ischaemia, 240 minutes recovery.	83
5-12.5	60 minutes ischaemia, 60 minutes recovery.	83
5-12.6	60 minutes ischaemia, 240 minutes recovery.	84
5-12.7	90 minutes ischaemia, 60 minutes recovery.	84
5-12.8	90 minutes ischaemia, 240 minutes recovery.	84
5-12.9	120 minutes ischaemia, 60 minutes recovery.	84
5-12.10	120 minutes ischaemia, 240 minutes recovery.	84
5-13	Electron microscopy of the visual cell inner segments.	85
5-13.1	15 minutes ischaemia, 60 minutes recovery.	85
5-13.2	15 minutes ischaemia, 240 minutes recovery.	85
5-13.3	30 minutes ischaemia, 60 minutes recovery.	85
5-13.4	30 minutes ischaemia, 240 minutes recovery.	85
5-13.5	60 minutes ischaemia, 60 minutes recovery.	85
5-13.6	60 minutes ischaemia, 240 minutes recovery.	86
5-13.7	90 minutes ischaemia, 60 minutes recovery.	86
5-13.8	90 minutes ischaemia, 240 minutes recovery.	86
5-13.9	120 minutes ischaemia, 60 minutes recovery.	87
5-13.10	120 minutes ischaemia, 240 minutes recovery.	87
5-14	Electron microscopy of the external limiting membrane.	87
5-15	Electron microscopy of the outer nuclear layer.	87
5-15.1	15 minutes ischaemia, 60 minutes recovery.	87
5-15.2	15 minutes ischaemia, 240 minutes recovery.	87
5-15.3	30 minutes ischaemia, 60 minutes recovery.	87
5-15.4	30 minutes ischaemia, 240 minutes recovery.	88
5-15.5	60 minutes ischaemia, 60 minutes recovery.	88
5-15.6	60 minutes ischaemia, 240 minutes recovery.	88
5-15.7	90 minutes ischaemia, 60 minutes recovery.	88
5-15.8	90 minutes ischaemia, 240 minutes recovery.	88
5-15.9	120 minutes ischaemia, 60 minutes recovery.	88
5-15.10	120 minutes ischaemia, 240 minutes recovery.	88
5-16	Electron microscopy of the outer plexiform layer.	90
5-16.1	15 minutes ischaemia, 60 and 240 minutes recovery.	90
5-16.2	30 minutes ischaemia, 60 and 240 minutes recovery.	90
5-16.3	60 minutes ischaemia, 60 minutes recovery.	90
5-16.4	60 minutes ischaemia, 240 minutes recovery.	90
5-16.5	90 minutes ischaemia, 60 minutes recovery.	90
5-16.6	90 minutes ischaemia, 240 minutes recovery.	90
5-16.7	120 minutes ischaemia, 240 minutes recovery.	90

	<u>Page.</u>
5-17 Electron microscopy of the inner nuclear layer.	91
5-17.1 15 minutes ischaemia, 60 and 240 minutes recovery.	91
5-17.2 30 minutes ischaemia, 60 and 240 minutes recovery.	92
5-17.3 60 minutes ischaemia, 60 minutes recovery.	92
5-17.4 60 minutes ischaemia, 240 minutes recovery.	92
5-17.5 90 minutes ischaemia, 60 minutes recovery.	92
5-17.6 90 minutes ischaemia, 240 minutes recovery.	93
5-17.7 120 minutes ischaemia, 60 minutes recovery.	93
5-17.8 120 minutes ischaemia, 240 minutes recovery.	94
5-18 Electron microscopy of the inner plexiform layer.	94
5-18.1 15 minutes ischaemia, 60 and 240 minutes recovery.	94
5-18.2 30 minutes ischaemia, 60 minutes recovery.	94
5-18.3 30 minutes ischaemia, 240 minutes recovery.	94
5-18.4 60 minutes ischaemia, 60 and 240 minutes recovery.	94
5-18.5 90 minutes ischaemia, 60 and 240 minutes recovery.	95
5-18.6 120 minutes ischaemia, 60 and 240 minutes recovery.	95
5-19 Electron microscopy of the ganglion cells.	95
5-19.1 15 minutes ischaemia, 60 and 240 minutes recovery.	95
5-19.2 30 minutes ischaemia, 60 and 240 minutes recovery.	95
5-19.3 60 minutes ischaemia, 60 and 240 minutes recovery.	96
5-19.4 90 minutes ischaemia, 60 minutes recovery.	96
5-19.5 90 minutes ischaemia, 240 minutes recovery.	96
5-19.6 120 minutes ischaemia, 60 minutes recovery.	96
5-19.7 120 minutes ischaemia, 240 minutes recovery.	96
5-20 Electron microscopy of the nerve fibre layer and internal limiting membrane.	96
5-21 Electron microscopy of the myelinated nerve fibre zone.	97
5-22 Electron microscopy of the choroidal endothelium.	98
5-23 Discussion.	99
 <u>Chapter 6 - Retinal function during and after ischaemia.</u>	 108
6-1 Introduction.	109
6-2 Dark adaptation.	109
6-3 Quantitation of the electroretinogram.	110
6-4 The ERG during acute total ocular ischaemia.	111
6-5 The pattern of post - ischaemic recovery of the ERG.	111
6-5.1 Post-ischaemic recovery of the 'a' wave.	111
6-5.2 Post-ischaemic recovery of the 'b' wave.	113
6-5.3 Post-ischaemic recovery of the 'n' wave.	114
6-5.4 Post-ischaemic recovery of the 'c' wave.	115
6-6 Discussion.	115
 <u>Chapter 7 - Discussion.</u>	 119
 <u>References.</u>	 127

LIST OF ILLUSTRATIONS.

Volumes I and II

VOLUME I:Chapter 1.

- Fig. 1-1 Light micrograph of normal rabbit retina.
 Fig. 1-2 Diagram of electroretinogram components.

Chapter 2.

- Fig. 2-1 Schematic diagram of experimental model.
 Fig. 2-2 Tables showing the number of animals employed.
 Fig. 2-3 Diagram showing the retinal positions from which tissue was examined.

Chapter 3.

- Fig. 3-1 Light micrograph of the visual streak.
 Fig. 3-2 Light micrograph of the peripheral retina.
 Fig. 3-3 Light micrograph of the horizontal nerve fibre zone.
 * Fig. 3-4 Light micrograph of the outer retina.
 Fig. 3-5 Light micrograph of the visual cells.
 Fig. 3-6 Light micrograph of the inner nuclear layer.
 * Fig. 3-7 Light micrograph of the inner retina.
 Fig. 3-8 Light micrograph of the myelinated fibre bundles and their associated blood vessels.
 Fig. 3-9 Electron micrograph of the retinal pigment epithelium.
 Fig. 3-10 Electron micrograph of the retinal pigment epithelium.
 Fig. 3-11 Electron micrograph of the apical surface of the retinal pigment epithelium.
 * Fig. 3-12 Electron micrographs of the retinal pigment epithelium.
 * Fig. 3-13 Electron micrographs of the five phagosome stages.
 * Fig. 3-14 Table showing the number and percentage distribution of the various phagosome stages.
 Fig. 3-15 Table showing the number of phagosomes at the various stages in the control tissue. Animals 1-8.
 Fig. 3-16 Table showing percentage distribution of the phagosome stages in the control tissue. Animals 1-8.
 Fig. 3-17 Table showing the number of phagosomes at the various stages in the control tissue. Animals 9-16.
 Fig. 3-18 Table showing the percentage distribution of the phagosome stages in the control tissue. Animals 9-16.
 Fig. 3-19 Table showing the number of phagosomes at the various stages in the control tissue. Animals 17-24.
 Fig. 3-20 Table showing the percentage distribution of the phagosome stages in the control tissue. Animals 17-24.
 Fig. 3-21 Electron micrograph of the visual cell outer segments.
 Fig. 3-22 Electron micrograph of the modified cilium between the inner and outer segments.
 Fig. 3-23 Electron micrograph of the visual cell inner segments.
 Fig. 3-24 Electron micrograph of the myoid region of the inner segments.
 Fig. 3-25 Electron micrograph of the outer nuclear layer.
 Fig. 3-26 Electron micrograph of the outer nuclear layer.
 Fig. 3-27 Electron micrograph of the outer plexiform layer.
 Fig. 3-28 Electron micrograph of the outer plexiform layer.

- Fig. 3-29 Electron micrograph of the inner nuclear layer.
- Fig. 3-30 Electron micrograph of the inner nuclear layer.
- Fig. 3-31 Electron micrograph of the inner retina.
- Fig. 3-32 Electron micrograph of the inner plexiform layer.
- Fig. 3-33 Electron micrograph of the ganglion cell.
- Fig. 3-34 Electron micrograph of the Müller cell cytoplasm.
- * Fig. 3-35 Electron micrograph of the internal limiting membrane.
- Fig. 3-36 Electron micrograph of the myelinated and unmyelinated nerve fibre zone.
- Fig. 3-37 Electron micrograph of the retinal blood vessel.

Chapter 4.

- Fig. 4-1 Light micrograph of retina - 15 minutes pressure ischaemia.
- Fig. 4-2 Light micrograph of retina - 60 minutes pressure ischaemia.
- Fig. 4-3 Light micrograph of retina - 120 minutes pressure ischaemia.
- Fig. 4-4 Light micrograph of retina - 60 minutes pressure ischaemia.
- Fig. 4-5 Light micrograph of outer retina - 60 minutes pressure ischaemia.
- Fig. 4-6 Light micrograph of inner and outer segments - 120 minutes pressure ischaemia.
- Fig. 4-7 Light micrograph of outer retina - 60 minutes pressure ischaemia.
- Fig. 4-8 Light micrograph of outer retina - 120 minutes pressure ischaemia.
- Fig. 4-9 Light micrograph of inner retina - 120 minutes pressure ischaemia.
- Fig. 4-10 Light micrograph of inner retina - 120 minutes pressure ischaemia.
- Fig. 4-11 Light micrograph of retina - 15 minutes post-mortem (room temperature).
- Fig. 4-12 Light micrograph of retina - 120 minutes post-mortem (room temperature).
- Fig. 4-13 Light micrograph of outer retina - 120 minutes post-mortem (room temperature).
- Fig. 4-14 Light micrograph of outer retina - 60 minutes post-mortem (room temperature).
- Fig. 4-15 Light micrograph of inner retina - 120 minutes post-mortem (room temperature).
- Fig. 4-16 Light micrograph of inner retina - 60 minutes post-mortem (room temperature).
- Fig. 4-17 Light micrograph of retina - 60 minutes post-mortem (room temperature).
- Fig. 4-18 Light micrograph of retina - 90 minutes post-mortem (room temperature).
- Fig. 4-19 Light micrograph of retina - 30 minutes post-mortem (37°C.).
- Fig. 4-20 Light micrograph of retina - 90 minutes post-mortem (37°C.).
- Fig. 4-21 Graph of number of macrophages in ischaemic tissue.
- Fig. 4-22 Electron micrograph of retinal pigment epithelium - 15 minutes pressure ischaemia.
- Fig. 4-23 Electron micrograph of retinal pigment epithelium - 60 minutes pressure ischaemia.
- Fig. 4-24 Electron micrograph of retinal pigment epithelium - 120 minutes pressure ischaemia.
- * Fig. 4-25 Electron micrograph of retinal pigment epithelium - 120 minutes pressure ischaemia.
- Fig. 4-26 Table showing the number of phagosomes in the ischaemic retinal pigment epithelium.
- Fig. 4-27 Table showing the percentage distribution of the various phagosome stages in the ischaemic pigment epithelium.
- Fig. 4-28 Electron micrograph of outer segments - 30 minutes pressure ischaemia.
- Fig. 4-29 Electron micrograph of outer segments - 120 minutes pressure ischaemia.

- Fig. 4-30 Electron micrograph of inner segments - 30 minutes pressure ischaemia.
- Fig. 4-31 Electron micrograph of inner segments - 60 minutes pressure ischaemia.
- Fig. 4-32 Electron micrograph of inner segments - 120 minutes pressure ischaemia.
- Fig. 4-33 Electron micrograph of external limiting membrane - 120 minutes pressure ischaemia.
- Fig. 4-34 Electron micrograph of macrophages in subretinal space - 120 minutes pressure ischaemia.
- Fig. 4-35 Electron micrograph of macrophagic cytoplasm - 90 minutes pressure ischaemia.
- Fig. 4-36 Electron micrograph of macrophagic cytoplasm - 60 minutes pressure ischaemia.
- Fig. 4-37 Electron micrograph of macrophagic cytoplasm - 60 minutes pressure ischaemia.
- Fig. 4-38 Electron micrograph of outer nuclear layer - 15 minutes pressure ischaemia.
- Fig. 4-39 Electron micrograph of outer nuclear layer - 60 minutes pressure ischaemia.
- Fig. 4-40 Electron micrograph of outer nuclear layer - 120 minutes pressure ischaemia.
- Fig. 4-41 Electron micrograph of receptor pedicles - 120 minutes pressure ischaemia.
- Fig. 4-42 Electron micrograph of inner nuclear layer - 60 minutes pressure ischaemia.
- Fig. 4-43 Electron micrograph of inner nuclear layer - 90 minutes pressure ischaemia.
- Fig. 4-44 Electron micrograph of inner nuclear layer - 120 minutes pressure ischaemia.
- Fig. 4-45 Electron micrograph of inner plexiform layer - 30 minutes pressure ischaemia.
- Fig. 4-46 Electron micrograph of inner plexiform layer - 90 minutes pressure ischaemia.
- Fig. 4-47 Electron micrograph of inner plexiform layer - 120 minutes pressure ischaemia.
- Fig. 4-48 Electron micrograph of ganglion cell - 30 minutes pressure ischaemia.
- Fig. 4-49 Electron micrograph of ganglion cell - 90 minutes pressure ischaemia.
- Fig. 4-50 Electron micrograph of inner limiting membrane - 15 minutes pressure ischaemia.
- Fig. 4-51 Electron micrograph of glial cell - 60 minutes pressure ischaemia.
- Fig. 4-52 Electron micrograph of retinal blood vessel - 60 minutes pressure ischaemia.
- Fig. 4-53 Electron micrograph of retinal pigment epithelium - 30 minutes post-mortem (room temperature).
- Fig. 4-54 Electron micrograph of retinal pigment epithelium - 90 minutes post-mortem (room temperature).
- Fig. 4-55 Electron micrograph of retinal pigment epithelium - 90 minutes post-mortem (room temperature).
- Fig. 4-56 Electron micrograph of outer segments - 60 minutes post-mortem (room temperature).
- Fig. 4-57 Electron micrograph of inner segments - 30 minutes post-mortem (room temperature).
- Fig. 4-58 Electron micrograph of inner segments - 60 minutes post-mortem (room temperature).

- Fig. 4-59 Electron micrograph of outer nuclear layer - 30 minutes post-mortem (room temperature).
- Fig. 4-60 Electron micrograph of outer nuclear layer - 60 minutes post-mortem (room temperature).
- Fig. 4-61 Electron micrograph of receptor pedicles - 60 minutes post-mortem (room temperature).
- Fig. 4-62 Electron micrograph of inner nuclear layer - 60 minutes post-mortem (room temperature).
- Fig. 4-63 Electron micrograph of inner plexiform layer - 90 minutes post-mortem (room temperature).
- Fig. 4-64 Electron micrograph of ganglion cell - 60 minutes post-mortem (room temperature).
- Fig. 4-65 Electron micrograph of myelinated nerve fibre zone - 90 minutes post-mortem (room temperature).
- Fig. 4-66 Electron micrograph of retinal pigment epithelium - 15 minutes post-mortem (37°C.).
- Fig. 4-67 Electron micrograph of retinal pigment epithelium - 90 minutes post-mortem (37°C.).
- Fig. 4-68 Electron micrograph of outer segments - 30 minutes post-mortem (37°C.).
- Fig. 4-69 Electron micrograph of inner nuclear layer - 90 minutes post-mortem.
- Fig. 4-70 Electron micrograph of inner plexiform layer - 60 minutes post-mortem (37°C.).

VOLUME II:Chapter 5.

- Fig. 5-1 Light micrograph of the retina - 15 minutes ischaemia, 60 minutes recovery.
- Fig. 5-2 Light micrograph of the retina - 30 minutes ischaemia, 60 minutes recovery.
- Fig. 5-3 Light micrograph of the retina - 60 minutes ischaemia, 60 minutes recovery.
- Fig. 5-4 Light micrograph of the retina - 90 minutes ischaemia, 60 minutes recovery.
- Fig. 5-5 Light micrograph of the retina - 120 minutes ischaemia, 60 minutes recovery.
- Fig. 5-6 Light micrograph of the retina - 90 minutes ischaemia, 60 minutes recovery.
- Fig. 5-7 Light micrograph of the retina - 15 minutes ischaemia, 240 minutes recovery.
- Fig. 5-8 Light micrograph of the retina - 30 minutes ischaemia, 240 minutes recovery.
- Fig. 5-9 Light micrograph of the retina - 60 minutes ischaemia, 240 minutes recovery.
- Fig. 5-10 Light micrograph of the retina - 120 minutes ischaemia, 240 minutes recovery.
- Fig. 5-11 Light micrograph of the retina - 15 minutes ischaemia, 240 minutes recovery.
- Fig. 5-12 Light micrograph of the retina - 90 minutes ischaemia, 240 minutes recovery.
- Fig. 5-13 Light micrograph of the outer retina - 60 minutes ischaemia, 240 minutes recovery.
- Fig. 5-14 Light micrograph of the inner nuclear layer - 60 minutes ischaemia, 240 minutes recovery.
- Fig. 5-15 Light micrograph of the outer retina - 90 minutes ischaemia, 240 minutes recovery.
- Fig. 5-16 Light micrograph of the visual cells - 90 minutes ischaemia, 240 minutes recovery.
- Fig. 5-17 Light micrograph of the inner nuclear layer - peripheral retina - 90 minutes ischaemia, 240 minutes recovery.
- Fig. 5-18 Light micrograph of the inner nuclear layer - visual streak - 90 minutes ischaemia, 240 minutes recovery.
- Fig. 5-19 Electron micrograph of the retinal pigment epithelium - 30 minutes ischaemia, 60 minutes recovery.
- Fig. 5-20 Electron micrograph of the retinal pigment epithelium - 120 minutes ischaemia, 60 minutes recovery.
- Fig. 5-21 Electron micrograph of the retinal pigment epithelium - 30 minutes ischaemia, 240 minutes recovery.
- Fig. 5-22 Electron micrograph of the basal infoldings - 90 minutes ischaemia, 240 minutes recovery.
- Fig. 5-23 Electron micrograph of the basal cell wall - 90 minutes ischaemia, 240 minutes recovery.
- Fig. 5-24 Electron micrograph of the basal cell wall - 90 minutes ischaemia, 240 minutes recovery.
- Fig. 5-25 Electron micrograph of the retinal pigment epithelium - 90 minutes ischaemia, 240 minutes recovery.
- Fig. 5-26 Electron micrograph of a junctional complex - 120 minutes ischaemia, 240 minutes recovery.

- Fig. 5-27 Table showing the number of phagosomes in animals 9-16.
- Fig. 5-28 Table showing the % distribution of phagosomes in animals 9-16.
- Fig. 5-29 Table showing the number of phagosomes in animals 17-24.
- Fig. 5-30 Table showing the % distribution of phagosomes in animals 17-24.
- Fig. 5-31 Graph of relation between % distribution of phagosomes in test and control tissue - 15 minutes ischaemia.
- Fig. 5-32 Graph of relation between % distribution of phagosomes in test and control tissue - 30 minutes ischaemia.
- Fig. 5-33 Graph of relation between % distribution of phagosomes in test and control tissue - 60 minutes ischaemia.
- Fig. 5-34 Graph of relation between % distribution of phagosomes in test and control tissue - 90 minutes ischaemia.
- Fig. 5-35 Electron micrograph of the outer segments - 30 minutes ischaemia, 60 minutes recovery.
- Fig. 5-36 Electron micrograph of the outer segments - 30 minutes ischaemia, 60 minutes recovery.
- Fig. 5-37 Electron micrograph of the outer segments - 90 minutes ischaemia, 60 minutes recovery.
- Fig. 5-38 Electron micrograph of the outer segments - 15 minutes ischaemia, 240 minutes recovery.
- Fig. 5-39 Electron micrograph of the outer segments - 60 minutes ischaemia, 240 minutes recovery.
- Fig. 5-40 Electron micrograph of the outer segments - 120 minutes ischaemia, 240 minutes recovery.
- Fig. 5-41 Electron micrograph of the inner segments - 60 minutes ischaemia, 60 minutes recovery.
- Fig. 5-42 Electron micrograph of the inner segments - 15 minutes ischaemia, 240 minutes recovery.
- Fig. 5-43 Electron micrograph of the outer retina - 60 minutes ischaemia, 240 minutes recovery.
- Fig. 5-44 Electron micrograph of the inner segments - 60 minutes ischaemia, 240 minutes recovery.
- Fig. 5-45 Electron micrograph of the outer retina - 90 minutes ischaemia, 240 minutes recovery.
- Fig. 5-46 Electron micrograph of the outer nuclear layer - 90 minutes ischaemia, 60 minutes recovery.
- Fig. 5-47 Electron micrograph of the outer nuclear layer - 30 minutes ischaemia, 240 minutes recovery.
- Fig. 5-48 Electron micrograph of the visual cells - 60 minutes ischaemia, 240 minutes recovery.
- Fig. 5-49 Electron micrograph of the visual cells - 60 minutes ischaemia, 240 minutes recovery.
- Fig. 5-50 Electron micrograph of the outer nuclear layer - 90 minutes ischaemia, 240 minutes recovery.
- Fig. 5-51 Electron micrograph of the outer nuclear layer - 90 minutes ischaemia, 240 minutes recovery.
- Fig. 5-52 Electron micrograph of the outer plexiform layer - 60 minutes ischaemia, 60 minutes recovery.
- Fig. 5-53 Electron micrograph of the receptor pedicles - 120 minutes ischaemia, 60 minutes recovery.
- Fig. 5-54 Electron micrograph of the outer plexiform layer - 90 minutes ischaemia, 240 minutes recovery.
- Fig. 5-55 Electron micrograph of the outer plexiform layer - 90 minutes ischaemia, 60 minutes recovery.
- Fig. 5-56 Electron micrograph of the inner nuclear layer - 90 minutes ischaemia, 60 minutes recovery.
- Fig. 5-57 Electron micrograph of the inner nuclear layer - 90 minutes ischaemia, 60 minutes recovery.
- Fig. 5-58 Electron micrograph of the inner nuclear layer - 60 minutes ischaemia, 240 minutes recovery.

- Fig. 5-59 Electron micrograph of the inner nuclear layer - 90 minutes ischaemia, 240 minutes recovery.
- Fig. 5-60 Electron micrograph of the inner nuclear layer - 90 minutes ischaemia, 240 minutes recovery.
- Fig. 5-61 Electron micrograph of the inner plexiform layer - 30 minutes ischaemia, 240 minutes recovery.
- Fig. 5-62 Electron micrograph of the inner plexiform layer - 90 minutes ischaemia, 240 minutes recovery.
- Fig. 5-63 Electron micrograph of the inner plexiform layer - 60 minutes ischaemia, 240 minutes recovery.
- Fig. 5-64 Electron micrograph of the ganglion cell layer - 90 minutes ischaemia, 240 minutes recovery.
- Fig. 5-65 Electron micrograph of the nerve fibre layer - 60 minutes ischaemia, 240 minutes recovery.
- Fig. 5-66 Electron micrograph of the ganglion cell layer - 90 minutes ischaemia, 240 minutes recovery.
- Fig. 5-67 Electron micrograph of the horizontal nerve fibre zone - 90 minutes ischaemia, 60 minutes recovery.
- Fig. 5-68 Electron micrograph of the horizontal nerve fibre zone - 90 minutes ischaemia, 240 minutes recovery.
- Fig. 5-69 Electron micrograph of the internal limiting membrane - 60 minutes ischaemia, 60 minutes recovery.
- Fig. 5-70 Electron micrograph of a choroidal vessel - 15 minutes ischaemia, 60 minutes recovery.
- Fig. 5-71 Electron micrograph of a choroidal vessel - 60 minutes ischaemia, 240 minutes recovery.

Chapter 6.

- Fig. 6-1 Electroretinograms during the course of dark adaptation.
- Fig. 6-2 Dark adaptation curves for the 'a', 'b' and 'n' waves.
- Fig. 6-3 Dark adaptation curves for the 'a', 'b' and 'n' waves of each eye of one animal.
- Fig. 6-4 Diagram to show method of measurement of the various wave forms.
- Fig. 6-5 Graph of the control 'b' wave during the ischaemic and post-ischaemic phases in the test eye.
- Fig. 6-6 Electroretinograms following the induction of ischaemia.
- Fig. 6-7 Electroretinograms during an experiment involving 15 minutes ischaemia.
- Fig. 6-8 Electroretinograms during an experiment involving 30 minutes ischaemia.
- Fig. 6-9 Electroretinograms during an experiment involving 60 minutes ischaemia.
- Fig. 6-10 Electroretinograms during an experiment involving 90 minutes ischaemia.
- Fig. 6-11 Electroretinograms during an experiment involving 120 minutes ischaemia.
- Fig. 6-12 Graph showing the post-ischaemic recovery of the 'a' wave.
- Fig. 6-13 Graph showing the standard deviation of the mean of the 'a' wave following 60 and 240 minutes recovery.
- Fig. 6-14 Electroretinograms showing the latency of the 'a' wave following 60 and 90 minutes ischaemia.
- Fig. 6-15 Electroretinograms with isolated 'a' waves.
- Fig. 6-16 Graph showing the post-ischaemic recovery of the 'b' wave.
- Fig. 6-17 Graph showing the mean and standard deviation of the 'b' wave following 60 and 240 minutes recovery.

- Fig. 6-18 Electroretinogram showing failure of the 'b' wave to rise above iso-electric line.
- Fig. 6-19 Electroretinograms showing the 'b' wave latency following 15 and 90 minutes ischaemia.
- Fig. 6-20 Graph showing the post-ischaemic recovery of the 'n' wave.
- Fig. 6-21 Graph showing the mean and standard deviation of the 'n' wave following 60 and 240 minutes recovery.

Acknowledgments.

This investigation was supported by the Medical Research Council (Grant No. 971/366/C) and their generous help is gratefully acknowledged.

The experimental procedures reported in this thesis were carried out in the Tennent Institute of Ophthalmology, Glasgow, and I am grateful to Professor W.S. Foulds for providing these facilities. I also wish to thank Professor W.S. Foulds for his valuable help and guidance throughout this study. My thanks also go to Professor J.A.J. Pateman for the use of the electron microscope in the Department of Genetics, Glasgow, to Dr. W.R. Lee, Senior Lecturer in Ophthalmic Pathology and Honorary Consultant, Tennent Institute of Ophthalmology, Glasgow, and the staff of the West of Scotland Ophthalmic Pathology Service for their help and consideration, to Dr. R. Strang, Department of Clinical Physics and Bio-Engineering, Glasgow, for his initial guidance and help with the electrophysiological equipment, to Mrs. Jane Bright and Mrs. Norma Verrico for secretarial help and to Mr. A. Ganzer for translating articles from the original German.

The work reported in this thesis is entirely the work of the author, except for the valuable technical assistance provided by Miss S. Minhas from September, 1973, to August, 1974.

Material from this thesis has been published and presented at conferences as shown below:

- (1) The effect of acute ischaemia on the structure and function of the rabbit retina. (In conjunction with W.S. Foulds and R. Strang).
Proc. 14th AER Edinburgh.
Exp. Eye Res. (1973) 17, 390.
- (2) Rabbit electroretinograms during recovery from induced ischaemia. (In conjunction with W.S. Foulds).
Trans. Ophthal. Soc. U.K. (1974) 94, 383.
- (3) Effects of acute ischaemia on the structure of the rabbit retina. Preliminary results.
Trans. Ophthal. Soc. U.K. (1974) 94, 394.

- (4) The effect of acute ischaemia on the structure of the retinal pigment epithelium of the rabbit.
Proc. Symposium on the application of electron microscopy to Ophthalmic Anatomy and Pathology.
Exp. Eye Res. (1974) 18, 415.
- (5) Phagocytosis in the normal and ischaemic rabbit retina.
Proc. II Meeting of the European Club for Ocular Fine Structure.
London, 1974.
- (6) Phagocytosis in the normal and ischaemic retinal pigment epithelium of the rabbit.
Exp. Eye Res. (1975) 20, 97.
- (7) Phagocytosis in the choroidal endothelium of the ischaemic rabbit eye.
Acta Ophthalmol. (1975) 53, 321.
- (8) The mechanical effects of pressure on the rabbit retina.
Proc. III Meeting of the European Club for Ocular Fine Structure.
Marburg 1975.
- (9) The electroretinogram during and after recovery from acute ocular ischaemia in the rabbit. (In conjunction with W.S. Foulds).
In "Vision and Circulation", Kimpton, London. (1976).
(Proc. III Mackenzie Symposium).
- (10) Electron microscopy of acute retinal ischaemia in the rabbit and a study of the pattern of recovery.
In "Vision and Circulation", Kimpton, London (1976).
(Proc. III Mackenzie Symposium).
- (11) Post-mortem changes in the rabbit retina.
A study by light microscopy.
Acta Ophthalmol. 1976 (In Press).
- (12) The occurrence of macrophages in the ischaemia rabbit eye.
Acta Ophthalmol. 1976 (In Press).

N.F. JOHNSON
September, 1976.

xx

Summary.

This thesis describes the function and structure of the rabbit retina during and after periods of total acute ischaemia. The function of the retina was determined by electroretinography while the retinal structure was investigated by light and electron microscopy.

Following a 2 hour period of dark adaptation, total acute ocular ischaemia was induced in one eye of each rabbit by raising the intraocular pressure above the systemic systolic blood pressure for varying periods (15, 30, 60, 90 and 120 minutes). The contralateral eye acted as the control. One group of animals were killed immediately after the period of ischaemia and investigated histologically. In another group of animals, the intraocular pressure was returned to normal for up to 4 hours, the function of the retina was monitored throughout by electroretinography under scotopic conditions. Groups of animals were killed one and 4 hours after the return of the ocular circulation to determine the histological pattern of post-ischaemic recovery.

Light and electron microscopy revealed that the individual cell types making up the retina possessed different tolerances to ischaemia. The visual cells were the least resistant to ischaemia, being susceptible to periods of ischaemia longer than 30 minutes. The Müller cells, the ganglion cells and the RPE were the most resistant to ischaemia, often showing only mild changes following 4 hours recovery from 90 and 120 minutes ischaemia. The neural cells of the inner nuclear layer exhibited an intermediate tolerance to ischaemia showing severe degenerative changes following periods of ischaemia longer than 60 minutes. A prominent feature of the ischaemic retina was the presence of macrophages in the subretinal space. The macrophages appeared to be actively engaged in the removal of outer segment debris. These cells were not a feature of the post-ischaemic retina. During the recovery phase the RPE was able

to increase its phagocytic activity. This appeared to be the main mechanism for the removal of outer segment debris during the post-ischaemic phase following periods of ischaemia not longer than 60 minutes. The histological changes arising from periods of ischaemia induced by high intraocular pressure may have arisen from the effects of ischaemia, the mechanical effect of pressure or a combination of the two factors. Post-mortem retinal tissue was investigated to determine the effects of total acute ocular ischaemia not involving raised intraocular pressure. There was a marked similarity between the pressure-induced ischaemic tissue and post-mortem tissue which suggested that the mechanical effects of raised intraocular pressure were small compared to the effects of ischaemia.

Following total ocular ischaemia, some recovery of ERG was found in all eyes exposed to ischaemia of up to 120 minutes, although after longer periods of ischaemia, recovery of the ERG was delayed and incomplete. After periods of ischaemia of 15, 30 or 60 minutes, a recordable 'b' wave appeared within 5 minutes of the restoration of circulation. After 90 minutes of ischaemia recovery of the 'b' wave can be seen some 15 to 20 minutes after restoration of circulation, while after 120 minutes of ischaemia, the appearance of a recordable 'b' wave was delayed for as long as half an hour. After longer periods of ischaemia, its recovery became progressively slower and less complete. After 30 minutes of ischaemia, the amplitude of the 'b' wave became temporarily larger than that in the control eye, this temporary supernormality lasting through the 4 hour period of observation. After 60 minutes of ischaemia, the amplitude of the 'b' wave returned to 80% of the value in the control eye in 4 hours, while after 90 minutes of ischaemia recovery ranged between 10 and 50% of the value in the other eye after 4 hours. Following 120 minutes ischaemia, the 'b' wave returned temporarily and was absent in all eyes

after 3 hours. In general the 'a' wave returned more rapidly than the 'b' wave after an ischaemic episode and the disparity became more marked the longer the period of ischaemia lasted. After 30 minutes of ischaemia, recovery of the 'a' wave started within 5 minutes on average, while after 60 minutes or 90 minutes of ischaemia 'a' wave recovery started between 5 and 10 minutes after restoration of circulation. A common finding after 15 and 30 minutes of ischaemia was an 'a' wave of increased amplitude. The 'c' wave was found to be more variable than the 'a' wave or 'b' wave. On occasion the 'c' wave was found to be of larger amplitude than in the pre-ischaemic ERG. A feature of the ERG during recovery from ischaemia was the occurrence of marked post-'b' wave negativity. Following the induction of ischaemia in the test eye, the 'b' wave of the contralateral control eye increased in amplitude.

There was a poor correlation between the alterations in the components of the ERG and the changes in the cells from which the components were thought to arise. The 'a' wave returned rapidly following ischaemia in spite of considerable damage to the inner and outer segments of the visual cells. However, there was a good correlation between the overall wave form of the ERG and the histological changes. A marked negativity of the ERG with reduced positive components was indicative of a severely damaged retina.

Chapter I - Introduction

1-1 Introduction.

This thesis reports an investigation into the effects of total acute ischaemia on the structure and function of the rabbit retina and the pattern of post-ischaemic recovery. The structure of the retina has been studied by light and electron microscopy and the function of the retina has been investigated by electroretinography.

The retina is a highly specialised tissue concerned with the conversion of radiant energy into electrical energy, which is transmitted to the visual cortex in the occipital lobe of the brain. This complicated set of events forms the basis of the visual process.

1-2 The organisation of the retina.

The specialised nature of the retina is reflected in the many cell types which occur and form well-defined layers. Eleven such layers can be easily identified with the light microscope (Fig. 1-1). These are - (1) the retinal pigment epithelium (RPE), (2) the outer segments, (3) the inner segments, (4) the external limiting membrane, (5) the outer nuclear layer, (6) the outer plexiform layer, (7) the inner nuclear layer, (8) the inner plexiform layer, (9) the ganglion cell layer, (10) the nerve fibre layer, and (11) the internal limiting membrane. Before light can stimulate the visual cells it has to pass through the majority of these layers. The visual cells are the sensory receptors in the visual pathway and their outer segments contain photopigments which initiate the excitatory process accompanying light stimulation. The cell bodies of the visual cells form the outer nuclear layer and their axons synapse with the dendrites of the bipolar cells in the outer plexiform layer. The bipolar cells are the first neurones of the visual

inner
 pathway. These latter cells lie in the ~~the~~ nuclear layer and their axons extend into the inner plexiform layer to synapse with ganglion cell dendrites. The ganglion cells are the second neurones of the visual pathway and their axons extend through the optic nerve to the chiasm and end in the lateral geniculate body. The third order neurones extend from the lateral geniculate body to the occipital cortex. Before the electrical impulses reach the level of the ganglion cells, there is considerable integration of the signals through the action of horizontal and amacrine cells. These cells are found in the inner nuclear layer. The horizontal cells have extensive connections in the outer plexiform layer whilst the amacrine cell connections are in the inner plexiform layer. The neural elements of the retina are surrounded by the cytoplasm of glial cells (Müller cells). The nuclei of the Müller cells lie in the inner nuclear layer and their cytoplasm extends from the internal limiting membrane and to the external limiting membrane where it forms a brush border in between the elements of the inner segments. The glial cell acts both as a structural and metabolic support for the retina.

1-3 The function of the retina.

The conversion of light into electrical energy results in a series of potential changes which spread through the retinal tissue. These potential changes can be recorded electrically and a portion of these changes form the familiar electroretinogram. In 1865 Holmgren described alterations in the standing potential of the eye following the onset of illumination. This response was independently discovered by Dewar and McKendrick in Scotland in 1873. It was not until 1903 that Gotch produced electroretinograms which would be recognisable to-day.

He described a small negative deflection preceding the main positive response to the onset of illumination. Minthoven and Jolly (1908) referred to various deflections of the response by the initial letters of the alphabet (Fig. 1-2) and attempted to separate the response into various components. Similar attempts were made by Waller (1909). The modern interpretation of the components of the electroretinogram stems from the extensive work of Granit. In 1933 Granit proposed three components P1, P11 and P111 (Fig. 1-2) corresponding to the 'c', 'b' and 'a' waves respectively. Granit's components are based on the selective loss of the various components with deepening ether anaesthesia. Since Granit's initial work many attempts have been made to determine the relationship between the components P1, P11 and P111 and the various cells within the retina. There is much evidence to suggest that the 'a' wave or P111 component is generated in the receptor cells (Brown and Wiesel 1961, Brown and Watanabe 1961, Arden and Brown 1965, Brown 1968, and Penn and Hagins 1969), the 'b' wave or P11 component originates from the Müller cells under ionic influence from the bipolar cells (Warblin and Dowling 1969, and Miller 1973) and the 'c' wave or P1 component is generated in the retinal pigment epithelium (Noel 1954, Heck and Papst 1957, and Steinberg, Schmidt and Brown 1970).

1-4 The blood supply of the retina.

The normal functioning retina has one of the highest metabolic rates of any tissue in the body. The nutritional requirements of the retina are met largely from its blood supply, in addition to a small proportion probably derived from the vitreous. In the rabbit, the entire retina is supplied from the choroidal circulation. In a great number of mammalian species the retina is nourished by separate retinal and

choroidal circulations. The retinal vessels supply the inner retina which includes the ganglion cell and inner nuclear layers. The arterial vessels of the retinal circulation are derived from the central retinal artery which in many mammals arises from a branch of the ophthalmic artery which penetrates the optic nerve before entering the globe. The choroidal vessels supply the outer retina which includes the visual cells and retinal pigment epithelium. The choroidal circulation is derived from the posterior ciliary arteries. Within the globe these arteries branch into large vessels which lie in the scleral margin of the choroid. These vessels divide into smaller arteries, as the vessels become closer to the retina their size decreases until they reach capillary size in the choriocapillaris which is adjacent to the retinal pigment epithelium. Within the choroidal vascular network many anastomoses occur.

Cessation of the entire blood supply to the retina results in a rapid loss of function. Prolonged cessation of the blood supply leads to an irreversible loss of function and degenerative changes in the retina. Interruption of the retinal circulation severely affects the function of the retina and results in pathological changes in the inner retina whilst the outer retina is spared. The reverse situation is observed following choroidal ischaemia with degenerative changes in the outer retina and little alteration in the inner retina.

1-5 Background to present study.

There is an extensive literature relating to the clinical and experimental manifestations of retinal ischaemia. In spite of this, speculation exists concerning the exact sites of ischaemic damage in the retina and the ability of retinal tissues to withstand and to recover from ischaemic insults.

A convenient method to induce total retinal ischaemia is to raise the intraocular pressure sufficiently to abolish the flow of blood to the retina. This technique has been employed here to study the effects of varying periods of total ischaemia on the structure and function of the rabbit retina. By lowering the raised intraocular pressure to normal after the ischaemic episode, the pattern of post-ischaemic recovery has been followed. An obvious problem with using high intraocular pressures to induce ischaemia is that the actual pressure may exert a direct effect on retinal tissues.

The mechanical effects of pressure on the retina have been studied. Light and electron microscopy have been used to establish the sites of ischaemic damage in the retina and to determine to what extent these alterations influence the pattern of post-ischaemic recovery. The structural findings are correlated with the functional findings provided by electroretinography.

The literature forming the background to this study can be divided into two main categories, that relating to total retinal ischaemia and that relating to partial retinal ischaemia.

1-6 Total retinal ischaemia.

The effects of total retinal ischaemia have been investigated using a variety of methods in several species using both histological and electrophysiological techniques.

1-6.1 Structural effects of total ischaemia.

Total retinal ischaemia has been studied histologically following section or ligation of the vessels supplying the choroidal and retinal circulations, the posterior ciliary arteries and central retinal arteries respectively, and by raising the intraocular pressure

sufficiently to abolish the blood flow to the eye. The former method has been employed in rabbits by Wagenman (1890) and Nichols (1938), in rats by Turnbull (1948) and in cats by Smith and Baird (1952). In addition total retinal ischaemia has been investigated in gerbils by clamping one or both common carotid arteries (Levine and Payan 1966). The histological effects of intraocular pressures sufficient to abolish blood flow to the eye have been studied in rats by Smith and Baird (1952), in monkeys by Fujino and Hamasaki (1967) and Anderson and Davis (1975), and in cats by Reinecke, Kuwabara and Cogan and Weis (1962). The findings of these studies show basic similarities irrespective of the method used to induce ischaemia. The initial change was the occurrence of oedema throughout the retina. The oedema was more prominent in the inner retina and was followed by degenerative changes in the ganglion and bipolar cells with the eventual involvement of the whole retina. Although in rabbits Nichols (1938) described the initial change to be in the outer retina. This may be related to the absence of a true retinal circulation in rabbits (Michelson 1954) whereas in the cat, rat, gerbil and monkey a dual circulation exists. There is considerable variation in the period of total ischaemia thought to induce irreversible changes. These periods ranged from 90 minutes (Reinecke et al 1962) to 15 minutes (Smith and Baird 1952). Complete retinal ischaemia is a rare occurrence clinically. It can occur following the failure of the general circulation as in hypotension or cardiac arrest, the blockage of the arterial flow to the eye accompanying surgery, thrombosis or trauma and after exsanguination. The pathological reports of complete retinal ischaemia indicate a similarity between clinical and experimental observations (Duke-Elder 1967). Although the pathological reports often detail end-stage pathology, little is known about the initial course of events in humans suffering from

complete retinal ischaemia.

Little detailed information could be traced in the literature concerning the structure of the retina during periods of post-ischaemic recovery. In addition, no detailed account of ultrastructural changes accompanying periods of total retinal ischaemia and post-ischaemic recovery was found in the literature.

1-6.2 Functional effects of total ischaemia.

The electroretinographic aspects of total retinal ischaemia induced by raised intraocular pressure have been studied in rabbits by Hoell (1951), Bornschein and Zwaiver (1952), Popp (1955), Arden and Greaves (1956) and Papst and Heck (1957), in monkeys by Hoell (1951 and 1952), Fujino and Hamasaki (1965) and Gerstle, Anderson and Hamasaki (1973) and in man by Bock, Bornschein and Honner (1960), Karlberg, Hedin and Bjornberg (1960) and Sipperly, Anderson and Hamasaki (1973). In addition Granit (1933) and Horsten and Winkelman (1957) have studied electroretinograms in cats following occlusion of the aorta. The experiments show that the electroretinogram is rapidly affected in the absence of any flow of blood to the eye. The response was extinguished 3 to 15 minutes after induction of ischaemia. The various components disappeared in a characteristic fashion, the 'c' wave being least resistant to ischaemia disappeared first, followed by the 'b' wave and finally the 'a' wave. The results of Arden and Greaves (1956) suggested that the order of disappearance was the 'a' and 'c' waves followed by the 'b' wave. The consensus of opinion favours the former situation. Once the blood flow is re-established to the eye, the 'a' wave appears first followed by the 'b' wave and later the 'c' wave. The recovery of the electroretinogram following periods of ischaemia is dependent on the duration of the ischaemic episode. A considerable variation occurs in the duration of

ischaemia necessary to provoke irreversible changes in the electroretinogram. The maximum period thought to be compatible with eventual recovery of the normal electroretinograms is 60-90 minutes (Fujino and Hamasaki 1967, Bock, Bornschein and Homner 1960 and Popp 1955). These studies provide little precise information concerning the changes in the various components during the post-ischaemic recovery phase.

1-7 Partial retinal ischaemia.

A substantial number of histological and electroretinographic investigations have been carried out into the effects of partial ischaemia in the retina. This is because partial ischaemia is a frequent clinical finding and can result in impaired vision or blindness. Partial ischaemia may accompany rises in intraocular pressure which are insufficient to cause complete cessation of the blood flow, or following occlusion of part or all of either the arterial or venous networks of the retinal or choroidal circulations.

1-7.1 Structural effects of partial ischaemia.

The histological changes accompanying periods of elevated intraocular pressure have been described in rabbits by Flocks, Tsukhara and Miller (1959), Kupfer (1962), De Carvalho (1962) and Ruusuvaara and Palkama (1974) and in monkeys by Fujino and Hamasaki (1967). The initial sign of damage is oedema in the nerve fibre and ganglion cell layers. The oedema is more marked following long periods of raised intraocular pressure which eventually results in vacuolation and disintegration of the ganglion cells and in severe cases, complete retinal atrophy. These experimentally-induced changes mirror to a great extent the alterations observed clinically during glaucoma (Duke-Elder 1967).

Partial ischaemia arising from insufficiency in either the venous or arterial side of the retinal circulation has been studied experimentally

by several authors. Histological investigations of the effect of disturbances in the arterial side of the retinal circulation have been studied in monkeys by Hayreh (1965), Kroll (1968), in cats by Smith and Baird (1952) and Stone (1969), in pigs by Ashton, Dollery, Henkind, Hill, Paterson, Ramalho and Shakib (1966) and in dogs by Gay, Golder and Smith (1964) and Golder and Gay (1967). Arterial insufficiency can lead to massive swelling of the inner retinal layers followed by necrosis. The changes can affect all the cells vitread to the outer nuclear layer, although the glial cells appear to remain normal as do the visual cells. The severity of the changes depend on where in the arterial network the disturbance occurs, the more major the vessel affected, the more severe are the degenerative changes.

Disturbance of the venous side of the retinal circulation affect the structure of the retina, although to a much more variable extent than arterial insufficiency. Experimentally-induced venous disturbances have been studied in cats by Becker and Fost (1951) and Campbell (1961), in monkeys by Hayreh (1965), Fujino, Curtin and Norton (1969), Kohner, Shakib, Henkind, Paterson, De Oliveria and Bulpitt (1970) and in pigs by Kohner et al (1970). The results of these experiments are generally similar and show that following venous disturbances, oedema occurs in the nerve fibre layer and inner nuclear layer. Haemorrhages also occur around vessels and in the inner retinal layers in the ischaemic region. The experimentally-induced changes accompanying both arterial and venous insufficiency of the retina show a similarity to the clinical and pathological findings in man (Duke-Elder 1967 and Wise, Dollery and Henkind 1971). Although in man, in many cases of retinal vascular disease, all parts of the vascular network are involved. It is frequently difficult to ascribe the initial pathology to either the venous or the arterial side of the circulation.

Disturbances in the choroidal circulation can also lead to partial ischaemia. The histological changes accompanying periods of choroidal ischaemia have been studied in monkeys by Hayreh and Raines (1972), Buettner, Machemer, Charles and Anderson (1973) and Anderson and Davies (1974), in cats by Collier (1967) and in dogs by Gay, Goldor and Smith (1964) and Goldor and Gay (1967), in rabbits by Nicholls (1938) and Wagenman (1890). Choroidal ischaemia primarily affects the pigment epithelium and visual cells. Prolonged periods of ischaemia result in necrosis of these two outer layers of the retina. Extracellular oedema is often a feature of the inner retinal layers. The organisation of the choroidal vascular network has an important bearing on the severity of ischaemic lesions following vessel occlusion. Many anastomoses occur between vessels and ischaemic lesions occur only after multiple occlusions of the choriocapillaris or occlusion of one or more posterior ciliary arteries. Occlusion of the larger choroidal vessels appears to have little effect on the overlying pigment epithelium and visual cells, whereas occlusive disorders of the retinal vascular system are well known clinical entities, occlusive disorders of the choroid have received less attention. There appears to be a good correlation between the experiment and clinical observations in choroidal ischaemia. (Hapburn, 1935, Duke-Elder 1967, Foulds, Lee and Taylor 1971, and Amalric 1971).

1-7.2 Functional effects of partial ischaemia.

The electroretinogram has been studied experimentally following disturbances of the retinal circulation in monkeys by Fujino and Hamasaki (1965), Brown and Watanabe (1962) and Hamasaki and Kroll (1968) and in cats by Brown and Watanabe (1962), and following choroidal ischaemia in monkeys by McLeod and Hayreh (1972), Buettner, Machemer, Charles and Anderson (1973) and Fujino and Hamasaki (1965).

Interruption of the retinal circulation abolishes the P11 component leaving the negative P111 component which appears to be maintained by the choroidal circulation. Choroidal occlusion also results in the loss of the P11 component, the remaining P111 component eventually being abolished also. An extensive literature exists on the clinical electroretinography of vascular disturbances. Since the initial work of Karpe (1945), it has been known that patients suffering from obstruction of the central retinal vessels generally show a pathologically altered electroretinogram. Karpe (1945) proposed a classification of patients according to the configuration of the electroretinogram. Electroretinograms with enlarged 'b' and 'a' waves are referred to as supernormal, and ERGs with an enlarged 'a' wave are referred to as negative. When the ERG has a marked 'a' wave and a normal or supernormal 'b' wave, they are designated as 'negative - plus'. An ERG which has a marked 'a' potential and a subnormal 'b' wave is classed as 'negative - minus'. An ERG in which the 'b' wave is diminished is referred to as 'sub-normal'. The prognosis was best amongst patients with supernormal, normal and negative plus ERGs and gradually worsened with negative minus, subnormal, and extinguished ERGs. A full range of these changes was found in patients with disturbances of the retinal circulation (Karpe 1945, Honkes 1953 and 1954 and Nilsson 1971). Less is known about the clinical electroretinogram following choroidal disturbances.

Occlusion of the posterior ciliary arteries occurs clinically in ischaemic optic neuropathy which is commonly due to temporal arteritis (Hayreh 1969 and 1971). The ERG is usually unaffected after ~~temporal~~ ischaemic optic neuropathy (Palm 1958, and Edmund and Jensen 1967). McLeod and Hayreh (1973) describe electroretinographic responses accompanying vascular occlusions due to temporal arteritis. In some instances both retinal and choroidal circulations were involved. Retinal involvement

resulted in selective loss of the 'b' wave leaving a large 'a' wave.

In the eyes with reduced flow in posterior ciliary arteries there was generally no alteration in the ERG, although a reduction in both 'a' and 'b' waves of the ERG was found when the circulation through the posterior arteries was severely reduced.

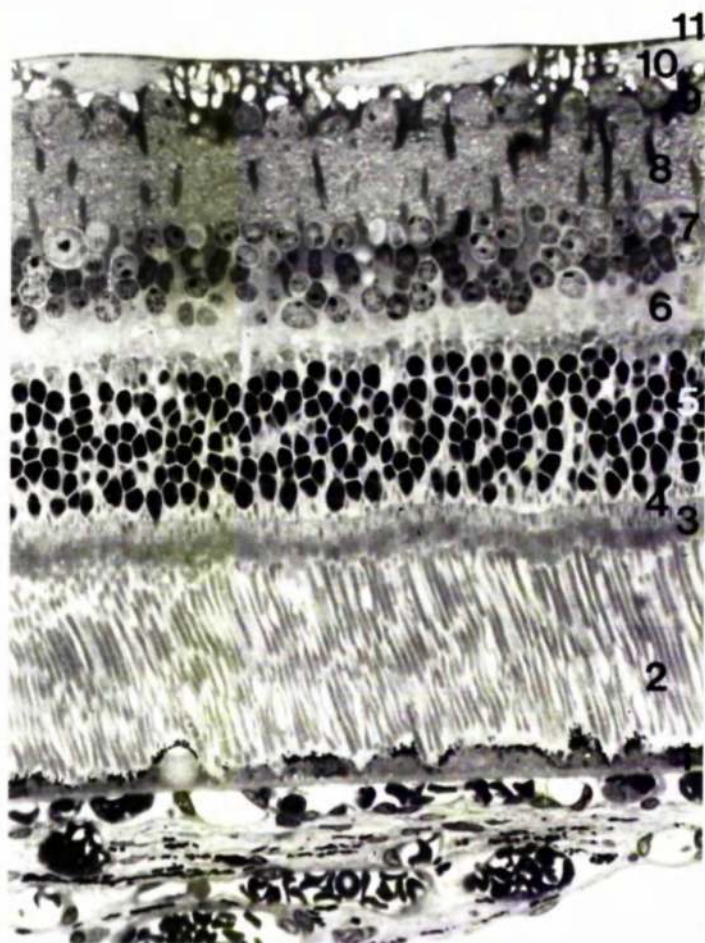


FIG. I-I Light micrograph of the rabbit retina showing the eleven recognisable layers; I- The retinal pigment epithelium; 2- The outer segments; 3- The inner segments; 4- The external limiting membrane; 5- The outer nuclear layer; 6- The outer plexiform layer; 7- The inner nuclear layer; 8- The inner plexiform layer; 9- The ganglion cell layer; 10- The nerve fibre layer; 11- The internal limiting membrane. (1,200 X)

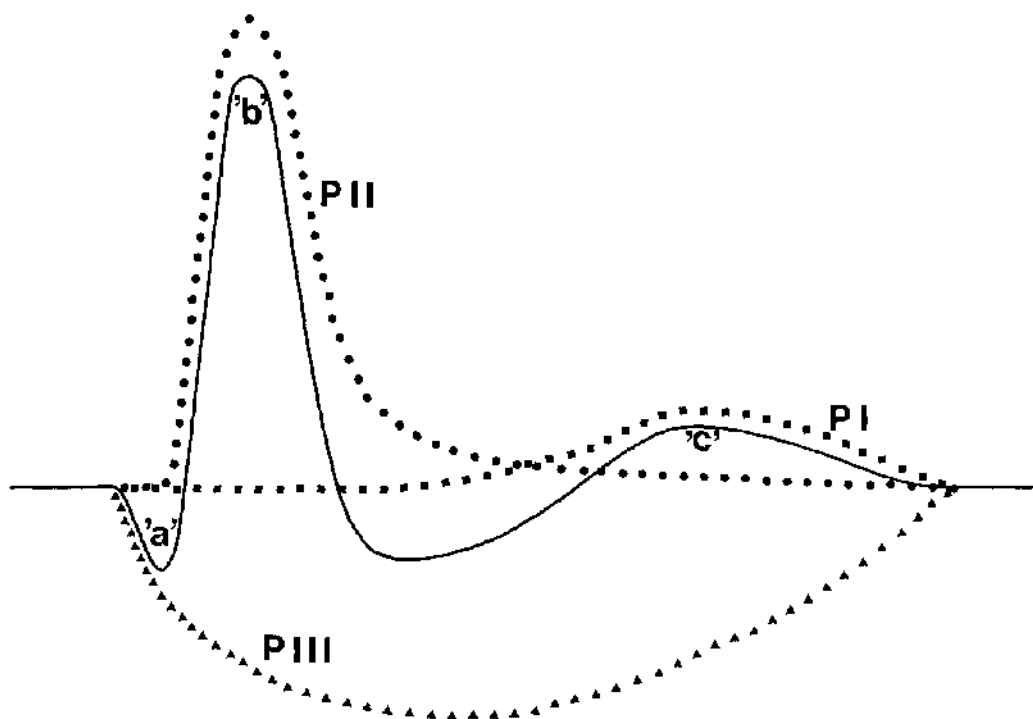


FIG.I-2 Schematic representation of the electroretinogram showing the 'a', 'b' and 'c' waves(after Einthoven and Jolly 1908) and their relation to the components PI,PII and PIII.(after Granit 1933)

Chapter 2 -- Materials and Methods

2-1 Material.

The material for this study was obtained from a total of 70 adult Dutch rabbits (Lepus cuniculus) weighing between 1.7 and 2.2 Kg.

2-2 Methods employed in investigation into pressure-induced ischaemia.

The animals were anaesthetised with 40% urethane (ethyl carbamate made up in sterile distilled water) administered slowly via the marginal ear vein until the corneal reflex disappeared. The dose of urethane was dependent on the weight of the animal, the amount given varied between 1.75 and 2.1 g. urethane/Kg. body weight. The pupils were maximally dilated with several drops of 1.0% cyclopentolate and 10% phenylephrine. Further drops were given hourly throughout the course of the experiment to keep the pupils fully dilated. A tracheostomy was performed. The abdominal aorta was cannulated via the femoral artery with a heparinised polythene cannula (0.75 mm. dia.). This cannula and its connections were filled with heparinised saline (1000 iu/500 ml.). The animal was placed in a prone position and the head secured in a head rest. The animal was covered, except for its head in a double felt blanket. This covering was found sufficient for the animal to maintain its normal body temperature (36-38°C.) without the need to apply external heat. The lids of both eyes were retracted by sutures prior to cannulation of both anterior chambers with heparinised gauge 23 needles. (These were modified prior to cannulation to enable them to act as electrodes. See 2-4.). The needles were carefully inserted to prevent leakage of aqueous humour around the needle. Leakage was sometimes a problem with gauge 23 needles because of their long bevel. The entire length of the bevel had to be inserted into the corneal stroma before the anterior chamber was penetrated. This prevented leakage during cannulation and during the course of the experiment.

Once the anterior chamber was penetrated, care was taken to avoid touching the iris, lens or corneal endothelium. The cannulae were held firmly in position by a series of clamps and rigid scaffolding attached to the operating table. The anterior chamber of one eye was linked by a three way tap and polythene tubing to a manometer and pump by which means it was possible to raise and maintain the intraocular pressure at any desired level. The femoral artery cannula was linked to a low volume pressure transducer (Bell and Howell L221) by way of a three way tap and tubing. All the connections used in the experiments and including the manometer were filled with heparinised saline (1000 iu/500 ml.). The pressure transducers were joined to a devices pen recorder. Fibre optic light guides were positioned so that their polished end plates (5 mm. dia.) were 2 cm. from the corneal surface on the optical axis of each eye. The light guides were linked by a 'Y' piece to a devices photic stimulator. By this arrangement it was possible to present simultaneous stimuli of equal intensity to both eyes. The light guides were held firmly in position by a series of clamps and scaffolding attached to the operating table. A modified gauge 23 needle (see 2-4) was placed subcutaneously above the orbit of each eye, similar electrodes were attached to the mouthpiece and operating table. A schematic diagram of the experimental model is shown in fig. 2-1. On completion of the operative procedures the animals were light adapted for 2 mins. (30 cps $37 \frac{3}{4}$ m joules/cm²/sec.). Following this the animals were dark adapted for at least two hours. One hour after the cannulation of the femoral artery, the animal was heparinised with 500 iu heparin, this dose was repeated after a further 4 hours. This was done in order to prevent the blood clotting in the cannulae. It was found necessary to wait an hour before administration as this gave time for the surgical wounds to clot and prevent blood loss during the experiment which otherwise occurred if the heparin was given immediately after surgery.

During the course of dark adaptation, electroretinograms were recorded. After this period the IOP in one eye was raised 10 mm.Hg. above the systemic systolic blood pressure. This pressure was maintained for 15, 30, 60, 90 or 120 minutes. The other eye was left as before and acted as the control. In one group of animals the experiment was terminated immediately after the ischaemic episode. In a further group of animals the IOP was allowed to return to normal for either 60 or 240 minutes. The number of animals investigated at each point in the experiment is shown in Table 1 (Fig. 2-2). During the ischaemic period and period of post-ischaemic recovery electroretinograms were recorded. At the termination of the various experiments tissue was taken for histological examination. The experiments were either concluded with an overdose of urethane or by perfusion with fixative.

2-3 Methods employed in the investigation into post-mortem changes in the retina.

The animals were killed with an overdose of urethane. In one group of animals the eyes were enucleated and bisected into anterior and posterior halves. The posterior halves were immediately fixed by immersion in 3% gluteraldehyde in Sorensen's phosphate buffer (pH 7.3 - 7.4) at room temperature. These animals were employed as controls. In another group of animals, the eyes were enucleated following death and placed in the dark in Dulbecco's phosphate buffer at either room temperature or at 37°C. The eyes were kept under these conditions for either 15, 30, 60, 90 or 120 minutes. In a further group the eyes were left in the cadaver to determine whether placing the eyes in phosphate buffer had any effects on the structure of the retina. The number of animals used at each point in the experiment is shown in Table 2 (Fig. 2-2). After the varying post-mortem periods the eyes were bisected and the

posterior halves immersed in fixative at room temperature for at least 4 hours before conventional processing for electromicroscopy (see 2-5).

2-4 Electoretinography.

Electoretinograms (ERG) were recorded throughout the series of experiments to study the functional aspects of pressure-induced ischaemia. This involved recording during a period of dark adaptation (not less than 2 hours), a period of ischaemia (up to 2 hours) and a period of post-ischaemic recovery (up to 4 hours). The ERGs were recorded usually at 5 or 10 minute intervals. Following the onset and cessation of the raised intraocular pressure ERGs were recorded more frequently, but never more than 1 per minute.

The electrodes used to record the signal from the eye at the onset of illumination were modified gauge 23 needles. The needle and the lead to the recording equipment were held in place by a plastic sheath. This arrangement appeared to produce an adequate contact between the two metal surfaces and yet provide a quick and convenient method of making electrodes. The anterior chamber cannulae acted as the active electrode, those in the scalp between the orbits acted as the indifferent electrodes and those attached to the mouth piece and operating table acted as the earth electrodes. The three electrodes from each side of the animal were linked to differential preamplifiers (Teckronix 122) prior to display on a dual beam dual trace storage oscilloscope (Teckronix 5103H). The displayed traces were photographed for subsequent analysis.

2-5 Tissue preparation for electromicroscopy.

At the termination of the particular experiment tissue was obtained for histological examination. In the series of experiments where the intraocular pressure was allowed to return to normal the animals were fixed

by intra-arterial perfusion via the femoral artery cannula. The jugular vein was cut as an exit channel for the expelled blood and spent fixative. The fixative was in all cases 2-3% buffered glutaraldehyde. The buffer was either 0.2M sodium cacodylate (pH 7.2 - 7.4) or Sorensen's phosphate buffer (pH 7.3 - 7.4). The fixative was injected into the cannula with the aid of a 50 ml. syringe at a rate of 50 ml. min. The amount of fixative used in each animal varied between 200 and 350 ml. Following perfusion the eyes were enucleated, bisected in the equatorial plane and the posterior halves immersed in fixative at room temperature. In the group of animals where the tissue was obtained immediately after the ischaemic episode the eyes were enucleated before fixation. Perfusion was impracticable as the blood supply to the ischaemic eye was completely abolished by the high intraocular pressures employed and this would prevent passage of fixative to the eye. Immediately following enucleation the eyes were bisected in the equatorial plane and the posterior halves immersed in fixative at room temperature. The posterior halves from this latter group were fixed for at least 4 hours. From this point, tissue from both the latter group and that from the post-mortem study were treated in a similar fashion. Before processing, pieces of tissue were obtained from predetermined regions (fig. 2-3) ^{and} during the subsequent processing the tissue from the various areas was kept separate and individually processed.

1 - 2 mm. x 2 - 3 mm. pieces of tissue comprising the sclera, choroid and retina were dissected out in solution of buffered 8% sucrose (Sorensen's phosphate buffer or Sodium cacodylate). This solution was used to remove all unbound glutaraldehyde prior to secondary fixation with buffered 1% osmium tetroxide. After osmification the tissue was again washed in 8% buffered sucrose. This was followed by dehydration in a graded series of alcohols. The tissue was then passed through a transitional fluid before embedding in araldite. The araldite-embedded tissue was cured for 2 days

at 55°C. The tissue blockswere then left at least two days before cutting.

2-6 Microscopy.

The tissue blocks were trimmed and sections cut with glass knives for both light and electron microscopy on an L.K.B. Ultratome III.

Following the trimming of the block, 1 micron thick sections were cut and collected with a platinum wire loop from the trough of the knife which contained 10% acetone in distilled water. The sections were transferred to a clean glass slide and dried gently on a hot plate. The sections were stained by heating (70 - 80°C.) for 1 minute with ripe Loeffler's methylene blue which had been filtered prior to use. The sections were then differentiated in 70% alcohol and then rapidly air dried. The sections were mounted in either araldite for permanency or in Harleco's synthetic resin for semi-permanency.

Loeffler's methylene blue was found to be the most convenient and easy stain to use from a range of basic dyes tried. The basic dyes, toluidine blue, methylene blue, basic fuschin and malachite green, often provide a rapid dichromatic or polychromatic staining effect especially when the stains are used in combination with each other. Toluidine and methylene blue are largely nuclear stains, basic fuschin acts as an overall stain while malachite green can enhance the effect of the nuclear stains. The following methods were tried, Richardson, Jarrett and Finke 1960 (methylene blue and azure 11), Huber, Parker and Caland 1968 (methylene blue, basic fuschin, and malachite green), Moore, Kumaw and Schoenberg 1960 (crystal violet and basic fuschin), Winkilestein, Kenefee, Gand and Bell 1963 (basic fuschin), Chandra and Skelton 1964 (toluidine blue and basic fuschin) Hoefert 1968 (azure blue, toluidine blue, methylene blue and paragon stain), Lee and Hopper 1965 (basic fuschin, and crystal violet), Grimley 1964 (toluidine blue, malachite green and basic fuschin), Martin, Lynn and

Wickey 1966 (Paragon stain), Grimley, Albrecht and Michelitch 1965 (azure blue, toluidine blue, malachite green and Stirling's gentian violet) and Feder and O'Brien 1968 (acid fuchsin and toluidine blue). While the majority of these stains worked, the contrast and differentiation obtained in retinal tissue was poor. This was often in association with lengthy staining periods. Three factors appeared to be important in staining araldite-embedded retinal tissue. These were pH of the stain, the temperature at which the staining was carried out and whether the stain was alcoholic. The best staining results were obtained with high pHs (9 - 11) and alcoholic stains with the staining carried out at 60 - 80°C. Although one disadvantage of using alcoholic stains was the presence of precipitates even after filtering. The procedure using Loeffler's methylene blue gave a rapid staining method and good tissue differentiation which was suitable for both light microscopy and photography.

Following the cutting of sections for light microscopy, the blocks were retrimmed for electron microscopy, 400 - 600² thick sections were collected on copper grids and stained with uranyl acetate and lead citrate and investigated with the aid of a Siemens 1A Elmiskop.

2-7 Animal selection - Pressure-induced ischaemia study.

Only those animals in which the diastolic blood pressure remained within 10% of its initial value throughout the course of the various experiments were used for histological and electrophysiological investigation.

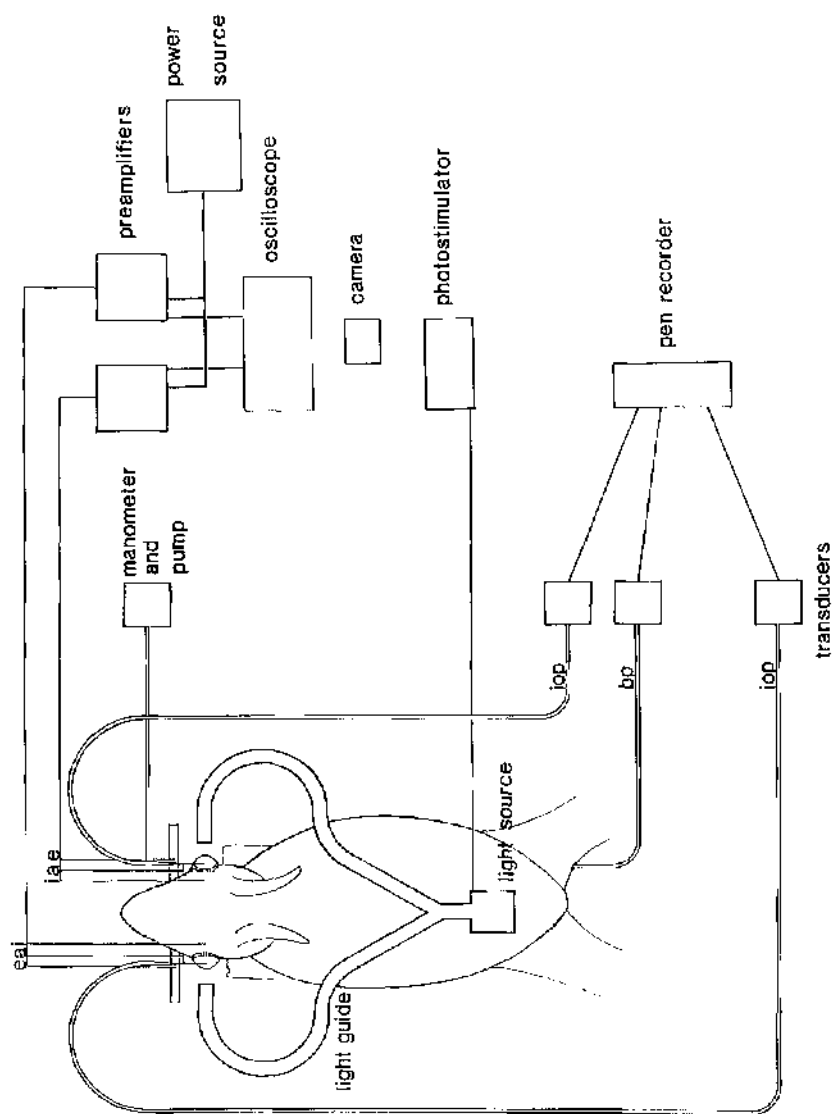


FIG.2-1 Schematic representation of the experimental model.

		Recovery Period (minutes)				
		0	60	180	210	240
Period of Ischaemia (minutes)	15	3 (3)	2 (2)	1		4 (3)
	30	3 (3)	2 (2)	1	1	4 (3)
	60	3 (3)	2 (2)			5 (3)
	90	3 (3)	2 (2)			5 (3)
	120	3 (3)	2 (2)			4 (2)
		Plus 6 animals for dark adaptation and anaesthetic controls.				

FIG.2-2 Table I. Table showing the number of animals used at each point in the electrophysiological experiments. The numbers in brackets represent the number of animals investigated histologically.

Post-mortem period (minutes)	Room temperature	37°C
0 (control)	-	4
15	3*	2
30	3*	2
60	2	2
90	3*	2
120	2	2

FIG.2-2 Table II. Table showing the number of animals investigated at the various post-mortem periods.* Denotes group in which 1 eye was left in the cadaver.

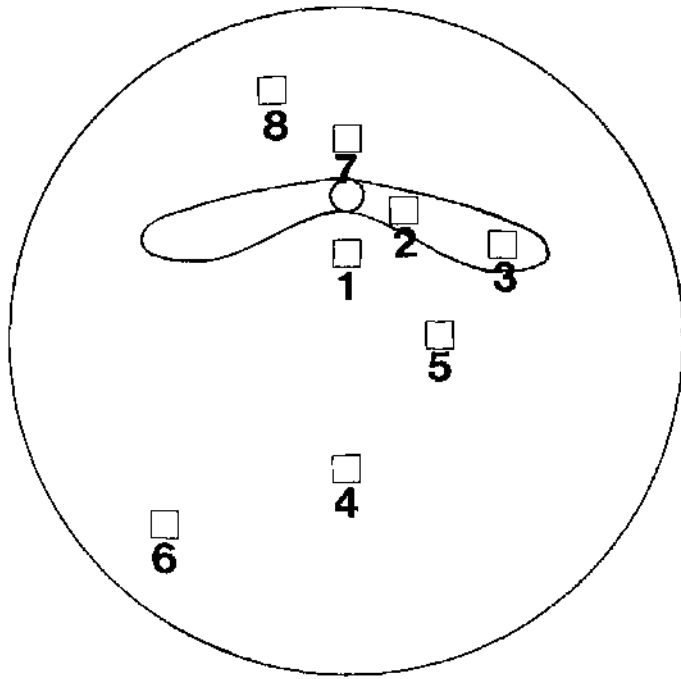


FIG.2-3 Diagram showing the areas from which the tissue blocks were taken.1- The visual streak,2 and 3- The horizontal nerve fibre zone,4,5,6,7, and 8- The peripheral retina.

Chapter 3 - Control Histological Observations

3-1 Introduction.

This chapter describes the organisation of the normal rabbit retina as observed by conventional light and electron microscopy. The structure of the retina of a wide range of mammalian species including the rabbit is well documented in the literature. As a result of the well-established nature of these observations, only the features necessary to allow a comparison to be made between control and experimental retinal tissue will be given.

3-2 Light Microscopy.

Histologically the rabbit retina could be divided into three regions, the visual streak, the periphery and the horizontal nerve fibre layer.

3-2.1 The visual streak (fig. 3-1).

This region was the thickest and most developed of the three regions. It corresponds in nature, although not in organisation, to the macular region of many primates including man. The visual streak was distinguished by the well developed visual cell outer segments, outer and inner nuclear layers, outer and inner plexiform layers and the single row of ganglion cell.

The following description of the various retinal layers can be generally applied to all the three regions. The characteristics which distinguish the layers of the visual streak are outlined.

The outer retina (figs. 3-4 and 3-5) includes the retinal pigment epithelium and the visual cells. The retinal pigment epithelium was a uniform layer of cells stretching from the optic nerve head to the ora serrata. The pigment granules lay towards the apical surface of the pigment epithelium. The cells had a prominent oval, basally situated nucleus and giant lipid granules which were characteristic of the rabbit

retina. The basement membrane of the cell formed part of Bruch's membrane which overlay the choroidal capillary network (choriocapillaris). Inner to the pigment epithelium were the visual cells. Two types of visual cell could be recognised - the rod and cone visual cells. The rabbit retina was dominated by rod cells. The rod visual cells had shorter inner segments and consequently longer outer segments than the cones. The rod nuclei were distinguished by their "coffee bean" chromatin pattern and were smaller and more oval than their cone counterparts. The cone nuclei were situated adjacent to the external limiting membrane and had a dispersed chromatin pattern (fig. 3-5). In the visual streak the number of cone cells was greater than in the other areas and the distinction between the inner and outer segments of rods and cones was less marked. The receptor pedicles formed the outer margin of the outer plexiform layer (figs. 3-5 and 3-6) and were of two types. The rod pedicles were spherical while those of the cone cells were conical and stained more intensely. The remainder of the outer plexiform layer was composed of the processes of the various cells in the inner nuclear layer. The inner nuclear layer (fig. 3-6) contained the nuclei of the Müller cells, the bipolar cells, the amacrine cells and the horizontal cells. The nuclei of these cells were often difficult to distinguish from one another. Generally, the Müller cell nuclei were found centrally in the layer, were angular in outline and stained more intensely than the other nuclei. The amacrine cell nuclei were found on the vitreal side of the layer and were characterised by an indented profile. The horizontal cells had pale-staining nuclei surrounded by a considerable amount of lightly staining cytoplasm. These nuclei were found on the scleral aspect of the inner nuclear layer and were larger than those of the bipolar cells. The nucleus of the bipolar cell stained in an intermediate fashion between that of the horizontal and Müller cell nuclei, and usually

possessed a prominent nucleolus. The bipolar cell nucleus was surrounded by a much smaller amount of cytoplasm than that of the horizontal cell.

Inner to the inner nuclear layer was the inner plexiform layer (fig. 3-6) which was composed of the processes of the amacrine, bipolar and ganglion cells. The ganglion cells lay inner to the inner plexiform layer (fig. 3-7) and in a section of the visual streak the cells formed a single and uninterrupted row. The nucleus and cytoplasm stained in a similar fashion. Both had a granular appearance. The nucleus was generally eccentrically placed on the vitreal side of the cell. A nucleolus was present in some cases. Inner to the layer of ganglion cells was the nerve fibre and the internal limiting membrane.

An important feature of the rabbit retina is its avascularity. The entire nutritive supply of the retina comes from the choroid. In the region of the visual streak the choroid was at its thickest and most developed.

3-2.2 The peripheral retina (fig. 3-2).

The architecture of this region which encompasses most of the retina was basically similar to that of the visual streak. All the layers of the retina were reduced in thickness when compared with the visual streak. The visual cells in the peripheral retina were almost entirely rods, the few cones present had long inner segments and shorter outer segments. The distinction between the rod and cone^s inner and outer segments was more pronounced in the peripheral retina than in the visual streak. In the inner nuclear layer the number of horizontal cells relative to the bipolar nuclei appeared to be greater. The ganglion cells formed an incomplete row and were more widely spaced than in the visual streak. The separation of the ganglion cells became greater with increasing distance from the visual streak. There were small scattered bundles of unmyelinated nerve fibres which formed the nerve fibre layer.

3-2.3 The horizontal nerve fibre layer. (fig. 3-3).

The horizontal nerve fibre zone was similar in organisation to the peripheral retina with the exception that bundles of myelinated nerve fibres extended^{ed} horizontally from the optic nerve head to the equator. Close to the optic nerve head, the bundles were large and the retina much reduced. Towards the equator the nerve fibre bundles diminished in size and the retina became thicker. The individual nerve fibres were up to 3 microns in diameter. Amongst these fibres were found frequent glial cells, which appeared to be of two main types. The more numerous type had an oval pale-staining nucleus and were thought to be astrocytes. The less common type had a more intensely staining nucleus and were thought to be oligodendrocytes. In association with the myelinated nerve fibre bundles were the retinal blood vessels. The vessels only occurred in this region and were generally extraretinal. Although they were occasionally found within the fibre bundles, they never penetrated the retina proper.

3-3 Electron microscopy.

The ultrastructure of the various cells of the retina was similar in all three retinal areas, although the overall organisation of the retina did vary with retinal location as was seen by light microscopy.

3-3.1 The retinal pigment epithelium (RPE).

Recent research on the ultrastructure and histochemistry on this layer of cells has revealed functions that were not suspected previously. Before the advent of electron microscopy and histochemistry, the functions of the RPE were thought to include, the support of the photoreceptors, to provide a pigmented absorptive source for the required by the photoreceptors and the transmission of nutrients from the choriocapillaris to the outer part of the retina. Additional functions of these cells are now known to include storage of vitamin A and its conversion to a form that can be utilised by the photoreceptors for the synthesis of rhodopsin, the

manufacture of some of the mucopolysaccharides that envelop the surface of the outer and inner segments of the visual cells and the phagocytosis and digestion of the rod outer segments discs and other substances from the retina. Many of the important functions of the RPE were reflected in the organisation of the cell and its organelles.

The cytoplasm of the RPE has an abundance of organelles necessary for the maintenance of its various functions (fig. 3-9). The cells had abundant mitochondria located in the basal cytoplasm adjacent to the infoldings of the basal cell wall (figs. 3-9 and 3-12). The association of the mitochondria and the infoldings of the cell wall is thought to be indicative of the cells involvement in fluid transport (Bernstein 1961).

The apical surface of the cell was also thrown into folds, these surface projections either embraced the tips of the outer segments or extended into the subretinal space (fig. 3-9). These projections surrounding the outer segments may play an important role in the attachment of the neural retina to the underlying RPE. The lateral cell wall by comparison had a relatively smooth outline. This cell wall was characterised by an apical junctional complex (fig. 3-12). This complex was usually composed of a gap junction, zonulae occludentes and adherents. The junctional complex is thought to have an important bearing on the functioning of the cell. There is strong circumstantial evidence that the gap junction mediates electrical coupling between cells (Revel, Yee and Hudspeth 1971). The electrical coupling of the pigment epithelium is of particular interest because it contributes to a normal response to light (the 'c' wave or P1 component). The zonulae occludentes seal off the intercellular spaces and form a barrier to diffusion (Peyman, Spitznas and Straatsma 1971). This restricts the transport of materials via an intercellular route from the choroid to the retina. The transfer of material from the choroid occurs across the pigment epithelium. This transcellular transfer is accomplished

by means of active transport through pinocytic vesicles (Bernstein and Hollenberg 1965). The pigment epithelium's high transepithelial resistance (the 'R' membrane) (Cohen 1965) and its role in the blood-retina barrier (Peyman, Spitznas and Straatsma 1971 and Peyman and Bok 1972) may also be due to the obliteration of the intercellular space by zonulae occludentes.

The cytoplasm contained very large amounts of smooth endoplasmic reticulum (SER) which occurred throughout the main body of the cell (figs. 3-9 and 3-12). Cisternae of rough endoplasmic reticulum (RER) occurred in the apical region of the cell as did the melanin granules (fig. 3-10). Free ribosomes occurred throughout the cytoplasm as did many small membrane-bound vacuoles, a proportion of which were coated vesicles (fig. 3-11). The Golgi apparatus was well developed and was frequently found close to the nucleus (fig. 3-12). The nuclei were basally situated and were oval with the long axis parallel to Bruch's membrane (fig. 3-10). A characteristic feature of the RPE of the rabbit was the large lipid granules which often distorted the apical surface of the cell. A prominent feature of the cytoplasm was the phagosomes. These phagosomes were involved in the removal and enzymic degradation of material originating in the visual cell outer segments. This disposal mechanism appears to be a major function of the normal RPE. The phagocytic process could be traced through several distinct ultrastructural stages (fig. 3-13). The phagosomes of the RPE in the control tissue as well as those in the experimental groups have been the subject of a quantitative analysis. The analysis was carried out on tissue from 24 control eyes. From each eye three tissue blocks were taken from both the visual streak and peripheral retina (5 mm. inferior to the visual streak). From each retinal position, the number of phagosomes was counted in 25 complete cell cross-sections. The sections were cut at 25 micron intervals to avoid the possibility of the same cell being counted at different levels. The phagosomes were counted in groups corresponding to

the five stages illustrated in Fig. 3-13.

The analysis showed that the number of phagosomes were more frequent with the increasing maturity of the phagosome (figs. 3-14, 3-15, 3-17 and 3-19). The initial stage accounted for up to 7% while the final stage, the residual body formed up to 38% of the total. The percentage distribution of the various stages remained similar in the two regions investigated (figs. 3-14, 3-16, 3-18 and 3-20). A noticeable difference between the two regions occurred in the actual number of phagosomes encountered in each 25 cell cross-sections. The number of phagosomes at each of the five stages was significantly lower ($P < 0.01$) in the periphery than the visual streak (fig. 3-14). There was a difference of up to 35% between the two regions. The disparity in the observed number of phagosomes between the two regions studied may have arisen from a difference in the rate at which the two groups of cells engulfed outer segment material. This rate may have been dependent on the number of visual cells impinging on each individual pigment epithelial cell. The number of outer segments in contact with each RPE cell in the regions was determined. A difference in either the number of visual cells or in the size of the RPE cells could not be demonstrated. It would appear that the greater phagocytic activity in the RPE of the visual streak region must be determined by some other factor. This may have been related to the turnover rate of the outer segment discs which would have been lower in the periphery or higher in the visual streak region to account for the observed situation. Although in the rhesus monkey, the turnover rate of the rod discs was similar in both the macular region and the periphery (Young 1967).

3-5.2 The visual cells and outer plexiform layer.

The visual cells were long slender cells which were divided into several distinct, but interconnecting morphological regions. This compartmentalisation signifies a special function of each region and for the

cell as a whole. The regions of the visual cells were the outer segments, the inner segments, the nuclei and the receptor pedicles.

The outer segments were composed of a series of discs superimposed on each other like a stack of plates (fig. 3-21) and surrounded by a cell membrane. The discs were stacked at right angles to the length of the outer segments. Each disc was a membrane envelope in whose wall the photopigment was incorporated. The rod outer segments were generally longer than those of the cones and consequently contained more discs. The distal ends of the outer segments were enveloped by the processes of the RPE and the proximal region by projections from the inner segments. The outer and inner segments were connected by a narrow neck of cytoplasm which contained a modified cilium (fig. 3-22). The cilium originated in the basal body which was located in the ellipsoid region of the inner segment. Some of the tubules of the cilium extended right to the end of the outer segments while others ended sooner. Bundles of root filaments originating from the basal body traversed the ellipsoid and terminated in the myoid region. The root fibres had a weak striation (fig. 3-22). The inner segments were divided into the ellipsoid and myoid regions (fig. 3-23). The ellipsoid region joined the outer segments and the myoid was continuous with the soma of the cells in the outer nuclear layer. The ellipsoid region contained many mitochondria whose long axis lay parallel to the length of the visual cells (fig. 3-23). The myoid region contained randomly orientated tubules of smooth endoplasmic reticulum, a few cisternae of rough endoplasmic reticulum free ribosomes and neurotubules (fig. 3-24). The Golgi apparatus was often well developed. The inner segments of the visual cells were separated from one another by the villous projections of the Müller cells (fig. 3-24). The projections extended past the external limiting membrane into the subretinal space. Mitochondria

inner to lay ~~these~~ these infoldings and suggested the cells' involvement in fluid transport (in much the same way as the similar arrangement in the IEL with the exception that the Müller cells do not overlie a capillary network). The mitochondria in this region of the Müller cells were usually poorly preserved (fig. 3-24). The inner segments were demarcated from the outer nuclear layer by the external limiting membrane (fig. 3-24). The external limiting membrane was composed of zonulae adherentes (Cohen 1965) formed by the Müller and visual cells. These junctions are thought to offer little resistance to the passage of substances from the inner to outer retina or vice versa (Peymon, Spitznas and Straatema, 1971). The outer nuclear layer contained the cell bodies of the rods and cones, (fig. 3-25). The rod and cone cell bodies were essentially similar. After passing through the external limiting membrane the rod and cone outer receptor fibres contained a few small mitochondria, tubules of smooth endoplasmic reticulum, free ribosomes and many neurotubules. The nuclei of the visual cells occupied much of the cell body (fig. 3-26). The nuclei of the cones were larger and had a more diffuse chromatin pattern than their rod counterparts (fig. 3-26) and lay adjacent to the external limiting membrane. The cell body was connected to the receptor pedicle by the internal receptor fibre. These fibres contained many neurotubules, the occasional mitochondrion, a few vesicles and some free ribosomes. The cone fibres were generally thicker than their rod counterparts. All the structures of the outer nuclear layer were surrounded by Müller cell cytoplasm.

The receptor pedicles were the terminations of the internal receptor fibres and lay at the scleral aspect of the outer plexiform layer (fig. 3-27). The rod receptor pedicle was oval and its internal surface was invaginated by several fibres originating from the cells of the inner nuclear layer (fig. 3-28). The invagination was associated with a single ribbon synapse

lying in the cytoplasm of the pedicle amongst randomly placed vesicles. Only one ribbon synapse was encountered in the rod pedicle. The lateral surfaces of the rod pedicles were frequently in close relationship to lateral extensions of the cone pedicles (fig. 3-28). The cone pedicles were larger and more electron-dense than the rods (fig. 3-28). The cone pedicles had several invaginations each associated with a single ribbon synapse. Cells of the inner nuclear layer also synapsed with the flat inner surface of the cone pedicle. The remainder of the outer plexiform layer was composed of the processes of the cells of the innernuclear layer (fig. 3-28). The origin of these processes is difficult to determine without serial reconstruction. Particularly large cell processes could frequently be followed over relatively long distances in the outer plexiform layer. These processes ran parallel to the plane of the layer and they were presumed to belong to the horizontal cells. These processes often had a lower electron density than many of the surrounding processes.

The different regions of the visual cells have separate functions. The outer segments contain the photopigment in a confined area, the ellipsoid region is involved in providing the cells' energy and the myoid region is concerned with the manufacture of proteins and other substances. The rod and cone fibres are similar to nerve axons and convey the signal generated in the outer segments to the receptor pedicles. The pedicle is a specialized synaptic region. The cell processes in the invagination of the pedicles are regarded as belonging to the horizontal and bipolar cells. This arrangement is thought to be responsible for the initial integration of the signal from the visual cells.

3-3.3 The inner nuclear and inner plexiform layer.

The inner nuclear layer contained the nuclei of the bipolar, horizontal, amacrine and Müller cells. The nuclei are difficult to differentiate without serial reconstruction, although a general classificati

could be made. The Müller cell nuclei were centrally placed within the layer and were angular in outline (fig. 3-29). The other nuclei had rounded outlines and lower electron density than the Müller cell nuclei (fig. 3-29). The cytoplasm of the Müller cell enveloped all the nuclei of the layer and often formed prominent radial fibres extending through the inner nuclear layer. In the region of the Müller cell nucleus the cytoplasm often contained cisternae of rough endoplasmic reticulum, scattered tubules of smooth endoplasmic reticulum, small clusters of glycogen-like particles and a Golgi apparatus (fig. 3-30). The cell bodies of the amacrine cells were located on the vitreal face of the inner nuclear layer. These cells were typified by large oval pale-staining nuclei which were generally indented and surrounded by a moderate amount of cytoplasm. The bipolar cell nuclei were characterised by their medium electron density and well-defined nucleolus. The bipolar cells lining the scleral margin of the inner nuclear layer had a greater amount of cytoplasm than the other bipolar cells (fig. 3-29). This cytoplasm contained many small mitochondria, scattered cisternae of rough endoplasmic reticulum, fibrils, neurotubules and Golgi apparatus. The remaining bipolar cells were found in the mid-region of the layer and had a narrow halo of perinuclear cytoplasm. The cell bodies of the horizontal cells lay on the scleral aspect of the inner nuclear layer (fig. 3-29). The volume of the horizontal cell cytoplasm was considerably larger than most of the other cells in the layer. The cytoplasm had a low electron density, containing few fibrils and mitochondria, scattered ribosomes and an occasional Golgi apparatus.

The inner plexiform layer lay vitread to the inner nuclear layer and was composed of the processes of the amacrine, the bipolar, the ganglion and Müller cells (fig. 3-31). Large radial pillars of Müller cell cytoplasm

traversed this layer. The cytoplasm was rich in glycogen, filaments and smooth endoplasmic reticulum. The nerve fibres of the inner nuclear layer formed a complex intertwined network (fig. 3-32). The classification of the various processes is difficult even with serial reconstruction. A small proportion of the processes could be identified by the way in which they synapsed with adjacent processes. Bipolar synapses were characterised by the presence of a synaptic ribbon similar to those of the receptor pedicles (fig. 3-32). The synaptic ending was often wedge-shaped containing the ribbon synapse orientated along the long axis, the ending often penetrated a short distance into the cleft between a pair of neighbouring nerve processes. The two post-synaptic processes could either be two amacrine processes or an amacrine and a ganglion cell process. This post-synaptic arrangement of more than one process allows the integration and modification of the visual signal in much the same way as in the outer plexiform layer. The amacrine processes often contained synaptic vesicles and a few small mitochondria. The ganglion cell processes were frequently larger and they possessed no vesicles and a few ribosomes may be present. Many other types of synapses occurred between these various processes and they reflected the complex nature of this layer. On this basis, a tentative analysis of some of the cell processes in the inner plexiform layer could be made.

3-3.4 The ganglion cell and nerve fibre layers.

The ganglion cell had a large pale uniformly staining nucleus and a nucleolus was frequently present. The nucleus was eccentrically located at the vitreal pole of the cell. The cytoplasm had a granular appearance and contained considerable amounts of rough endoplasmic reticulum and free ribosomes. Lysosomal-like bodies, neurotubules and smooth endoplasmic reticulum also occurred throughout the cytoplasm (fig. 3-33). The Golgi

apparatus was well-developed. The mitochondria were generally difficult to preserve and appeared as small rounded structures with few cristae and a matrix of low electron density. The ganglion cell processes that formed the nerve fibre layer contained many neurotubules and neurofibrils, some free ribosomes and mitochondria. The ganglion cells and axons were surrounded by the massive inner ends of the Müller cells. The cytoplasm of the Müller cell at this level was easy to identify, being more electron-dense than other components and containing numerous filaments, scattered glycogen-like particles and some unbound ribosomes (fig. 3-34). In this tissue glycogen was not particularly prominent which was in contrast to the situation described by Magalhães and Coimbra (1972). The inner margin of the Müller cells formed the boundary between the retina and vitreous, the basement membrane of the cell formed the internal limiting membrane (fig. 3-35).

In the peripheral retina and in the visual streak, the fibres in the nerve fibre layer were unmyelinated. These fibres became myelinated before they entered the optic nerve. These myelinated fibres formed the horizontal nerve fibre zone (fig. 3-36). This region was the only area of the retina to be associated with a vascular supply (fig. 3-37), although this was not a true retinal blood supply as the vessels remain outside the retina (Tripathi and Ashton 1971). The horizontal myelinated nerve fibre zone contained myelinated as well as some unmyelinated fibres (fig. 3-36). Considerable variation was seen in the size of both these types of fibres, the myelinated nerve fibres were 0.1 - 3.0 microns, and the unmyelinated fibres 0.02 - 1.0 microns in diameter. Many small glial cell processes were found amongst the nerve fibres in this layer. In this region two main types of glial cells were found, the astrocytes and oligodendrocytes. The astrocytes had large round nuclei which were centrally placed in a considerable amount of cytoplasm (fig. 3-36). The cytoplasm contained mitochondria, rough endoplasmic

reticulum, free ribosomes, glycogen granules and a Golgi apparatus. Fibrils were a characteristic feature of the astrocyte cytoplasm. These were arranged mainly parallel to each other. These filaments were found throughout the cytoplasm and they extended into the farthest reaches of the processes. The astrocyte processes frequently extended to the retina-vitreous barrier and in some areas provided the basement membrane forming the internal limiting membrane (fig. 3-37). In other instances the processes extended through the internal limiting membrane to envelop the retinal blood vessels.

The oligodendrocytes had smaller and more elliptical nuclei than those of the astrocytes. The nucleus was surrounded by a small amount of cytoplasm of relatively high electron density. The cytoplasm contained many neurotubules and a few mitochondria. The processes were generally smaller than those of the astrocytes and were characterized by their high electron density and the presence of neurotubules (fig. 3-36).

The astrocytes appear to have both a nutritive and a supportive role amongst the nerve fibres of the horizontal myelinated nerve fibre zone. This is a similar role to the Müller cells whose cytoplasm envelops all the structures of the neural retina apart from the inner and outer segments of the visual cells. The inner segments were, however, separated from one another by the villous projections of the Müller cells.

In the rabbit the retinal blood vessels were generally either found free in the vitreous or surrounded by astrocyte processes. Occasionally blood vessels were seen within the nerve fibre bundles. The endothelium of the blood vessels was unremarkable and resembled that of other unfenestrated blood vessels. Tight junctional complexes occurred between adjacent endothelial cells and are thought to be barriers to diffusion. This blood-retinal barrier infers a transendothelial transfer of material from the lumen of the vessel to the structures of the horizontal myelinated nerve fibre zone.

The organization of the control rabbit retina observed in this study was similar to previous descriptions of normal rabbit tissue (Davis 1929 and Sjostrand and Nilsson 1964).

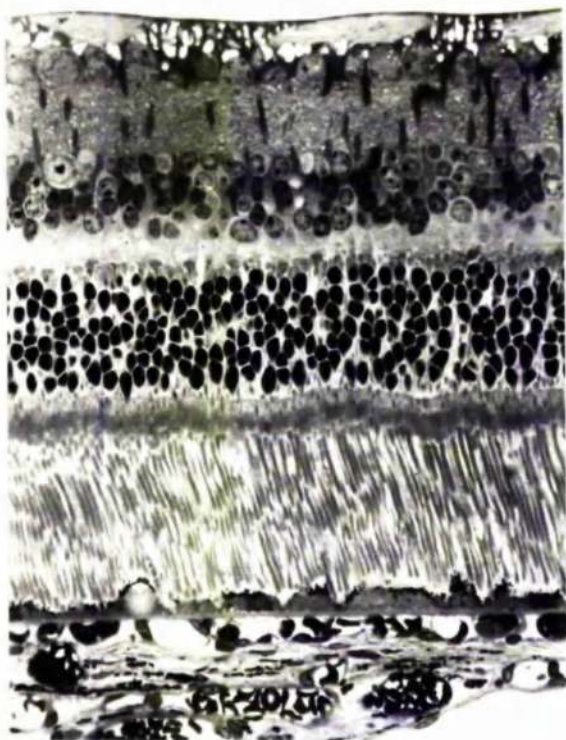


FIG.3-1 Light micrograph
of the visual streak region
showing the well developed
visual cells.(550 X)

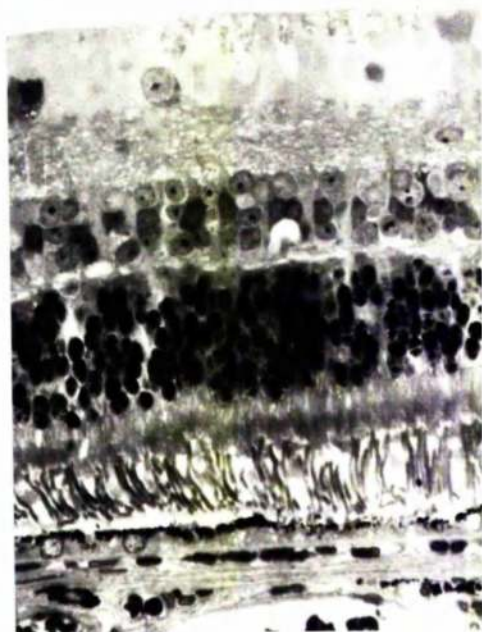


FIG.3-2 Light micrograph
of the peripheral retina.
(550 X)

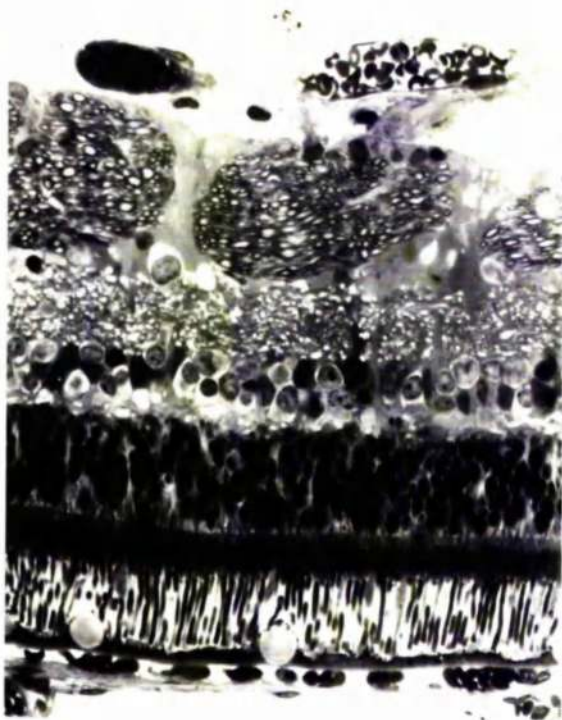


FIG.3-3 Light micrograph of the horizontal nerve fibre layer showing the myelinated nerve fibres and their associated blood vessels.(550 X)

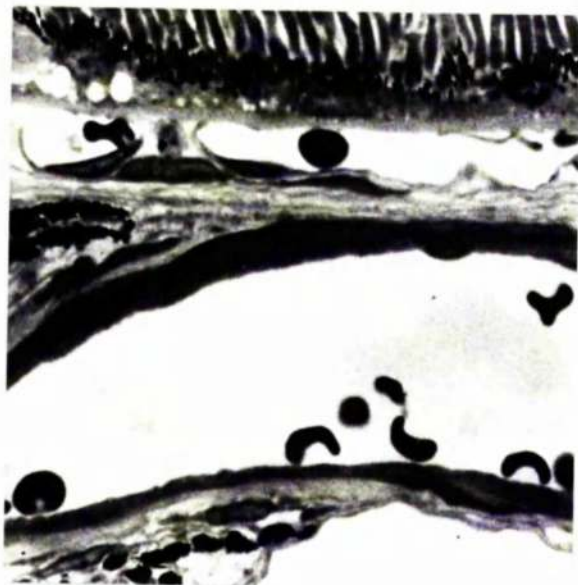


FIG.3-4 Light micrograph of the outer retina showing the visual cell outer segments and the retinal pigment epithelium and the under lying choroid (I,500 X).

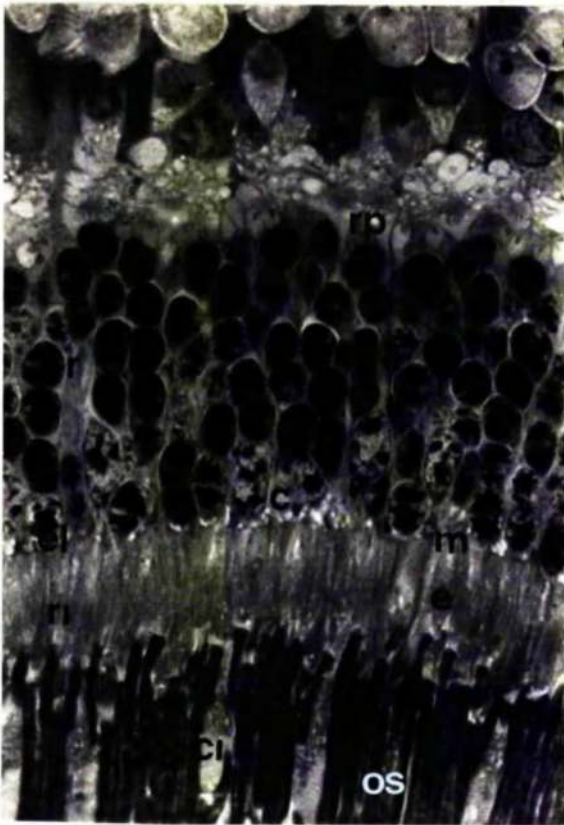


FIG.3-5 Light micrograph of the visual cells showing the outer segments(OS),the cone inner segments(CI),the rod inner segments(RI),the ellipsoid region(E),the myoid region(M),the cone nuclei(C), the rod nuclei(R) and the receptor pedicles(RP).The external limiting membrane (EL) lies between the inner segments and the visual cell nuclei.(I,500 X)

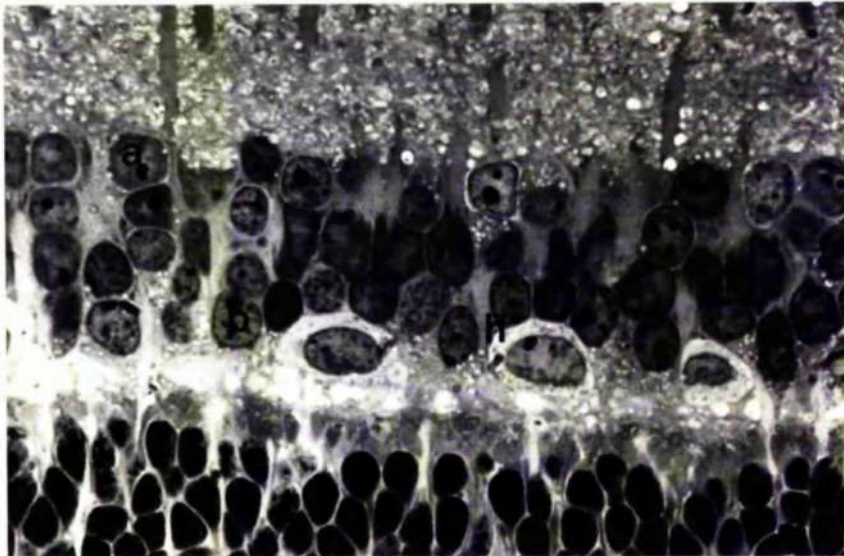


FIG3-6 Light micrograph of the inner nuclear layer,the outer plexiform layer and the inner plexiform layer.The inner nuclear layer contains the nuclei of the horizontal cells(H),the Muller cells(M),the bipolar cells(B) and the amacrine cells(A).(I,500 X)

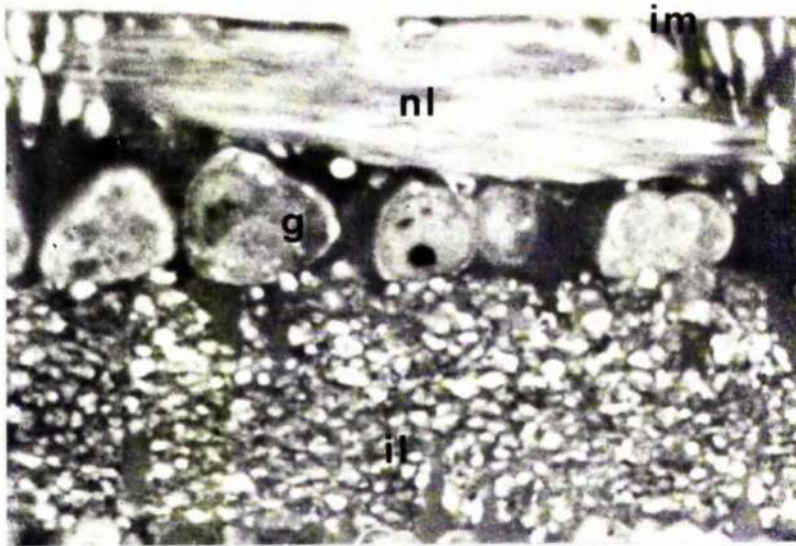


FIG.3-7 Light micrograph of the inner retina showing the inner plexiform layer(IL),the ganglion cells(G),the nerve fibre layer(NL) and the internal limiting membrane(IM) (I,500 X).

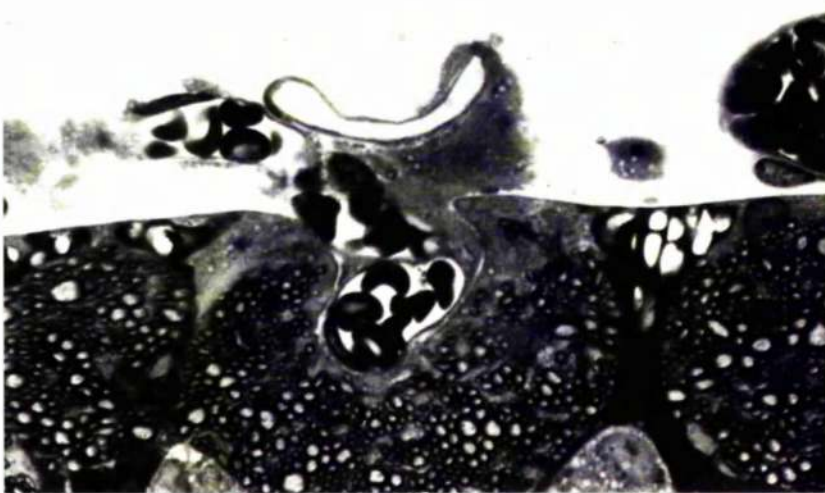


FIG.3-8 Light micrograph of the myelinated nerve fibre bundles and their associated blood vessels.(I,500 X)

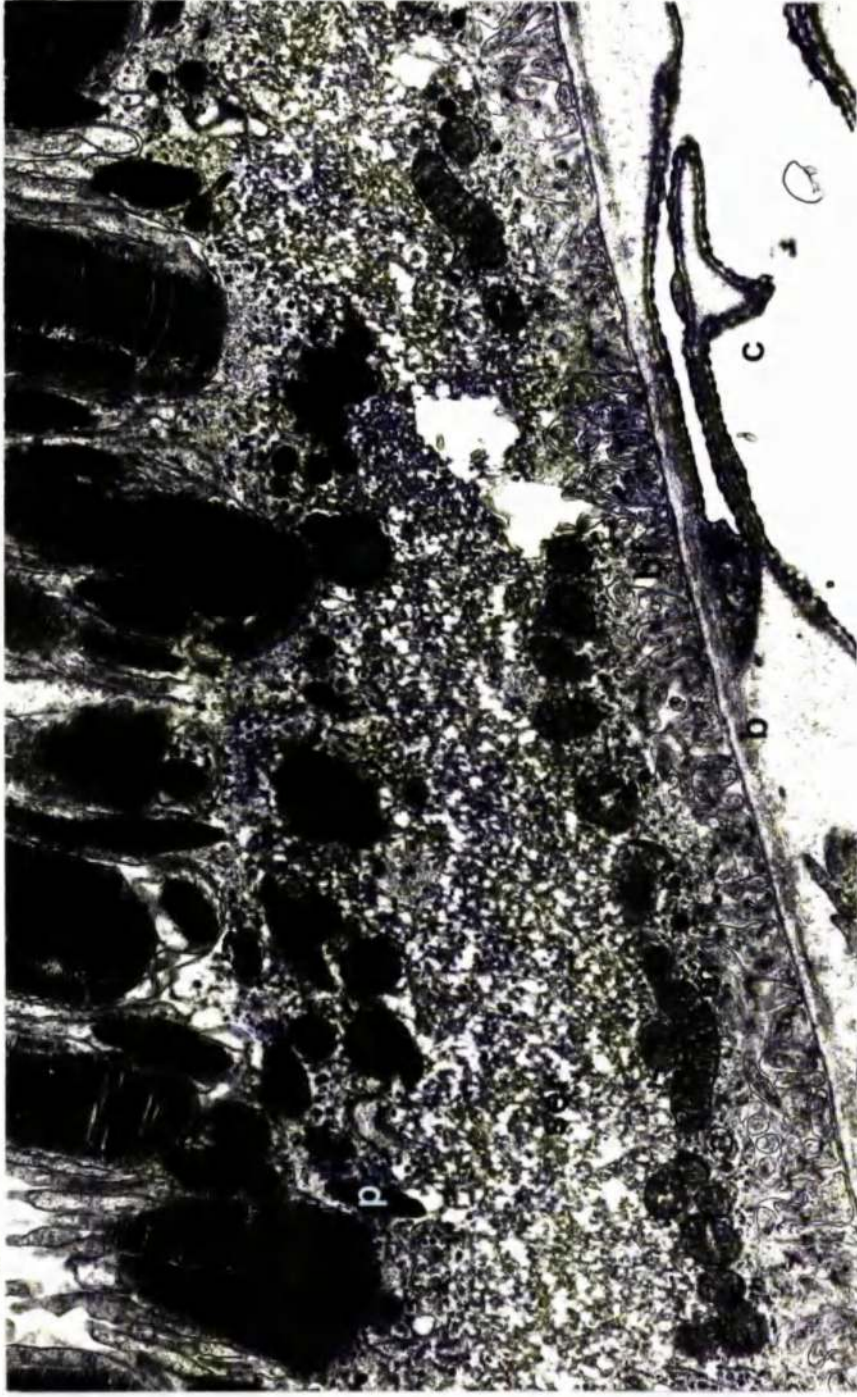


FIG. 3-9 Electron micrograph of the retinal pigment epithelium showing the basal infoldings (BF), the mitochondria (M), the smooth endoplasmic reticulum (SER) and the pigment granules (P). Bruch's membrane (B) lies between the basal infoldings and the fenestrated endothelial wall of the choriocapillaris (C). (12,000 X)

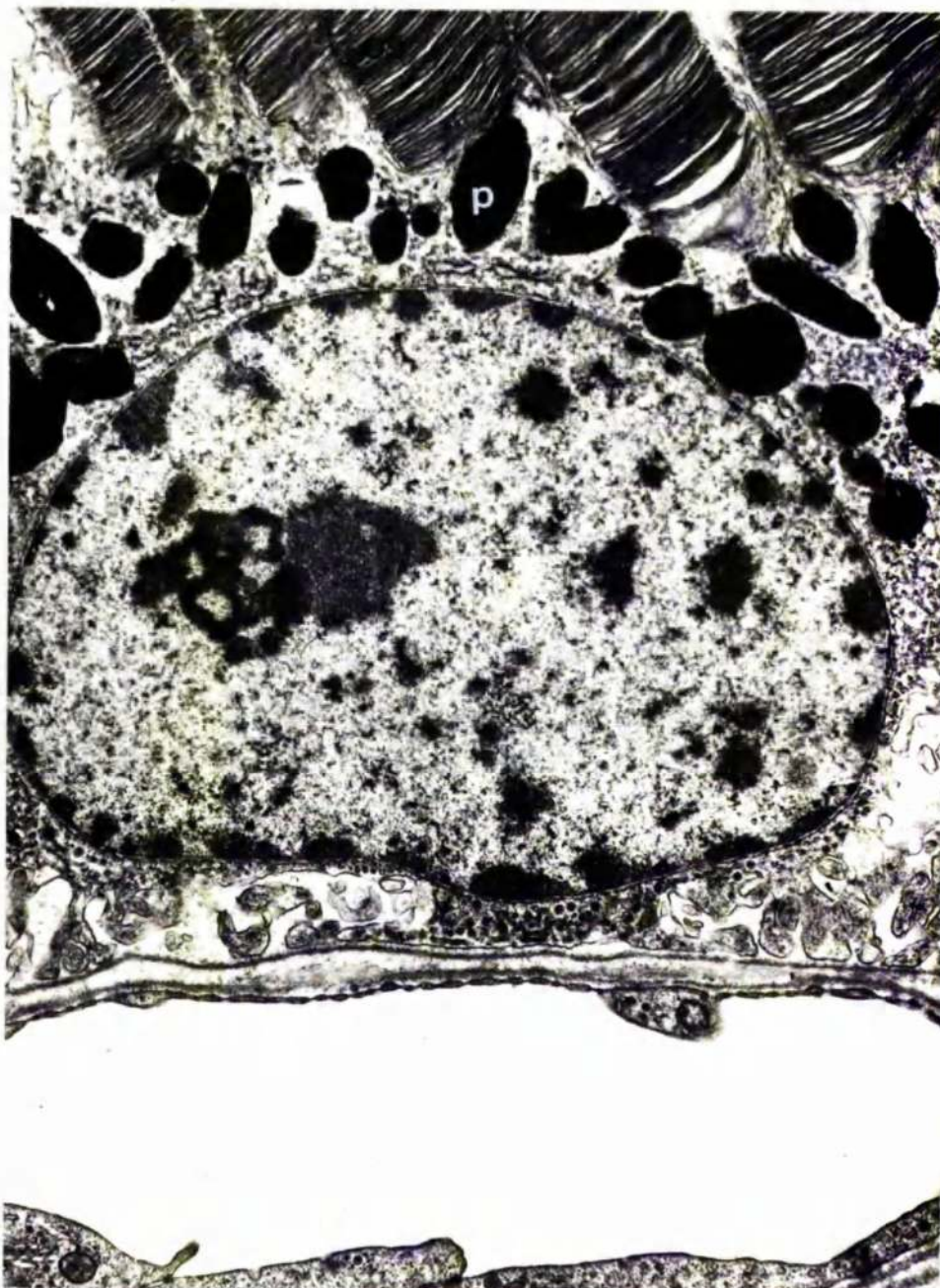


FIG.3-10 Electron micrograph of the pigment epithelium showing the nucleus. The apical region of the cell is associated with outer segments of the visual cells(OS). The rough endoplasmic reticulum(R) and the pigment granules(P) are found in the apical part of the cell. (12,000 X)

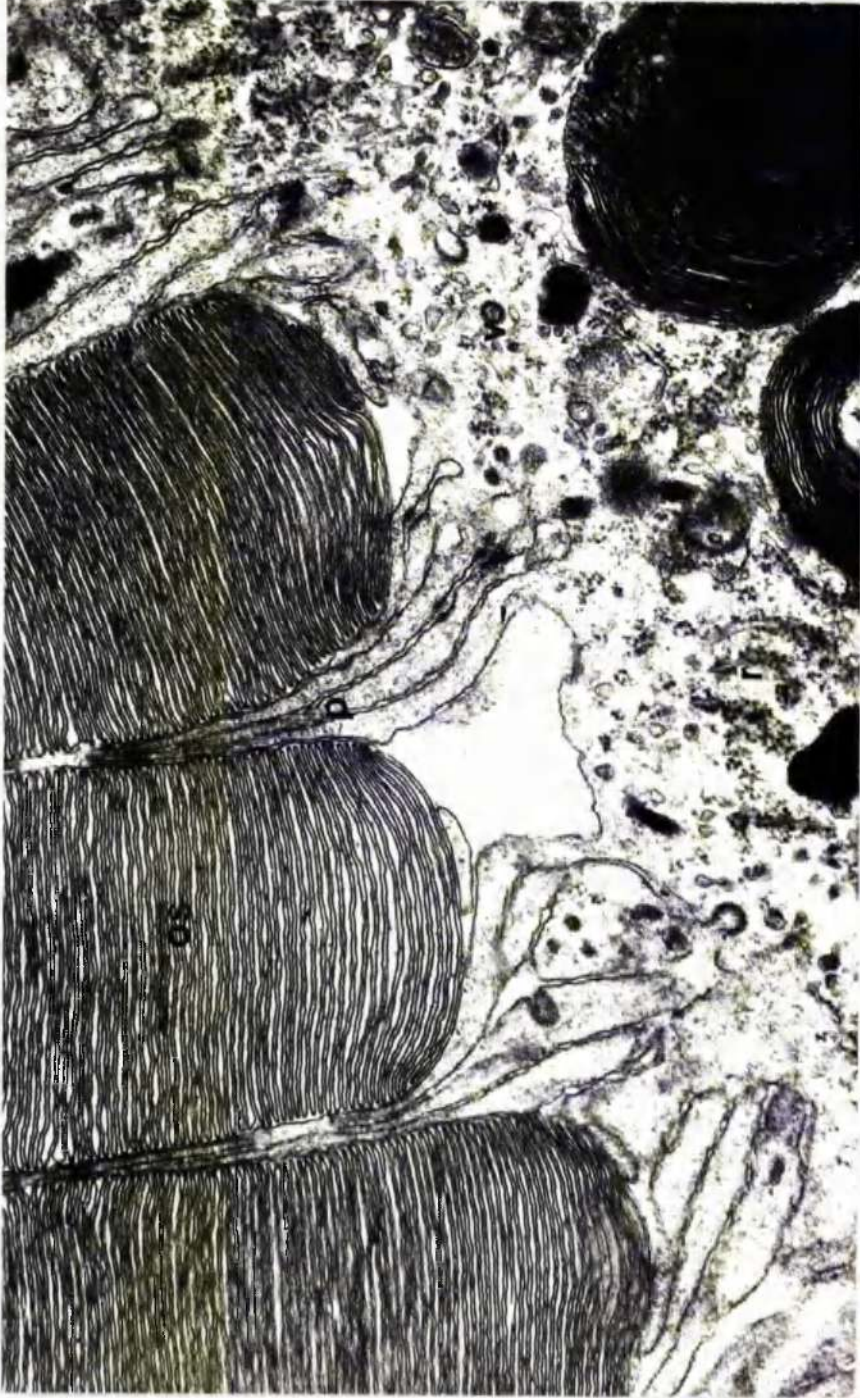


FIG. 3-II Electron micrograph of the apical surface of the retinal pigment epithelium. Finger like projections(P) extend between the outer segments(OS) of the visual cells. The cytoplasm of the pigment epithelium contains coated vesicles(V) and rough endoplasmic reticulum(R). (40,000 X)

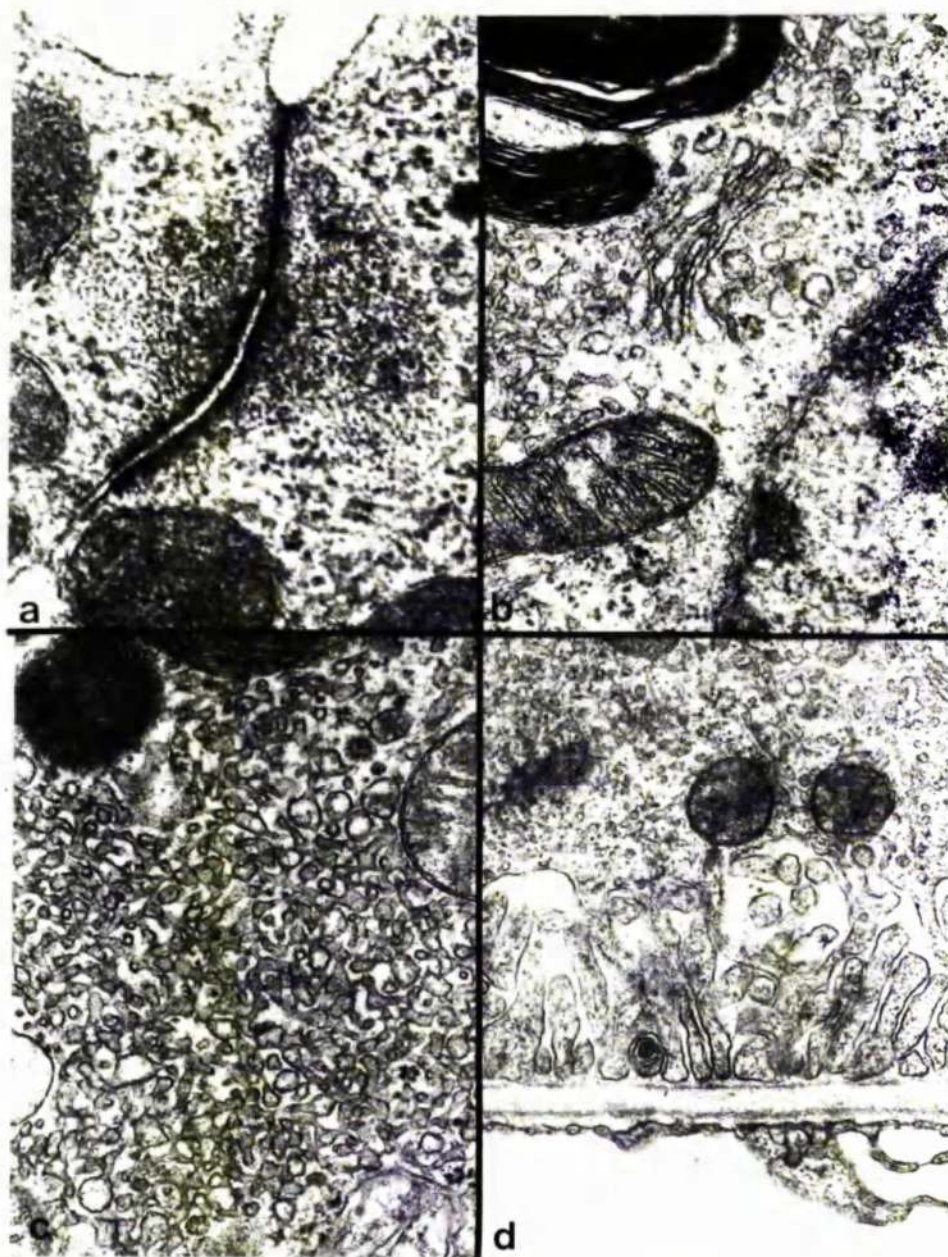


FIG.3-I2 Electron micrographs of various cellular components of the pigment epithelium;a) the apical junctional complex(35,000 X); b) the Golgi apparatus(25,000 X);c) the smooth endoplasmic reticulum (30,000 X) and d) the basal infoldings(25,000 X)

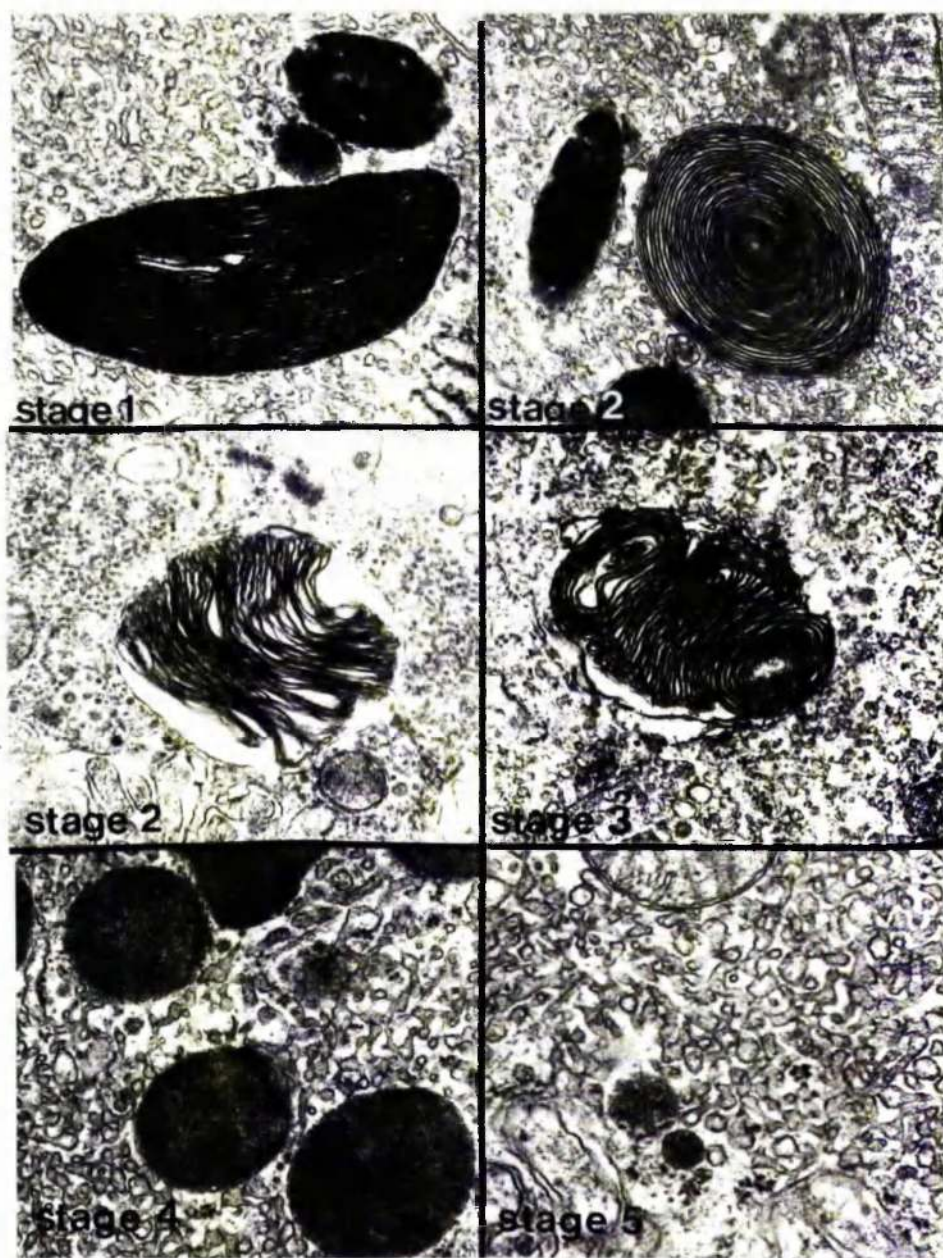


FIG.3-13 Electron micrographs showing the various phagosome stages involved in the degradation of outer sement material by the RPE. The initial stages(I-3) contain recognisable outer segment material, stage 5 represents the residual body(R). (stages I-3, X 30,000, stages 4 and 5, X 45,000)

a)

Stage	Mean V	S. D.	Mean P	S. D.	Wilcoxon rank
1	43 ± 11		33 ± 8		P < 0.01
2	88 ± 19		70 ± 18		P < 0.01
3	154 ± 25		130 ± 27		P < 0.01
4	206 ± 34		170 ± 23		P < 0.01
5	278 ± 36		228 ± 27		P < 0.01

b)

Stage	Mean V	S. D.	Mean P	S. D.
1	5.66 ± 0.87		5.14 ± 0.69	
2	11.43 ± 1.71		10.94 ± 1.82	
3	20.11 ± 1.71		20.58 ± 2.05	
4	26.84 ± 1.58		26.94 ± 1.08	
5	35.96 ± 2.22		36.36 ± 2.73	

FIG.3-14 Tables showing;a) the number of phagosomes at each stage of development in the visual streak(V) and periphery(P) and b) the % distribution of the phagosome stages in the visual streak(V) and periphery(P) of the control tissue.The number of phagosomes is significantly lower in the periphery however the distribution in visual streak and periphery is similar.The % distribution of the individual phagosome stages increases with increasing maturity of the phagosomes.

a)

Stage	V	P	V	P	V	P	V	P	V	P	V	P	V	P
1	31	30	38	26	49	27	55	37	43	32	62	46	94	26
2	67	58	70	40	74	51	80	58	89	59	104	90	43	37
3	115	112	146	97	186	128	208	156	144	134	102	157	128	102
4	138	155	185	137	253	166	267	172	205	176	239	194	157	133
5	243	209	284	192	276	214	306	262	263	213	299	260	236	206
Animal key	1	2	3	4	5	6	7	8						

FIG.3-I5 Table showing the number of phagosomes occurring at each stage of degradation in the visual streak(V) and peripheral retina(P).Animals I-8.

b)

Stage	V	P	V	P	V	P	V	P	V	P	V	P	V	P
1	8.2	5.3	5.2	5.2	4.8	4.6	6.0	5.4	5.8	5.2	7.7	8.1	5.7	5.2
2	11.3	10.3	10.4	9.2	8.8	8.7	8.7	8.5	12.0	9.6	12.9	13.1	7.2	7.3
3	19.3	19.9	20.0	19.4	22.2	21.8	22.7	22.8	19.4	21.8	12.7	20.8	21.4	20.2
4	23.4	27.5	25.4	27.5	30.2	28.3	28.1	25.1	27.6	28.7	29.7	25.7	28.3	28.4
5	40.8	37.1	39.0	38.6	32.9	36.5	33.4	36.2	35.3	34.7	37.1	34.4	39.5	40.9
Animal key	1	2	3	4	5	6	7	8						

FIG.3-I6 Table showing the percentage distribution of the phagosome stages occurring in the visual streak(V) and peripheral retinal(P).Animals I-8.

a)

	V	P	V	P	V	P	V	P	V	P	V	P	V	P	V	P
Stage																
1	38	31	32	28	61	53	49	45	34	26	42	27	44	31	50	37
2	91	72	86	61	118	97	98	88	91	73	96	87	101	91	92	86
3	182	159	179	128	163	103	152	181	133	118	157	129	168	140	143	124
4	256	219	231	173	257	210	239	193	176	150	192	166	209	164	183	167
5	320	298	291	190	316	251	288	238	243	208	289	234	268	245	236	197
Animal key	9		10		11		12		13		14		15		16	

FIG.3-17 Table showing the number of phagosomes occurring at each stage of degradation in the visual streak(V) and peripheral retina(P).Animals 9-16.

b)

	V	P	V	P	V	P	V	P	V	P	V	P	V	P	V	P
Stage																
1	4.4	4.0	3.9	4.8	6.7	6.8	6.0	6.1	5.0	4.5	5.4	4.2	5.4	4.5	7.1	6.1
2	10.2	9.2	10.5	10.6	12.9	12.1	11.7	11.8	13.4	12.7	12.4	13.5	16.0	13.2	13.0	14.1
3	20.4	20.4	21.9	21.8	17.8	24.0	18.5	24.4	19.5	20.8	20.2	20.1	20.5	20.3	20.3	20.3
4	29.0	28.1	28.2	29.9	28.1	28.1	29.1	26.0	26.0	26.2	24.7	25.8	25.5	28.8	25.8	27.3
5	36.0	38.3	35.5	32.9	34.5	31.2	34.8	31.8	35.9	36.0	37.2	36.4	32.7	35.5	33.7	32.3
Animal key	9		10		11		12		13		14		15		16	

FIG.3-18 Table showing the percentage distribution of the phagosome stages occurring in the visual streak(V) and the peripheral retina(P).Animals 9-16.

a)

	V	P	V	P	V	P	V	P	V	P	V	P	V	P
Stage														
1	35	29	29	24	49	35	28	22	41	33	35	26	61	59
2	96	89	92	85	107	84	70	57	96	87	76	48	104	68
3	153	132	170	125	162	143	126	106	151	91	136	78	182	141
4	203	188	225	185	216	164	182	138	193	162	173	148	223	165
5	268	231	271	206	266	232	227	224	303	259	277	222	296	216
Animal key	17		18		19		20		21		22		23	24

FIG.3-19 Table showing the number of phagosomes occurring at each stage of degeneration in the visual streak(V) and peripheral retina(P).Animals I7-24.

b)

	V	P	V	P	V	P	V	P	V	P	V	P	V	P
Stage														
1	4.5	4.3	3.7	3.8	7.1	5.3	4.3	4.0	5.2	5.5	5.0	5.0	7.0	6.2
2	12.6	13.3	11.7	13.6	12.9	12.8	11.5	10.4	12.2	9.5	10.9	8.8	12.0	10.8
3	19.7	19.7	21.6	20.0	21.9	21.7	20.6	19.4	19.3	15.1	19.5	15.0	21.0	22.3
4	26.1	28.2	28.6	29.6	26.0	24.9	26.5	25.2	24.6	26.9	24.8	26.5	25.8	28.1
5	37.1	34.5	34.4	33.0	32.2	35.9	37.2	41.0	38.6	43.0	39.7	42.7	34.2	34.5
Animal key	17		18		19		20		21		22		23	24

FIG.3-20 Table showing the percentage distribution of the phagosomes stages occurring in the visual streak(V) and peripheral retina(P).Animals I7-24.



FIG.3-2I Electron micrograph of the outer segments of the visual cells, they are composed of stacks of membrane bound discs.(12,000 X)

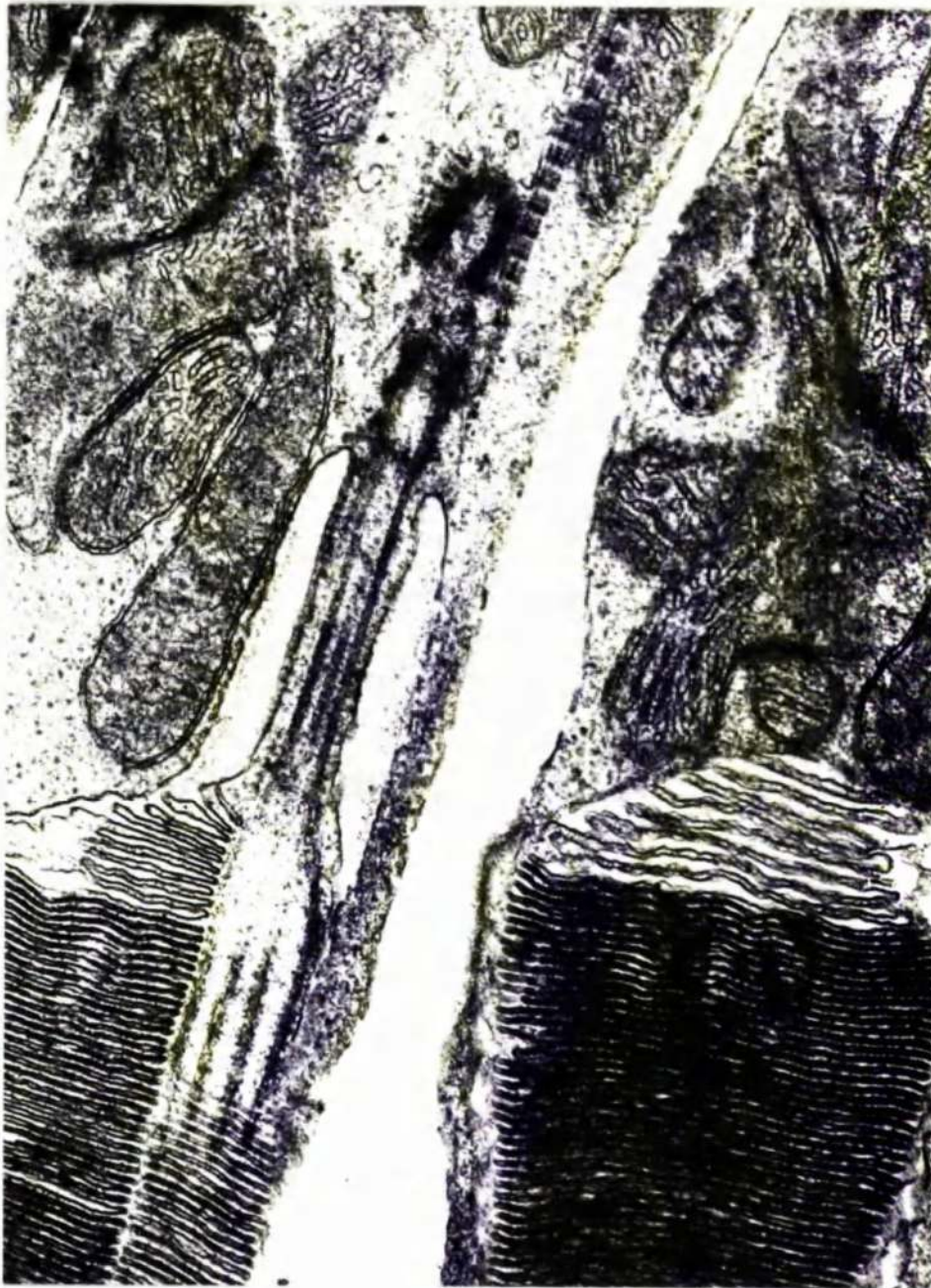


FIG. 5-22 Electron micrograph of the proximal region of the outer segment and the distal portion of the inner segments showing the connecting cilium and basal body. (40,000 X)



FIG. 3-23 Electron micrograph of the inner segments showing the ellipsoid region(E) and the myoid region(M).The ellipsoid region contains numerous mitochondria and the myoid region contains the Golgi apparatus and bound and free ribosomes.(12,000 X)

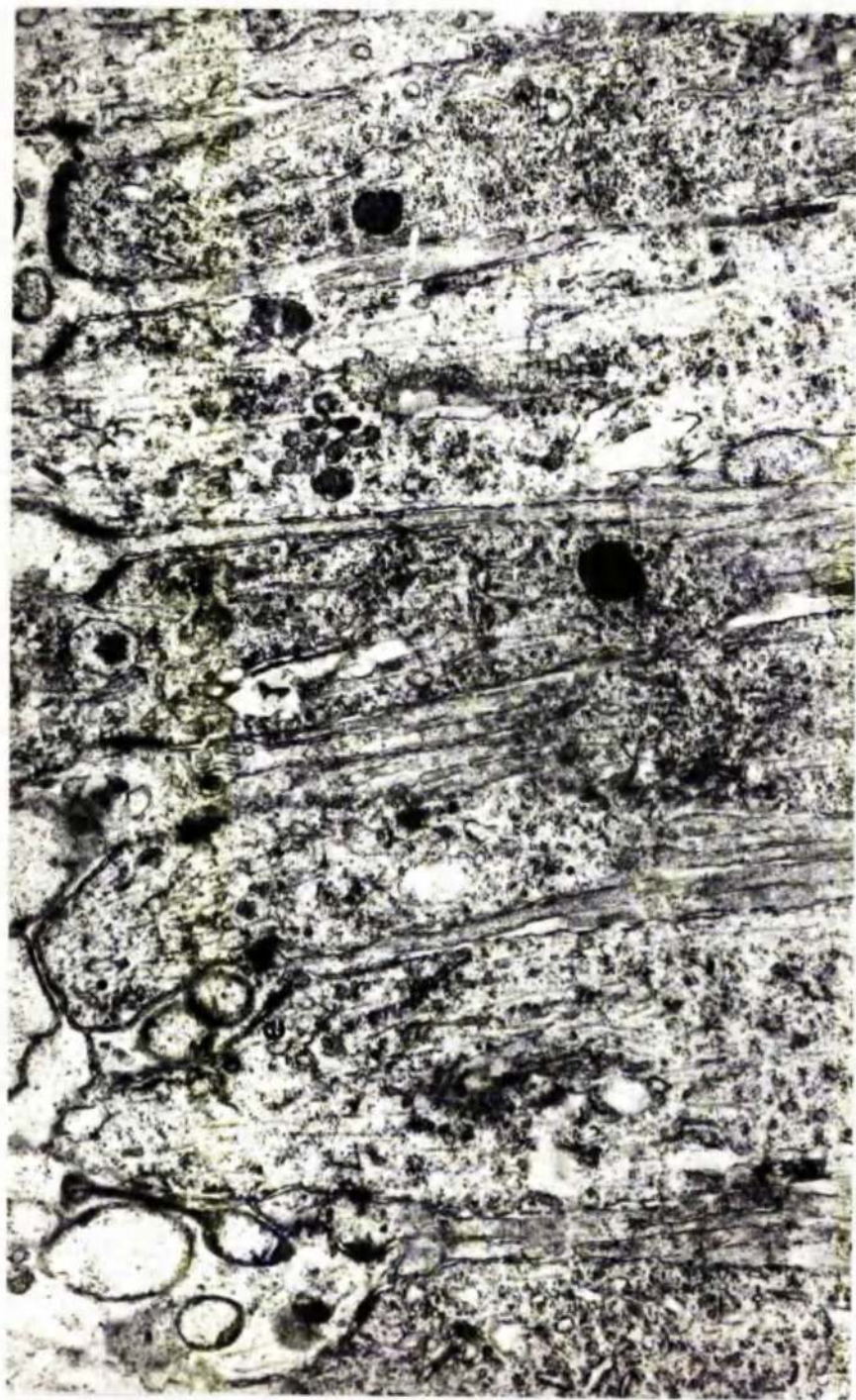


FIG. 1-24 Electron micrograph of the myoid region of the inner segments and the external limiting membrane (E). Processes of the Muller cells extend through the external limiting membrane and lie between the individual inner segments. (17,000 X)

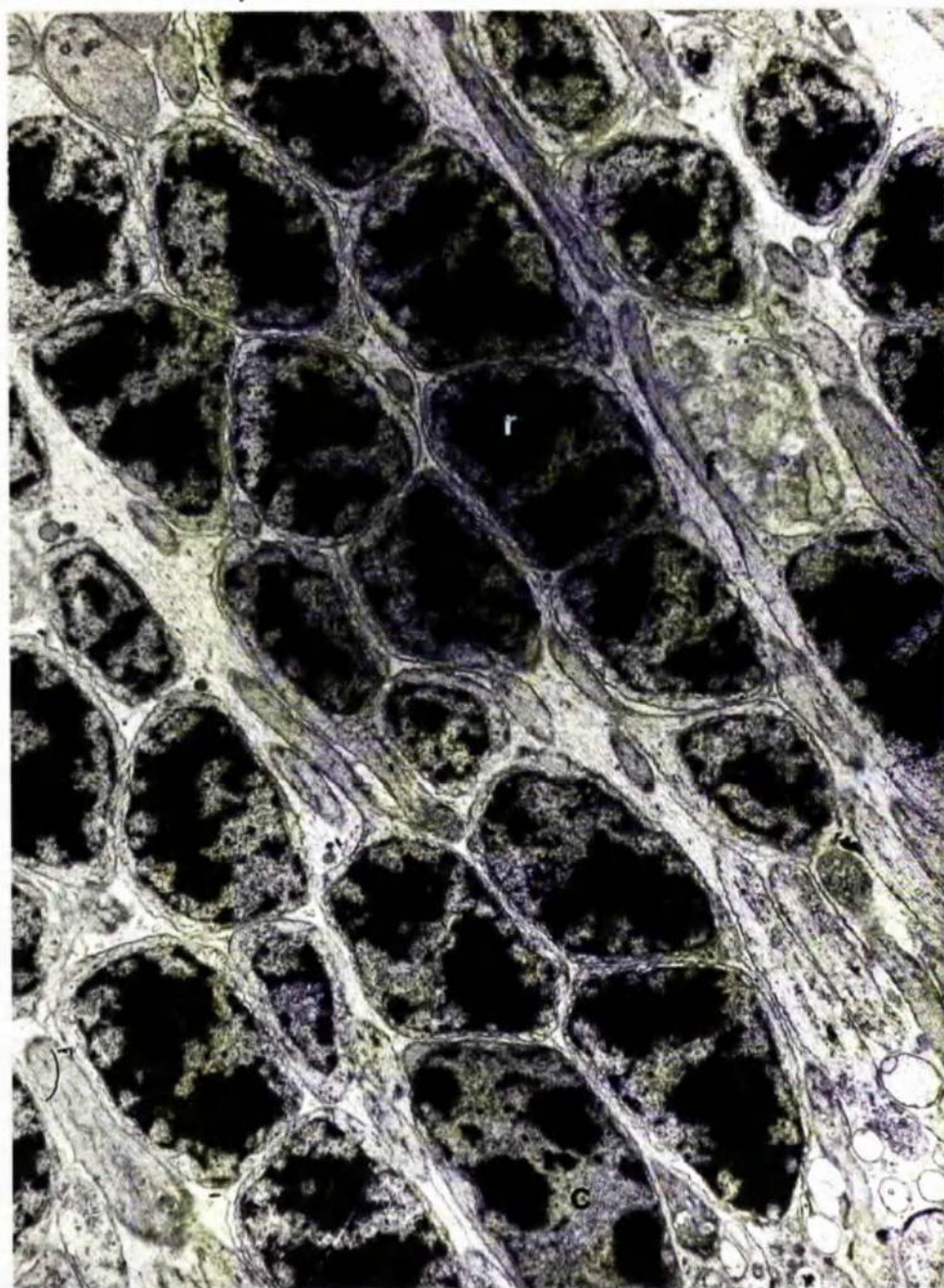


FIG. 3-25 Electron micrograph of the outer nuclear layer showing both rod(R) and cone nuclei(C) and the receptor fibres(F).(8,000 X)

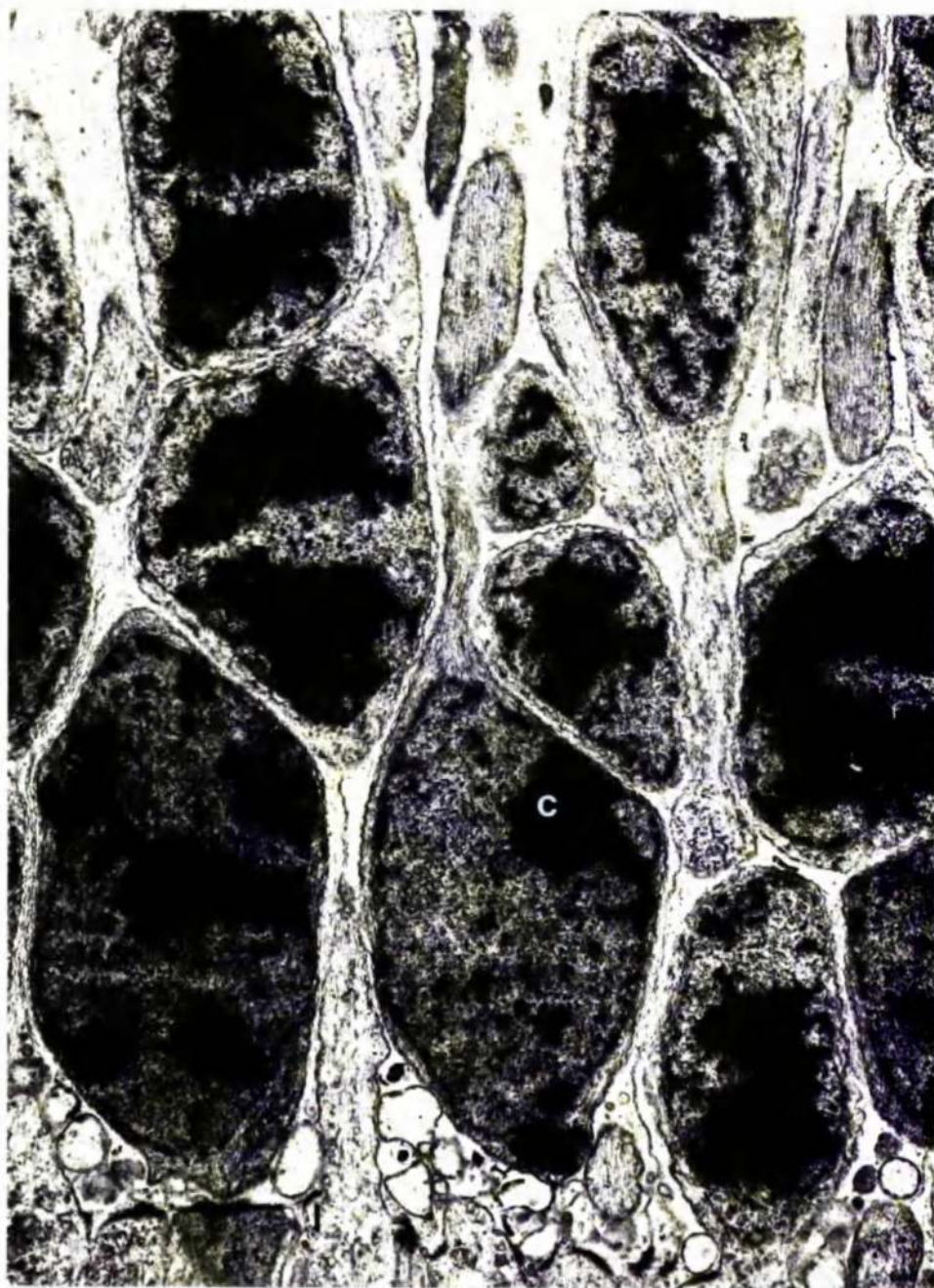


FIG.3-26 Electron micrograph of the outer nuclear layer showing the cone nuclei(C) adjacent to the internal limiting membrane(L), (17,000 X)

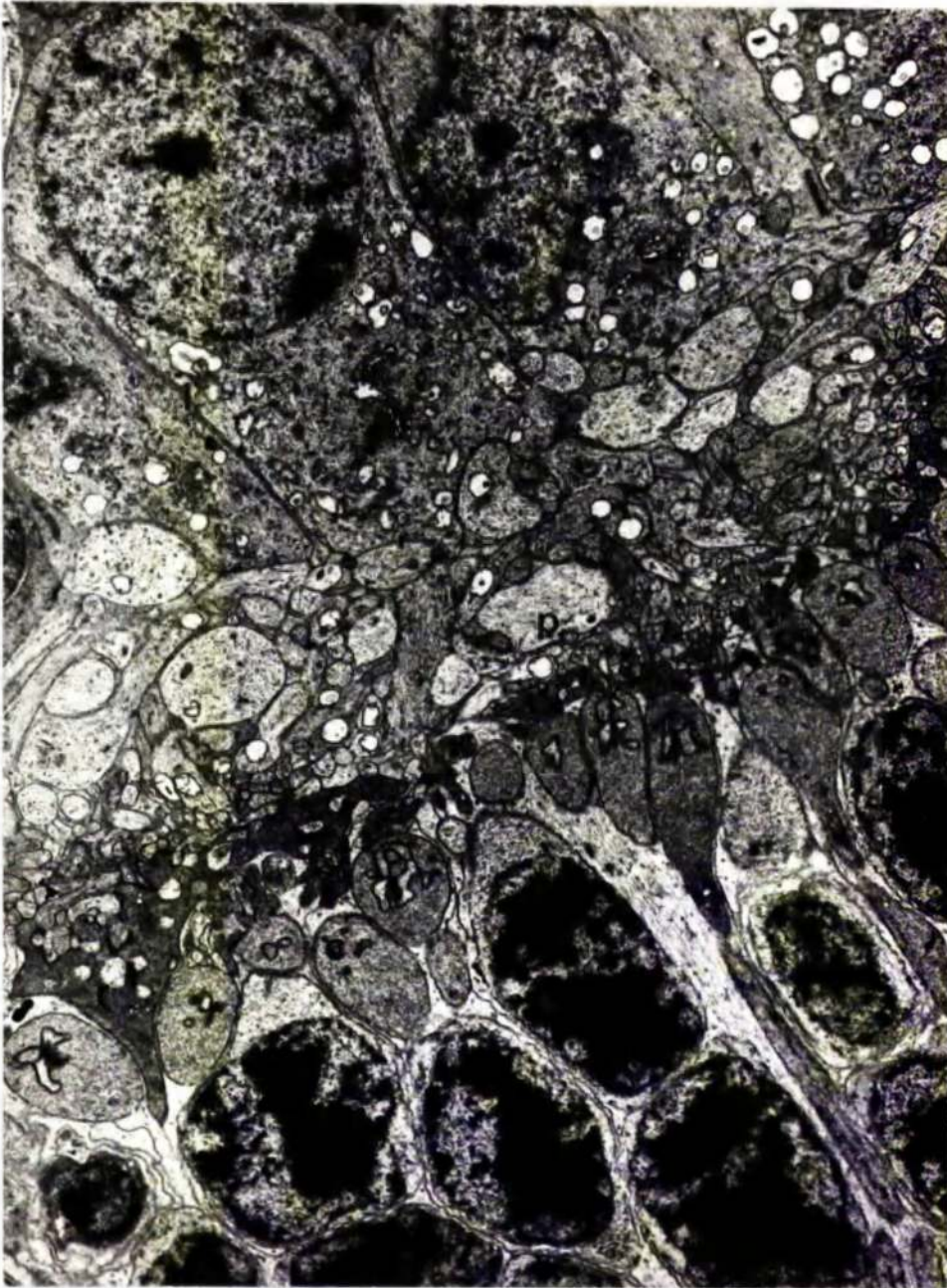


FIG.3-27 Electron micrograph of the outer plexiform layer showing the cone(C) and rod(R) pedicles and the processes(P) of the cells in the inner nuclear layer(L).(8,000 X)

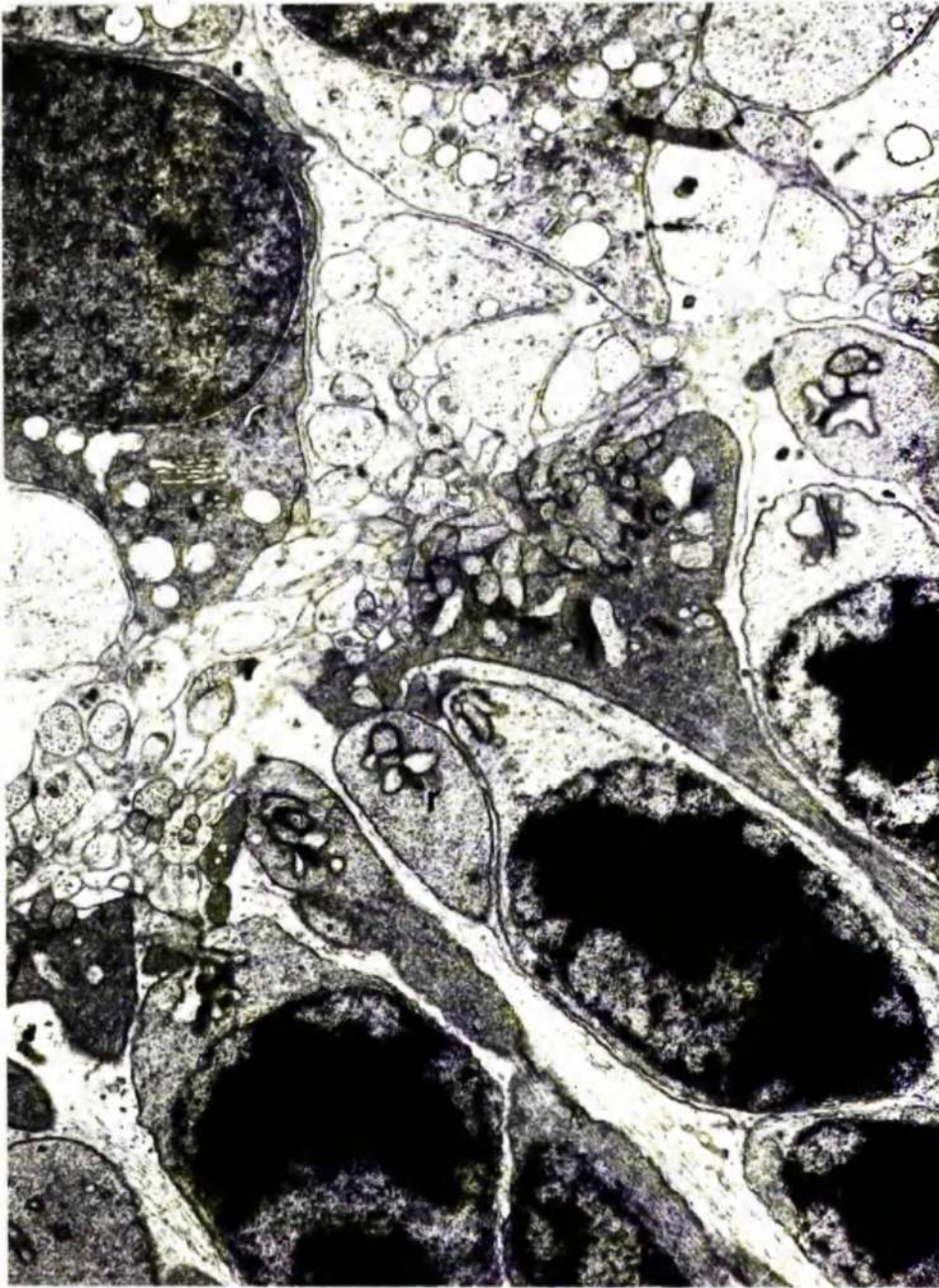


FIG.3-28 Electron micrograph of the rod(R) and cone(C) receptor pedicles.(14,000 X).

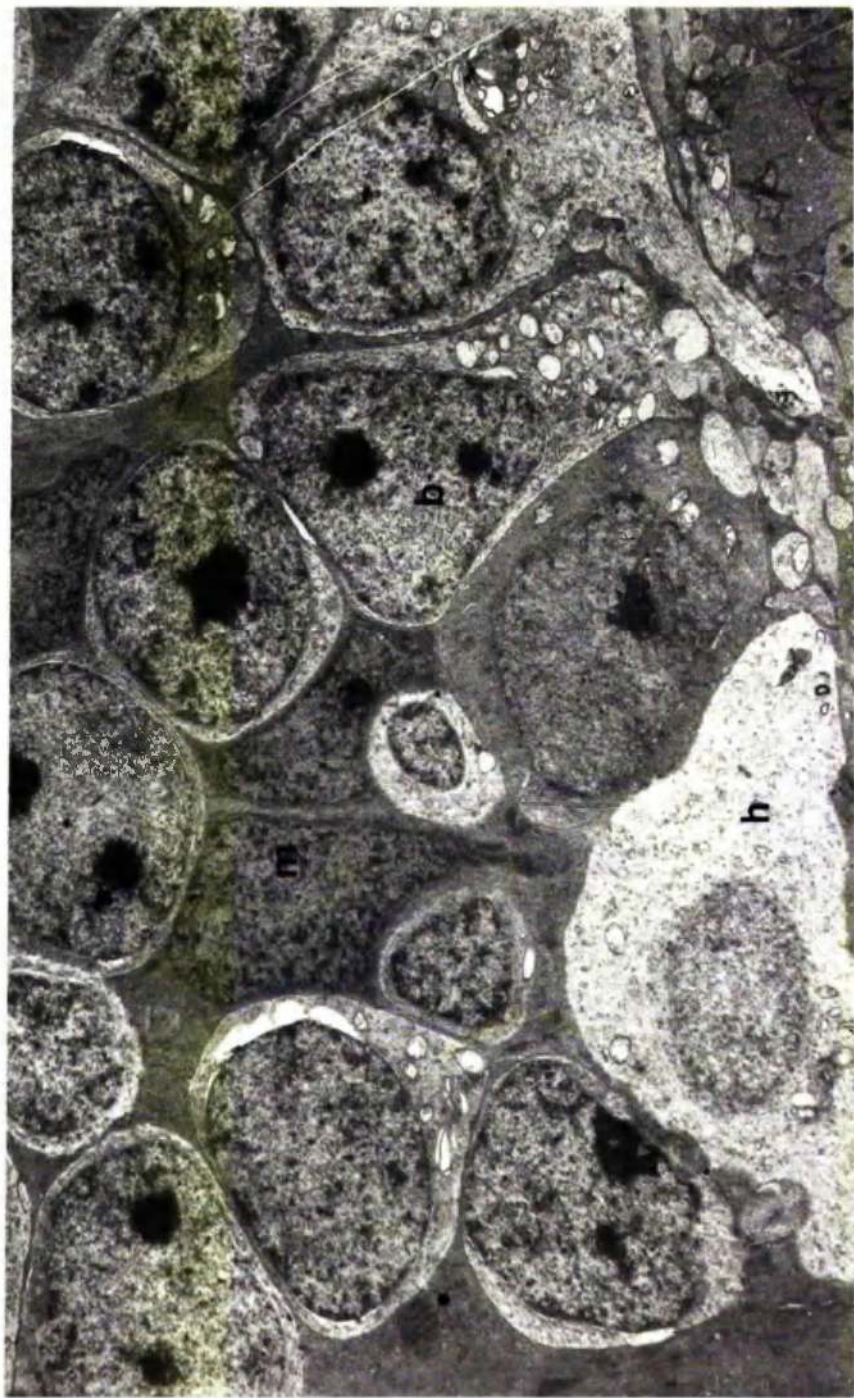


FIG.3-29 Electron micrograph of the inner nuclear layer showing the nuclei of the bipolar cells(P), the horizontal cells(H) and the Muller cells(M).(10,000 X)



FIG.3-30 Electron micrograph of the inner nuclear layer showing a nucleus of a Muller cell(M) and its surrounding cytoplasm.(25,000 X)



FIG.3-3I Electron micrograph of the inner retina showing the relationship between the inner nuclear layer(I),the inner plexiform layer(P),the ganglion cells(G) and the nerve fibre layer(N).(7,000 X)

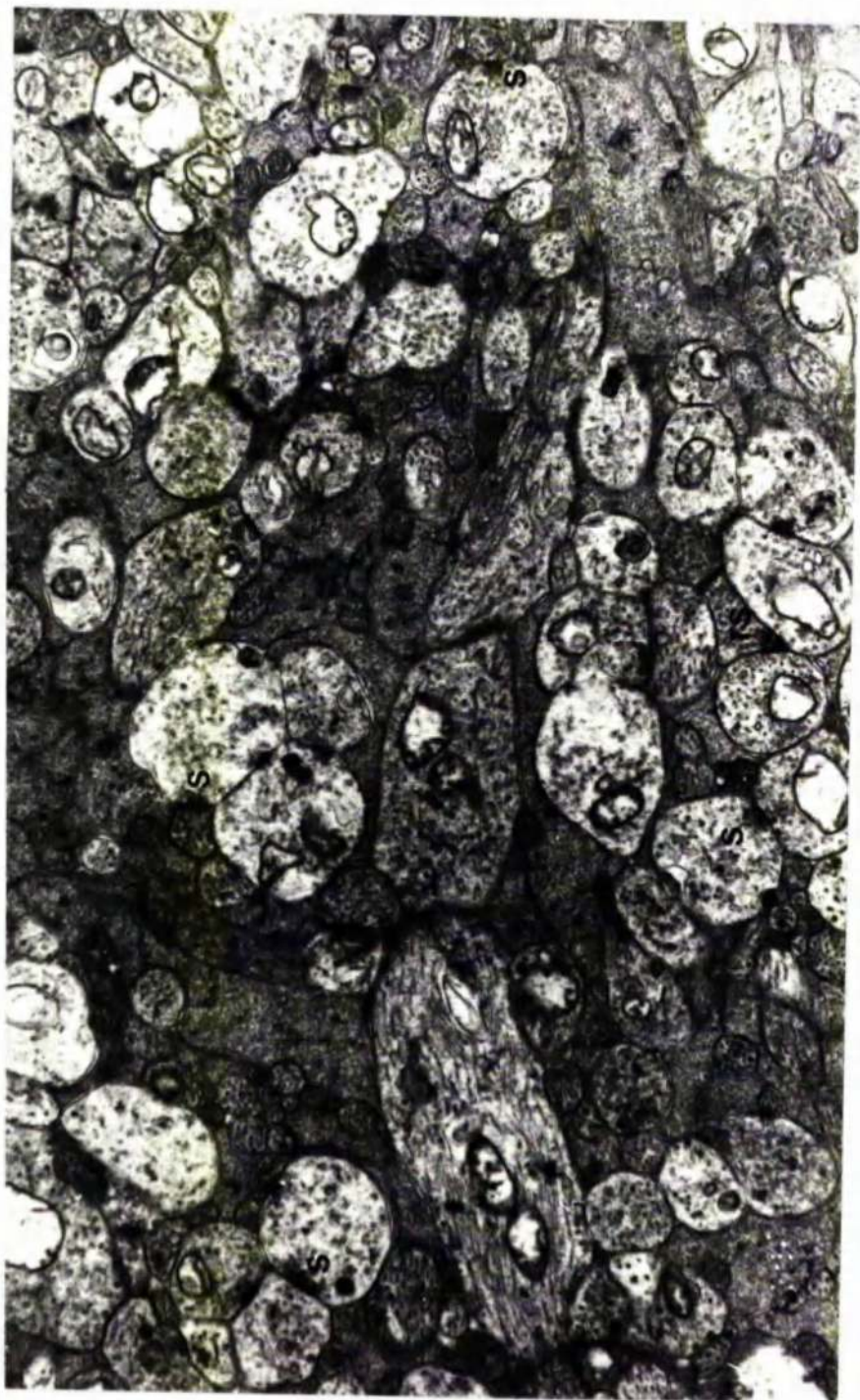


FIG. 3-32 Electron micrograph of the inner plexiform layer showing the numerous synapses (S) including those of the bipolar cells with their distinctive ribbon synapses(RS). (12,000 X)



FIG. 3-33 Electron micrograph of a ganglion cell showing the prominent nature of the rough endoplasmic reticulum(R) within the cytoplasm. (20,000 X)

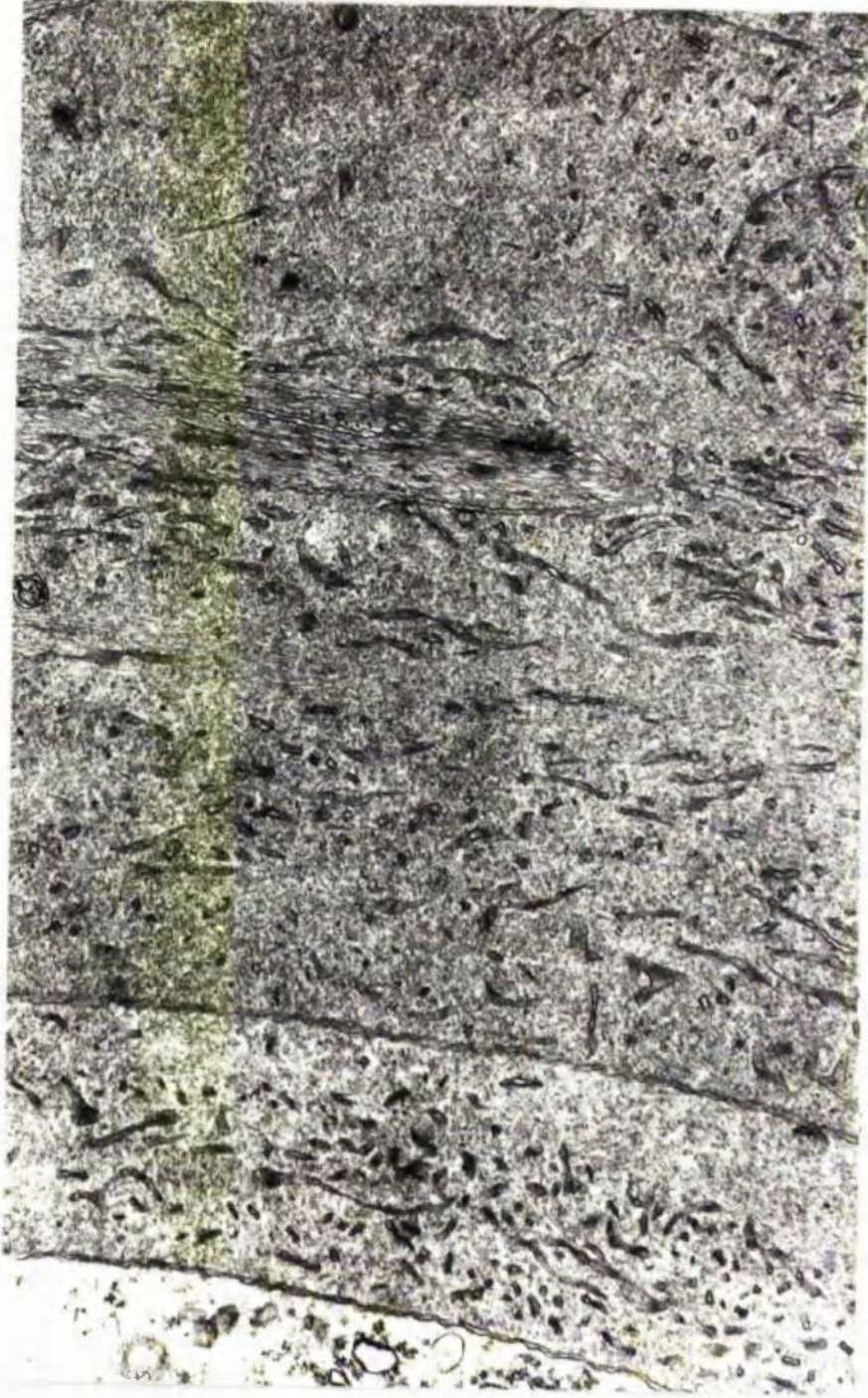


FIG. 3-34 Electron micrograph of the cytoplasm of the Muller cells at the level of the ganglion cells. The cytoplasm contains tubules of smooth endoplasmic reticulum and many fibrils. (17,000 X)

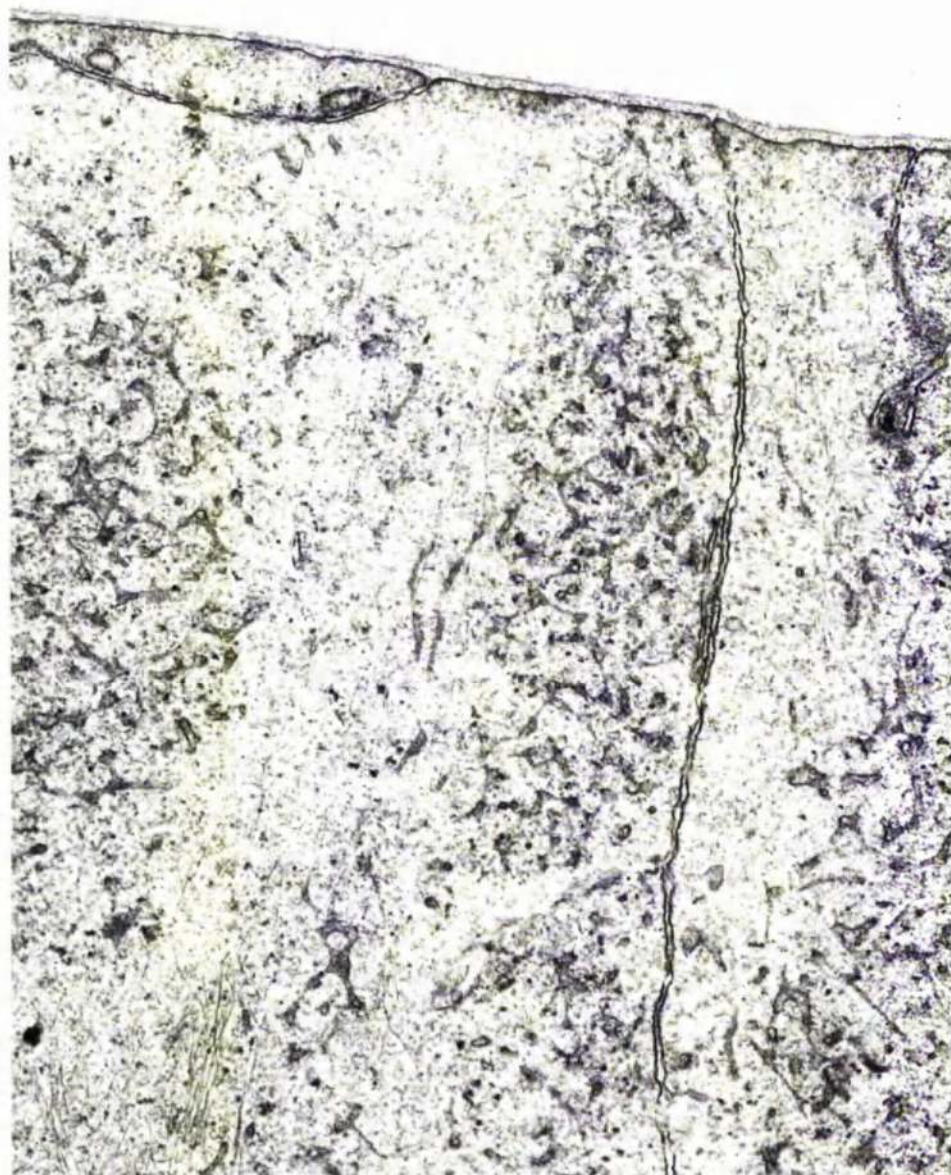


FIG.3-35 Electron micrograph of the Muller cell cytoplasm underlying the the internal limiting membrane.(30,000)



FIG.3-36 Electron micrograph of the myelinated and non-myelinated fibres of the horizontal nerve fibre zone.Glial cells(G) are a common feature of this region.(8,000 X)

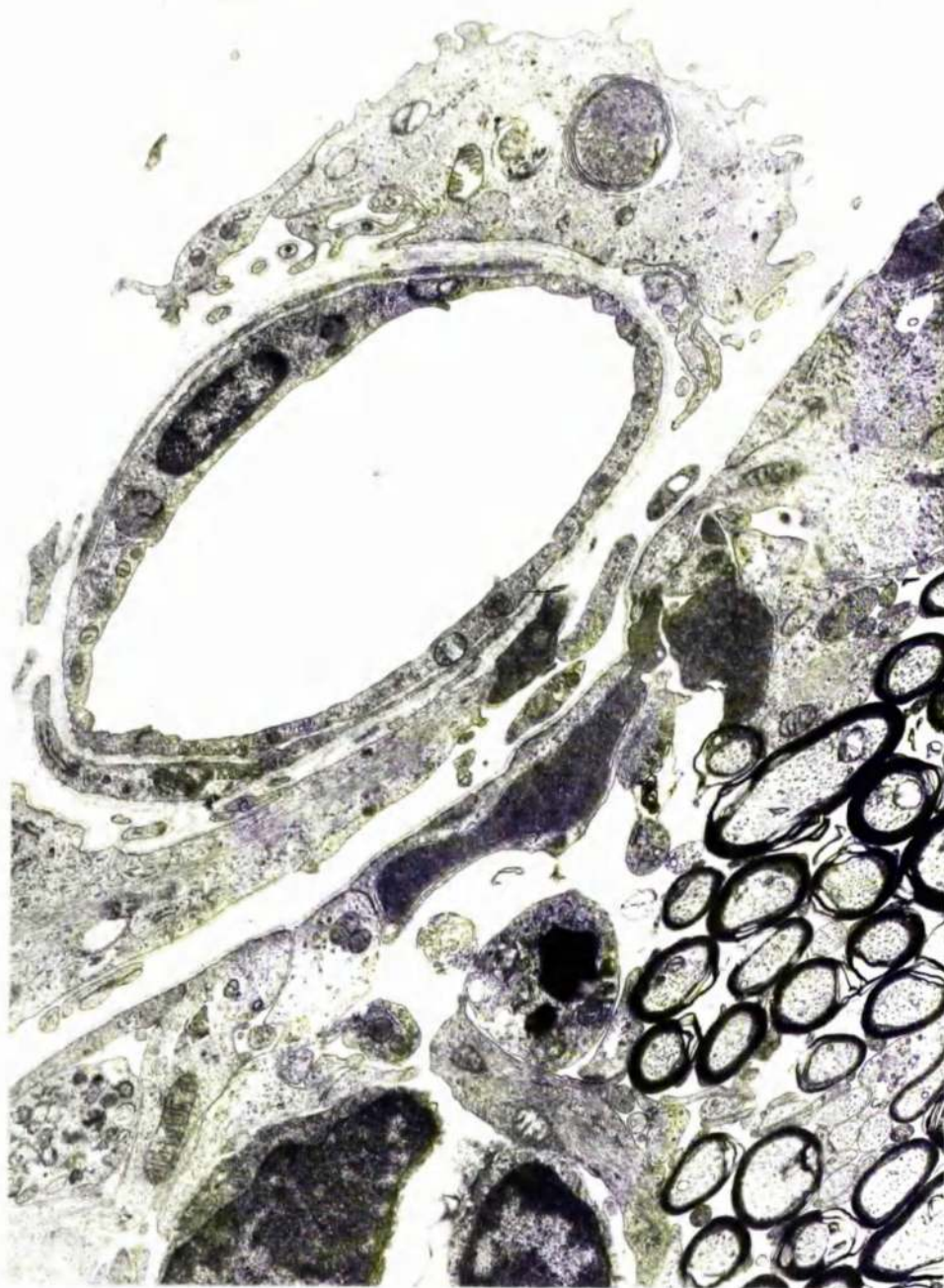


FIG.3-37 Electron micrograph of a retinal blood vessel lying above the retina of the horizontal nerve fibre zone.(6,000 X)

Chapter 4 - The effect of Total Acute Ischaemia
on the Structure of the Retina.

4-1 Introduction.

This chapter describes the structural changes accompanying varying periods of total acute ischaemia. Total acute ischaemia has been induced in two ways, by raising the intraocular pressure and by the severance of all the blood vessels supplying the eye (enucleation). Ischaemia induced in these ways produced similar overall changes in the rabbit retina. This relationship, however, only held true for the post-mortem tissue maintained at room temperature and it is this tissue that is described in conjunction with the pressure-induced ischaemic tissue. The effect of maintaining post-mortem tissue at 37°C. is described briefly at the end of the chapter. The similarities in the former tissues were sufficient to allow the ensuing description to cover the structural changes resulting from both methods used to induce the ischaemia. However, dissimilarities did occur, especially in the retinal pigment epithelium and for this reason the ultrastructural changes occurring in this cell layer are described separately for the two methods used to induce ischaemia. The significance of the similarities and dissimilarities observed in the retina following varying periods of ischaemia induced by the above two methods are discussed.

The retinal layers will be discussed from the retinal pigment epithelium inwards.

4-2 Light microscopy of the retinal pigment epithelium.

At the resolution afforded by conventional light microscopy the changes occurring in the retinal pigment epithelium appeared similar in both the ischaemic and post-mortem (room temperature) tissue. In the retinal pigment epithelium vacuolation became evident following periods of ischaemia longer than 15 minutes. The short periods of ischaemia (15-30 minutes) were associated with small vacuoles in the basal region of the cell. With longer periods of ischaemia the vacuoles were larger and were widespread

throughout the cell (fig. 4-2, 5 and 15), although they still tended to be located basally. The giant lipid granules that were a characteristic feature of the control tissue appeared to be resistant to even the longest period of ischaemia, the apical surface of the retinal pigment epithelium was often conversely distorted with a patchy distribution of the pigment granules (fig. 4-8). In spite of the considerable disturbance seen in the pigment epithelium, this single layer of cells remained intact and formed an uninterrupted covering of Bruch's membrane. The changes in the retinal pigment epithelium appeared similar in the three histological regions studied.

4-3 Light microscopy of the neural retina.

In the neural retina, short periods of ischaemia were in general accompanied by mild changes limited mainly to the visual cells (figs. 4-1, 4-11) moderate periods of ischaemia were followed by degenerate changes in the outer retina with some involvement of the inner retina (fig. 4-2), while immediately after the long periods of ischaemia marked degenerative changes were observed throughout the retina (figs. 4-3, 4-12).

4-3.1 The outer segments.

The changes in the retina following 15 minutes of complete ischaemia were limited to the outer segments of the visual cells (figs. 4-1, 4-11). These were often disorientated and fragmented. These features were more marked towards the terminal regions of the outer segments. With longer periods of ischaemia the fragmentation of the outer segments was more severe (fig. 4-5), with the fragments forming swollen saccules (figs. 4-6, 4-13). These changes occurred to a similar extent in the three regions of the retina. In many cases the intimate relationship between the terminal portions of the outer segments and the retinal pigment epithelium was lost. This was most noticeable after the long periods of ischaemia (60 - 120 minutes) where there was marked degeneration of the outer segments.

4-3.2 The inner segments.

In the visual cells' inner segments vacuolation accompanied periods of ischaemia longer than 15 minutes (figs. 4-2, 4-3 and 4-12). The vacuolation became more severe as the periods of ischaemia increased. The vacuolation was at first restricted to the ellipsoid region, although the myoid region was affected following the longer ischaemic episodes (figs. 4-6 and 4-13). Ninety and 120 minutes ischaemia was often associated with fragmentation of the inner segments (figs. 4-6, 4-13). An overall effect of ischaemia was to shorten the inner segments compared with their control counterparts.

4-3.3 Macrophages.

A prominent feature of the ischaemic retina was the accumulation of cellular debris in the subretinal space. The debris originated from the damaged inner and outer segments of the visual cells. Accompanying this accumulation of debris were macrophages containing darkly staining inclusion bodies (figs. 4-8, 4-14). The macrophages were 10-22 microns in diameter with an ovoid nucleus 5-12 microns in diameter (fig. 4-8). The nucleus often possessed a prominent chromatin mass. The cytoplasm of the macrophages was vacuolated and contained many small dark staining inclusion bodies. All the macrophages appeared mature and were adjacent to the apical surface of the retinal pigment epithelium. The number of macrophages increased with increasing periods of ischaemia. Following the longer periods of ischaemia the macrophages were frequently found in clumps (fig. 4-8) whereas with the shorter periods, the cells were frequently solitary (fig. 4-7). The nature of the increase in the number of macrophages has been determined by counting the number of these cells occurring in 100 μ m. of tissue obtained from the peripheral retina. Sections were cut at 25 μ m intervals to avoid the possibility of counting the same cell twice. The results are shown in fig. 4-21. In both the pressure-induced ischaemic tissue and the post-mortem tissue, macrophages were more numerous with increasing periods of ischaemia. Following

15 minutes ischaemia, the macrophages were rare, while after 120 minutes ischaemia they were commonly found. In both groups of tissue the increases were of the same order, although the cells were more frequent following periods of pressure-induced ischaemia than in the post-mortem tissue.

4-3.4 The outer nuclear layer.

Changes in the outer nuclear layer were not immediately obvious after the shortest period of ischaemia (figs. 4-1 and 4-11). The first degenerative signs were evident following 30 minutes ischaemia, with the rounding up of the nuclei followed by a loss of the normal chromatin pattern and a more intense staining reaction (figs. 4-10 and 4-15). The internuclear cytoplasm was often oedematous especially after long periods of ischaemia (90 and 120 minutes)(figs. 4-10 and 4-15). In some cases microcystic spaces occurred, these spaces were associated with severely pyknotic regions of the outer nuclear layer (fig. 4-3). A feature of all the tissue examined was the better preservation of the cone nuclei compared with those of the rod cells (fig. 4-6). The changes in the outer nuclear layer occurred uniformly throughout the retina.

4-3.5 The outer plexiform and inner nuclear layers.

In the outer plexiform layer oedematous changes were noticeable in the retina exposed to periods of ischaemia longer than 30 minutes (figs. 4-10 and 4-15). This was a generalised swelling which was more prominent following the long periods of ischaemia and could not be localised to any definite part of the layer. Some processes and synaptic pedicles were swollen while others appeared little affected.

Changes in the bipolar, horizontal and amacrine nuclei of the inner nuclear layer were evident after 60 minutes ischaemia (fig. 4-2). These nuclei were often rounded and less intensely stained than their control counterparts, and were frequently surrounded by a translucent area. These changes were more pronounced after 90-120 minutes ischaemia (figs. 4-9 and 4-15). In extreme cases, occasional nuclei possessed several small condensed

chromatin masses (fig. 4-10). These nuclei were almost entirely confined to the tissue subjected to 120 minutes ischaemia. In general the mitotic changes in the inner nuclear layer were less marked than those seen in the outer nuclear layer. The nuclei of the Müller cells appeared to be unaffected by even the longest period of ischaemia (120 minutes) (figs. 4-10 and 4-15). The changes in the neural cells of the inner nuclear layer were similar throughout the various regions of the retina.

4-3.6 The inner plexiform and ganglion cell layers.

The inner plexiform layer behaved in a similar fashion to the outer plexiform layer, showing a generalised swelling that became more pronounced with the longer periods of ischaemia (figs. 4-10 and 4-15).

The ganglion cells were affected in a similar way to the neural elements of the inner nuclear layer with oedematous changes in the cytoplasm and a less intensely staining nucleus (figs. 4-9 and 4-15). The intracellular oedema often created an electron-translucent region in the periphery of the cell. The cytoplasmic contents were often condensed and formed a mass adjacent to the nucleus.

The nerve fibre zone was also oedematous following periods of ischaemia longer than 60 minutes, although changes were not obvious in the bundles of myelinated nerves or their associated blood vessels (fig. 4-16).

In addition to these cellular changes, the overall organisation of the retina was often disturbed. With ischaemic periods longer than 60 minutes, folds in the retina were often observed. The folding generally involved the whole neural retina (figs. 4-4 and 4-17) although on occasion only the outer layers of the retina were involved (fig. 4-18).

4-4 Electron microscopy - Introduction.

The ultrastructural changes in the retinal pigment epithelium following pressure-induced ischaemia and post-mortem conditions are described separately. The description of the remainder of the retina applies to both the methods used to induce ischaemia.

4-5 Electron microscopy of the effect of pressure-induced ischaemia on the retinal pigment epithelium.

Complete ischaemia can produce marked changes in the organisation of the pigment epithelium. The changes were more severe with the longer periods of ischaemia.

Immediately following 15 minutes ischaemia the changes were mild and limited to the mitochondria and the smooth endoplasmic reticulum (fig. 4-22). The latter was focally condensed, the areas of condensation were up to 2 μ in diameter and were found throughout the cell. In any one complete cell cross-section, up to three such areas of condensation were found. An alteration in some mitochondrial profiles was evident with this period of ischaemia. These mitochondria had lost their tubular appearance and were oval in outline without any apparent change in the cristae or matrix. The changes were seen in less than half of the mitochondria. Abnormal and normal mitochondria occurred together in most cells.

The remaining cell organelles in the retinal pigment epithelium were similar to those observed in the control tissue.

With periods of ischaemia longer than 15 minutes the changes in the retinal pigment epithelium were more severe and widespread. The most evident changes occurred in the smooth endoplasmic reticulum, the mitochondria and the basal infoldings.

Thirty minutes ischaemia was accompanied by the rounding and distension of the majority of the mitochondria. In the more severely affected organelles there was a diminution of the electron density of the matrix and a shortening of the cristae. This latter situation was seen in the majority of the mitochondria following 60 minutes ischaemia (fig. 4-23). Ninety and 120 minutes ischaemia was characterised by considerable mitochondrial distension which was often sufficient to cause the mitochondria to rupture (fig. 4-24).

Many of the ruptured mitochondria contained a nodule of smooth endoplasmic reticulum (fig. 4-25). With the long periods of ischaemia the cristae were frequently small or absent and the matrix electron-translucent, (fig. 4-24).

The focal condensation of the smooth endoplasmic reticulum observed after 15 minutes ischaemia was more widespread with longer periods of ischaemia. With 30 minutes ischaemia the foci of smooth endoplasmic reticulum were more frequent and following 60 minutes ischaemia almost all the smooth endoplasmic reticulum was condensed (fig. 4-23). Little change from this situation was seen after 90 and 120 minutes ischaemia (fig. 4-24). There was a loss or reduction in the matrix surrounding the compressed tubules of smooth endoplasmic reticulum (fig. 4-25).

Periods of ischaemia longer than 15 minutes were also accompanied by alterations in the infoldings of the basal and apical cell surfaces. The infoldings of the basal cell wall were patchily widened and shortened (fig. 4-23). These areas were more frequent after the longer periods of ischaemia (fig. 4-24). A general disorganisation occurred in the apical processes after 30 minutes ischaemia, longer periods than this were associated with compression of the processes against the main body of the cell (fig. 4-23). This disorientation of the apical processes affected their close relationship with the outer segments of the visual cells. The tips of the outer segments were less deeply embedded in the processes and in many cases the outer segments appear detached from the processes. This loosening and eventual separation of the retinal pigment epithelium and the outer segments was more evident after 90 and 120 minutes ischaemia. Whereas the apical and basal cell walls were affected, the lateral cell wall was little affected by even the longest period of ischaemia employed in this study. The junctional complexes appeared intact in all the tissue examined.

The Golgi apparatus was generally well preserved although occasionally after 90 and 120 minutes ischaemia the cisternae were distended and disorganised (fig. 4-25).

The phagosomes were also generally unaffected except in some cases the larger phagosomes containing lamellar material were compressed and elongated following 120 minutes ischaemia. A quantitative analysis similar to that undertaken in the control retinal pigment epithelium was undertaken on tissue subjected to varying periods of pressure-induced ischaemia. This analysis showed that immediately after the ischaemic episode there was no significant change in either the number of phagosomes or their distribution at any of the periods of ischaemia studied (figs. 4-26 and 4-27), as compared with the corresponding control tissue. The identification of the later stages in the phagocytic process in the most severely affected cells was often difficult. These cells were limited to the tissue exposed to 120 minutes ischaemia and it was for this reason that no quantitative analysis was undertaken on this tissue.

The pigment granules were structurally unaltered even after the longest period of ischaemia, although their distribution was affected especially after 90 and 120 minutes ischaemia. The even distribution seen in the control tissue was lost. In the cells with a convex apical surface, the granules were located within the apex of the convexity, and were less frequently found towards the lateral cell wall.

The rough endoplasmic reticulum unlike the smooth endoplasmic, remained normal in appearance throughout the various periods of ischaemia (fig. 4-24).

The nucleus was likewise unaffected by periods of ischaemia up to 120 minutes, although there was a tendency for the nuclei to be slightly flattened after the longer periods of ischaemia.

The effect of pressure-induced ischaemia on some organelles in the retinal pigment epithelium was difficult or impossible to determine because of the compression observed in the smooth endoplasmic reticulum. Organelles such as coated vesicles, lysosomal-like bodies, smooth coated vesicles and free ribosomes were found randomly amongst tubules of smooth endoplasmic reticulum in the normal retinal pigment epithelium. Compression of the tubules following ischaemia obscured these organelles and the events accompanying the varying periods of ischaemia could not be determined.

4-6 Electron microscopy of post-mortem changes in the retinal pigment epithelium.

The main differences between this tissue and the pressure-induced ischaemic tissue involved the smooth endoplasmic reticulum and the basal infoldings.

The smooth endoplasmic reticulum did not show any condensation until 90 minutes post-mortem (fig. 4-54). Up to this time, many of the tubules were rounded and contained material with a low electron density (fig. 4-53). The absence of the condensation of the smooth endoplasmic reticulum enabled many of the smaller cell organelles to be identified after the shorter periods of ischaemia. The coated vesicles were often a prominent feature of the cytoplasm and it was thought that this may, in fact, reflect an increase in the number of these organelles, although no quantitative analysis was carried out (fig. 4-53). Coated vesicles were associated both with the apical and basal cell surfaces (fig. 4-53). Smooth coated vesicles were frequently found in the apical region of the cell, although these may have been cross-sections of diverticula of the apical surface. Frequent lysosomal bodies occurred throughout the cytoplasm. These appeared to be of two main types, one containing highly electron-dense material which formed a condensed mass, while the other type contained a more floccular material with a moderate electron density. The cisternae of rough endoplasmic reticulum were often

swollen and contained floccular material. An unusual feature of the pigment epithelium was the occasional immature melanosome (fig. 4-53), but these were rarely seen in the control tissue.

The other major difference compared with the pressure-induced tissue was the rapid reduction in the basal infoldings in the post-mortem retinal pigment epithelium. Fifteen minutes post-mortem there was little change in the basal infoldings, but by 30 minutes post-mortem the infoldings were much reduced and in some regions absent (fig. 4-53). The regions in which the basal infoldings were absent were more extensive with the longer ischaemic episodes. In post-mortem tissue the mitochondria appeared to be more readily affected than those of the pressure-induced ischaemic tissue (fig. 4-53). The sequence of degenerative mitochondrial changes were similar to that described previously for the pressure-induced ischaemic tissue, although the time span of the changes was generally shorter in the post-mortem tissue.

The nuclei behaved in a similar fashion to those of the pressure-induced ischaemic tissue and exhibited little change from that seen in the control tissue (fig. 4-55).

The apical processes underwent similar changes in both groups of ischaemic tissue, this was also true of the pigment granules, the lateral cell walls and the Golgi apparatus.

From here on the description of the various retinal layers applies to both the post-mortem tissue and tissue subjected to pressure-induced ischaemia.

4-7 Electron microscopy of the visual cells.

The visual cells were readily affected by periods of ischaemia. The changes occurring in the various regions of the visual cells, the outer and inner segments, the outer nuclear layer and the receptor pedicles (see fig. 1-1) will be described separately.

4-7.1 The outer segments.

Immediately following 15 minutes ischaemia, the terminal portions of the outer segments were disorganised and disorientated. Some fragments of outer segment material were present in the subretinal space adjacent to the retinal pigment epithelium. In some of these fragments and in a few proximal regions of the outer segments the inter-disc space was wider than normal. In addition, the orderly arrangement of the pile of discs was disturbed in a few outer segments. Following 30 minutes ischaemia, fragments of outer segment material were commonly found. Within these fragments the discs were often broken and disorganised (fig. 4-28). Some of the outer segments contained varicosities possessing the characteristics of the fragments described above. Although at this stage an occasional outer segment of normal appearance could be seen. Sixty minutes ischaemia was accompanied by extensive fragmentation of the outer segments. Many of the fragments were in the form of swollen saccules containing disorientated and disrupted discs (fig. 4-56). Varicosities in the outer segments were also frequent. Following the two longer periods of ischaemia (90 and 120 minutes) the great majority of the outer segments were fragmented with the fragments often being grossly distended (fig. 4-29). In severe cases, the membrane surrounding the fragments was ruptured. With these periods of ischaemia the ruptured and unruptured fragments contained small saccules formed from the disorganised discs (fig. 4-29).

4-7.2 The inner segments.

Marked changes were also apparent in the inner segments and these alterations like those observed in the outer segments were more severe with the longer periods of ischaemia.

The ellipsoid region of the inner segment which contains numerous mitochondria was readily affected by ischaemia. Fifteen minutes ischaemia was accompanied by a limited swelling of the mitochondria, although the matrix and cristae appeared normal. The distension was more severe following 30

minutes ischaemia with a subsequent diminution in the electron density of the matrix (fig. 4-57). At this stage, small intracellular spaces were present amongst the generally oedematous cytoplasm of the myoid region. The cell organelles in this region, however, appeared normal (fig. 4-30 and 4-57). The inner segments as a whole appeared to be considerably shorter than their control counterparts (fig. 4-30). The changes after 60 minutes ischaemia were more severe with many of the mitochondria being rounded with disorganised cristae and electron-translucent matrix (fig. 4-31). Following 90 and 120 minutes ischaemia, the majority of the mitochondria were rounded and oedematous. The distension was often severe enough to cause the mitochondria to rupture. In addition, with these long periods of ischaemia, the inner segments were often fragmented and ruptured (figs. 4-29 and 4-32). With the longer periods of ischaemia, the Golgi apparatus which was located in the myoid region was often grossly distended. The smooth endoplasmic reticulum, which was also in the myoid region, was rounded following 90 and 120 minutes ischaemia.

The degeneration in the inner and outer segments was associated with the presence of macrophages. A prominent feature of the macrophage cytoplasm was the many inclusion bodies (fig. 4-34). They consisted almost entirely of phagosomes containing outer segment material (fig. 4-35). The inclusion bodies were similar to some phagosomes present in the retinal pigment epithelium. A similarity existed between the pigment epithelial phagosomes involved in the early stages of degradation of outer segment material (fig. 3-13). An unusual feature of the macrophage's phagosomes was the presence of more than one fragment of outer segment material (fig. 4-35), whereas the retinal pigment epithelial phagosomes contained only one such fragment.

The macrophagic cytoplasm contained many distended mitochondria with an electron-translucent matrix and disrupted and shortened cristae (figs. 4-35 and 4-36). In some instances the mitochondrial membranes were ruptured. Many membrane bound vesicles occurred within the cytoplasm (fig. 4-37). Amongst

the various types of vesicles were found smooth and coated vesicles and lysosomal-like bodies. The smooth vesicles varied considerably in size (0.02 - 0.15 microns in diameter) and were more numerous around the Golgi apparatus which was often well developed (fig. 4-37). The coated vesicles were found more generally distributed throughout the cytoplasm. The lysosomal-like bodies contained a granular electron-dense substance and were irregular in shape and variable in size (0.2 - 2.0 microns)(fig. 4-36). The membrane systems were not particularly well developed. The rough endoplasmic reticulum was more prominent than the smooth endoplasmic reticulum. The cell membranes were often thrown into fringe-like projections which were frequently compressed between adjacent cells (fig. 4-34). The cells lacked a basement membrane and had a smooth outline free of pinocytic vacuoles.

The ultrastructure of these cells suggest that they were mature macrophages involved in the removal of outer segment material.

4-7.3 The outer nuclear layer and external limiting membrane.

The external limiting membrane which was formed by the cell junctions (zonulae adherentes) between the Müller cells and the visual cells appeared to remain intact even after the longest period of ischaemia (fig. 4-33). Following 120 minutes ischaemia, however, the cell membranes of some visual cells were ruptured although the zonulae adherentes appeared intact. These ruptures may cause discontinuities in the length of the external limiting membrane. The mitochondria of the Müller cells which lie just inner to the external limiting membrane were considerably distended following the various periods of ischaemia (fig. 4-58). Although the precise nature and course of the distension was hard to determine, in view of the poor preservation of these organelles in the control tissue.

The earliest changes in the outer nuclear layer were observed after 15 minutes ischaemia. The change involved small focal dilations of the nuclear envelope (fig. 4-38). Following 30 minutes ischaemia pyknotic

changes were evident in the rod nuclei. The majority of these nuclei were rounded with frequent focal distensions of the nuclear envelope. The perinuclear cytoplasm was swollen and was more electron-translucent than that observed in the control tissue (fig. 4-59). Periods of ischaemia longer than 30 minutes were accompanied by further rounding of the rod nuclei with a condensation of the chromatin (fig. 4-39). The distinctive "coffee bean" chromatin pattern of the normal rod nuclei was generally lost. In addition, with periods of ischaemia longer than 30 minutes, the perinuclear cytoplasm was more oedematous and the distension of the nuclear envelope more extensive. The nuclei of the cone cells were much more resistant to ischaemic changes than their rod counterparts (figs. 4-40, 4-58). Following the longest period of ischaemia there was only limited focal distensions of the nuclear envelope, slight rounding of the nuclei and a more diffuse chromatin pattern (fig. 4-40). The outer and inner receptor fibres of the rod cells were affected more severely than those of the cone cells, being electron-dense and containing numerous small electron-translucent vacuoles. The Müller cell cytoplasm enveloping the visual cell nuclei was also oedematous after 30 minutes of ischaemia. With progressively longer ischaemic episodes the oedema was more severe and gave prominence to the cytoplasmic fibrils of the Müller cells (fig. 4-40).

4-8 Electron microscopy of the outer plexiform layer.

The rod receptor pedicles like the rod nuclei were more severely affected than their cone counterparts following periods of complete ischaemia. The initial change was observed after 60 minutes ischaemia with the appearance of small vacuoles randomly scattered throughout the pedicle (fig. 4-61). This was followed by an increase in the electron density and a reduction in volume of the pedicle. In spite of these

changes, the synaptic ribbon appeared to remain intact (fig. 4-41). Even following 120 minutes ischaemia the pedicles of the cone cells had a normal appearance (fig. 4-41).

The processes of the outer plexiform layer were often swollen, the swelling was more severe and widespread (fig. 4-41) after the longer periods of ischaemia. The cells giving rise to the affected processes could not be identified. Although many of the large horizontal running fibres which may belong to the horizontal cells were distended after the long periods of ischaemia (60-120 minutes). The distension of the fibres was of a generalised nature, but in severe cases the fibres contained a floccular material and the number of neurotubules and fibrils appeared to be greatly reduced and in some cases absent. In spite of the considerable distension seen in some fibres, the cell membranes appeared intact.

4-2 Electron microscopy of the inner nuclear layer.

In the inner nuclear layer, changes became apparent after 30 minutes ischaemia. The initial changes were focal separations of the membrane of the nuclear envelope, slight mitochondrial swelling and dilation of the cisternae of the Golgi apparatus. This was followed by a generalised change in the neural cells of the layer (the horizontal amacrine and bipolar cells) which was manifest after 60 minutes ischaemia (figs. 4-42 4-62). This change was a diffuse swelling of the cytoplasm which was more extensive with longer periods of ischaemia. The oedematous cytoplasm was floccular and contained few organelles. The remaining cell organelles were frequently found as a mass adjacent to the nucleus, (fig. 4-43). This mass contained fibrils, neurotubules, distended cisternae of rough endoplasmic reticulum, swollen mitochondria, lysosomal-like bodies, free ribosomes and glycogen-like particles. The swollen mitochondria contained a floccular material with a few cristae, although these were often absent.

The Golgi apparatus could not be identified in the majority of the cases. The volume of the cell contents appeared to be reduced following the various ischaemic episodes compared with the control counterparts. Following 120 minutes some neural cells of the inner nuclear layer were severely affected. The cytoplasm was entirely oedematous and the nuclei showed advanced pyknotic changes (fig. 4-44). The chromatin had prominent electron dense masses amongst an electron-translucent background. The cell membranes were also frequently ruptured in these cells. In spite of the changes seen in the neural cells, the Müller cell nuclei appeared to be relatively unaffected even after 120 minutes ischaemia, although the cytoplasm was a little more electron-translucent which gave prominence to the cytoplasmic fibrils (fig. 4-42). On occasion, the cisternae of rough endoplasmic reticulum of the Müller cells which was found in this region were distended whereas the Golgi apparatus appeared normal.

4-10 Electron microscopy of the inner plexiform layer.

The processes forming the inner plexiform layer were initially affected after 30 minutes ischaemia. Some of the processes were swollen with few neurotubules and synaptic vesicles. The occasional process appeared to have ruptured membranes (fig. 4-45). Identification of the origin of these processes was difficult. The bipolar cell processes which were identified by virtue of their synaptic ribbons appeared to be little affected except by mild vacuolation. With the longer periods of ischaemia (60-120 minutes) the swelling of the processes was more universal (fig. 4-47, 4-63). Many of the processes had ruptured membranes and the cytoplasm was generally floccular (fig. 4-46). The number of neurotubules and fibrils were greatly reduced or entirely absent, in addition, many of the synaptic vesicles had disappeared or were fewer in number (fig. 4-46). The synaptic ribbon was often observed, although the vesicles were reduced

or absent and the overall changes seen in the other processes were also evident in these recognisable bipolar cell processes (fig. 4-45, 4-63). The large radial pillars of the Müller cells remained essentially normal in appearance following the various periods of ischaemia up to and including 120 minutes (fig. 4-47). As a result of the unaltered nature of the Müller cell cytoplasm at this level of the retina the cytoplasm had a higher electron density than the surrounding processes of the neural cells. This difference in electron density may provide an identification of some of the processes belonging to the Müller cells in the inner plexiform layer after long periods of ischaemia.

4-11 Electron microscopy of the ganglion cells and inner retina.

In the ganglion cells, degenerative changes were observed following 30 minutes ischaemia (fig. 4-48). Focal separation of the nuclear membranes occurred. These separations often formed diverticula, containing a floccular material. There also appeared to be some distension of the mitochondria, although the extent of this change was difficult to determine because of the poor preservation of the mitochondria in the control tissue. With longer periods of ischaemia the cytoplasm was oedematous ~~which became~~ ^{which was} more pronounced with increasing durations of ischaemia. The oedematous changes were accompanied by a reduction in the volume of the cell contents, which were frequently found as a mass adjacent to the nucleus in a similar fashion to that observed in the neural cells of the inner nuclear layer (fig. 4-49, 4-64). The axons of the ganglion cells were affected by periods of ischaemia longer than 15 minutes. The initial changes were limited to an oedematous swelling of the larger unmyelinated fibres which occurred in the peripheral retina (fig. 4-50). The oedema was accompanied by a reduction in the number of neurotubules and neurofibrils. The smaller unmyelinated fibres were frequently unaffected by even the longest period of ischaemia. The ganglion cell

axons become myelinated and formed the horizontal myelinated nerve fibre zone before they passed into the optic nerve. Changes in the myelinated nerve fibres were also apparent after 30 minutes ischaemia. The changes generally occurred in the larger fibres and involved a swelling of the axon and distortions of the myelin lamellae. In addition, there was also a loss of the filaments and neurotubules and their replacement by a floccular material (fig. 4-65). The myelinated nerve zone was associated with glial cells and blood vessels. The glial cells were generally unaltered following periods of ischaemia although there was some mitochondrial swelling (fig. 4-51). In some astrocytes, there were frequent secondary lysosomal-like bodies containing membranous material and material of high electron density (fig. 4-51). Such cells were rarely, if ever, observed in control tissue. The cells containing these inclusion bodies were often found vitreal to the inner limiting membrane.

The retinal blood vessels were readily affected by ischaemic conditions. With periods of ischaemia longer than 15 minutes the endothelium was vacuolated and the mitochondria distended (fig. 4-52). The vacuolation and the mitochondrial swelling were more severe after the longer periods of ischaemia. The vacuolation appeared to be the result of pinocytosis. An overall change in the endothelial cells was the shortening of their profiles which gave an apparent reduction in the diameter of the vessel lumen.

4-12 Electron microscopy of post-mortem changes in tissue kept at 37°C

Degenerative changes observed in this group were similar to those seen in the post-mortem tissue maintained at room temperature, and pressure-induced ischaemic tissue, although the alterations in the retina occurred more rapidly in the tissue kept at 37°C. Light microscopy revealed that 15 minutes post-mortem was associated with disruption of the terminal regions of the outer segment in addition to mild vacuolation in the retinal

pigment epithelium. After 30 minutes at 37°C. there were degenerative changes throughout the retina (fig. 4-19). These changes were more marked in the outer retina, often with considerable disturbance in the outer nuclear layer. Following 60, 90 and 120 minutes ischaemia, the degeneration was more severe. At 120 minutes post-mortem, the outer retina was disrupted with little evidence of any organisation in the outer or inner segments (fig. 4-20). The pigment epithelium was often undulated and heavily vacuolated. The visual cell nuclei and those of the inner nuclear layer were severely pyknotic. Pronounced oedema was evident in the outer and inner plexiform layers. The ganglion cells had extensive intracellular oedema. Electron microscopy confirmed the findings of light microscopy which showed a more rapid deterioration of the retinal tissue when maintained at 37°C. rather than at room temperature.

Macrophages were also evident in tissue maintained at 37°C. (fig. 4-21). They were slightly more numerous at each post-mortem period compared with tissue maintained at room temperature, but less than those observed in the pressure-induced ischaemic tissue.

In keeping with the light microscopic findings, electron microscopy showed similar, but more rapid, changes than the tissue maintained at room temperature (figs. 4-66 to 70).

4-13 Discussion.

Total acute ocular ischaemia whether as a result of raised intraocular pressure or post-mortem conditions was observed by light microscopy to result initially in damage to the visual cells and later to the retinal pigment epithelium and inner retina. These results were similar to those described by Wagonman (1890) and Nicholls (1938) who induced total acute ocular ischaemia by sectioning the posterior ciliary arteries. Electron microscopy revealed cellular changes before any

alteration evident by light microscopy. These early changes affected the mitochondria of the retinal pigment epithelium and the inner segments of the visual cells. These changes were followed by intracellular oedema throughout the inner retina.

Ischaemia caused rapid and marked changes in the mitochondria throughout the retinal cells. The resulting impaired mitochondrial function may have lead to an imbalance in the electrolyte content with a subsequent accumulation of water in the cytoplasm. Similar mitochondrial changes and oedema have been described in isolated rabbit retina following anoxia (Webster and Ames 1965), in the rat liver following ischaemia (Bassi and Bernelli-Zazzera 1964), anoxia (Cudeo 1963) and hypoxia (Bassi, Bernelli-Zazzera and Bassi 1960 and Sulkin and Sulkin 1965), in the rat heart following ischaemia (Bryant, Thomas and O'Neal 1958) and hypoxia (Sulkin and Sulkin 1965), following myocardial ischaemia in rabbits (Gaulfield and Klionsky 1959) and hypoxia in the brain tissues of the hamster (Hager, Hirschberger and Scholz 1960).

Following the longer periods of ischaemia the retinal oedema may only in part have been due to the mitochondrial changes. The oedema may have been influenced by the proteins and ions, notably potassium which would have been released into the intercellular space from the ruptured cells.

The normal retinal pigment epithelium has an important function in the maintenance of the fluid balance in the retina, particularly in the outer retina. This was thought to be especially true of the rabbit retina, where the entire diffusion of nutrients, fluids and ions from the blood to the retina and vice versa has to pass across the pigment epithelial layer. A modification of the cell thought to enable it to accomplish this role was the close association of the basal infoldings

and the mitochondria (Bernstein 1961). Both these structures have been shown to be readily affected by ischaemia and particularly by post-mortem conditions. Alterations in the basal infoldings have been noted in other situations where the blood flow through the choroid was affected. In the ageing human eye, they were reduced (Hogan 1971). In tissue cultured cells they were reduced and then absent (Luo, Albert and Zimmerman 1973). They were also reduced following choroidal ischaemia (Anderson and Davis 1975) and during hibernation (Munzberg 1975). A relationship may exist between the infoldings and the choroidal blood flow. The infoldings being absent or reduced when the blood flow has been abolished or limited and more plentiful with a higher blood flow. This aspect may repay further attention. How the changes in the basal infoldings and the adjacent mitochondria following ischaemia or post-mortem conditions affected or influenced the course of the retinal oedema was not fully understood. The distension of the mitochondria must have influenced the fluid imbalance, although the area over which fluid can pass must have been reduced. In spite of these changes cellular oedema was not a marked feature of the retinal pigment epithelium. Another important function of the normal retinal pigment epithelium is thought to be the metabolic support it provides for the visual cells, especially the outer segments. The functional impairment of the retinal pigment epithelium may have also played a role in the changes observed in the outer segments of the visual cells. Ischaemia initially caused disorientation and fragmentation of the distal portions of the outer segments. The proximal regions were affected later. The fragments were swollen and sometimes ruptured after the longer ischaemic episodes. Similar changes have been shown to occur in the retina following administration of sodium fluoride (Orzalesi, Grignolo and Calabria 1967) and sodium iodate (Grignolo, Orzalesi and Calabria 1966). Both these substances primarily affect the retinal pigment epithelium with

secondary effects on the outer segments. In this present investigation a direct effect of ischaemia may also have occurred in the outer segments in addition to the influence of the changes occurring in the inner segments. The ionic concentration in the subretinal space must have changed as a result of the mitochondrial changes in the inner segments and retinal pigment epithelium. The fragmentation and swelling of the outer segments following ischaemia closely resembled the results described by Cohen (1971) who investigated the changes in the photoreceptor outer segments in response to osmotic stress.

In the outer nuclear and outer plexiform layers the cone nuclei and pedicles were less affected than their rod counterparts. This preferential damage to the rod cells was not understood and probably could not be explained on an ultrastructural basis considering the close similarity in the ultrastructure of the rod and cone cells in the rabbit.

An interesting aspect of this study was the better preservation of the inner retina which was furthest from the blood supply as compared to the outer retina, which was adjacent to the capillary network of the choriocapillaris. A feature of the normal rabbit retina, although it was not well demonstrated in the control tissue, is the high concentration of glycogen in the inner retina (Kuwabara and Cogan 1961). This supply of glycogen may have enabled the rabbit retina to withstand the effects of short periods of ischaemia. Although Weiss (1972) showed that it was not the actual amount of glycogen that was important, but rather the ability to utilise it. Weiss (1972) showed that following 60 minutes pressure-induced ischaemia, the rate of glycolysis declined rapidly in spite of adequate supply of glycogen. This period of 60 minutes agreed in general with the ultrastructural changes which became evident in the inner retina at this period. The glycogen is largely found in the Müller cells. The glycogen particles

are more numerous in the inner regions of the cell than the outer areas (Magalhães and Coimbra 1972 and Uga and Smelser 1973). This form of distribution may have accounted for the pattern of ischaemic damage seen in the Müller cells. The outer regions of these cells which embraced the visual cell nuclei were generally more oedematous than the inner retinal pillars of cytoplasm. Overall the Müller cells were better preserved than the neural components of the retina. This was not unexpected in view of the fact that gliosis and loss of the retinal neural elements occurred following long-standing glaucoma (Duke-Elder 1967) and experimental long-term elevations of intraocular pressure in rabbits (Flocks, Tsuchihara and Miller 1959, and de Carvalho 1962).

It has been shown that animals without a retinal blood supply generally have a higher concentration of glycogen in the inner retina than their counterparts with a retinal blood supply (Kuwabara and Cogan 1961). This may explain the difference in the effect of ischaemia has on the inner retina of species with and without retinal circulations. In the former case, complete ischaemia results in oedema throughout the retina. The oedema was more prominent in the inner retina and was followed by degeneration in the ganglion and bipolar cells with the eventual involvement of the whole retina (Turnbull 1948, Smith and Baird 1952, Reinecke, Kuwabara, Cogan and Weiss, 1962, Levine and Pavan 1966, and Fujino and Kamasaki 1967).

Ischaemia resulted in a considerable amount of outer segment debris in the outer segments. Associated with this debris were mature macrophages which were a prominent feature of the ischaemic retina. Even though the retina was no longer nourished by fresh blood, some cells of the retina or choroid were able to proliferate and engulf outer segment material. Speculation exists concerning the site of origin of these cells in the outer retina. Free and fixed macrophages are generally thought to arise from

circulatory monocytes, although they can derive from tissue histiocytes and in the central nervous system from microglia (Sarr 1973). A circulatory origin for the retinal macrophages in this instance may have been unlikely. In both the pressure-induced ischaemic and post-mortem tissue, the blood flow to the eye was abolished. The macrophages would have had to transform from the small number of monocytes present in the blood trapped within the eye. There was no evidence of any transformation of monocytes into macrophages which one would expect if the latter cells were of circulatory origin. In addition the number of circulating white blood cells may have been reduced in the pressure-induced ischaemic tissue by the use of urethane as the anaesthetic agent (Haddow and Lexton 1946). A histiocytic or microglial origin of the macrophages also seemed unlikely in view of the small number of such cells found in the choroid and retina respectively, as well as the lack of evidence of their migration and transformation. The retinal pigment epithelium appeared to be a likely source of the macrophages. Although the exact way in which they could be derived from this cell layer was unknown. Whatever the mechanism for the formation of the macrophages, it must occur rapidly as the cells were observed after only 15 minutes of ischaemia. The rapid appearance of these mature macrophages may preclude transformation from a cell type not already involved in phagocytosis. The retinal pigment epithelium was able under normal circumstances to engulf outer segment material. If the site of origin was the retinal pigment epithelium then the retinal macrophages may have been whole RPE cells which had migrated from their attachment to Bruch's membrane, cells "budded" off from the RPE or cells formed by very rapid mitosis. In spite of the considerable amount of tissue investigated no evidence was seen for any of the above mechanisms.

Marshall, Fuldhauser, Lotmar and Reulien (1971) speculated that proliferation of the RPE at the edge of a photoocoagulation lesion occurred by cell budding as they found no evidence of rapid mitosis or incorporation of ³H-thymidine during epithelial regeneration. However, Gloor (1969), Wallow and Tso (1973), Ishikawa, Uga and Imai (1973) and Ishikawa and Imai (1974) showed mitotic figures in proliferating RPE cells.

Macrophages in the subretinal space also occurred following photic damage (Tso 1973), light coagulation (Gloor 1969), damage resulting from radiant energy (Friedman and Kuwabara 1968) and cryosurgery (Lincoff and Kreissig 1971). Their origin was considered to be the monocytes circulating in the choriocapillaris (Tso 1973), the retinal histiocyte (Friedman and Kuwabara 1968) and the retinal pigment epithelium (Gloor 1969 and Lincoff and Kreissig 1971).

The macrophages in this study increased with increasing durations of ischaemia. This increase in number paralleled the degree of damage observed in the outer segments. The difference in the number of cells occurring in the pressure-induced ischaemic tissue and that in the post-mortem tissue maintained at room temperature was not understood. The degenerative changes in the outer retina appear similar in both cases. The slightly smaller number of macrophages in the post-mortem tissue maintained at room temperature compared to that kept at 37°C. may be a reflection of the presumed greater metabolic activity in the latter.

In the pressure-induced ischaemic tissue the macrophagic removal of the outer segment material appeared to be the main mechanism for the disposal of this debris. The quantitative analysis carried out on the number of phagosomes within the retinal pigment epithelium revealed no change in the phagocytic process. This suggested that during the varying periods of ischaemia the retinal pigment epithelium was unable to ingest any extra outer segment material.

There was a striking similarity between post-mortem tissue maintained at room temperature and tissue made ischaemic by high intraocular pressures. Apart from the pigment epithelium this similarity extended to all the layers of the retina, even to the outer segments where one might have expected to observe some deformation as a result of the high intraocular pressures employed to induce ischaemia. This suggested that the mechanical effects of pressure were minimal even at the level of resolution afforded by electron microscopy. The effects of pressure did not appear to be a problem in the interpretation of ischaemic changes following periods of raised intraocular pressure. Post-mortem tissue may provide a good and convenient model for studying complete ischaemia, although it does not allow recovery studies to be undertaken. The exception to the similarity between the pressure-induced ischaemic and post-mortem tissue was the retinal pigment epithelium. The underlying reason for the difference was not understood. It was unlikely that the mechanical effects of pressure could have retarded the degenerative changes in the basal infoldings and mitochondria, although it may have accounted for the compression of the smooth endoplasmic reticulum.



FIG.4-1 Light micrograph of the retina following 15 minutes ischaemia, apart from the disorganised outer segments the retina appears normal. (550 X)

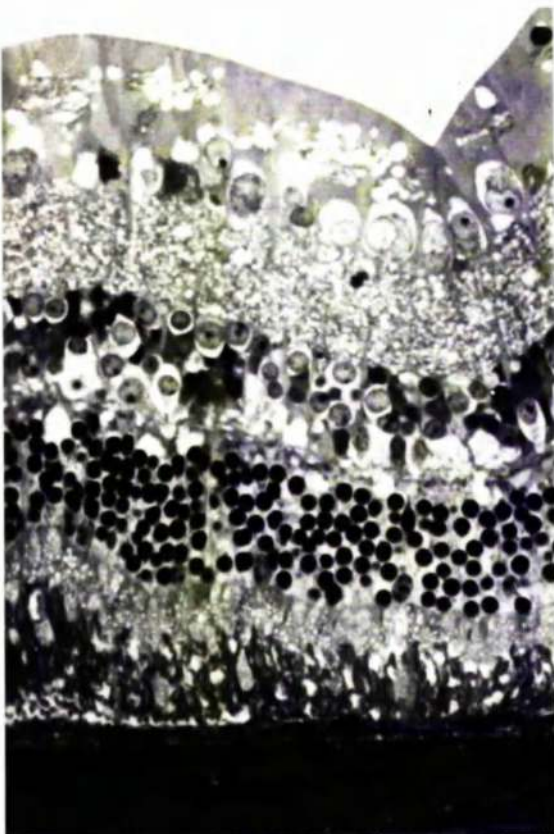


FIG.4-2 Light micrograph of the retina following 60 minutes ischaemia. Degenerative changes occur throughout the retina although the outer retina appears more severely affected than the inner retina. (550 X)



FIG.4-3 Light micrograph of the retina following 120 minutes ischaemia showing extensive changes throughout the retina. Microcystic spaces are a prominent feature of the outer nuclear layer.(550 X)



FIG.4-4 Light micrograph of the retina following 60 minutes ischaemia illustrating the retinal folding that can accompany periods of ischaemia. (300 X)

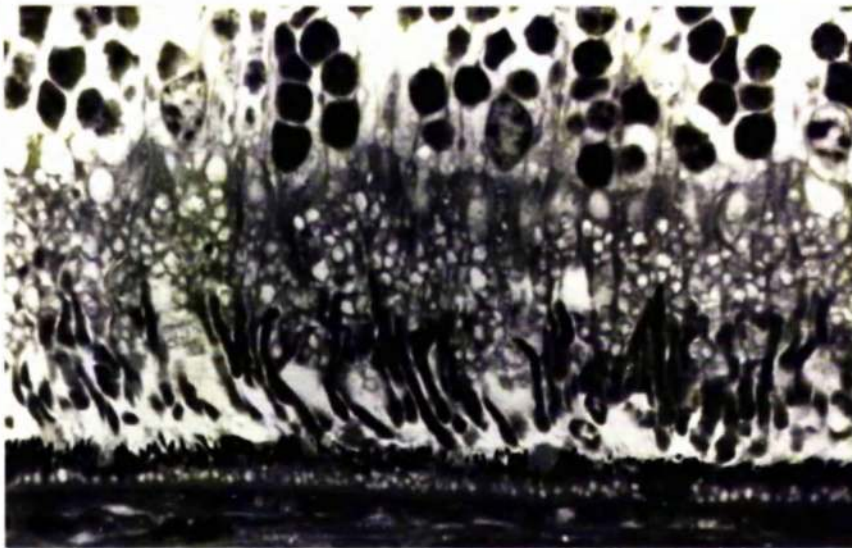


FIG.4-5 Light micrograph of the outer retina after 60 minutes ischaemia. Many vacuoles occur in the pigment epithelium. The outer segments are disrupted and some swollen fragments occur. The ellipsoid region of the inner segments are vacuolated. Pyknotic changes are evident in the outer nuclear layer. (I,500 X)

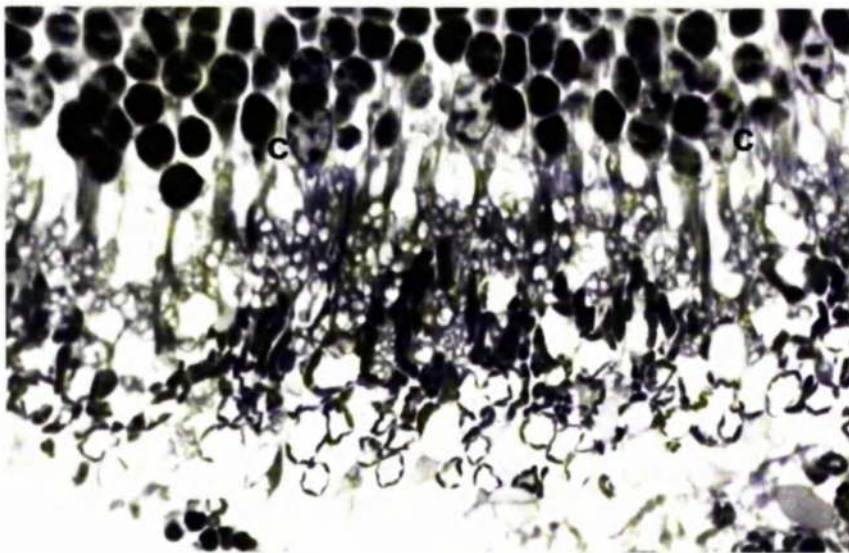


FIG.4-6 Light micrograph of the inner and outer segments after 120 minutes ischaemia, both regions are disrupted and fragmented. The outer segment fragments form swollen saccules. The cone nuclei (C) are better preserved than their rod counterparts. (I,500 X)

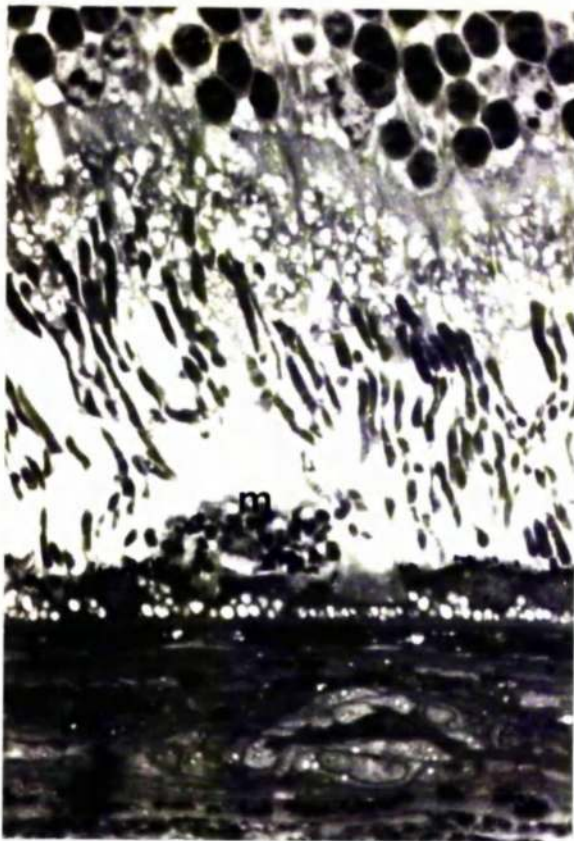


FIG.4-7 Light micrograph of the outer retina after 60 minutes ischaemia showing a solitary macrophage(X) adjacent to the pigment epithelium.(I,500 X)

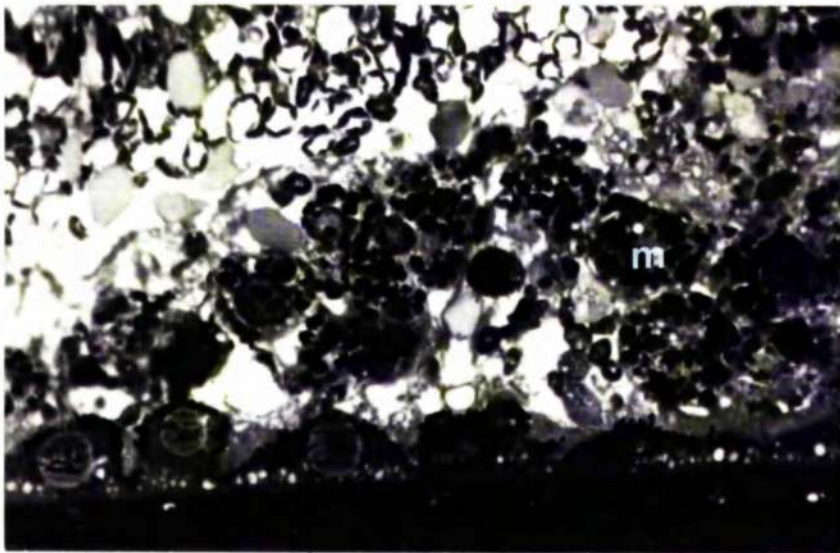


FIG.4-8 Light micrograph of the outer retina after 120 minutes ischaemia showing the many macrophages which are often present after long periods of ischaemia.(I,500 X)



FIG.4-9 Light micrograph of the inner retina after 120 minutes ischaemia. Oedematous changes are evident throughout the region. The ganglion cell (G) cytoplasm is often observed as a mass close to the nucleus. (1,500 X)



FIG.4-10 Light micrograph of the inner retina after 120 minutes ischaemia showing the advanced pyknotic changes in the inner nuclear layer. (1,500 X)

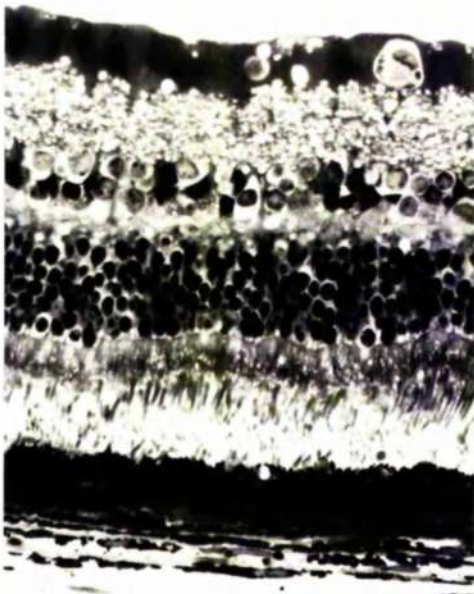


FIG.4-II Light micrograph of the retina 15 minutes post-mortem. The changes are related to the outer retina especially the outer segments. (550 X)



FIG.4-I2 Light micrograph of the retina 120 minutes post-mortem. Extensive degenerative changes are evident throughout the retina. (550 X)

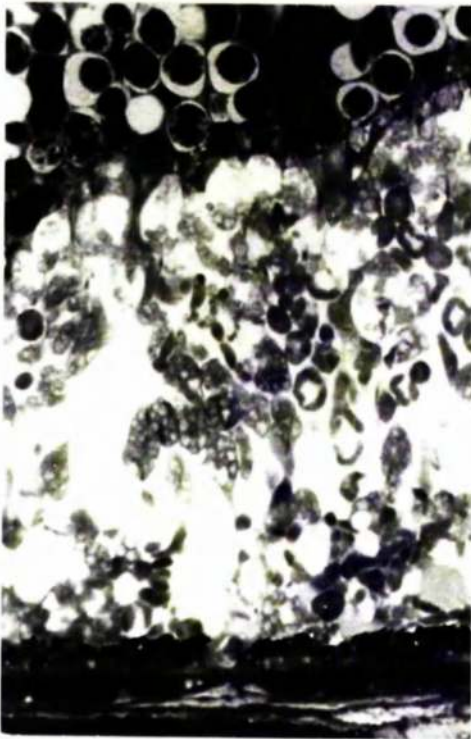


FIG.4-I3 Light micrograph of the outer retina 120 minutes post-mortem. The inner and outer segments are disrupted and fragmented. The nuclei of the outer nuclear layer are pyknotic. (1,500 X)

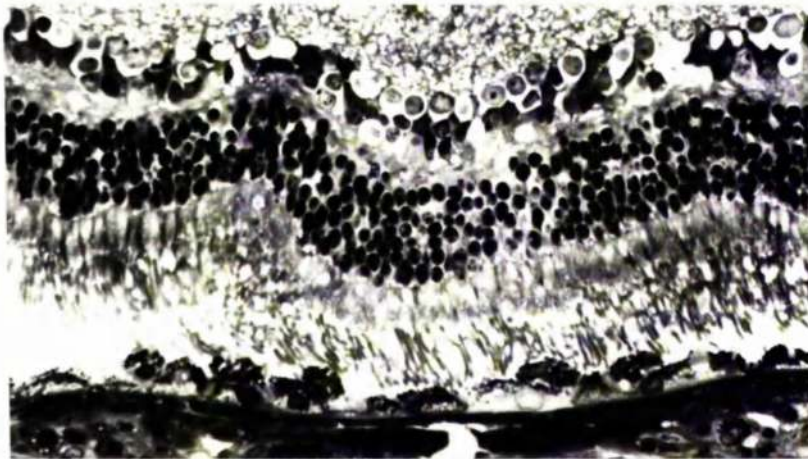


FIG.4-I4 Light micrograph of the outer retina 60 minutes post-mortem. Macrophages are prominent adjacent to the vacuolated pigment epithelium. (550 X)

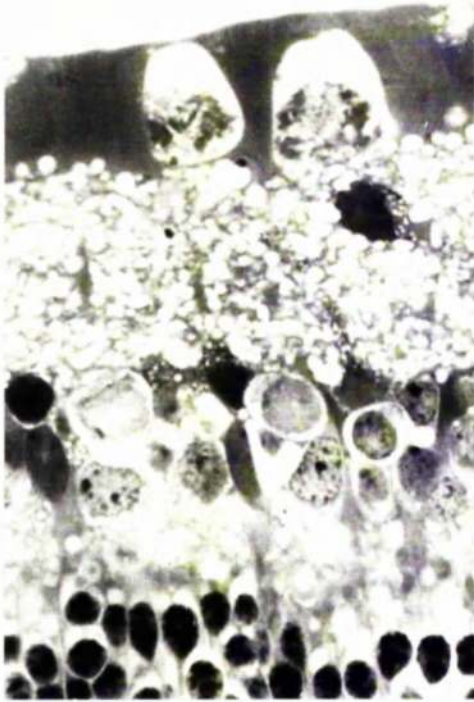


FIG.4-I5 Light micrograph of the inner retina 120 minutes post-mortem. Oedematous changes are evident throughout the inner retina. (1,500 X)

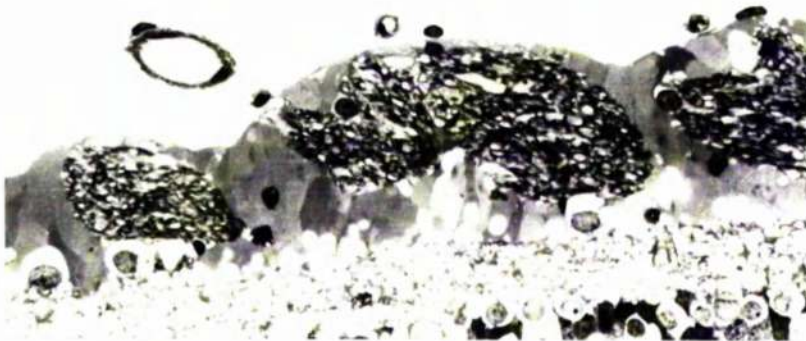


FIG.4-I6 light micrograph of the inner retina in the myelinated nerve fibre zone 60 minutes post-mortem. The myelinated nerve fibres and their associated blood vessels appear normal. (550 X)



FIG.4-17 Light micrograph of the retina 60 minutes post-mortem which illustrates the folding that occurs in post-mortem retinal tissue. The folding involves all the layers of the retina. (550 X)

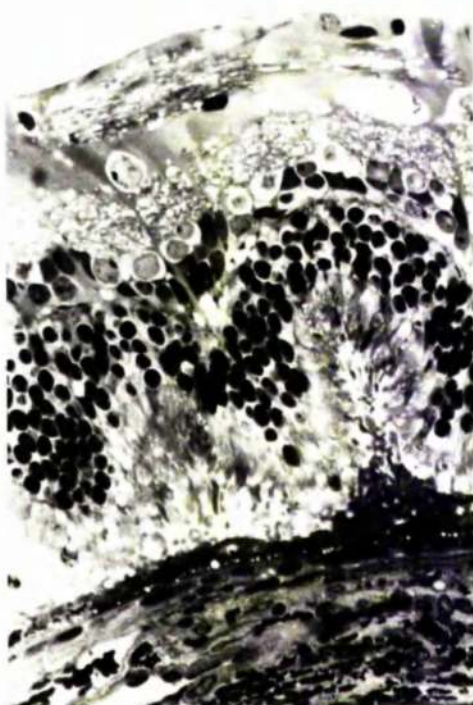


FIG.4-18 Light micrograph of the retina 90 minutes post-mortem. The retinal folding involves mainly the outer retina. (550 X)



FIG.4-19 Light micrograph of the retina maintained at 37°C for 30 minutes post-mortem. Considerable degenerative changes are evident throughout the retina.(550 X)



FIG4-20 Light micrograph of the retina maintained at 37°C for 90 minutes post-mortem. The visual cells are severely degenerate and the inner retina is extensively affected.(550 X)

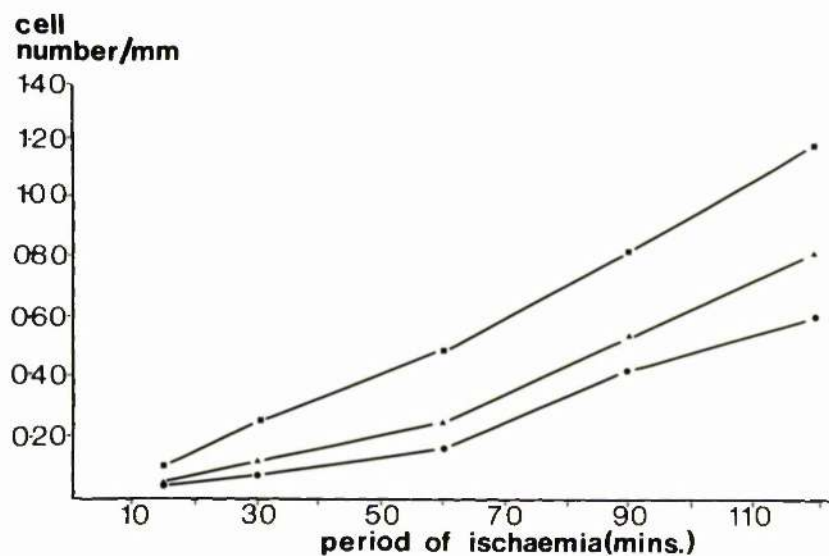


FIG.4-2I Graph showing the number of macrophages occurring in 100mm. of retinal tissue following various periods of ischaemia. ■-Pressure induced ischaemia. ▲-Post-mortem tissue maintained at 37°C. ●-Post-mortem tissue maintained at room temperature.

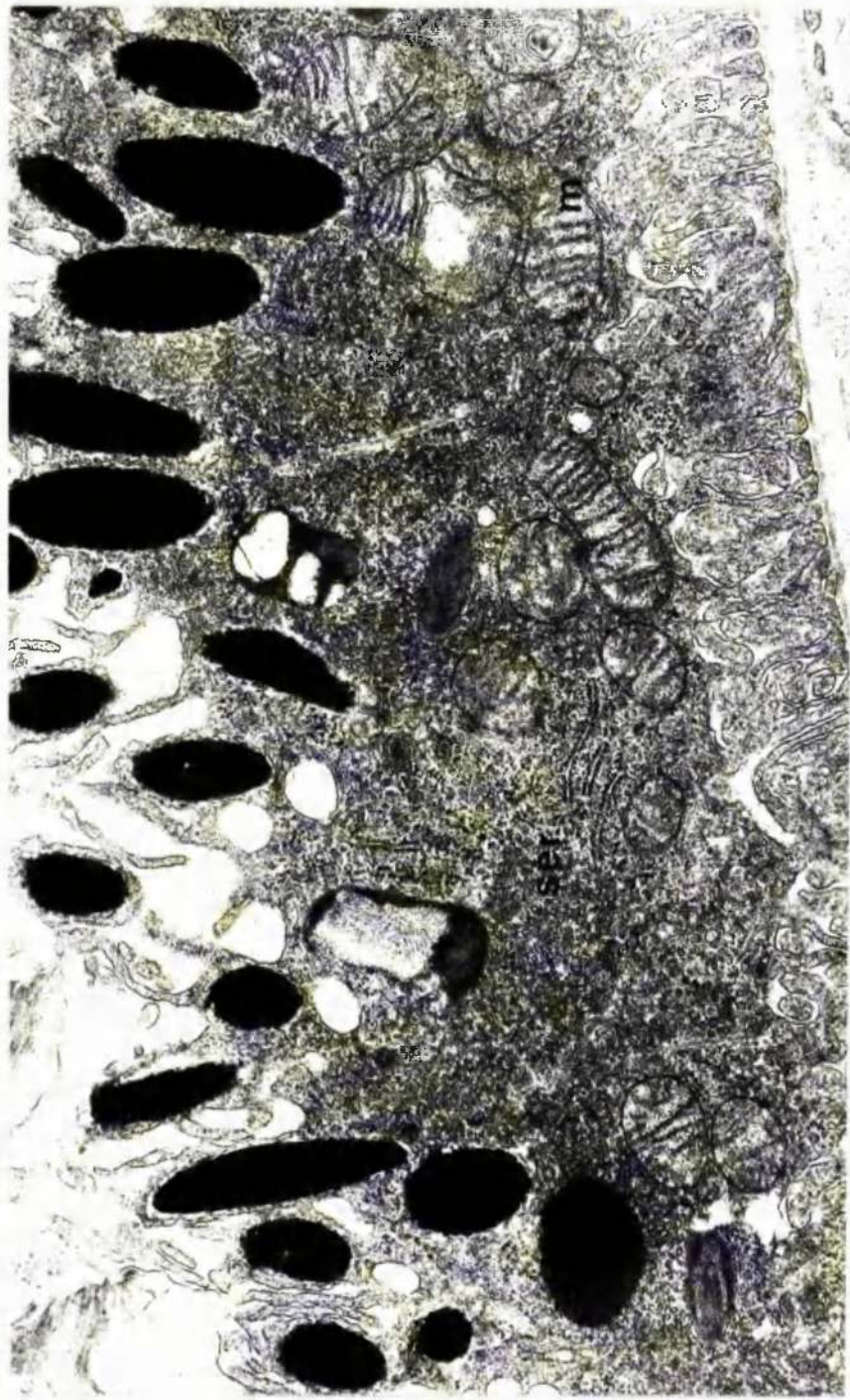


FIG.4-22 Electron micrograph of the retinal pigment epithelium after 15 minutes ischemia illustrating its normal appearance apart from the focal condensation of the smooth endoplasmic reticulum(SER) and the occasional distended mitochondria(M). (17,000 X)

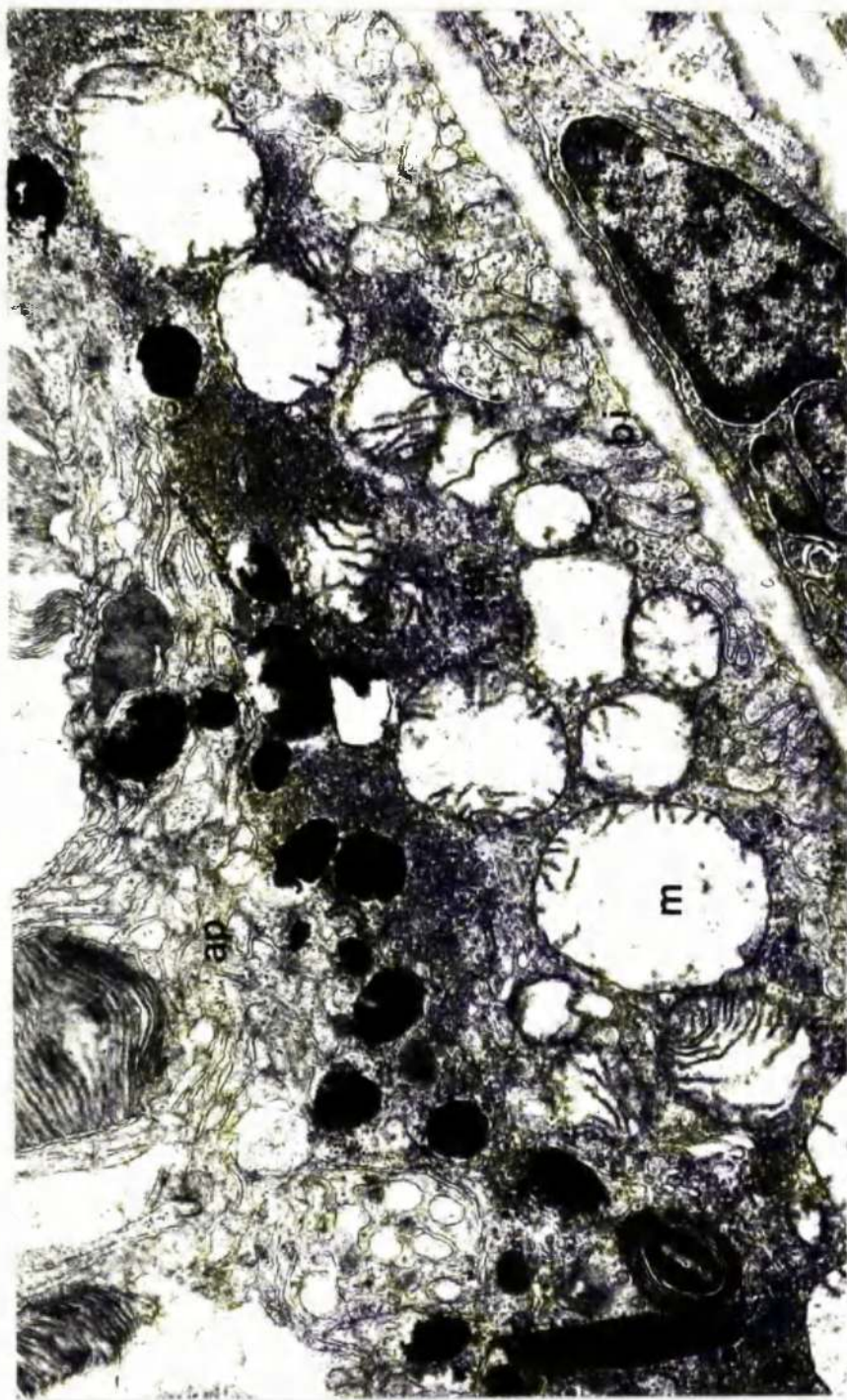


FIG.4-25 Electron micrograph of the retinal pigment epithelium after 60 minutes ischemia showing the many grossly distended mitochondria(M), condensed smooth endoplasmic reticulum (SER), compressed apical processes(AP) and widened basal infoldings(BI).(21,000 X)

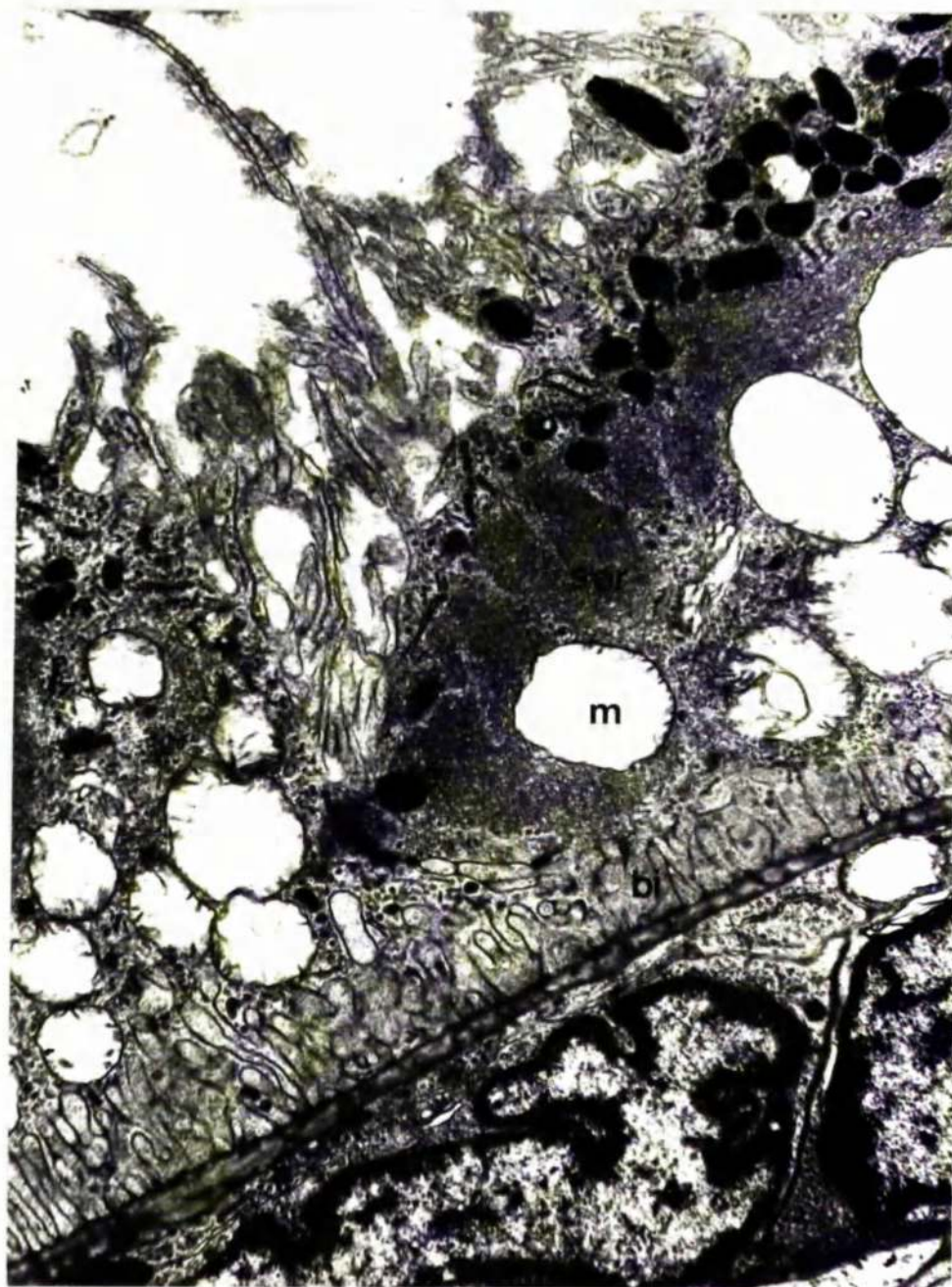


FIG.4-24 Electron micrograph of the retinal pigment epithelium after 120 minutes ischaemia showing the condensed smooth endoplasmic reticulum(SER),distended and ruptured mitochondria(M) and altered basal infoldings(BI).The cell is convexly distorted with patchily distributed pigment granles and apparently intact junctional complex.(16,000 X)

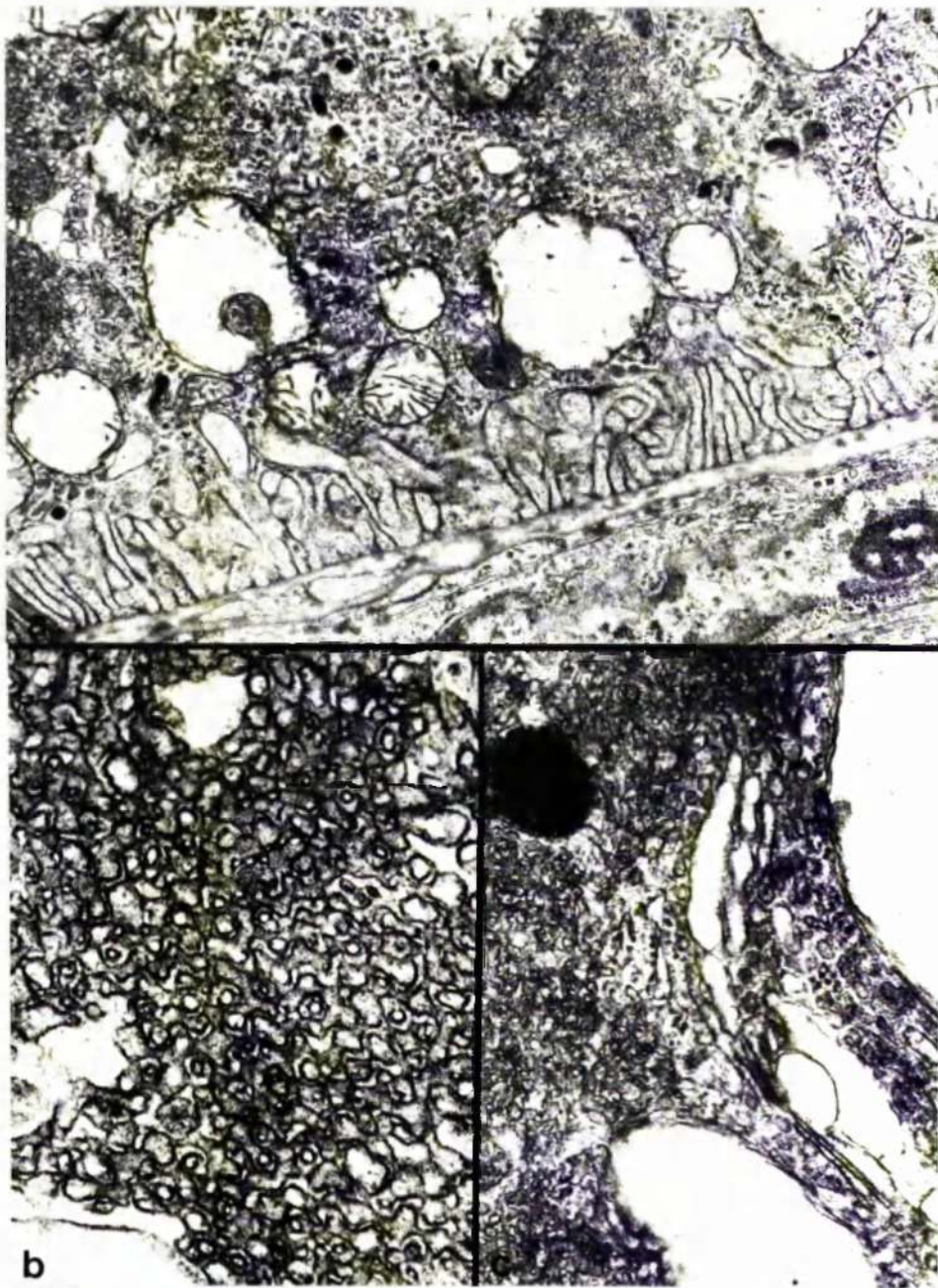


FIG.4-25 Electron micrographs of the various components of the retinal pigment epithelium after 120 minutes ischaemia.a) The basal infoldings are widened and the adjacent mitochondria are distended with few cristae and electron translucent matrix.The occasional mitochondrion contains a nodule of smooth endoplasmic reticulum. (21,000 X),b) The smooth endoplasmic reticulum is compressed. (35,000 X),c) The Golgi apparatus is distended.(22,000 X)

PERIOD OF ISCHAEMIA (MINUTES)

a)

Stage	15				30				60				90			
	V	P	V	P	V	P	V	P	V	P	V	P	V	P	V	P
1	25	21	33	24	41	34	72	49	58	49	52	44	32	27	29	26
2	62	53	68	59	75	46	87	64	95	72	83	67	67	61	56	56
3	117	108	130	119	189	141	232	186	167	155	162	144	132	107	124	103
4	135	109	147	124	256	174	263	215	181	176	186	160	165	154	143	141
5	241	210	272	229	289	218	346	263	294	231	279	224	241	199	237	205
Animal key	1		2		3		4		5		6		7		8	

FIG.4-26 Table showing the number of phagosomes occurring at each stage of degradation immediately after the period of ischaemia in the visual streak(V) and the peripheral retina.(P)

PERIOD OF ISCHAEMIA (MINUTES)

b)

Stage	15				30				60				90			
	V	P	V	P	V	P	V	P	V	P	V	P	V	P	V	P
1	4.3	4.2	5.1	4.2	4.8	5.5	7.0	6.3	7.3	7.1	6.7	6.8	5.0	4.9	4.9	4.9
2	10.7	10.6	10.5	10.5	8.8	7.6	8.5	8.2	11.9	10.5	12.0	10.4	10.5	11.1	9.5	10.5
3	20.2	21.2	20.0	21.5	22.3	23.0	22.7	23.9	21.0	23.0	21.0	22.3	20.7	19.5	21.1	19.4
4	23.3	21.8	22.6	22.4	30.2	28.4	27.7	27.7	22.6	25.7	24.1	25.7	25.9	26.1	24.3	26.6
5	41.6	42.1	41.8	41.3	33.9	35.6	34.1	33.8	37.0	33.7	36.1	34.7	37.8	36.3	40.2	38.6
Animal key	1		2		3		4		5		6		7		8	

FIG.4-27 Table showing the percentage distribution of the various phagosome stages immediately after the period of ischaemia in the visual streak(V) and peripheral retina(P).



Fig.4-28 Electron micrograph of the fragmented and focally distended visual cell outer segments after 30 minutes ischaemia. An occasional relatively normal outer segment(OS) occurs. (15,000 X)



FIG.4-29 Electron micrograph of the outer segments after 120 minutes ischaemia showing their disorganised and fragmented nature. Many of the outer segment fragments are swollen and found amongst fragments originating from the inner segments(IS). (15,000 X)



FIG.4-30 Electron micrograph of the inner segments following 30 minutes ischaemia. The mitochondria(M) have a reduced matrix electron density and are slightly swollen. The cytoplasm of the myoid region is generally oedematous with the occasional intracellular space(LS).(10,000 X)

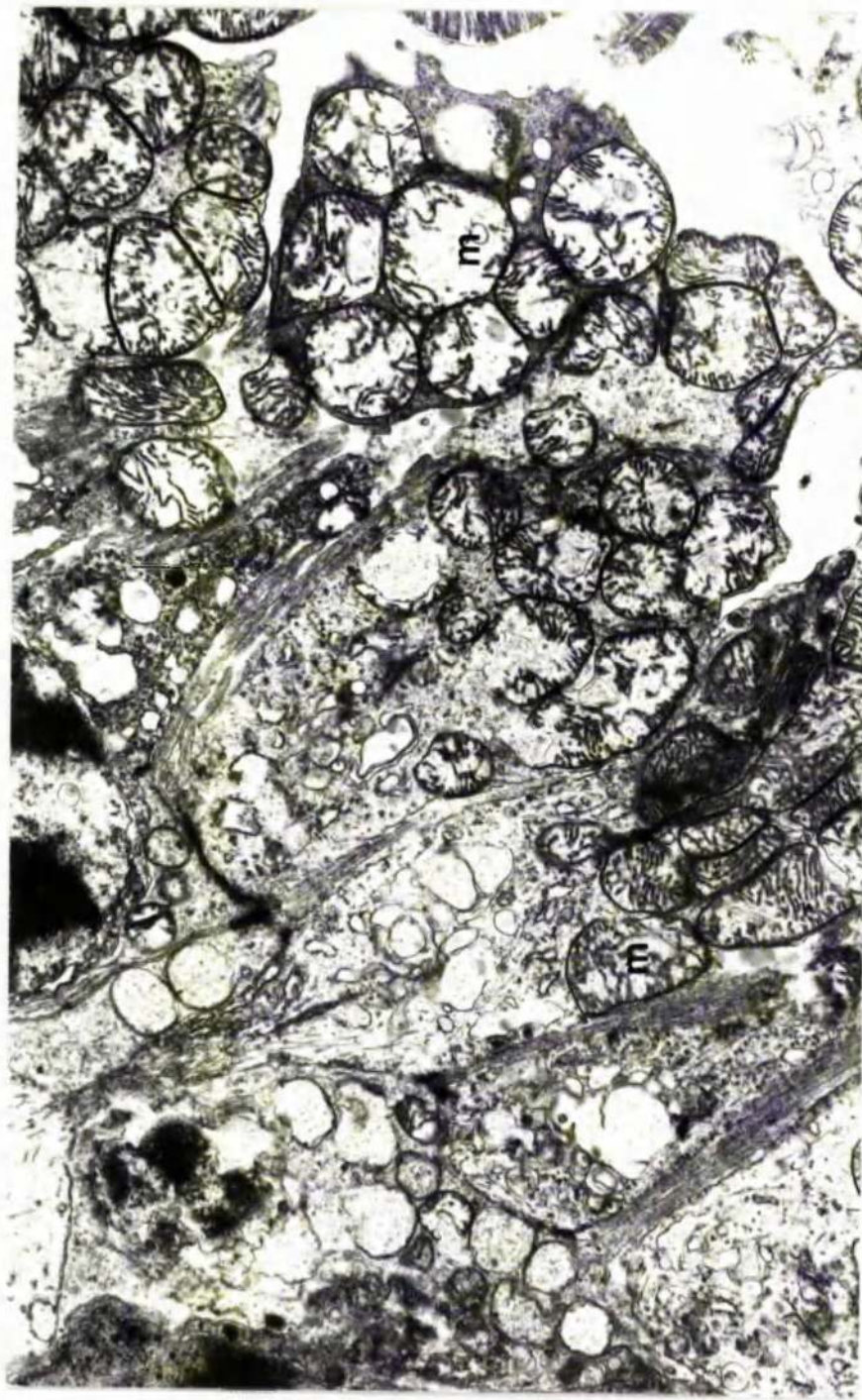


FIG.4-51 Electron micrograph of the inner segments after 60 minutes ischaemia. The mitochondria (M) are rounded and distended with a matrix of low electron density. The cristae are often abnormal and the occasional mitochondria are ruptured. (15,000 X)

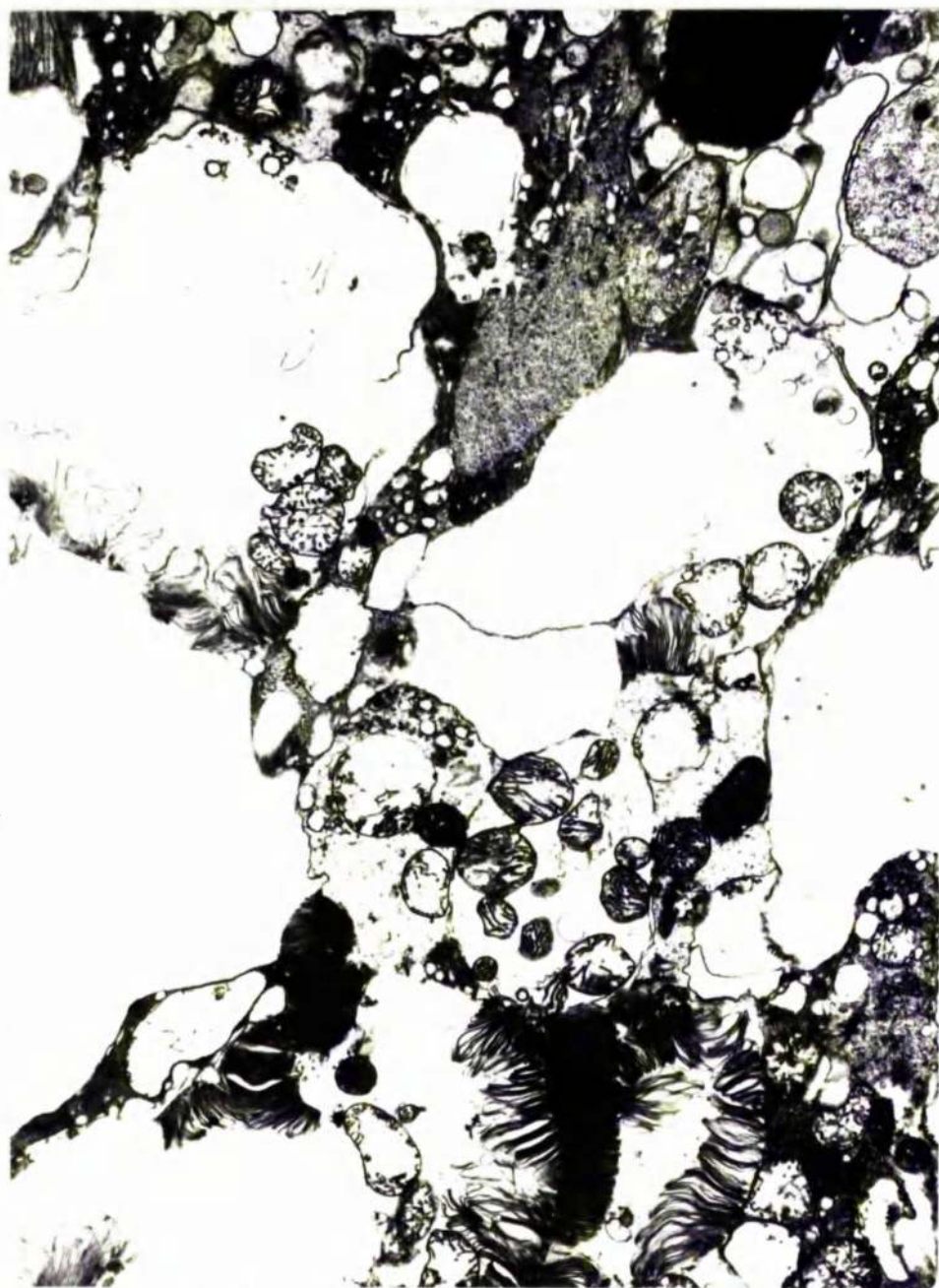


FIG.4-32 Electron micrograph of the inner segments after 120 minutes ischaemia, they are frequently swollen and ruptured. The cytoplasm of the inner segments is electron translucent. (10,000X)

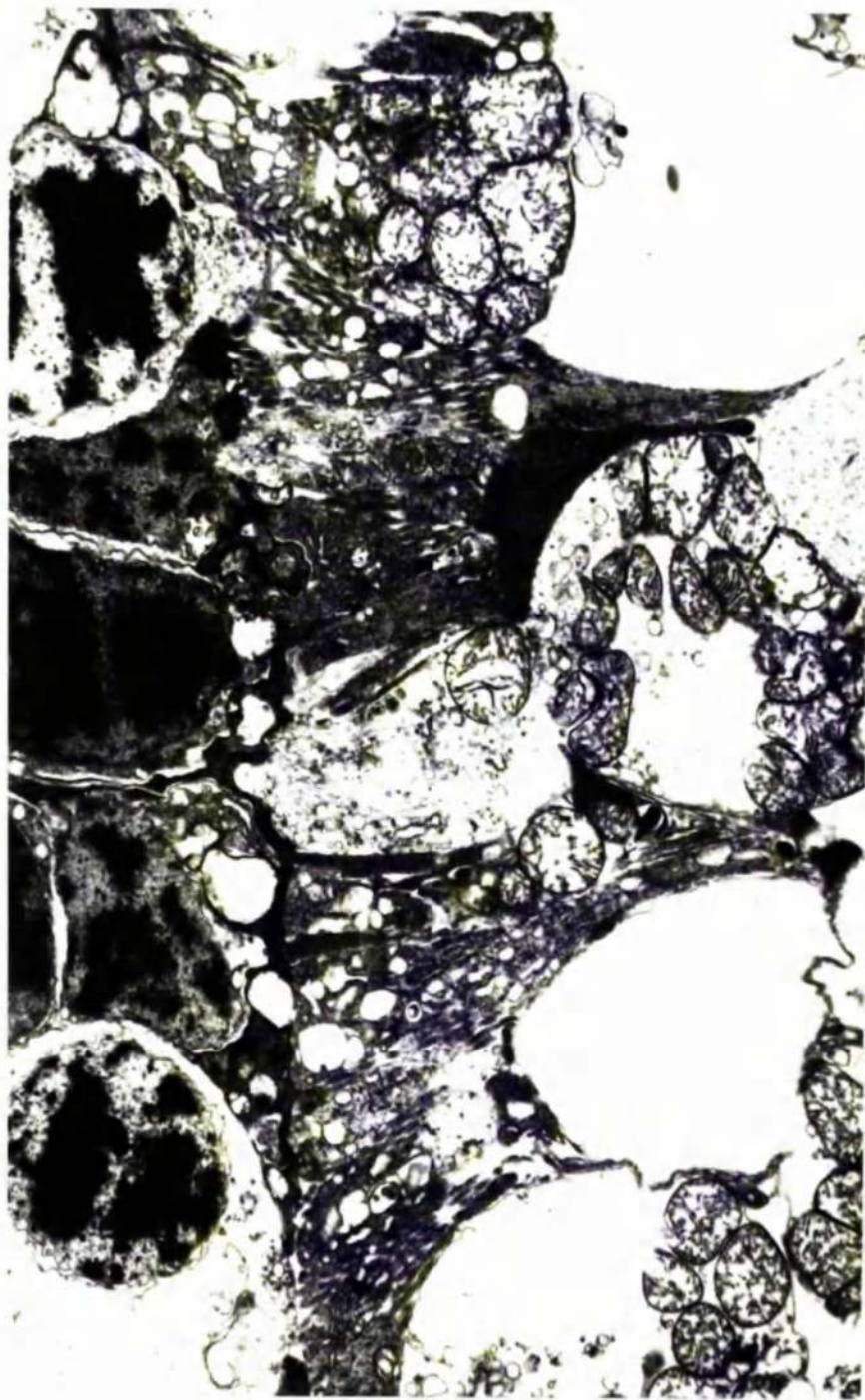


FIG.4-33 Electron micrograph of the external limiting membrane after 120 minutes ischaemia.
The junctions between the Muller cells and the visual cells remain intact. (15,000 X)

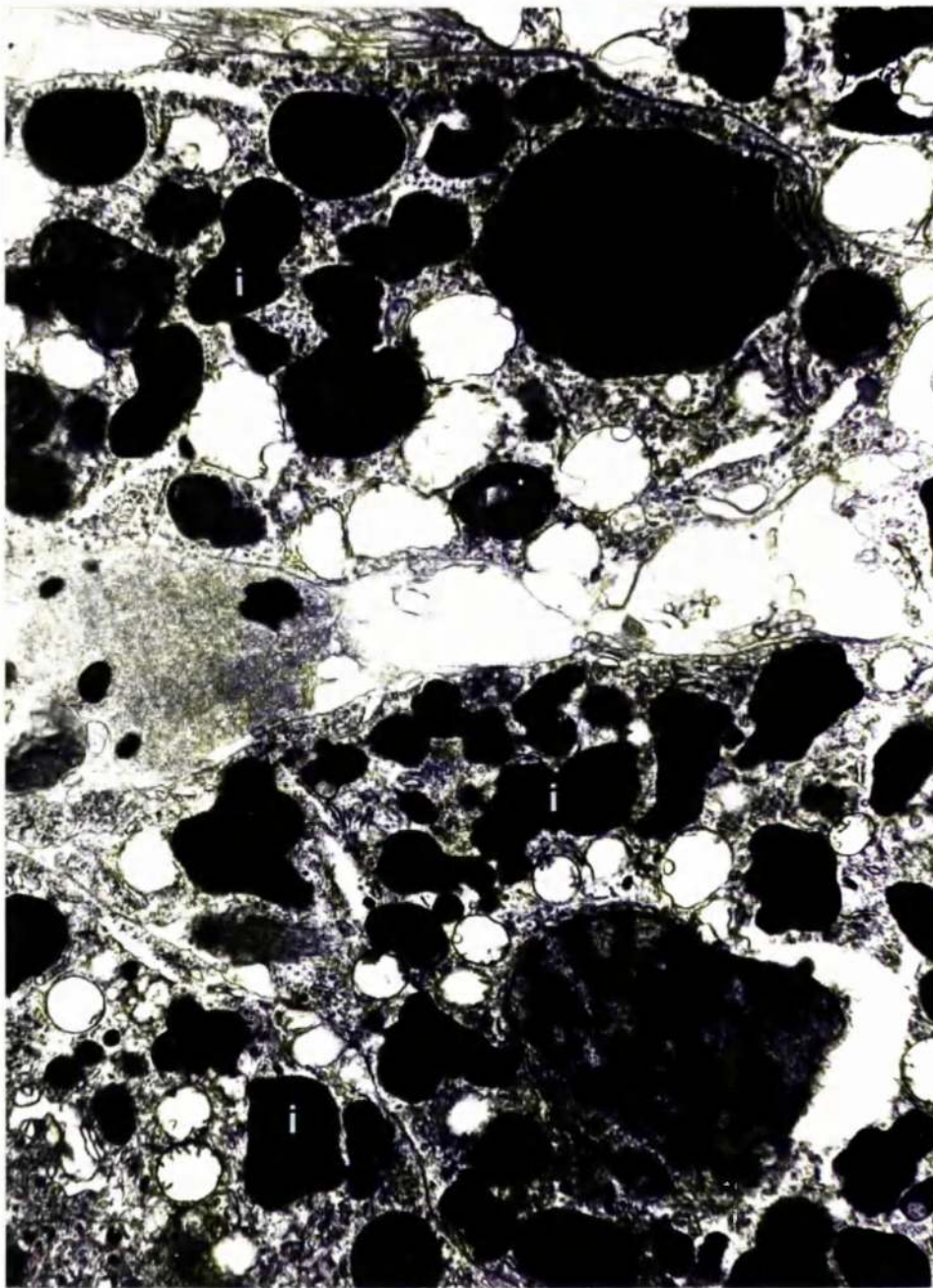


FIG.4-34 Electron micrograph of the macrophages which are commonly observed following periods of ischaemia. The cells contain many electron dense inclusion bodies(I) and swollen mitochondria. (120 minutes ischaemia, 6,000 X)

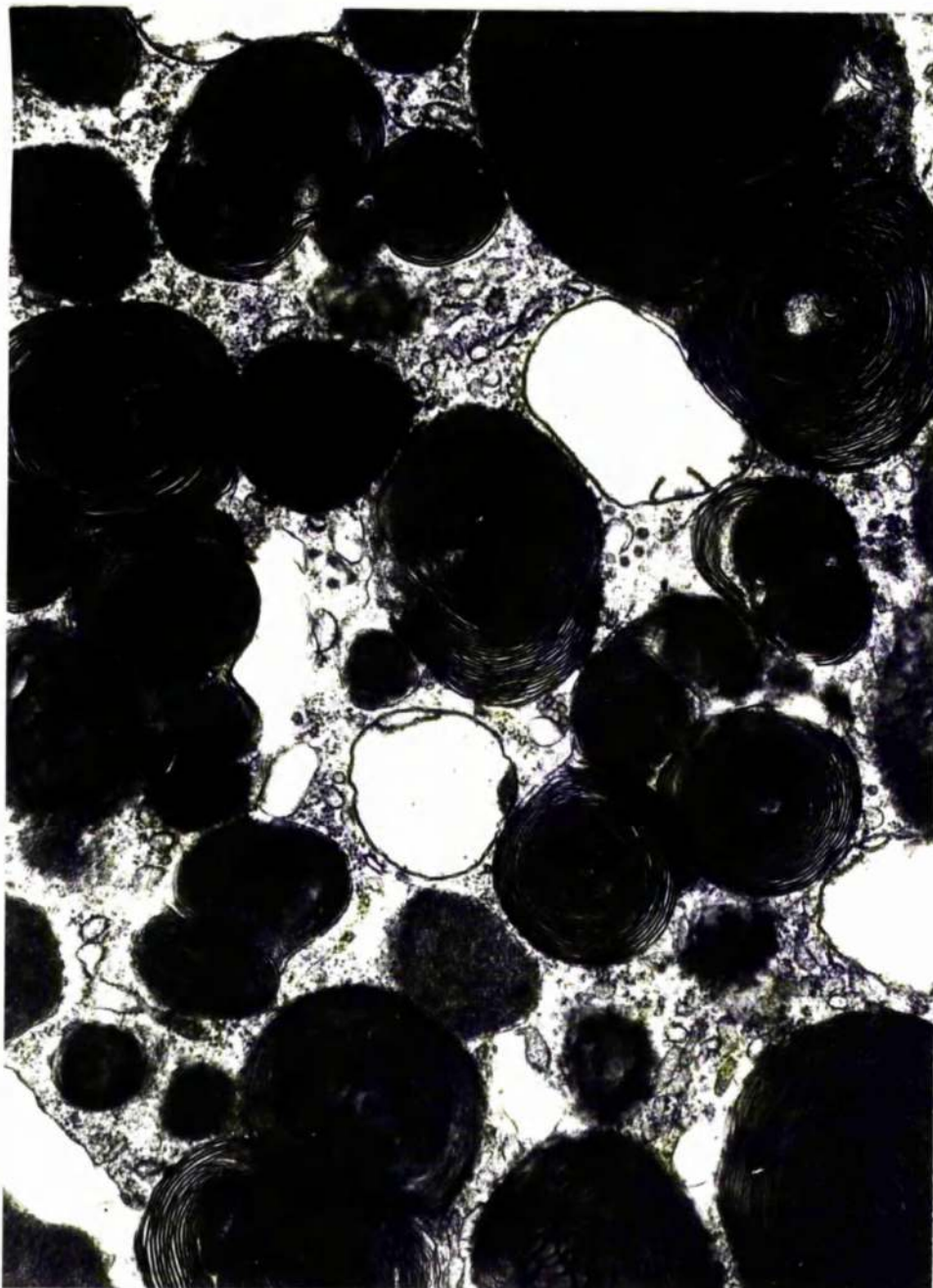


FIG.4-35 Electron micrograph of the macrophagic inclusion bodies containing membranous material. The distended mitochondria have few cristae and an electron translucent matrix. Smooth and rough endoplasmic reticulum occur within the cytoplasm. (90 minutes ischaemia, 30,000 X)

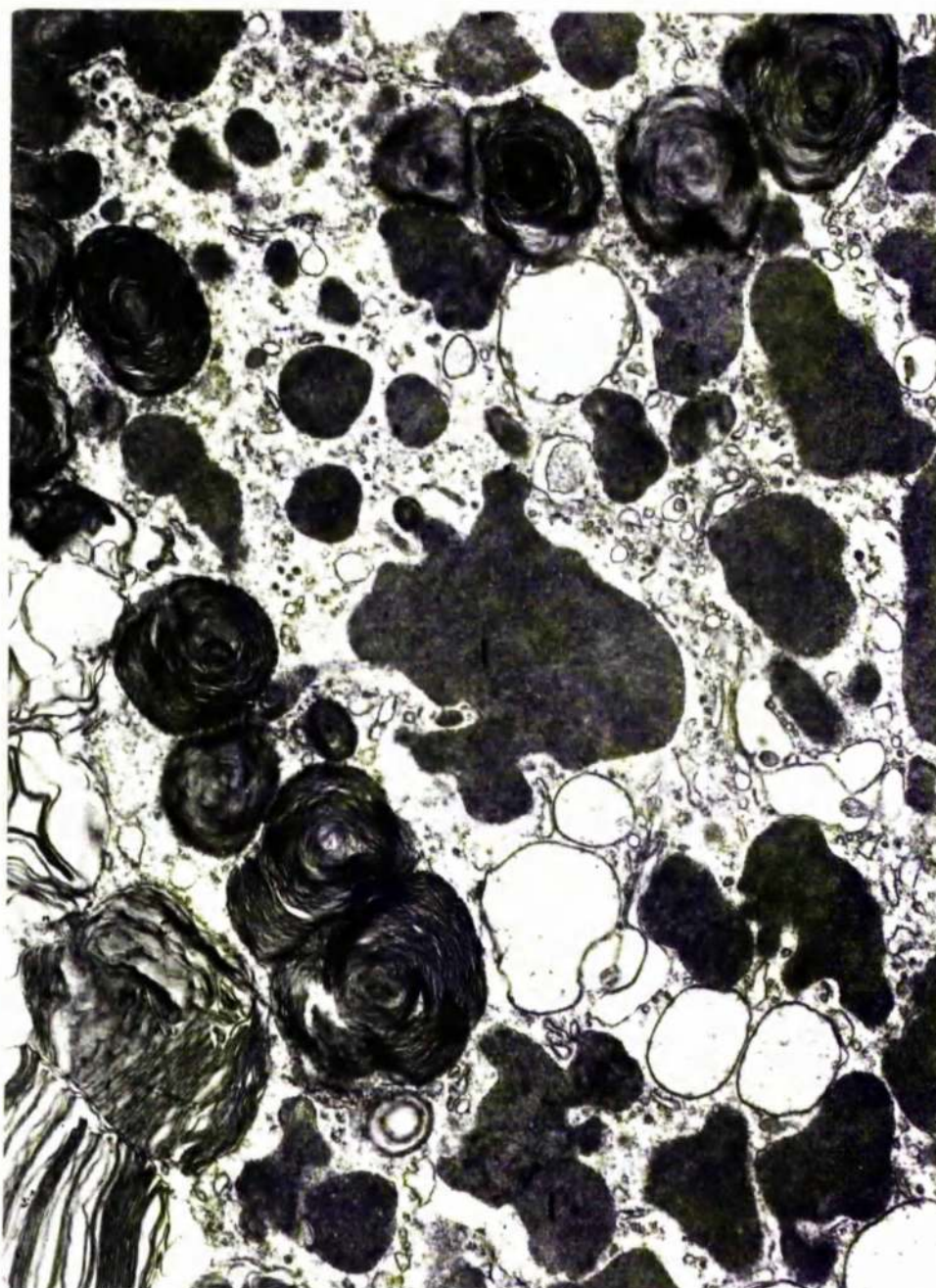


FIG.4-36 Electron micrograph illustrating the wide size range of the often irregularly shaped lysosomal bodies(L) which occur within the macrophagic cytoplasm.(60 minutes ischaemia, 20,000 X)

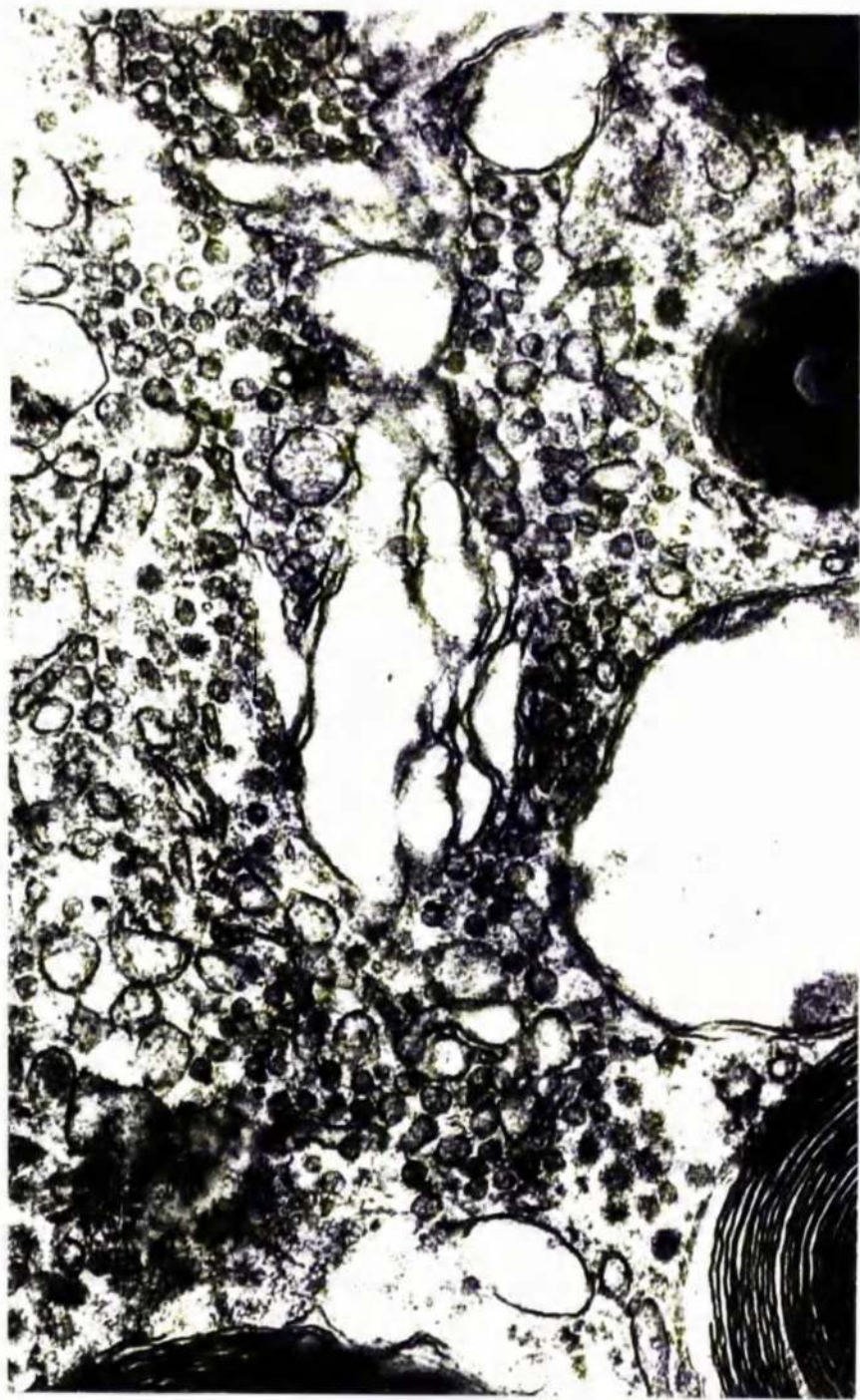


FIG. 4-37 Electron micrograph of the Golgi apparatus and surrounding cytoplasm of a macrophage found in the sub-retinal space after 60 minutes ischaemia. Many smooth and rough coated vesicles are seen close to the Golgi apparatus although the former are more frequent. (45,000 X)

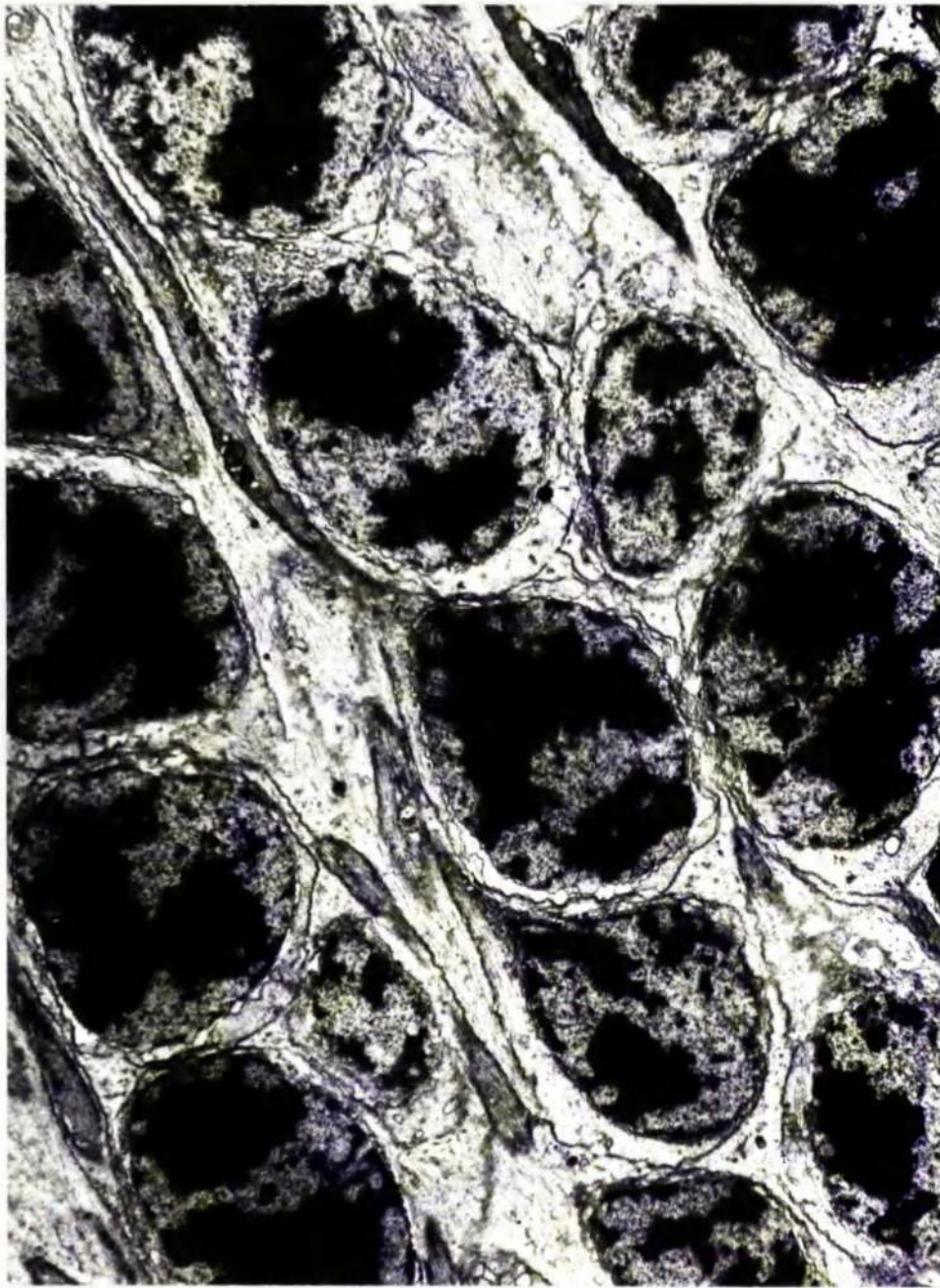


FIG.4-38 Electron micrograph of the outer nuclear layer following 15 minutes ischaemia. There are limited focal separations of the membranes of the nuclear envelope, the nuclei otherwise appear normal. (11,000 X)

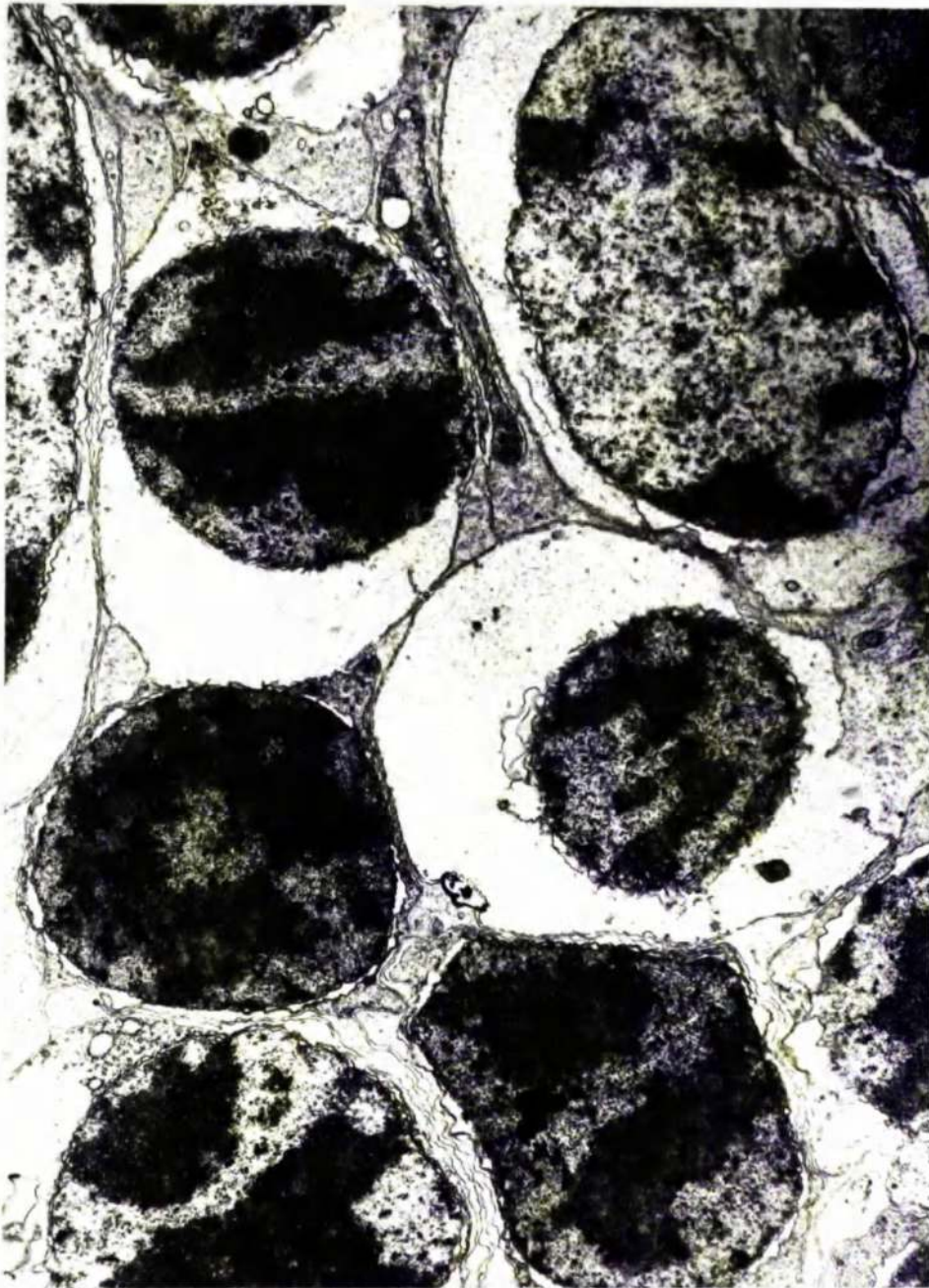


FIG.4-39 Electron micrograph of the outer nuclear layer after 60 minutes ischaemia. The rounded nuclei are surrounded by a halo of oedematous cytoplasm. (18,000 X)

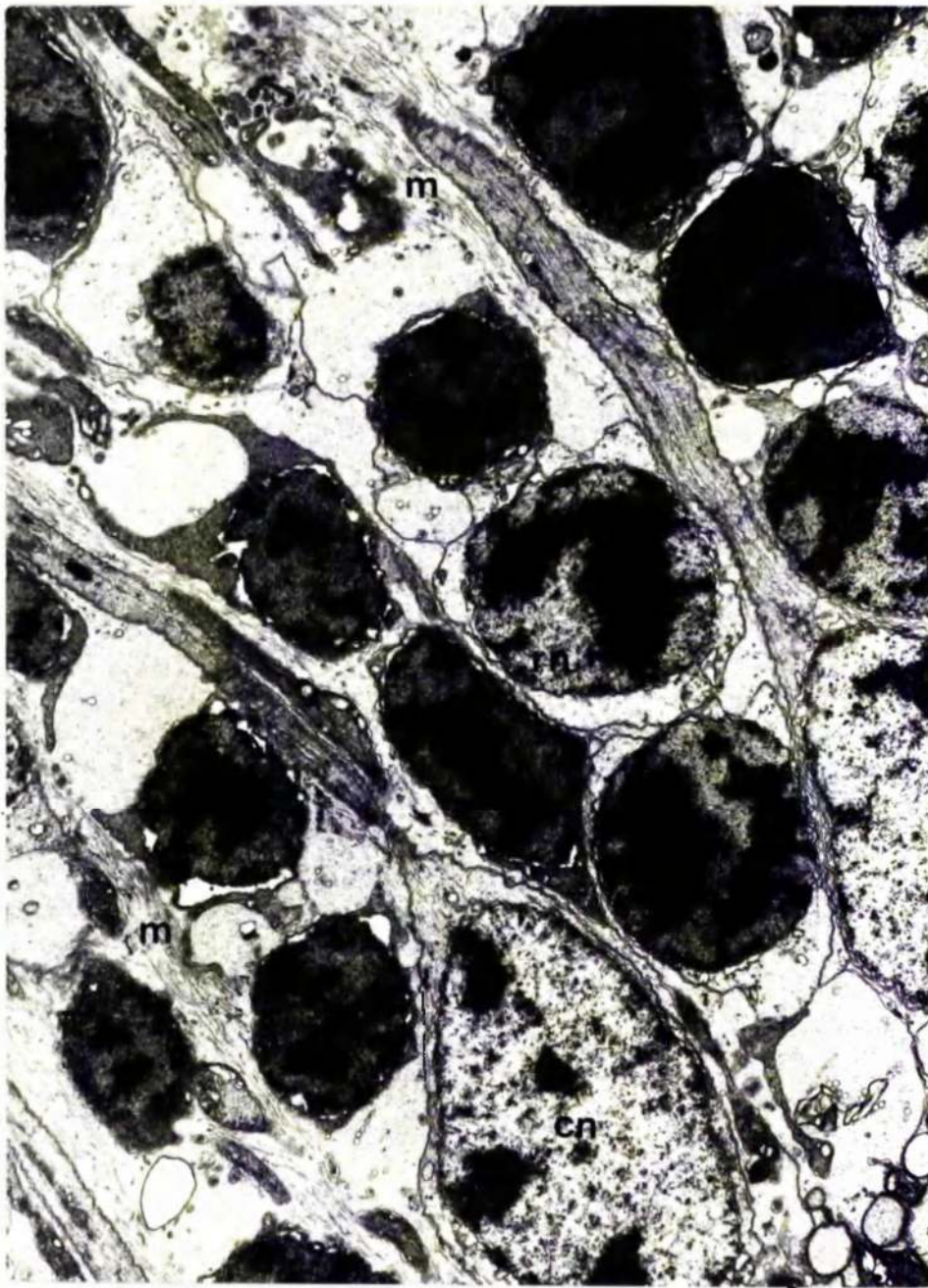


FIG.4-40 Electron micrograph of the outer nuclear layer after 120 minutes ischaemia. The cone nuclei (CN) are less affected than their rod counterparts (RN). The inner and outer receptor fibres are affected by mild vacuolation. The oedematous nature of the Muller cell (X) cytoplasm exposes the fibrillar content of the cell. (10,000 X)

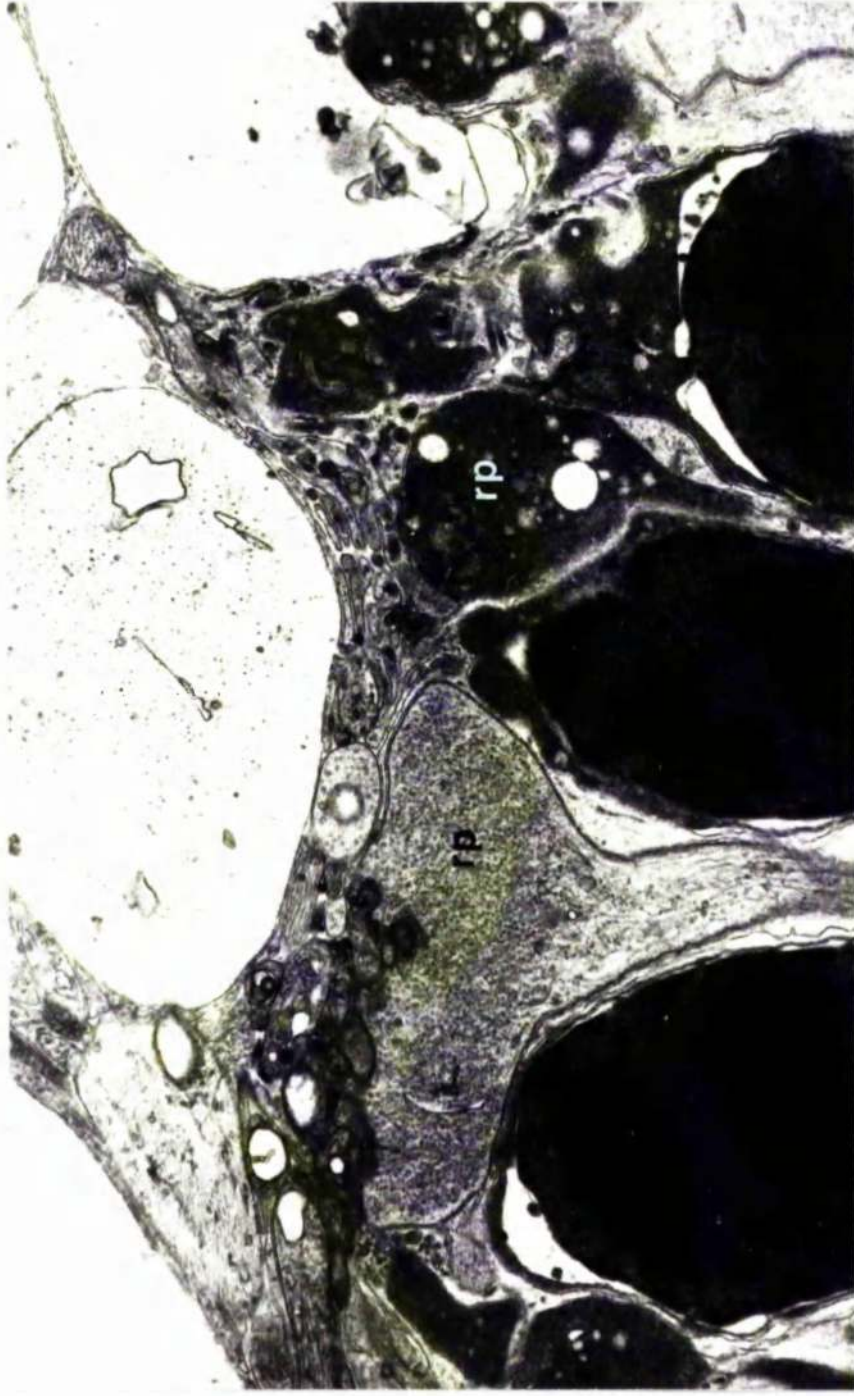


FIG.4-41 Electron micrograph of the receptor pedicles following 120 minutes ischaemia showing the extreme degeneration that can occur in the rod pedicles(rp).The cone pedicle(cp) is relatively unaffected.Several of the processes of the outer plexiform layer are severely distended.(14,000 X)

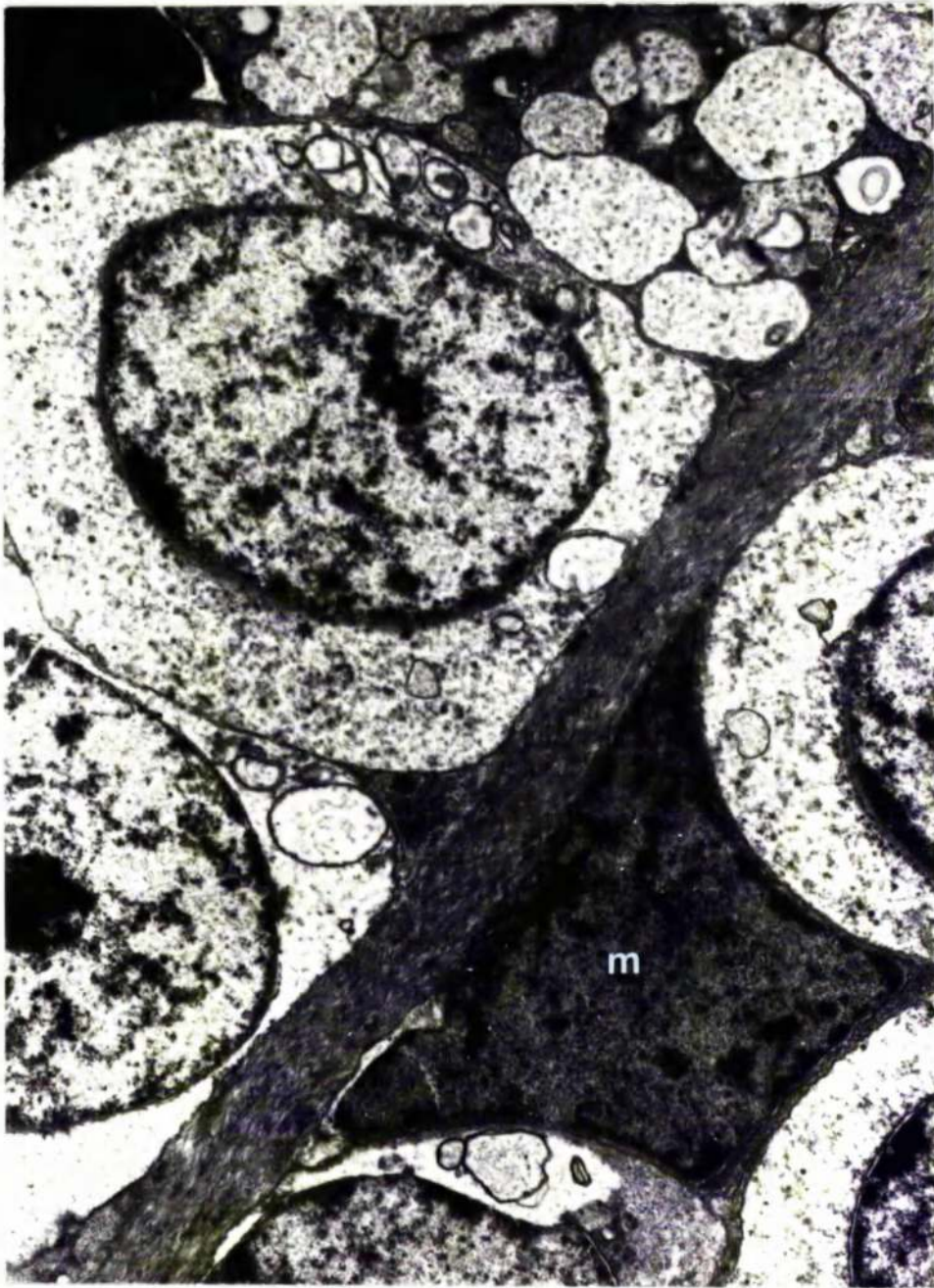


FIG.4-42 Electron micrograph of the inner nuclear layer following 60 minutes ischaemia. There is a generalised swelling of the cytoplasm of the neural cells while the Muller cells(M) appears relatively normal. (15,000 X)

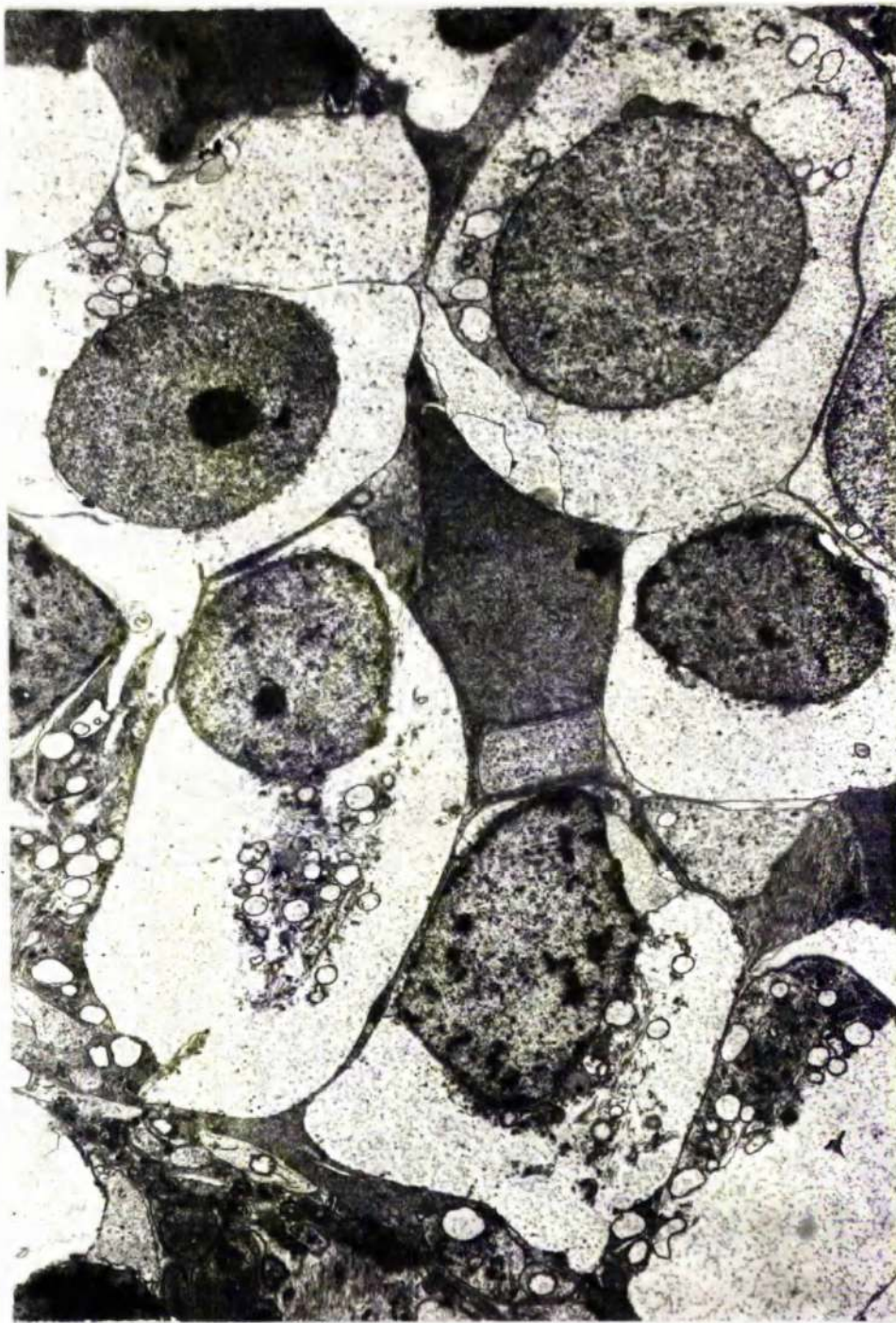


FIG. 4-43 Electron micrograph of the inner nuclear layer after 90 minutes ischaemia. The cytoplasm of the neural cells is extremely oedematous. The cell organelles often form a clump adjacent to the nucleus. The Muller cells appears normal. (10,000 X)

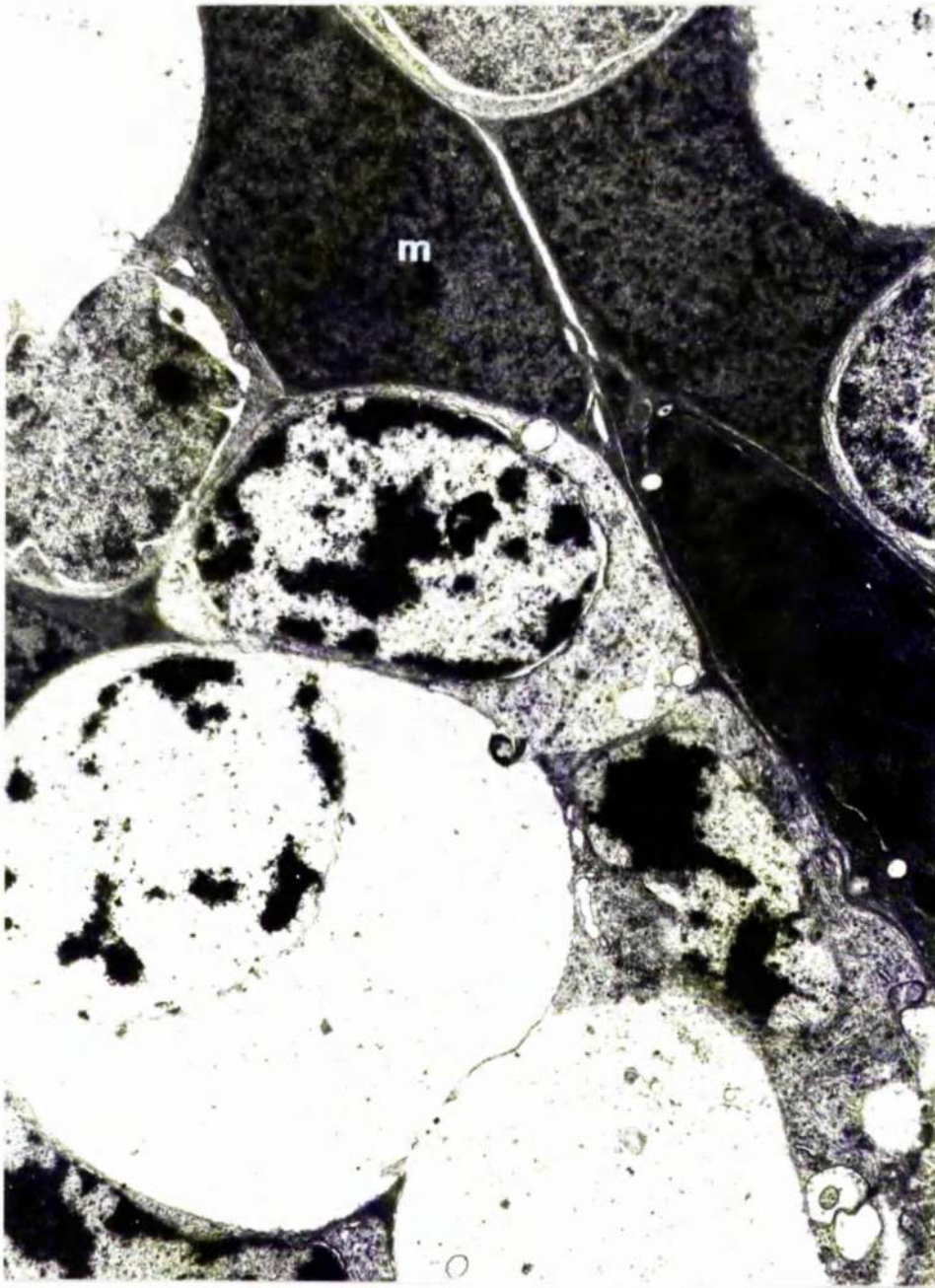


FIG.4-44 Electron micrograph of the inner nuclear layer following 120 minutes ischaemia. The neural cells have pyknotic nuclei and an oedematous cytoplasm. In spite of these degenerate cells the adjacent Muller cells (M) remain normal in appearance. (15,000 X)

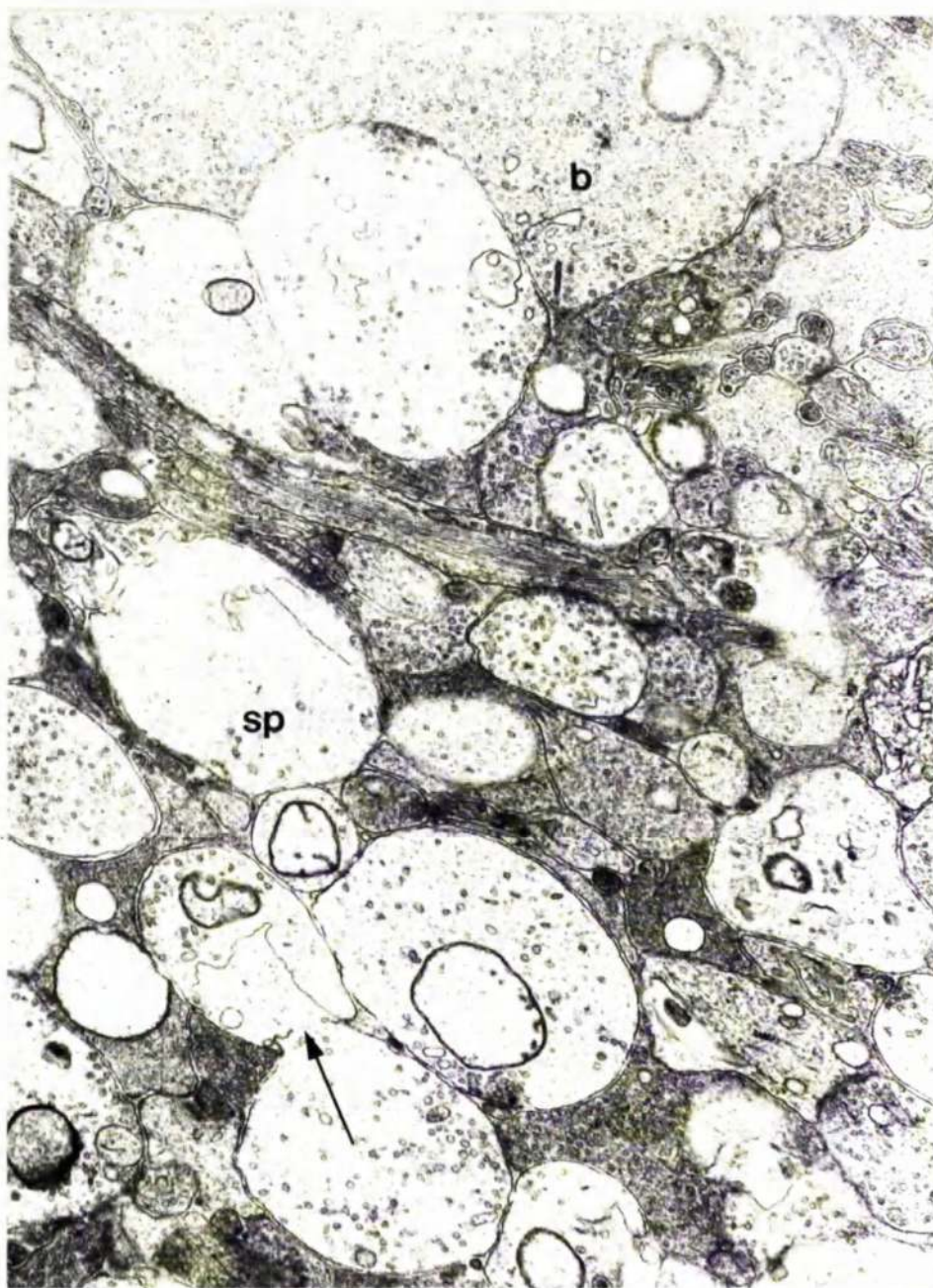


FIG.4-45 Electron micrograph of the inner plexiform layer after 30 minutes ischaemia. Some of the processes appear to be swollen (SP) and this is occasionally associated with ruptured cell membranes (arrow). The recognisable bipolar cell processes appear normal (B). (17,000 X)

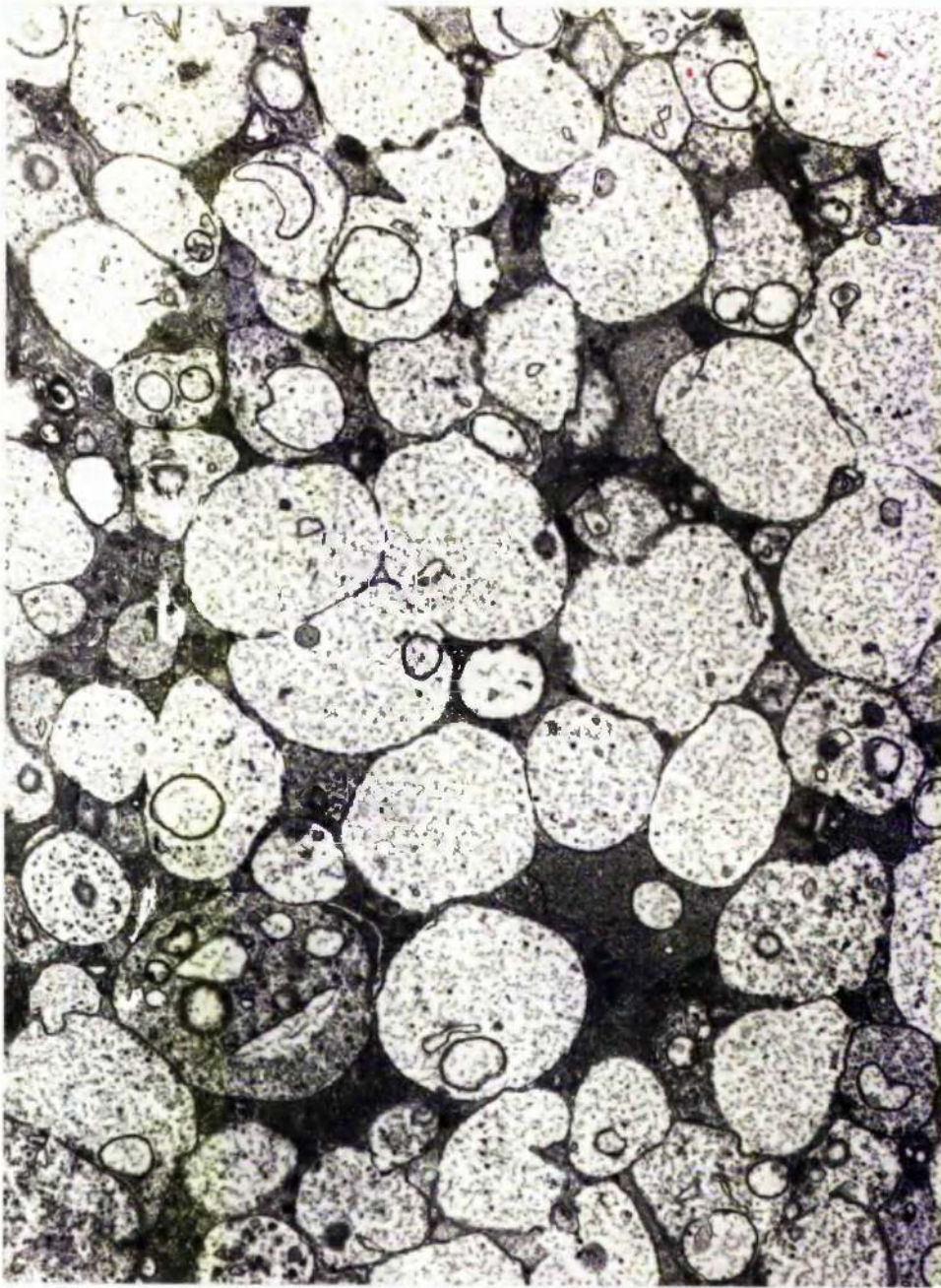


FIG.4-46 Electron micrograph of the inner plexiform layer after 90 minutes ischaemia. The majority of the processes have a flocular cytoplasm containing a few neurotubules, neurofibrils and vesicles. Processes with ruptured membranes are frequently observed. (12,000 X)



FIG.4-47 Electron micrograph of the inner plexiform layer after 120 minutes ischaemia showing the oedematous nature of many of the processes. Ribbon synapses(RS) can still be identified in the processes of the bipolar cells. The Muller cell cytoplasm(MC) is more electron dense than the surrounding cytoplasm. (10,000 X)



FIG.4-48 Electron micrograph of the ganglion cells after 30 minutes ischaemia. Focal distensions of the nuclear envelope are present(F). (19,000 X)

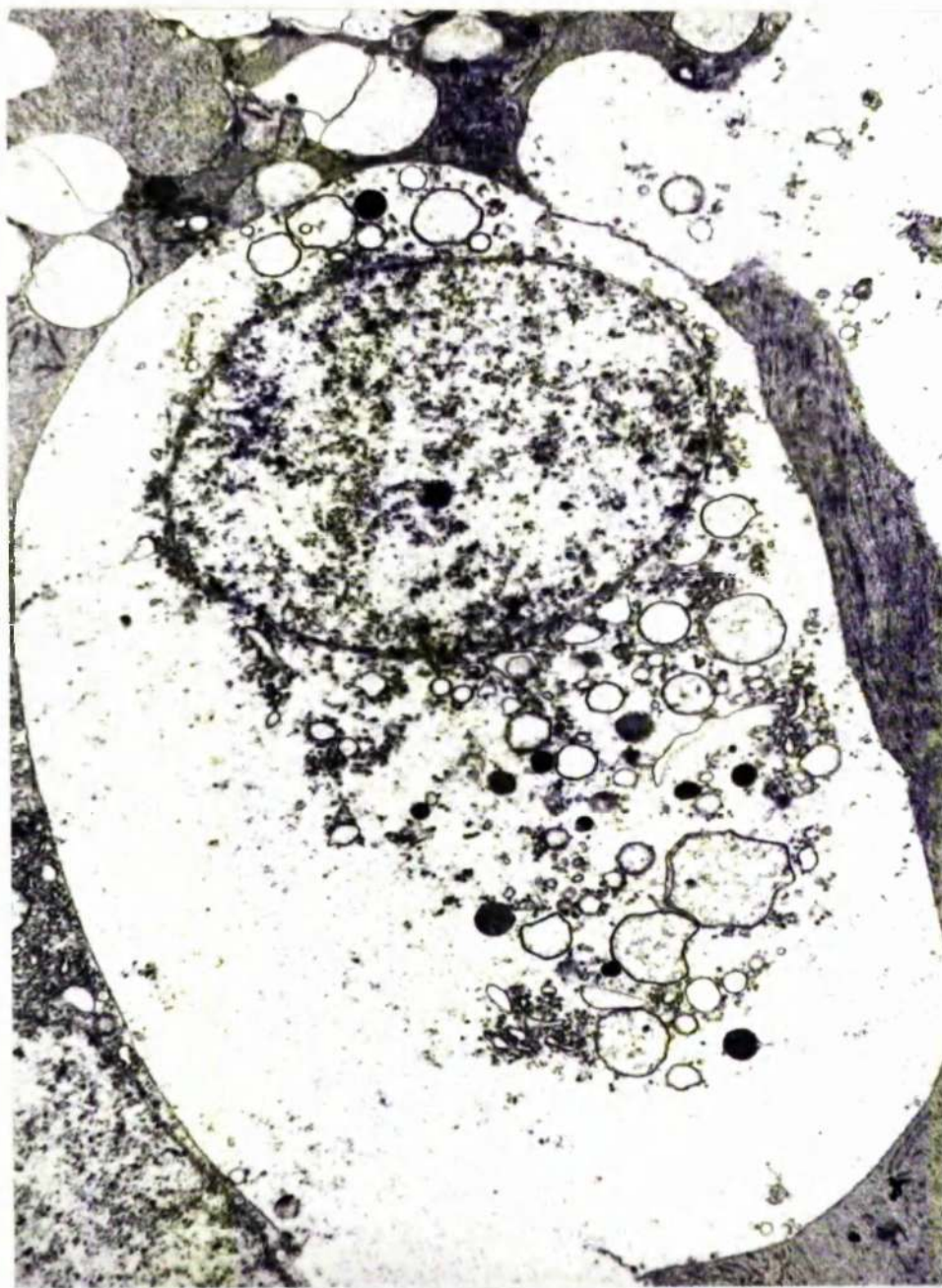


FIG.4-49 Electron micrograph of the ganglion cell layer after 90 minutes ischaemia showing the oedematous nature of the cytoplasm of a ganglion cell. The cell contents form a mass adjacent to the nucleus. (20,000 X)

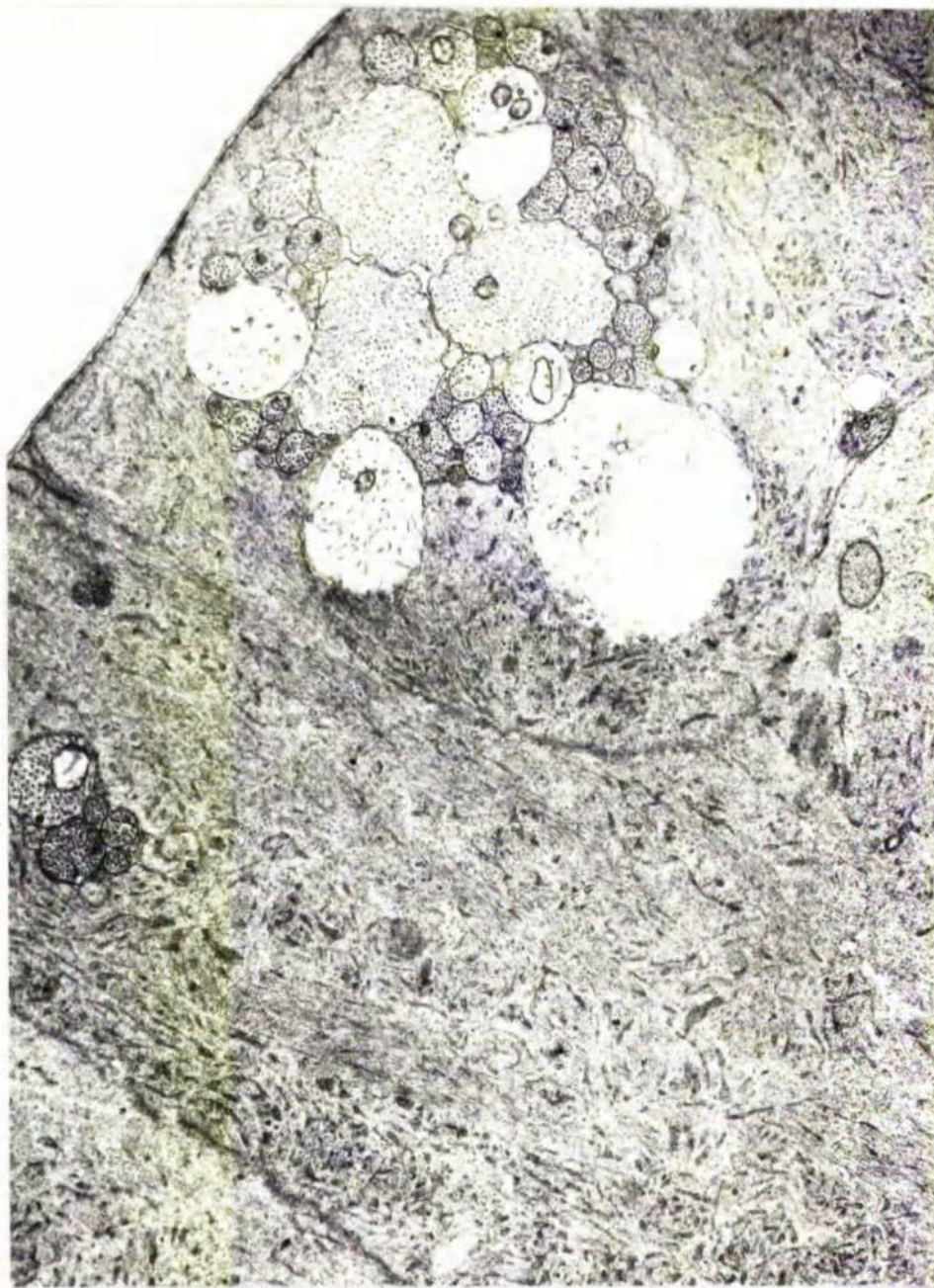


FIG.4-50 Electron micrograph of the unmyelinated nerve fibres of the peripheral retina after 15 minutes ischaemia. The smaller fibres appear normal while the larger fibres are swollen with a loss or reduction in the number of the neurotubules and neurofibrils contained within them. (13,000 X)



FIG.4-5I Electron micrograph of the cytoplasm of a glial cell following 60 minutes ischaemia showing several inclusion bodies containing membranous and electron dense debris.(13,000 X)

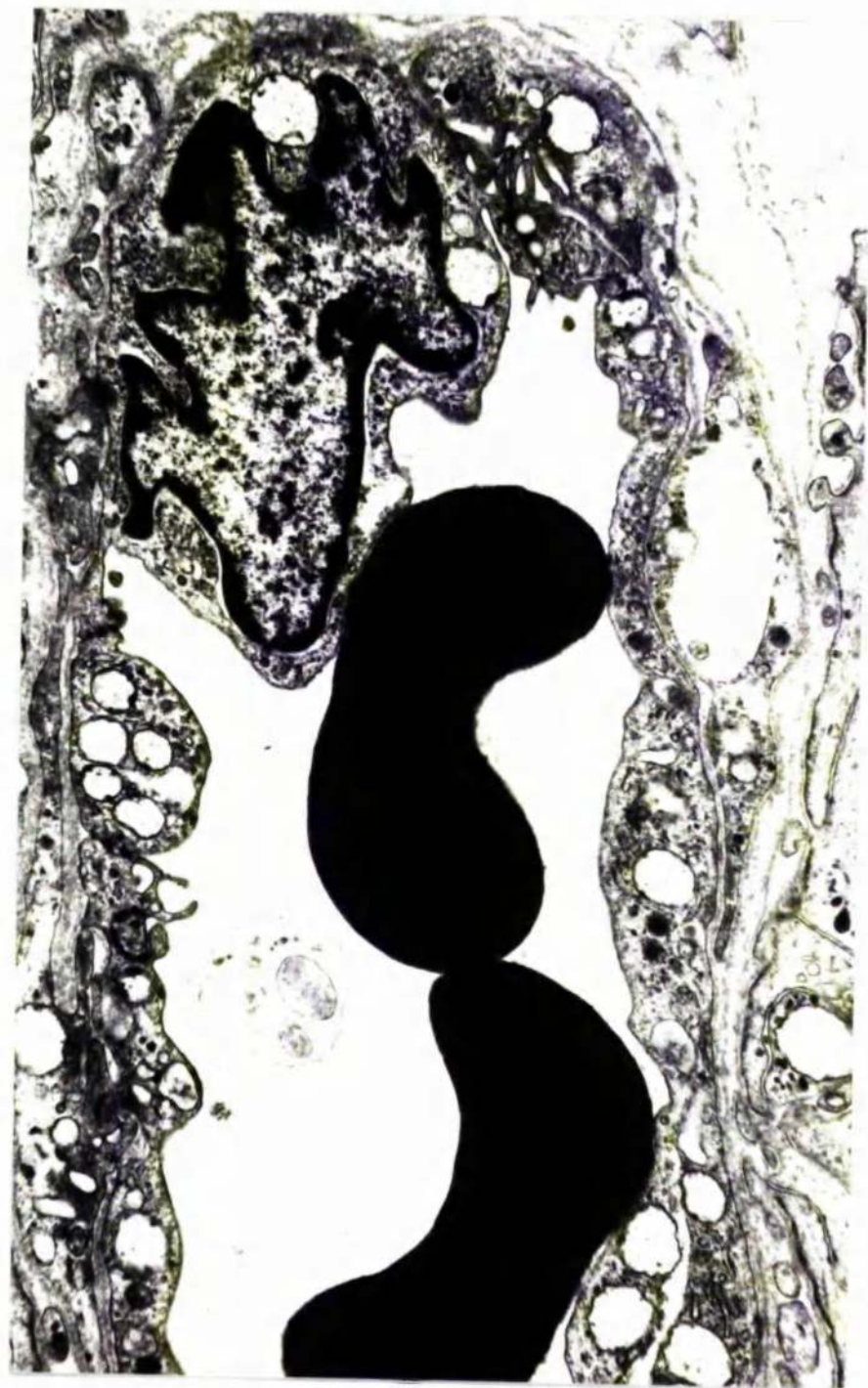


FIG.4-52 Electron micrograph of a retinal blood vessel after 60 minutes ischaemia showing the frequent vacuoles which occur in the endothelial wall of the vessel. The endothelial wall however appears intact. (10,000 X)

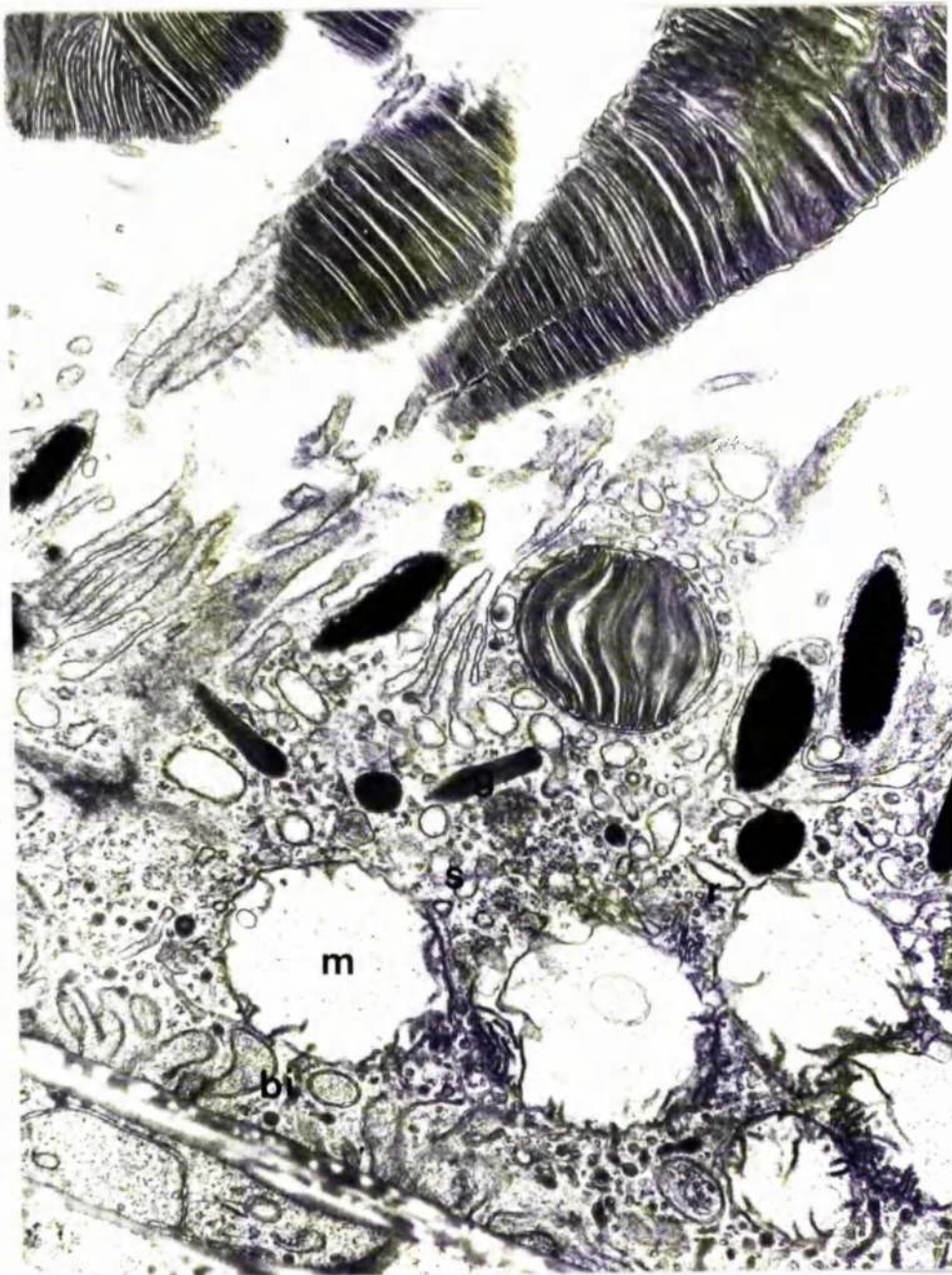


FIG.4-53 Electron micrograph of the pigment epithelium 30 minutes post-mortem(room-temperature).The basal infoldings(BI) and the mitochondria(R) are severely affected.The rough endoplasmic reticulum(R) and the smooth endoplasmic reticulum(S) are swollen.The occasional immature melanin granule(G) is seen in the cytoplasm. (12,000 X)



FIG.4-14 Electron micrograph of the pigment epithelium 90 minutes post-mortem (room-temperature). The cell is severely degenerate with condensed smooth endoplasmic reticulum and distended mitochondria. (15,000 X)



FIG. 4-55 Electron micrograph of a pigment epithelial nucleus 90 minutes post-mortem (room-temperature). The nucleus appears relatively normal. The apical surface of the cell is associated with swollen fragments of outer segment material. (16,000 X)



FIG.4-56 Electron micrograph of the outer segments 60 minutes post-mortem(room-temperature).The outer segments are fragmented, some of which are swollen and ruptured.Fragments of inner segment material also occur.(II,000 X)



FIG.4-57 Electron micrograph of the inner segments 30 minutes post-mortem(room-temperature).The mitochondria of the ellipsoid region are swollen and there is an apparent shortening of the inner segments.(14,000 X)

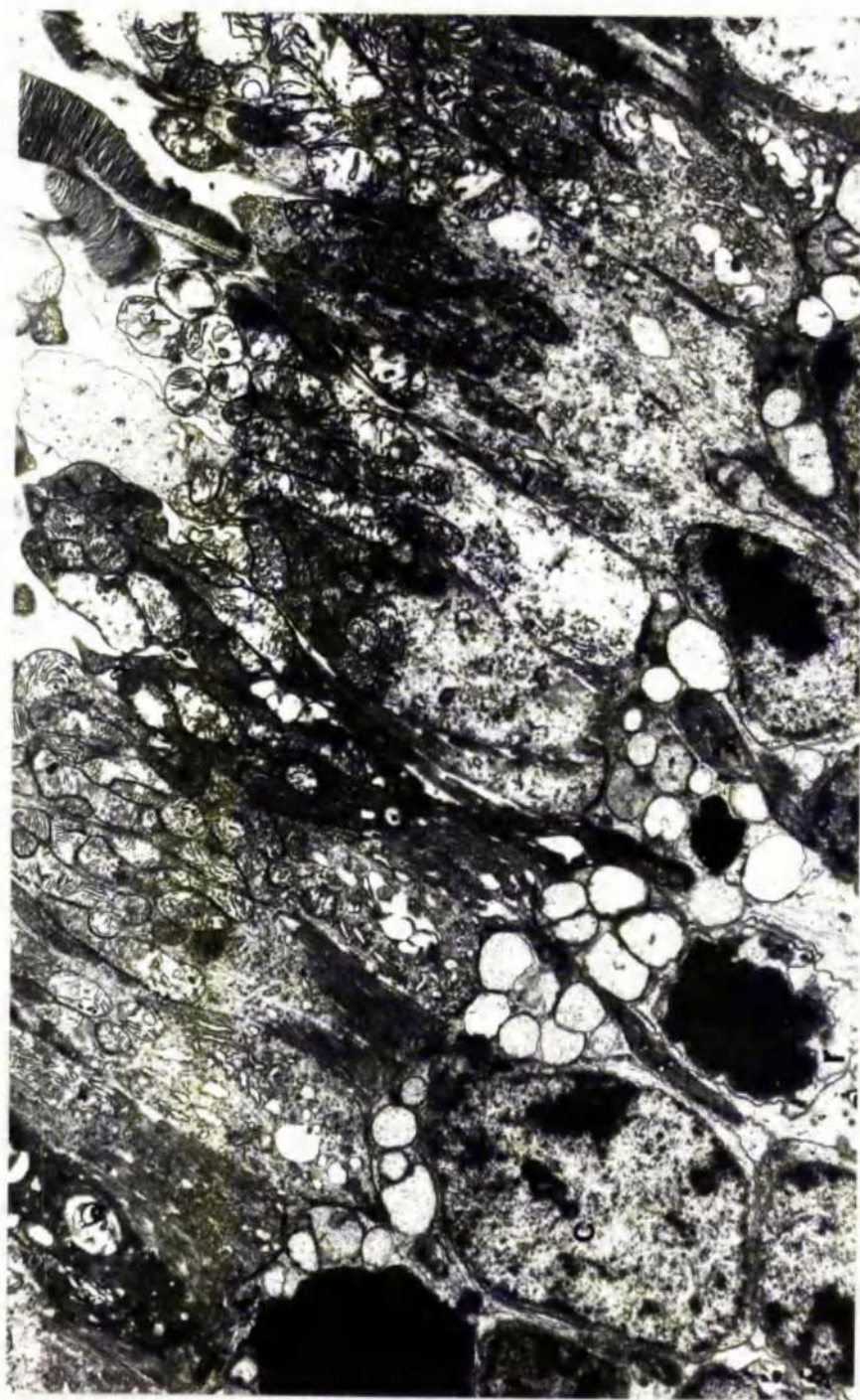


FIG.4-58 Electron micrograph of the inner segments and the outer nuclear layer 60 minutes post-mortem(room-temperature).The cone nuclei(C) are less affected than their rod counterparts(R).
(11,000 X)

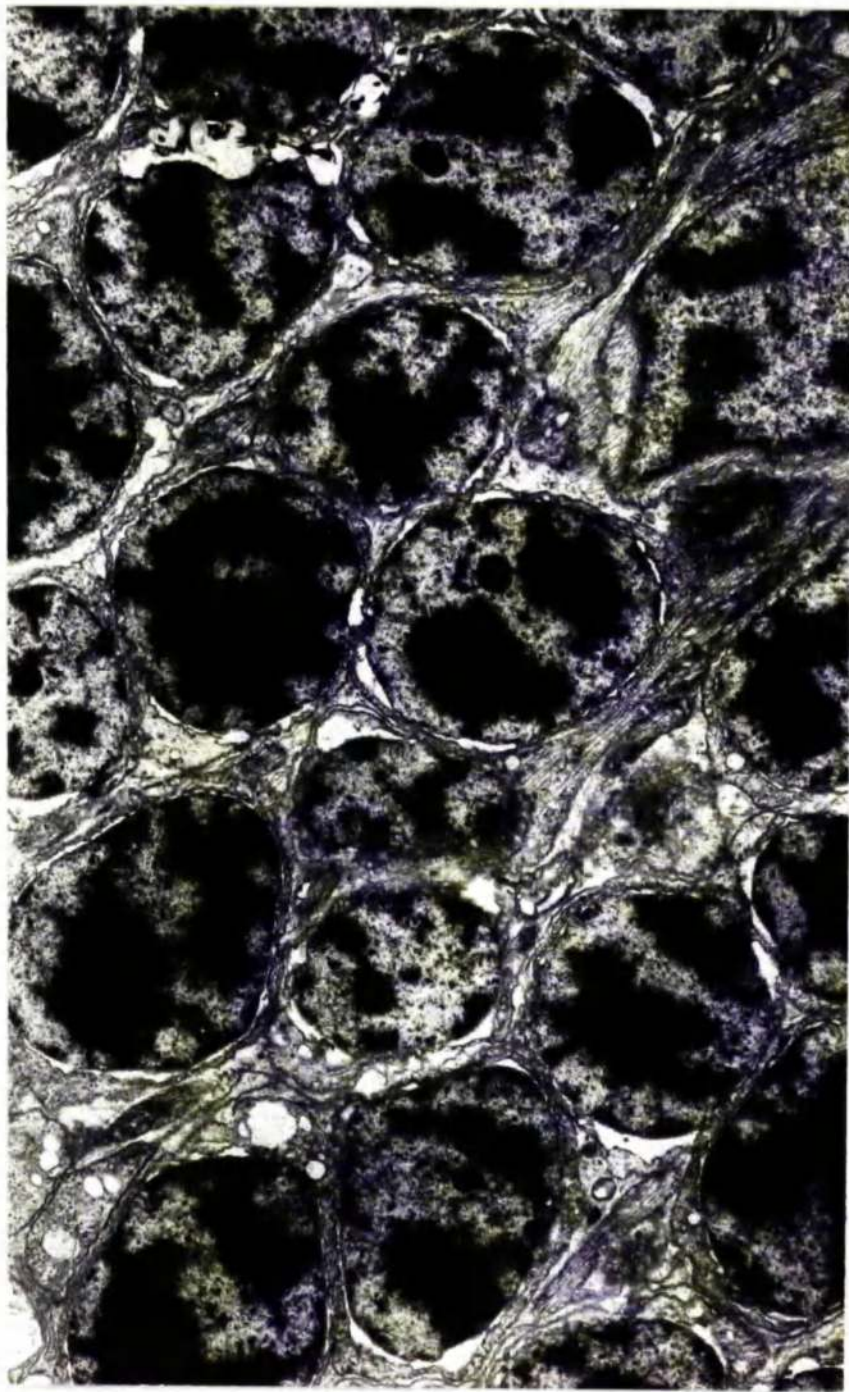


FIG. 4-59 Electron micrograph of the outer nuclear layer 30 minutes post-mortem (room-temperature). The visual cell nuclei are surrounded by a nuclear envelope which is focally distended. The nuclei of the rod cells are more rounded than their control counterparts. (12,000 X)

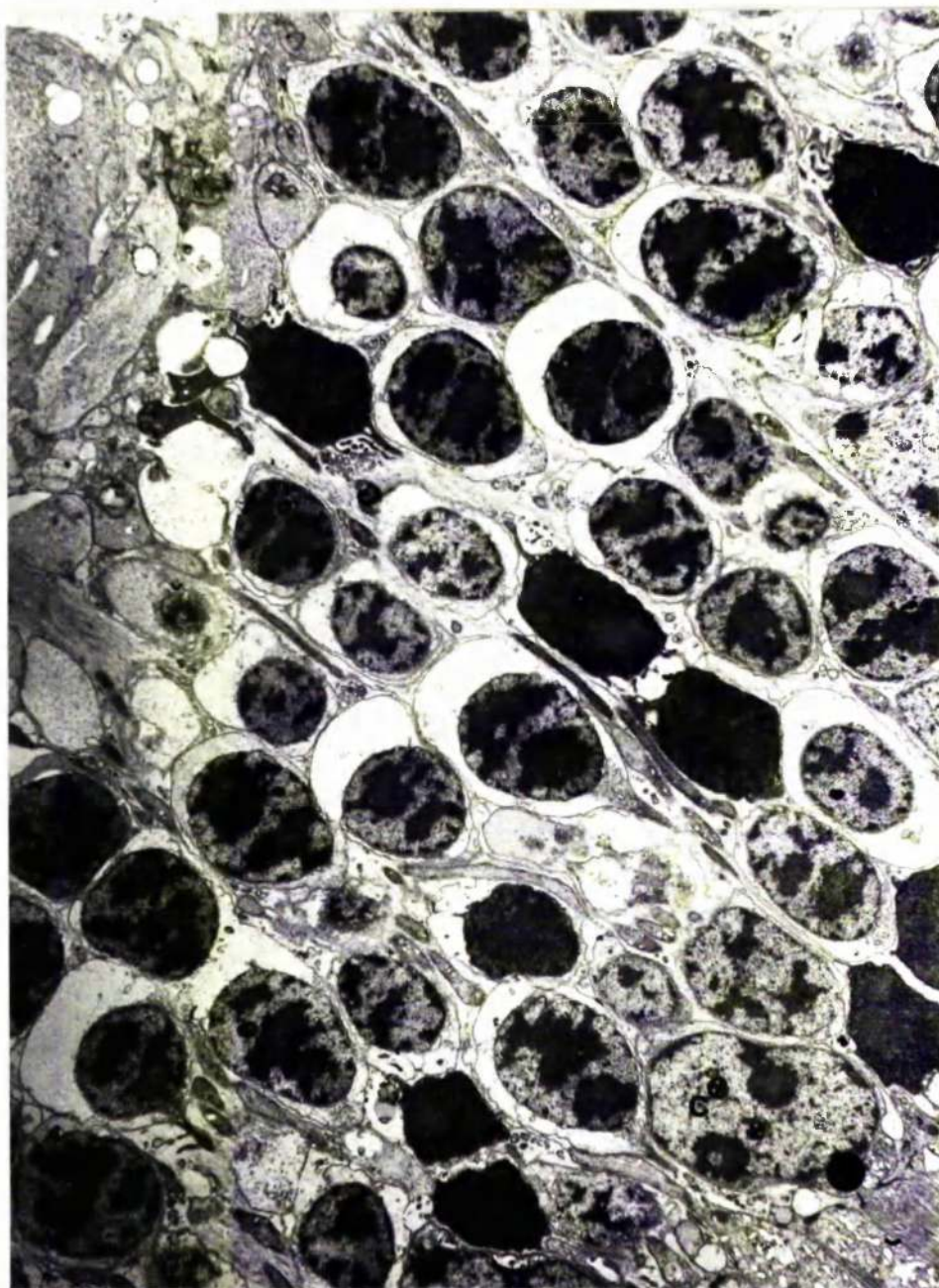


FIG.4-60 Electron micrograph of the outer nuclear layer 60 minutes post-mortem(room-temperature).The majority of the rod nuclei show pyknotic changes while the cone nucleus(C) remains relatively normal, (8,000 X)

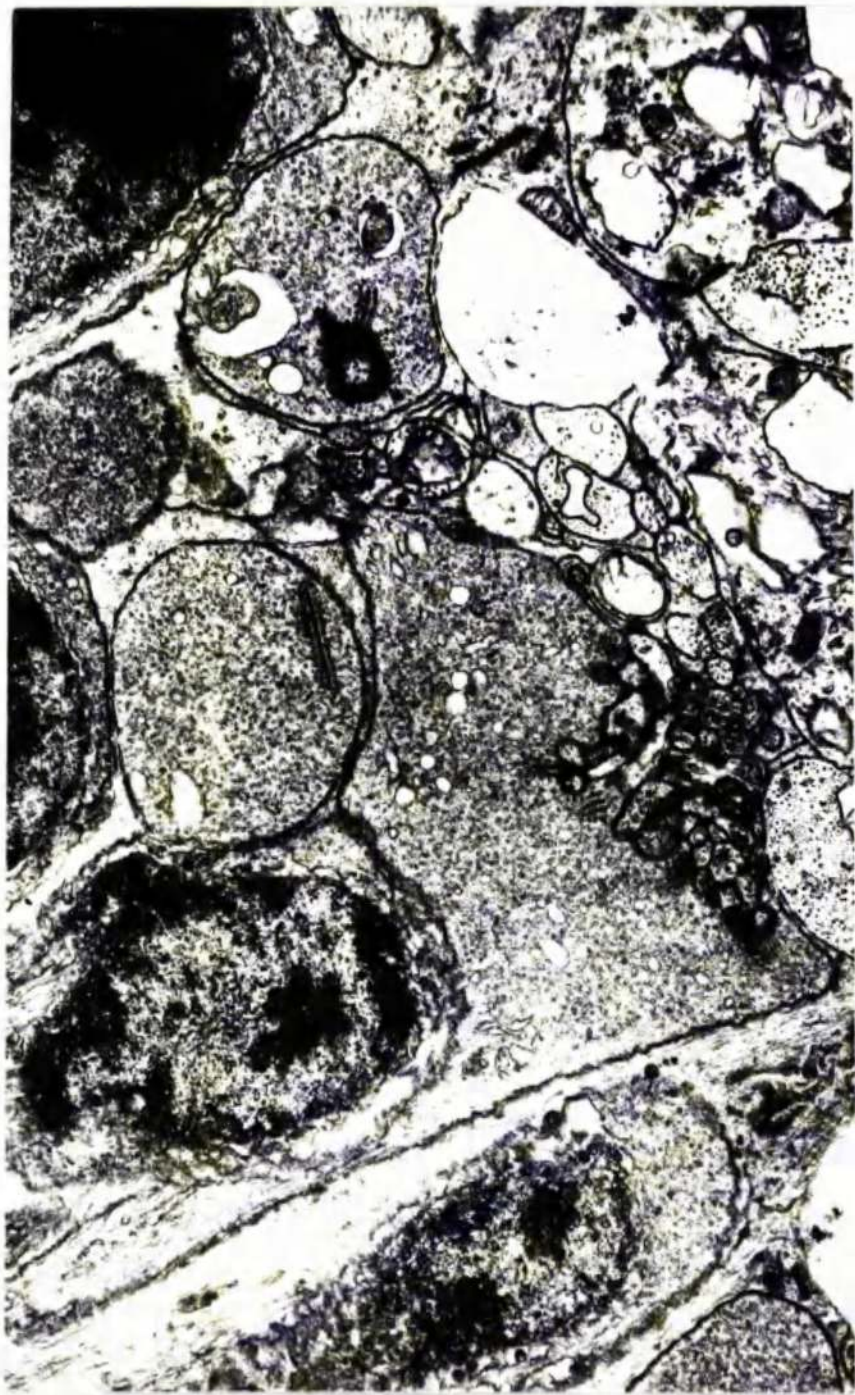


FIG. 4-6I Electron micrograph of the receptor pedicles 60 minutes post-mortem (room-temperature). The receptor pedicles of both the cone and rod cells are vacuolated, although the ribbon synapses are unaffected. (15,000 X)



FIG.4-62 Electron micrograph of the inner nuclear layer 60 minutes post-mortem(room-temperature).The cytoplasm of the neural cells shows early oedematous changes and there is often focal distensions of the nuclear envelope.The processes of the outer plexiform layer are swollen.(10,000 X)

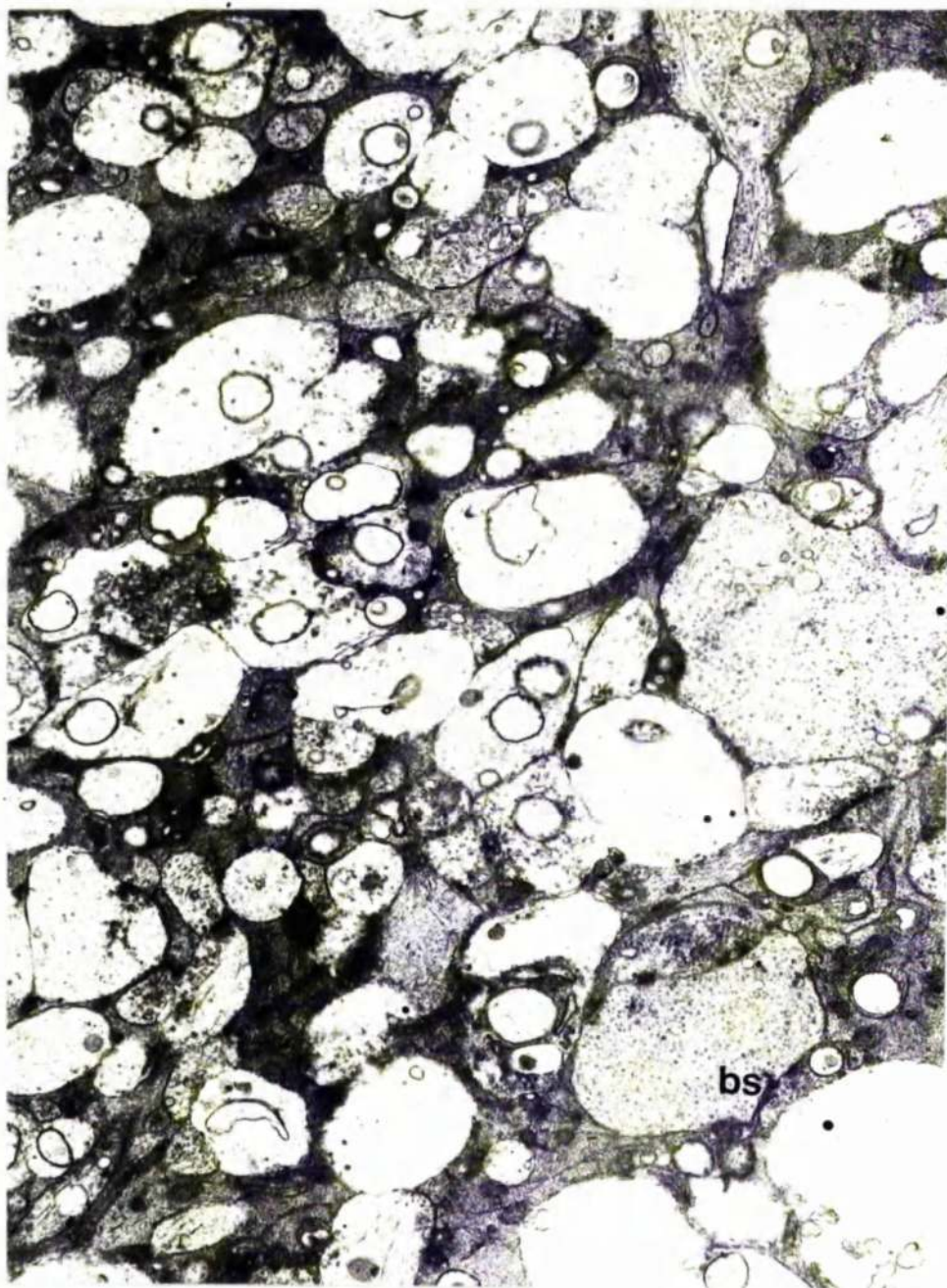


FIG.4-63 Electron micrograph of the inner plexiform layer 90 minutes post-mortem(room- temperature).Many of the processes are distended,however the occasional bipolar ribbon synapse(BS) can still be identified.(9,000 X)



FIG.4-64 Electron micrograph of a ganglion cell 60 minutes post-mortem(room-temperature).The cytoplasm is oedematous and a focal swelling of the nuclear envelope is present.The majority of the cell contents are found as a mass adjacent to the nucleus.(15,000 X)



FIG.4-65 Electron micrograph of the myelinated nerve fibres 90 minutes post-mortem(room-temperature).The myelin lamellae are often disturbed and there is a loss or a reduction in the number of neurotubules and neurofibrils.(25,000 X)



FIG.4-66 Electron micrograph of the pigment epithelium 15 minutes post-mortem(37°C). There is advanced degenerative changes in the mitochondria and the basal infoldings. The rough endoplasmic reticulum is swollen. (12,000 X)

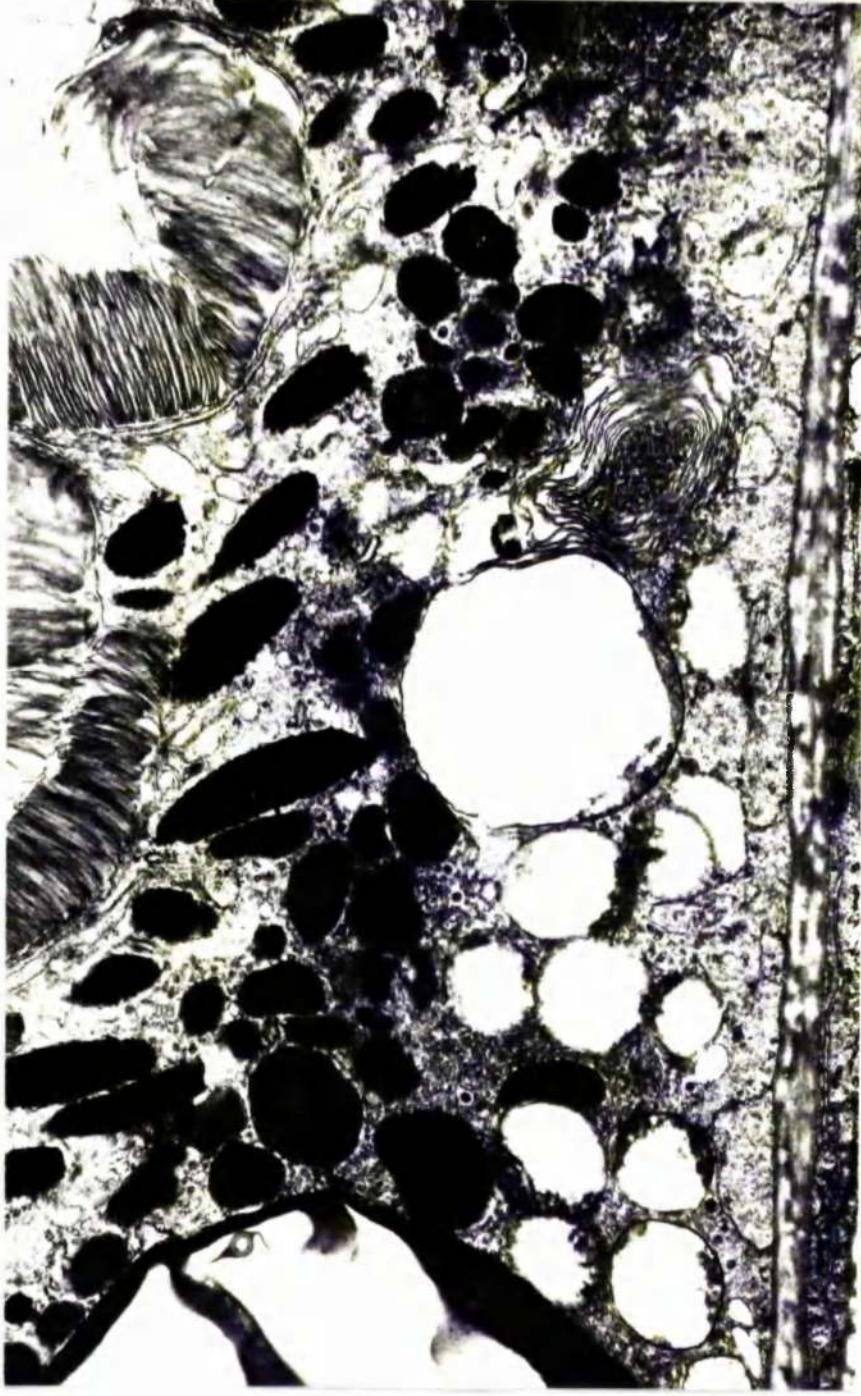


FIG.4-67 Electron micrograph of the pigment epithelium 90 minutes post-mortem (37°C). The cell is severely degenerate, the mitochondria are distended with few small cristae. The basal cell surface is almost smooth. The smooth endoplasmic reticulum is compressed. (19,000 X)



FIG.4-68 Electron micrograph of the inner and outer segments 30 minutes post-mortem(37°C). Both these structures are fragmented, many of the fragments are swollen. The mitochondria of the inner segments are distended, although few are ruptured. (10,000 X)



FIG.4-69 Electron micrograph of the inner nuclear layer 90 minutes post-mortem(37°C).The nuclei are severely pyknotic and the cytoplasm oedematous.(10,000 X)

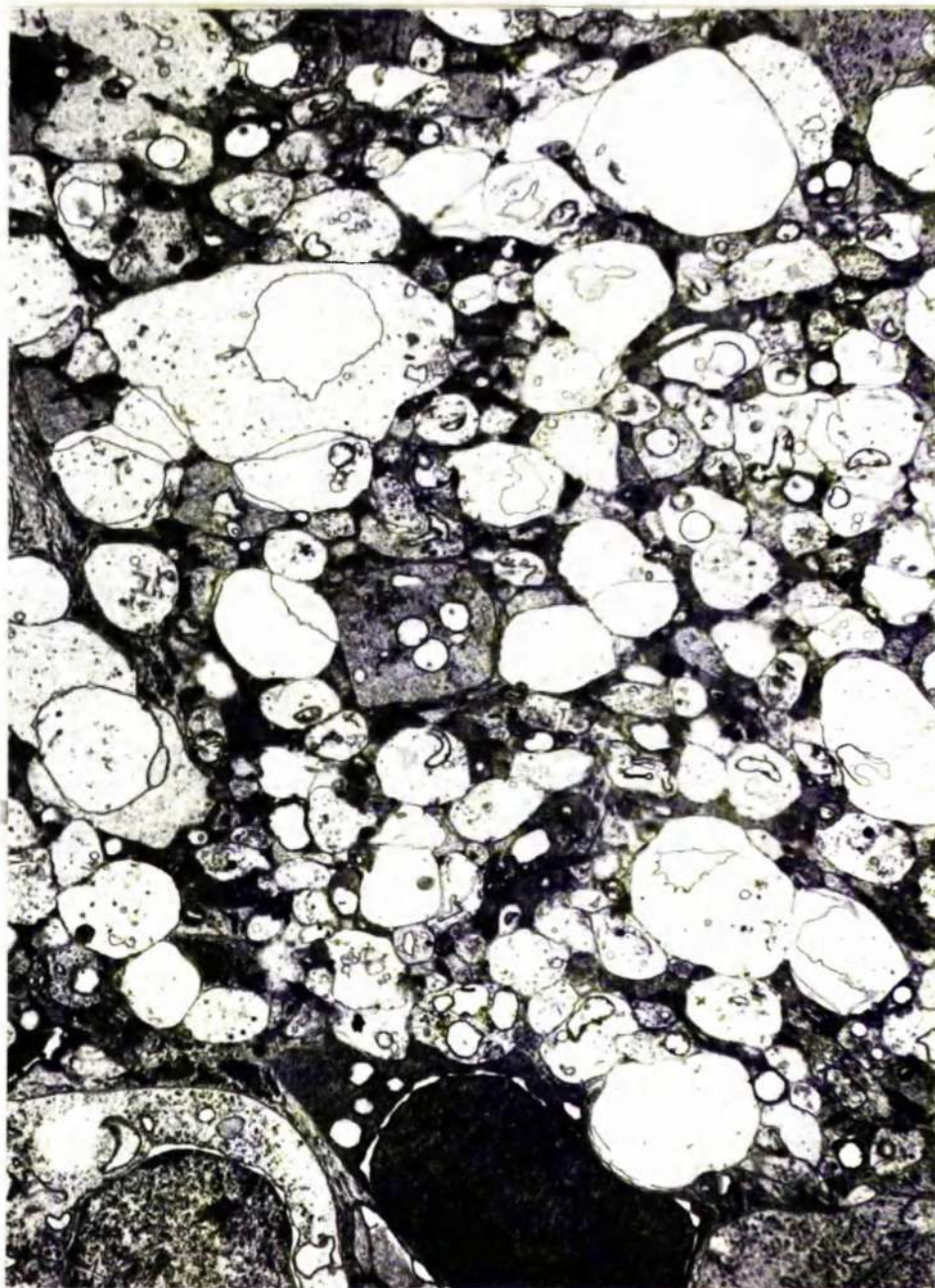


FIG.4-70 Electron micrograph of the inner plexiform layer 60 minutes post-mortem(37°C).The majority of the processes are swollen and ruptured.The cytoplasm of the processes is generally oedematous. (10,000 X)

THE EFFECT OF TOTAL ACUTE ISCHAEMIA ON THE STRUCTURE
AND FUNCTION OF THE RABBIT RETINA AND THE PATTERN OF
POST-ISCHAEMIC RECOVERY.

Volume II

Thesis
4566
Copy 2.
Vol. 2



List of Contents.

List of tables and illustrations	xxvix
Summary	xxxiv

<u>Chapter 5 - The structure of the rabbit retina during post-ischaemic recovery.</u>	67
5-1 Introduction.	68
5-2 Light microscopy of the retinal pigment epithelium.	69
5-2.1 30 minutes ischaemia, 60 and 240 minutes recovery.	69
5-2.2 30 minutes ischaemia, 60 minutes recovery.	69
5-2.3 30 minutes ischaemia, 240 minutes recovery.	69
5-2.4 60 minutes ischaemia, 60 minutes recovery.	69
5-2.5 60 minutes ischaemia, 240 minutes recovery.	69
5-2.6 90 minutes ischaemia, 60 and 240 minutes recovery.	69
5-2.7 120 minutes ischaemia, 60 and 240 minutes recovery.	70
5-3 Light microscopy of the outer segments.	70
5-3.1 15 minutes ischaemia, 60 and 240 minutes recovery.	70
5-3.2 30 minutes ischaemia, 60 minutes recovery.	70
5-3.3 30 minutes ischaemia, 240 minutes recovery.	70
5-3.4 60 minutes ischaemia, 60 minutes recovery.	70
5-3.5 60 minutes ischaemia, 240 minutes recovery.	70
5-3.6 90 minutes ischaemia, 60 minutes recovery.	71
5-3.7 90 minutes ischaemia, 240 minutes recovery.	71
5-3.8 120 minutes ischaemia, 60 and 240 minutes recovery.	71
5-4 Light microscopy of the visual cell inner segments.	71
5-4.1 15 minutes ischaemia, 60 and 240 minutes recovery.	71
5-4.2 30 minutes ischaemia, 60 and 240 minutes recovery.	71
5-4.3 60 minutes ischaemia, 60 minutes recovery.	71
5-4.4 60 minutes ischaemia, 240 minutes recovery.	71
5-4.5 90 minutes ischaemia, 60 and 240 minutes recovery.	72
5-4.6 120 minutes ischaemia, 60 and 240 minutes recovery.	72
5-5 Light microscopy of the external limiting membrane and the outer nuclear layer.	72
5-5.1 15 minutes ischaemia, 60 and 240 minutes recovery.	72
5-5.2 30 minutes ischaemia, 60 and 240 minutes recovery.	72
5-5.3 60 minutes ischaemia, 60 minutes recovery.	72
5-5.4 60 minutes ischaemia, 240 minutes recovery.	72
5-5.5 90 minutes ischaemia, 60 minutes recovery.	73
5-5.6 90 minutes ischaemia, 240 minutes recovery.	73
5-5.7 120 minutes ischaemia, 60 and 240 minutes recovery.	73
5-6 Light microscopy of the outer plexiform and inner nuclear layers.	73
5-6.1 15 minutes ischaemia, 60 and 240 minutes recovery.	73
5-6.2 30 minutes ischaemia, 60 and 240 minutes recovery.	74
5-6.3 60 minutes ischaemia, 60 minutes recovery.	74
5-6.4 60 minutes ischaemia, 240 minutes recovery.	74
5-6.5 90 minutes ischaemia, 60 minutes recovery.	74
5-6.6 90 minutes ischaemia, 240 minutes recovery.	74
5-6.7 120 minutes ischaemia, 60 minutes recovery.	75
5-6.8 120 minutes ischaemia, 240 minutes recovery.	75
5-7 Light microscopy of the inner plexiform and ganglion cell layers.	75
5-7.1 15 minutes ischaemia, 60 and 240 minutes recovery.	75
5-7.2 30 minutes ischaemia, 60 and 240 minutes recovery.	75
5-7.3 60 minutes ischaemia, 60 minutes recovery.	75
5-7.4 60 minutes ischaemia, 240 minutes recovery.	76
5-7.5 90 minutes ischaemia, 60 minutes recovery.	76
5-7.6 90 minutes ischaemia, 240 minutes recovery.	76
5-7.7 120 minutes ischaemia, 60 minutes recovery.	76
5-7.8 120 minutes ischaemia, 240 minutes recovery.	76

5-8	Light microscopy of the nerve fibre and myelinated nerve fibre layers.....	76
5-9	General retinal organisation.....	76
5-10	Electron microscopy - Introduction.....	77
5-11	Electron microscopy of the retinal pigment epithelium.....	77
5-11.1	15 minutes ischaemia, 60 minutes recovery.....	77
5-11.2	15 minutes ischaemia, 240 minutes recovery.....	77
5-11.3	30 minutes ischaemia, 60 minutes recovery.....	78
5-11.4	30 minutes ischaemia, 240 minutes recovery.....	78
5-11.5	60 minutes ischaemia, 60 minutes recovery.....	78
5-11.6	60 minutes ischaemia, 240 minutes recovery.....	79
5-11.7	90 minutes ischaemia, 60 minutes recovery.....	80
5-11.8	90 minutes ischaemia, 240 minutes recovery.....	80
5-11.9	120 minutes ischaemia, 60 minutes recovery.....	82
5-11.10	120 minutes ischaemia, 240 minutes recovery.....	82
5-12	Electron microscopy of the visual cell outer segments.....	83
5-12.1	15 minutes ischaemia, 60 minutes recovery.....	83
5-12.2	15 minutes ischaemia, 240 minutes recovery.....	83
5-12.3	30 minutes ischaemia, 60 minutes recovery.....	83
5-12.4	30 minutes ischaemia, 240 minutes recovery.....	83
5-12.5	60 minutes ischaemia, 60 minutes recovery.....	83
5-12.6	60 minutes ischaemia, 240 minutes recovery.....	84
5-12.7	90 minutes ischaemia, 60 minutes recovery.....	84
5-12.8	90 minutes ischaemia, 240 minutes recovery.....	84
5-12.9	120 minutes ischaemia, 60 minutes recovery.....	84
5-12.10	120 minutes ischaemia, 240 minutes recovery.....	84
5-13	Electron microscopy of the visual cell inner segments.....	85
5-13.1	15 minutes ischaemia, 60 minutes recovery.....	85
5-13.2	15 minutes ischaemia, 240 minutes recovery.....	85
5-13.3	30 minutes ischaemia, 60 minutes recovery.....	85
5-13.4	30 minutes ischaemia, 240 minutes recovery.....	85
5-13.5	60 minutes ischaemia, 60 minutes recovery.....	85
5-13.6	60 minutes ischaemia, 240 minutes recovery.....	86
5-13.7	90 minutes ischaemia, 60 minutes recovery.....	86
5-13.8	90 minutes ischaemia, 240 minutes recovery.....	86
5-13.9	120 minutes ischaemia, 60 minutes recovery.....	87
5-13.10	120 minutes ischaemia, 240 minutes recovery.....	87
5-14	Electron microscopy of the external limiting membrane.....	87
5-15	Electron microscopy of the outer nuclear layer.....	87
5-15.1	15 minutes ischaemia, 60 minutes recovery.....	87
5-15.2	15 minutes ischaemia, 240 minutes recovery.....	87
5-15.3	30 minutes ischaemia, 60 minutes recovery.....	87
5-15.4	30 minutes ischaemia, 240 minutes recovery.....	88
5-15.5	60 minutes ischaemia, 60 minutes recovery.....	88
5-15.6	60 minutes ischaemia, 240 minutes recovery.....	88
5-15.7	90 minutes ischaemia, 60 minutes recovery.....	88
5-15.8	90 minutes ischaemia, 240 minutes recovery.....	89
5-15.9	120 minutes ischaemia, 60 minutes recovery.....	89
5-15.10	120 minutes ischaemia, 240 minutes recovery.....	89
5-16	Electron microscopy of the outer plexiform layer.....	90
5-16.1	15 minutes ischaemia, 60 and 240 minutes recovery....	90
5-16.2	30 minutes ischaemia, 60 and 240 minutes recovery....	90
5-16.3	60 minutes ischaemia, 60 minutes recovery.....	90
5-16.4	60 minutes ischaemia, 240 minutes recovery.....	90
5-16.5	90 minutes ischaemia, 60 minutes recovery.....	90
5-16.6	90 minutes ischaemia, 240 minutes recovery.....	91
5-16.7	120 minutes ischaemia, 240 minutes recovery.....	91

5-17	Electron microscopy of the inner nuclear layer.	9
5-17.1	15 minutes ischaemia, 60 and 240 minutes recovery.	9
5-17.2	30 minutes ischaemia, 60 and 240 minutes recovery.	9
5-17.3	60 minutes ischaemia, 60 minutes recovery.	9
5-17.4	60 minutes ischaemia, 240 minutes recovery.	9
5-17.5	90 minutes ischaemia, 60 minutes recovery.	9
5-17.6	90 minutes ischaemia, 240 minutes recovery.	9
5-17.7	120 minutes ischaemia, 60 minutes recovery.	9
5-17.8	120 minutes ischaemia, 240 minutes recovery.	9
5-18	Electron microscopy of the inner plexiform layer.	9
5-18.1	15 minutes ischaemia, 60 and 240 minutes recovery.	9
5-18.2	30 minutes ischaemia, 60 minutes recovery.	9
5-18.3	30 minutes ischaemia, 240 minutes recovery.	9
5-18.4	60 minutes ischaemia, 60 and 240 minutes recovery.	9
5-18.5	90 minutes ischaemia, 60 and 240 minutes recovery.	9
5-18.6	120 minutes ischaemia, 60 and 240 minutes recovery.	9
5-19	Electron microscopy of the ganglion cells.	9
5-19.1	15 minutes ischaemia, 60 and 240 minutes recovery.	9
5-19.2	30 minutes ischaemia, 60 and 240 minutes recovery.	9
5-19.3	60 minutes ischaemia, 60 and 240 minutes recovery.	9
5-19.4	90 minutes ischaemia, 60 minutes recovery.	9
5-19.5	90 minutes ischaemia, 240 minutes recovery.	9
5-19.6	120 minutes ischaemia, 60 minutes recovery.	9
5-19.7	120 minutes ischaemia, 240 minutes recovery.	9
5-20	Electron microscopy of the nerve fibre layer and internal limiting membrane.	9
5-21	Electron microscopy of the myelinated nerve fibre zone.	9
5-22	Electron microscopy of the choroidal endothelium.	9
5-23	Discussion.	9

Chapter 6 - Retinal function during and after ischaemia.

6-1	Introduction.	10
6-2	Dark adaptation.	10
6-3	Quantitation of the electroretinogram.	11
6-4	The ERG during acute total ocular ischaemia.	11
6-5	The pattern of post-ischaemic recovery of the ERG.	11
6-5.1	Post-ischaemic recovery of the 'a' wave.	11
6-5.2	Post-ischaemic recovery of the 'b' wave.	11
6-5.3	Post-ischaemic recovery of the 'n' wave.	11
6-5.4	Post-ischaemic recovery of the 'c' wave.	11
6-6	Discussion.	11

Chapter 7 - Discussion.

<u>References.</u>	12
-------------------------	----

List of Tables and Illustrations.

Volume II:Chapter 5.

- Fig. 5-1 Light micrograph of the retina - 15 minutes ischaemia, 60 minutes recovery.
- Fig. 5-2 Light micrograph of the retina - 30 minutes ischaemia, 60 minutes recovery.
- Fig. 5-3 Light micrograph of the retina - 60 minutes ischaemia, 60 minutes recovery.
- Fig. 5-4 Light micrograph of the retina - 90 minutes ischaemia, 60 minutes recovery.
- Fig. 5-5 Light micrograph of the retina - 120 minutes ischaemia, 60 minutes recovery.
- Fig. 5-6 Light micrograph of the retina - 90 minutes ischaemia, 60 minutes recovery.
- Fig. 5-7 Light micrograph of the retina - 15 minutes ischaemia, 240 minutes recovery.
- Fig. 5-8 Light micrograph of the retina - 30 minutes ischaemia, 240 minutes recovery.
- Fig. 5-9 Light micrograph of the retina - 60 minutes ischaemia, 240 minutes recovery.
- Fig. 5-10 Light micrograph of the retina - 120 minutes ischaemia, 240 minutes recovery.
- Fig. 5-11 Light micrograph of the retina - 15 minutes ischaemia, 240 minutes recovery.
- Fig. 5-12 Light micrograph of the retina - 90 minutes ischaemia, 240 minutes recovery.
- Fig. 5-13 Light micrograph of the outer retina - 60 minutes ischaemia, 240 minutes recovery.
- Fig. 5-14 Light micrograph of the inner nuclear layer - 60 minutes ischaemia, 240 minutes recovery.
- Fig. 5-15 Light micrograph of the outer retina - 90 minutes ischaemia, 240 minutes recovery.
- Fig. 5-16 Light micrograph of the visual cells - 90 minutes ischaemia, 240 minutes recovery.
- Fig. 5-17 Light micrograph of the inner nuclear layer - peripheral retina - 90 minutes ischaemia, 240 minutes recovery.
- Fig. 5-18 Light micrograph of the inner nuclear layer - visual streak - 90 minutes ischaemia, 240 minutes recovery.
- Fig. 5-19 Electron micrograph of the retinal pigment epithelium - 30 minutes ischaemia, 60 minutes recovery.
- Fig. 5-20 Electron micrograph of the retinal pigment epithelium - 120 minutes ischaemia, 60 minutes recovery.
- Fig. 5-21 Electron micrograph of the retinal pigment epithelium - 30 minutes ischaemia, 240 minutes recovery.
- Fig. 5-22 Electron micrograph of the basal infoldings - 90 minutes ischaemia, 240 minutes recovery.
- Fig. 5-23 Electron micrograph of the basal cell wall - 90 minutes ischaemia, 240 minutes recovery.
- Fig. 5-24 Electron micrograph of the basal cell wall - 90 minutes ischaemia, 240 minutes recovery.
- Fig. 5-25 Electron micrograph of the retinal pigment epithelium - 90 minutes ischaemia, 240 minutes recovery.
- Fig. 5-26 Electron micrograph of a junctional complex - 120 minutes 240 minutes recovery.

- Fig. 5-27 Table showing the number of phagosomes in animals 9-16.
- Fig. 5-28 Table showing the % distribution of phagosomes in animals 9-16.
- Fig. 5-29 Table showing the number of phagosomes in animals 17-24.
- Fig. 5-30 Table showing the % distribution of phagosomes in animals 17-24.
- Fig. 5-31 Graph of relation between % distribution of phagosomes in test and control tissue - 15 minutes ischaemia.
- Fig. 5-32 Graph of relation between % distribution of phagosomes in test & control tissue - 30 minutes ischaemia.
- Fig. 5-33 Graph of relation between % distribution of phagosomes in test and control tissue - 60 minutes ischaemia.
- Fig. 5-34 Graph of relation between % distribution of phagosomes in test and control tissue - 90 minutes ischaemia.
- Fig. 5-35 Electron micrograph of the outer segments - 30 minutes ischaemia 60 minutes recovery.
- Fig. 5-36 Electron micrograph of the outer segments - 30 minutes ischaemia 60 minutes recovery.
- Fig. 5-37 Electron micrograph of the outer segments - 90 minutes ischaemia 60 minutes recovery.
- Fig. 5-38 Electron micrograph of the outer segments - 15 minutes ischaemia 240 minutes recovery.
- Fig. 5-39 Electron micrograph of the outer segments - 60 minutes ischaemia 240 minutes recovery.
- Fig. 5-40 Electron micrograph of the outer segments - 120 minutes ischaemia 240 minutes recovery.
- Fig. 5-41 Electron micrograph of the inner segments - 60 minutes ischaemia 60 minutes recovery.
- Fig. 5-42 Electron micrograph of the inner segments - 15 minutes ischaemia, 240 minutes recovery.
- Fig. 5-43 Electron micrograph of the outer retina - 60 minutes ischaemia, 240 minutes recovery.
- Fig. 5-44 Electron micrograph of the inner segments - 60 minutes ischaemia, 240 minutes recovery.
- Fig. 5-45 Electron micrograph of the outer retina - 90 minutes ischaemia, 240 minutes recovery.
- Fig. 5-46 Electron micrograph of the outer nuclear layer - 90 minutes ischaemia, 60 minutes recovery.
- Fig. 5-47 Electron micrograph of the outer nuclear layer - 30 minutes ischaemia, 240 minutes recovery.
- Fig. 5-48 Electron micrograph of the visual cells - 60 minutes ischaemia, 240 minutes recovery.
- Fig. 5-49 Electron micrograph of the visual cells - 60 minutes ischaemia, 240 minutes recovery.
- Fig. 5-50 Electron micrograph of the outer nuclear layer - 90 minutes ischaemia, 240 minutes recovery.
- Fig. 5-51 Electron micrograph of the outer nuclear layer - 90 minutes ischaemia, 240 minutes recovery.
- Fig. 5-52 Electron micrograph of the outer plexiform layer - 60 minutes ischaemia, 60 minutes recovery.
- Fig. 5-53 Electron micrograph of the receptor pedicles - 120 minutes ischaemia, 60 minutes recovery.
- Fig. 5-54 Electron micrograph of the outer plexiform layer - 90 minutes ischaemia, 240 minutes recovery.
- Fig. 5-55 Electron micrograph of the outer plexiform layer - 90 minutes ischaemia, 60 minutes recovery.
- Fig. 5-56 Electron micrograph of the inner nuclear layer - 90 minutes ischaemia, 60 minutes recovery.
- Fig. 5-57 Electron micrograph of the inner nuclear layer - 90 minutes ischaemia, 60 minutes recovery.

- Fig. 5-58 Electron micrograph of the inner nuclear layer - 60 minutes ischaemia, 240 minutes recovery.
- Fig. 5-59 Electron micrograph of the inner nuclear layer - 90 minutes ischaemia, 240 minutes recovery.
- Fig. 5-60 Electron micrograph of the inner nuclear layer - 90 minutes ischaemia, 240 minutes recovery.
- Fig. 5-61 Electron micrograph of the inner plexiform layer - 30 minutes ischaemia, 240 minutes recovery.
- Fig. 5-62 Electron micrograph of the inner plexiform layer - 90 minutes ischaemia, 240 minutes recovery.
- Fig. 5-63 Electron micrograph of the inner plexiform layer - 60 minutes ischaemia, 240 minutes recovery.
- Fig. 5-64 Electron micrograph of the ganglion cell layer - 90 minutes ischaemia, 240 minutes recovery.
- Fig. 5-65 Electron micrograph of the nerve fibre layer - 60 minutes ischaemia, 240 minutes recovery.
- Fig. 5-66 Electron micrograph of the ganglion cell layer - 90 minutes ischaemia, 240 minutes recovery.
- Fig. 5-67 Electron micrograph of the horizontal nerve fibre zone - 90 minutes ischaemia, 60 minutes recovery.
- Fig. 5-68 Electron micrograph of the horizontal nerve fibre zone - 90 minutes ischaemia, 240 minutes recovery.
- Fig. 5-69 Electron micrograph of the internal limiting membrane - 60 minutes ischaemia, 60 minutes recovery.
- Fig. 5-70 Electron micrograph of a choroidal vessel - 15 minutes ischaemia 60 minutes recovery.
- Fig. 5-71 Electron micrograph of a choroidal vessel - 60 minutes ischaemia 240 minutes recovery.

Chapter 6.

- Fig. 6-1 Electroretinograms during the course of dark adaptation.
- Fig. 6-2 Dark adaptation curves for the 'a', 'b' and 'n' waves.
- Fig. 6-3 Dark adaptation curves for the 'a', 'b' and 'n' waves of each eye of one animal.
- Fig. 6-4 Diagram to show method of measurement of the various wave forms.
- Fig. 6-5 Graph of the control 'b' wave during the ischaemic and post-ischaemic phases in the test eye.
- Fig. 6-6 Electroretinograms following the induction of ischaemia.
- Fig. 6-7 Electroretinograms during an experiment involving 15 minutes ischaemia.
- Fig. 6-8 Electroretinograms during an experiment involving 30 minutes ischaemia.
- Fig. 6-9 Electroretinograms during an experiment involving 60 minutes ischaemia.
- Fig. 6-10 Electroretinograms during an experiment involving 90 minutes ischaemia.
- Fig. 6-11 Electroretinograms during an experiment involving 120 minutes ischaemia.
- Fig. 6-12 Graph showing the post-ischaemic recovery of the 'a' wave.
- Fig. 6-13 Graph showing the standard deviation of the mean of the 'a' wave following 60 and 240 minutes recovery.
- Fig. 6-14 Electroretinograms showing the latency of the 'a' wave following 60 and 90 minutes ischaemia.
- Fig. 6-15 Electroretinograms with isolated 'a' waves.
- Fig. 6-16 Graph showing the post-ischaemic recovery of the 'b' wave.
- Fig. 6-17 Graph showing the mean and standard deviation of the 'b' wave following 60 and 240 minutes recovery.

- * Fig. 6-18 Electroretinogram showing failure of the 'b' wave to rise above iso-electric line.
- * Fig. 6-19 Electroretinograms showing the 'b' wave latency following 15 and 90 minutes ischaemia.
- Fig. 6-20 Graph showing the post-ischaemic recovery of the 'n' wave.
- Fig. 6-21 Graph showing the mean and standard deviation of the 'n' wave following 60 and 240 minutes recovery.

Summary.

This thesis describes the function and structure of the rabbit retina during and after periods of total acute ischaemia. The function of the retina was determined by electroretinography while the retinal structure was investigated by light and electron microscopy.

Following a 2 hour period of dark adaptation, total acute ocular ischaemia was induced in one eye of each rabbit by raising the intraocular pressure above the systemic systolic blood pressure for varying periods (15, 30, 60, 90 and 120 minutes). The contralateral eye acted as the control. One group of animals were killed immediately after the period of ischaemia and investigated histologically. In another group of animals, the intraocular pressure was returned to normal for up to 4 hours, the function of the retina was monitored throughout by electroretinography under scotopic conditions. Groups of animals were killed one and four hours after the return of the ocular circulation to determine the histological pattern of post-ischaemic recovery.

Light and electron microscopy revealed that the individual cell types making up the retina possessed different tolerances to ischaemia. The visual cells were the least resistant to ischaemia, being susceptible to periods of ischaemia longer than 30 minutes. The Müller cells, the ganglion cells and the RPE were the most resistant to ischaemia, often showing only mild changes following 4 hours recovery from 90 and 120 minutes ischaemia. The neural cells of the inner nuclear layer exhibited an intermediate tolerance to ischaemia showing severe degenerative changes following periods of ischaemia longer than 60 minutes. A prominent feature of the ischaemic retina was the presence of macrophages in the subretinal space. The macrophages appeared to be actively engaged in the removal of outer segment debris. These cells were not a feature of the post-ischaemic retina. During the recovery phase the RPE was able

to increase its phagocytic activity. This appeared to be the main mechanism for the removal of outer segment debris during the post-ischaemic phase following periods of ischaemia not longer than 60 minutes. The histological changes arising from periods of ischaemia induced by high intraocular pressure may have arisen from the effects of ischaemia, the mechanical effect of pressure or a combination of the two factors. Post-mortem retinal tissue was investigated to determine the effects of total acute ocular ischaemia not involving raised intraocular pressure. There was a marked similarity between the pressure-induced ischaemic tissue and post-mortem tissue which suggested that the mechanical effects of raised intraocular pressure were small compared to the effects of ischaemia.

Following total ocular ischaemia, some recovery of ERG was found in all eyes exposed to ischaemia of up to 120 minutes, although after longer periods of ischaemia, recovery of the ERG was delayed and incomplete. After periods of ischaemia of 15, 30 or 60 minutes, a recordable 'b' wave appeared within 5 minutes of the restoration of circulation. After 90 minutes of ischaemia recovery of the 'b' wave can be seen some 15 to 20 minutes after restoration of circulation, while after 120 minutes of ischaemia, the appearance of a recordable 'b' wave was delayed for as long as half an hour. After longer periods of ischaemia, its recovery became progressively slower and less complete. After 30 minutes of ischaemia, the amplitude of the 'b' wave became temporarily larger than that in the control eye, this temporary supernormality lasting through the 4 hour period of observation. After 60 minutes of ischaemia, the amplitude of the 'b' wave returned to 80% of the value in the control eye in 4 hours. While after 90 minutes of ischaemia recovery ranged between 10 and 50% of the value in the other eye after 4 hours. Following 120 minutes ischaemia, the 'b' wave returned temporarily and was absent in all eyes.

after 3 hours. In general the 'a' wave returned more rapidly than the 'b' wave after an ischaemic episode and the disparity became more marked the longer the period of ischaemia lasted. After 30 minutes of ischaemia recovery of the 'a' wave started within 5 minutes on average, while after 60 minutes or 90 minutes of ischaemia 'a' wave recovery started between 5 and 10 minutes after restoration of circulation. A common finding after 15 and 30 minutes of ischaemia was an 'a' wave of increased amplitude. The 'c' wave was found to be more variable than the 'a' wave or 'b' wave. On occasion the 'c' wave was found to be of larger amplitude than in the pre-ischaemic ERG. A feature of the ERG during recovery from ischaemia was the occurrence of marked post-'b' wave negativity. Following the induction of ischaemia in the test eye, the 'b' wave of the contralateral control eye increased in amplitude.

There was a poor correlation between the alterations in the components of the ERG and changes in the cells from which the components were thought to arise. The 'a' wave returned rapidly following ischaemia in spite of considerable damage to the inner and outer segments of the visual cells. However, there was a good correlation between the overall wave form of the ERG and the histological changes. A marked negativity of the ERG with reduced positive components was indicative of a severely damaged retina.

Chapter 5 - The Pattern of Structural Recovery
following periods of Ischaemia.

5 - 1 Introduction.

This chapter describes the histological features of post-ischaemic recovery. Following the various periods of ischaemia, the intraocular pressure was allowed to return to normal. Animals were killed one or four hours after the return of normal intraocular pressure. The retina was examined to determine the pattern of post-ischaemic recovery.

The mild changes seen in the outer retina immediately following the shorter periods of ischaemia (15 and 30 minutes) generally remained unchanged after four hours recovery. During recovery from 60 minutes ischaemia, there was some evidence of structural recovery in the outer retina. The post-ischaemic phase following 90 and 120 minutes ischaemia was, however, associated with little or no improvement in the structure or organisation of the outer retina. In addition, the degenerative changes were frequently more advanced during the recovery phase than immediately after the period of ischaemia. Recovery from 90 and 120 minutes ischaemia was also associated with degenerative changes in the inner retina.

A marked feature of the post-ischaemic retina was the absence of macrophages in the subretinal space. In the ischaemic tissue macrophages were prominent and involved in the removal of outer segment material. During the recovery phase the retinal pigment epithelium appeared to act as an auxiliary macrophage in the removal of the outer segment material in the subretinal space.

In the following description of the pattern of post-ischaemic recovery in the rabbit retina, the light microscopic changes are covered before the electron microscopic findings. The various layers of the retina will be described from the retinal pigment epithelium inwards to the internal limiting membrane.

5-2 Light microscopy of the retinal pigment epithelium.

5-2.1 15 minutes ischaemia, 60 and 240 minutes recovery.

The retinal pigment epithelium appeared normal and this was similar to the situation observed immediately after this period of ischaemia (fig. 5-1 and 5-11).

5-2.2 30 minutes ischaemia and 60 minutes recovery.

The retinal pigment epithelium contained small basally situated vacuoles, apart from this feature the cells appeared normal and were of similar appearance to the cells studied immediately after the period of ischaemia.

5-2.3 30 minutes ischaemia and 240 minutes recovery.

The retinal pigment epithelium appeared normal. There was no evidence of vacuolation (fig. 5-8).

5-2.4 60 minutes ischaemia and 60 minutes recovery.

Following this period of recovery the pigment epithelium contained few vacuoles and the apical surface was ragged and undulating. The cytoplasm stained intensely (fig. 5-3). The number of vacuoles was much reduced compared with the tissue investigated immediately after the ischaemic episode. In addition, this latter tissue was less intensely stained.

5-2.5 60 minutes ischaemia and 240 minutes recovery.

The intense cytoplasmic staining evident with the shorter recovery period was not present after 4 hours recovery (figs. 5-9 and 5-13). The apical surface remained undulating and the cytoplasm was devoid of vacuoles.

5-2.6 90 minutes ischaemia, 60 and 240 minutes recovery.

The retinal pigment epithelium was similar in appearance to that seen after 60 minutes recovery from 60 minutes ischaemia. The cytoplasm contained a few vacuoles and stained intensely. The apical surface was

ragged. The tissues following these two recovery periods were indistinguishable from one another (figs. 5-4, 5-6, 5-12 and 5-15).
 5-2.7 120 minutes ischaemia, 60 and 240 minutes recovery.

As with the two previous periods of ischaemia, recovery from this length of ischaemia was associated with an intensely stained cytoplasm and an irregular apical surface (figs. 5-5 and 5-10).

5-3 Light microscopy of the outer segments.

5-3.1 15 minutes ischaemia, 60 and 240 minutes recovery.

The mild disturbance of the terminal portions of the outer segments seen immediately after the ischaemia episode was still present following these two periods of recovery (figs. 5-1 and 5-7).

5-3.2 30 minutes ischaemia and 60 minutes recovery.

The outer segments were disturbed and fragments were often seen in the region adjacent to the apical surface of the retinal pigment epithelium. This situation was similar to that seen immediately after the period of ischaemia (fig. 5-2).

5-3.3 30 minutes ischaemia and 240 minutes recovery.

Following 4 hours recovery, the disorganisation in the outer segments was less severe than after the shorter recovery period (fig. 5-8). However, the occasional fragment still occurred and a few of these were swollen.

5-3.4 60 minutes ischaemia and 60 minutes recovery.

The outer segments were fragmented and disorganised and had a similar appearance to the outer segments observed immediately after the period of ischaemia (fig. 5-3).

5-3.5 60 minutes ischaemia and 240 minutes recovery.

Four hours recovery was associated with some reorganisation of the outer segments. Amongst the many remaining fragments intact outer segments occurred (figs. 5-9 and 5-13).

5-3.6 90 minutes ischaemia and 60 minutes recovery.

The severe fragmentation and disruption of the outer segments seen immediately after the period of ischaemia was still evident (fig. 5-4).

5-3.7 90 minutes ischaemia and 240 minutes recovery.

Some reorganisation was evident, although this was less than seen after 60 minutes ischaemia and 240 minutes recovery. There were few intact outer segments. The majority of the outer segments were fragmented, with many of the fragments forming swollen saccules (figs. 5-12 and 5-15).

5-3.8 120 minutes ischaemia, 60 and 240 minutes recovery.

Following these two recovery periods the outer segments were indistinguishable from those seen immediately after the period of ischaemia. The degenerative changes were severe, the majority of outer segment fragments were swollen, (figs. 5-5 and 5-10).

5-4 Light microscopy of the visual cell inner segments.

5-4.1 15 minutes ischaemia, 60 and 240 minutes recovery.

The inner segments were indistinguishable from normal. There was no change from the situation seen immediately after the period of ischaemia (figs. 5-1 and 5-7).

5-4.2 30 minutes ischaemia, 60 and 240 minutes recovery.

The inner segments appeared normal (figs. 5-2 and 5-8). The mild vacuolation evident immediately after the period of ischaemia was not evident following these two recovery periods.

5-4.3 60 minutes ischaemia and 60 minutes recovery.

The inner segments were vacuolated and much shorter than their control counterparts (fig. 5-3). This appearance was similar to that seen immediately after the ischaemic episode.

5-4.4 60 minutes ischaemia and 240 minutes recovery.

Following 4 hours recovery, the appearance of individual inner segments varied considerably. Some were round, swollen and uniformly stained. In these inner segments, no distinction between the myoid and

ellipsoid regions could be made. The remaining inner segments were long and slender and stained more intensely (figs. 5-9 and 5-13).

5-4.5 90 minutes ischaemia, 60 and 240 minutes recovery.

The inner segments were indistinguishable from those observed immediately after the period of ischaemia. There was marked vacuolation and fragmentation of the inner segments (figs. 5-4 and 5-16).

5-4.6 120 minutes ischaemia, 60 and 240 minutes recovery.

The severe disruption and fragmentation of the inner segments seen immediately after this period of ischaemia was still evident following these two recovery periods (figs. 5-5 and 5-10).

5-5 Light microscopy of the external limiting membrane and the outer nuclear layer.

5-5.1 15 minutes ischaemia, 60 and 240 minutes recovery.

The external limiting membrane and the outer nuclear layer were normal in appearance (figs. 5-1, 5-7 and 5-11).

5-5.2 30 minutes ischaemia, 60 and 240 minutes recovery.

The external limiting membrane and the outer nuclear layer were normal in appearance. The mild pyknotic changes seen in the outer nuclear layer immediately after the period of ischaemia were not evident after 60 minutes recovery (figs. 5-2 and 5-8).

5-5.3 60 minutes ischaemia and 60 minutes recovery.

The external limiting membrane appeared normal. The outer nuclear layer was indistinguishable from that seen immediately after the period of ischaemia. The rod nuclei were rounded and intensely stained. The surrounding cytoplasm was oedematous. Pyknotic changes were not present in the cone nuclei (fig. 5-3).

5-5.4 60 minutes ischaemia and 240 minutes recovery.

The external limiting membrane remained normal. Following 4 hours recovery there was some evidence of structural recovery in the outer nuclear layer. Several of the visual cell nuclei were oval and possessed

a "coffee bean" chromatin pattern. These were similar to their control counterparts. However, other nuclei were abnormal, remaining round and heavily stained (fig. 5-13).

5-5.5 90 minutes ischaemia and 60 minutes recovery.

The external limiting membrane remained intact. The outer nuclear layer was similar to that seen immediately after the period of ischaemia with one exception (fig. 5-4) which was seen in three tissue blocks from two animals. A split occurred in the outer aspect of the layer and this differed from the usual picture of retinoschisis in which the split occurs in the plexiform layers (fig. 5-6). The visual cell nuclei were extremely pyknotic and microcystic spaces were often present.

5-5.6 90 minutes ischaemia and 240 minutes recovery.

Following 4 hours recovery there was little change in the outer nuclear layer. What changes there were depended to some extent on retinal location. In the peripheral retina, the visual cell nuclei were round and heavily stained and distributed in a more random manner than previously. The surrounding cytoplasm was oedematous (fig. 5-16). In the area of the visual streak, the nuclei were less pyknotic and were normally distributed (fig. 5-18).

5-5.7 120 minutes ischaemia, 60 and 240 minutes recovery.

The visual cell nuclei were severely degenerated and surrounded by oedematous Müller cell cytoplasm. The degenerative changes were more advanced than those seen immediately after the period of ischaemia (figs. 5-5 and 5-10).

5-6 Light microscopy of the outer plexiform and inner nuclear layers.

5-6.1 15 minutes ischaemia, 60 and 240 minutes recovery.

The outer plexiform and inner nuclear layers were normal in appearance (figs. 5-1 and 5-7).

5-6.2 30 minutes ischaemia, 60 and 240 minutes recovery.

The outer plexiform and inner nuclear layers were normal in appearance (figs. 5-2 and 5-8).

5-6.3 60 minutes ischaemia and 60 minutes recovery.

Following 60 minutes recovery, there was a generalised swelling in the outer plexiform layer which was similar to that seen immediately after the period of ischaemia. The nuclei of the inner nuclear layer were similar in appearance to those occurring immediately after the ischaemic episode. They were lightly stained and surrounded by a halo of clear cytoplasm (fig. 5-3).

5-6.4 60 minutes ischaemia and 240 minutes recovery.

Following 4 hours recovery the nuclei remained rounded although they were stained in a normal manner. The Müller cell nuclei appeared to be altered at this stage with a loss of their previous angular outline and were stained less intensely (fig. 5-14). This was the first appearance of any change in the Müller cell nuclei. These changes were uniform and independent of the retinal location of the tissue.

The generalised swelling in the outer plexiform layer present after 60 minutes recovery was less in evidence after 4 hours recovery.

5-6.5 90 minutes ischaemia and 60 minutes recovery.

The marked oedematous changes in the outer plexiform and inner nuclear layers observed immediately after the period of ischaemia remained after 60 minutes recovery (fig. 5-4).

5-6.6 90 minutes ischaemia and 240 minutes recovery.

Following 4 hours recovery the outer plexiform layer remained oedematous (figs. 5-17 and 5-18). In the area of the visual streak the receptor pedicles were heavily stained (fig. 5-18). The nuclei of the inner nuclear layer were often more severely damaged than after the shorter period of recovery. This was especially true of the visual streak. In

this region frequent nuclei were condensed and intensely stained, others contained many dark chromatin masses. The remaining nuclei were rounded and swollen (fig. 5-18). In the peripheral retina, the nuclei were generally rounded (fig. 5-17), and were similar to the rounded nuclei of the visual streak region. The cytoplasm surrounding the nuclei in both the visual streak and peripheral retina remained oedematous.

5-6.7 120 minutes ischaemia and 60 minutes recovery.

The outer plexiform and inner nuclear layers were similar in appearance to these seen immediately following the period of ischaemia. The outer plexiform layer was oedematous and the inner nuclear layer was severely degenerate (fig. 5-5).

5-6.8 120 minutes ischaemia and 240 minutes recovery.

Following 4 hours recovery, the appearance of the outer plexiform and inner nuclear layers was similar to that seen following 90 minutes ischaemia. The pyknotic changes in the inner nuclear layer were more pronounced in the visual streak region than in the peripheral retina. Overall the changes following this period of recovery were more marked with 120 minutes ischaemia than with 90 minutes ischaemia.

5-7 Light microscopy of the inner plexiform and ganglion cell layers.

5-7.1 15 minutes ischaemia, 60 and 240 minutes recovery.

The inner plexiform and ganglion cell layers were indistinguishable from their control counterparts (figs. 5-1, 5-7 and 5-11).

5-7.2 30 minutes ischaemia, 60 and 240 minutes recovery.

The inner plexiform and ganglion cell layers appeared normal (figs. 5-2 and 5-8).

5-7.3 60 minutes ischaemia and 60 minutes recovery.

There was a generalised swelling of the inner plexiform layer and intracellular oedema in the ganglion cells. The changes were similar to those observed immediately after the period of ischaemia.

5-7.4 60 minutes ischaemia and 240 minutes recovery.

Following a 4 hour recovery period, the inner plexiform and ganglion cell layers were normal in appearance. The oedema seen previously was no longer evident.

5-7.5 90 minutes ischaemia and 60 minutes recovery.

Pronounced oedema was evident in both the inner plexiform and ganglion cell layers which was identical to that seen immediately following the period of ischaemia (fig. 5-4).

5-7.6 90 minutes ischaemia and 240 minutes recovery.

The oedema remained in the inner plexiform layer (figs. 5-17 and 5-18). However, the ganglion cells were often condensed and intensely stained (fig. 5-12).

5-7.7 120 minutes ischaemia and 60 minutes recovery.

The marked oedema in the inner plexiform layer and the severe intracellular oedema in the ganglion cells present immediately after the period of ischaemia remained after 60 minutes recovery.

5-7.8 120 minutes ischaemia and 240 minutes recovery.

The inner plexiform layer in the retinae examined after 4 hours recovery was similar in appearance to the tissue examined after 60 minutes recovery. In the ganglion cells the intracellular oedema seen previously was no longer evident. The cells were condensed and heavily stained.

5-8 Light microscopy of the nerve fibre and myelinated nerve fibre layers.

The nerve fibre layer, the myelinated nerve fibre bundles and their associated blood vessels were indistinguishable from normal following all the various periods of ischaemia and recovery (figs. 5-7, 5-8, 5-9 and 5-10).

5-9 General retinal organisation.

The prominent retinal folding which was frequently present immediately after the ischaemic episode was less marked following 60 minutes

recovery and generally absent after 4 hours recovery.

5-10 Electron microscopy - Introduction.

The various layers of the retinal will be described from the retinal pigment epithelium inwards and each of the layers will be described separately for every period of ischaemia and recovery.

5-11 Electron microscopy of the retinal pigment epithelium.

5-11.1 15 minutes ischaemia and 60 minutes recovery.

The retinal pigment epithelium was ultrastructurally normal. The focal condensation of the smooth endoplasmic reticulum and the mild mitochondrial changes seen immediately after this period of ischaemia were not evident after one hour's recovery. However, one departure from normal was the more frequent appearance of phagosomes in the initial stages of degredation. A quantitative analysis similar to that undertaken for the control tissue was carried out (see Chapter 3, section 3 for details) to determine the number and distribution of the various phagosome stages. With this period of recovery (60 minutes) from 15 minutes ischaemia, the number and percentage distribution of the two initial stages increased. The increases occurred in both the peripheral retina and in the visual streak region (figs. 5-27 and 5-28). The average distribution of the five phagosome stages in the visual streak and periphery of the test eyes was compared to the distribution in similar regions of the corresponding control eyes during the recovery phase. This comparison revealed that the increases in both the initial stages in the visual streak were in the order of 150% while in the peripheral retina the increases were in the order of 160-180% (fig. 5-31).

5-11.2 15 minutes ischaemia and 240 minutes recovery.

The retinal pigment epithelium remained normal although an increase in the number and percentage distribution of the first two phagosome stages was still evident (figs. 5-29 and 5-30). The increases were of the same

order when compared with the shorter period of recovery. A comparison of the respective test and control eyes showed no further increases in stage 2 phagosomes. However, a further small increase in stage 1 phagosomes occurred. The increase was more pronounced in the peripheral retina (fig. 5-32).

5-11.3 30 minutes ischaemia and 60 minutes recovery.

Apart from some mitochondrial swelling the cells appeared normal (fig. 5-19). The changes apparent in the smooth endoplasmic reticulum and the basal and apical infoldings immediately after the period of ischaemia were absent after 60 minutes recovery.

Increases occurred in the number ^{and} percentage distribution of the two initial phagosome stages (figs. 5-27 and 5-28). A comparison of the corresponding test and control eyes showed a greater increase in stage 1 phagosomes than stage 2 in both the visual streak and peripheral retina. In both the regions, the increases in stage 1 and 2 were of the same order 160-170% and 110-120% respectively (figs. 5-32).

5-11.4 30 minutes ischaemia and 240 minutes recovery.

The cells appeared normal, the mitochondrial swelling present after 60 minutes recovery was no longer evident. Phagosomes were frequently prominent in the cytoplasm (fig. 5-21). The number and percentage distribution of the two initial phagosome stages showed dramatic increases (figs. 5-29 and 5-30). A comparison of corresponding test and control eyes showed increases in the first two stages in both the visual streak and peripheral retina. The increases were considerable compared with the shorter recovery period. In the visual streak, the increases in stage 1 and 2 were 240% and 150% respectively. The increases in the peripheral retina were marked stage 1 increased by 340% and stage 2 by 210% (fig. 5-32).

5-11.5 60 minutes ischaemia and 60 minutes recovery.

Following this recovery period some reorganisation was evident in the retinal pigment epithelium. The patchy widening of the basal infoldings

which occurred immediately after the period of ischaemia was not present. The basal infoldings were indistinguishable from normal. Immediately after the ischaemic episodes, the smooth endoplasmium was condensed throughout the cell. This widespread condensation was less evident after this period of recovery. Changes also occurred in the mitochondria. The marked rounding and reduction in the matrix electron density present immediately after ischaemia was less pronounced in the post- ischaemic tissue. The apical processes were generally normal although on occasion they remained compressed against the main cell body in a similar fashion to that seen immediately after the period of ischaemia. In addition to these alterations, the number of phagosomes within the retinal pigment epithelium was increased. In contrast to the other periods of ischaemia, the increase in number and percentage distribution only occurred in stage 2 phagosomes (figs. 5-27 and 5-28). Comprison of the corresponding control and test eyes showed similar increases (190-200%) in stage 2 phagosomes in the visual streak region and peripheral retina (fig. 5-33).

5-11.6 60 minutes ischaemia and 240 minutes recovery.

Further reorganisation was evident with this longer period of recovery. The condensation of the smooth endoplasmic reticulum was less marked. Foci of condensation occurred along with areas of normal smooth endoplasmic reticulum (figs. 5-39 and 5-43). The mitochondria were relatively normal, although they were frequently more rounded than their control counterparts. The cells appeared relatively normal apart from the condensed smooth endoplasmic reticulum. The number and percentage distribution of stage 2 phagosomes increased considerably (figs. 5-29 and 5-30). The other four stages appeared unaffected. Comparison of the corresponding control and test eyes showed a more marked increase in the peripheral retina (280%) than in the region of the visual streak (210%).

5-11.7 90 minutes ischaemia, 60 minutes recovery.

There was little if any reorganisation in the retinal pigment epithelium at this stage. The condensation of the smooth endoplasmic reticulum was similar in appearance to that observed immediately after the period of ischaemia. In some mitochondria there were marked changes. Such mitochondria possessed a matrix of high electron density and had prominent cristae. These mitochondria were found along with swollen and ruptured mitochondria in most cells of the layer. These latter mitochondria were indistinguishable from those seen immediately after ischaemia. The widening and reduction of the basal infoldings evident in the ischaemic tissue was more marked in the post-ischaemic tissue. The number and distribution of the phagosomes appeared to be unaltered (figs. 5-27, 5-28 and 5-34).

5-11.8 90 minutes ischaemia and 240 minutes recovery.

This period of ischaemia and recovery was associated with marked degenerative changes in the retinal pigment epithelium.

The tubules of smooth endoplasmic reticulum were shrunken and electron-dense (fig. 5-22). The surrounding matrix was floccular and of medium electron density. Frequently clefts occurred in the cytoplasm. The clefts contained little or no electron-dense material.

The majority of the mitochondria were swollen and rounded. The matrix was floccular and there were few cristae (fig. 5-22). An occasional tubular mitochondrion occurred which had a matrix of high electron density and wide cristae.

The reduction in the basal infolding was more extensive than following the shorter period of ischaemia (figs. 5-22). Widespread areas were devoid of infoldings, while in the remaining areas the infoldings were small and abnormal. In a few instances, the basal cell wall was ruptured (figs. 5-23 and 5-24). These ruptures exposed the contents of the cell to

Bruch's membrane, although no cellular material was seen within Bruch's membrane. The cells adjacent to these ruptured cells possessed long, finger-like projections which extended along Bruch's membrane in the area of the rupture (figs. 5-23).

The lateral junctional complexes were intact (fig. 5-26) with the exception of the cells with a ruptured cell membrane. In these cells the apical gap junctions could not be identified although the zonula adherens appeared intact (fig. 5-23).

The apical surface appeared intact after 4 hours recovery in spite of a considerable disturbance of the apical process (figs. 5-25 and 5-45). The processes were in addition often compressed by the swollen terminal portions of the outer segments. In some areas of the retinal pigment epithelium the cells were attenuated so that the thickness of the cell was as little as 1-2 microns (fig. 5-25). This attenuation was usually associated with swollen saccules of outer segment material adjacent to the apical surface. The apical surface of the pigment epithelial layer was ragged and undulating (fig. 5-45). This was in marked contrast to the relatively flat apical surface seen after recovery from shorter periods of ischaemia.

The quantitative analysis of the various phagosome stages revealed no increases or changes in distribution (figs. 5-29 and 5-30). Comparison of the test and control eyes therefore showed no differences (Fig. 5-34).

The distribution of the pigment granules within the cells was often abnormal at this stage. In some instances the apical region of the cell was devoid of pigment granules while in others granules were 3 or 4 deep (fig. 5-45).

The remaining organelles such as the nucleus, rough endoplasmic reticulum and the Golgi apparatus appeared generally normal in the intact cells. In the cells with a ruptured basement membrane the rough endoplasmic reticulum was swollen and formed vacuoles containing a floccular material.

The cytoplasm contained many vacuoles ^{and} ~~in~~ the smooth endoplasmic reticulum was abnormal (fig. 5-24).

5-11.9 120 minutes ischaemia and 60 minutes recovery.

The retinal pigment epithelial cells at this stage were generally similar in appearance to the tissue described after 60 minutes recovery from 90 minutes ischaemia. There was again little reorganisation of the cell. In addition, a few cells were more severely affected. The smooth endoplasmic reticulum formed a reticular mass which obscured much of the cytoplasmic detail. Mitochondria were similar to those found in the RPE after 90 minutes ischaemia and 60 minutes recovery and were generally the only organelles recognisable within the cytoplasm (fig. 5-20). As a result of the difficulty in distinguishing cell organelles a quantitative analysis of the various phagosome stages was not carried out.

5-11.10 120 minutes ischaemia and 240 minutes recovery.

This tissue was again similar to that seen after an identical period of recovery from 90 minutes ischaemia, although the changes were more widespread after the longer period of ischaemia. The smooth endoplasmic reticulum was abnormal. The basal infoldings were reduced or absent and ruptures in the basal cell wall were more frequently found than after 90 minutes ischaemia. In the intact cells the apical junctional processes appeared intact. These cells often possessed round or tubular mitochondria which had a matrix of high electron density and wide cristae (fig. 5-26). These mitochondria were less frequently encountered than following 90 minutes of ischaemia. The majority of the mitochondria after 4 hours recovery from 120 minutes of ischaemia were rounded and had a floccular matrix and randomly orientated cristae.

A quantitative analysis of the various phagosomes was not carried out on this tissue.

5-12 Electron microscopy of the visual cell outer segments.

5-12.1 15 minutes ischaemia and 60 minutes recovery.

The outer segments remained similar in appearance to those observed immediately after the period of ischaemia. The terminal portions of the outer segments were disorganised and disorientated.

5-12.2 15 minutes ischaemia and 240 minutes recovery.

The outer segments were indistinguishable from those studied after the shorter period of recovery (fig. 5-38). The outer segments were generally intact, although the discs were less well ordered at the distal end than in the normal retina. When the outer segments were cut perpendicularly they appeared wavy as they went in and out of the plane of section. In the normal retina, the outer segments formed straight pillars.

5-12.3 30 minutes ischaemia and 60 minutes recovery.

The fragmentation seen immediately following the period of ischaemia was less evident after 60 minutes recovery. This period of recovery was associated with some abnormalities. In the terminal regions of the outer segments there was some fragmentation and disorganisation (fig. 5-35). In some areas there were focal disturbances of the discs which were usually associated with ruptures of the cell membrane (fig. 5-36).

5-12.4 30 minutes ischaemia and 240 minutes recovery.

Many of the outer segments were intact but disorganised in a similar fashion to that seen after recovery from 15 minutes ischaemia. The ruptured cell membranes which were seen after 60 minutes recovery were not a feature of the tissue after 4 hours recovery. Some fragments of outer segment material still remained and these were generally found adjacent to the apical surface of the retinal pigment epithelium. These fragments often contained disorganised discs.

5-12.5 60 minutes ischaemia and 60 minutes recovery.

The outer segments were extensively fragmented, with many of the fragments forming swollen saccules. This situation was similar to that seen immediately after the period of ischaemia.

5-12.6 60 minutes ischaemia and 240 minutes recovery.

Following this recovery period relatively normal outer segments could be seen as well as abnormal fragments of outer segment material (fig. 5-43). Grossly distended fragments occurred only occasionally. The near normal outer segments often showed a focal area of disturbed discs although this area was not associated with a rupture of the cell membranes (fig. 5-39).

5-12.7 90 minutes ischaemia and 60 minutes recovery.

The outer segments remained in a similar state to that observed immediately after the period of ischaemia. Fragmentation was very pronounced with many of the fragments containing abnormal discs.

5-12.8 90 minutes ischaemia and 240 minutes recovery.

Some reorganisation was evident in the outer segments. Frequent long lengths of relatively normal outer segment material occurred, although few complete outer segments were observed (fig. 5-45). The apical surface of the retinal pigment epithelium was covered by many swollen outer segment fragments containing disorganised disc material. Frequently these distended fragments were ruptured and contained few discs amongst an electron-translucent material (figs. 5-25 and 5-45).

5-12.9 120 minutes ischaemia and 60 minutes recovery.

The outer segments were unchanged from the situation observed immediately after the period of ischaemia. The outer segments were extensively fragmented with many of the fragments being ruptured and containing abnormal discs.

5-12.10 120 minutes ischaemia and 240 minutes recovery.

At this stage there was little change from the situation seen immediately after the ischaemic episode and following 60 minutes recovery. However small portions of relatively normal outer segment material were present (fig. 5-40). These portions were much smaller and less frequent than after a similar period of recovery from 90 minutes ischaemia.

5-13 Electron microscopy of the visual cell inner segments.

5-13.1 15 minutes ischaemia and 60 minutes recovery.

The inner segments appeared generally normal. The mild mitochondrial distension seen immediately after the ischaemic episode was no longer present after 60 minutes recovery. There was however a limited swelling of the Golgi apparatus.

5-13.2 15 minutes ischaemia and 240 minutes recovery.

The inner segments remained normal in appearance except for the distension of the cisternae of the Golgi apparatus (fig. 5-42). This swelling was more severe than following the shorter period of recovery.

5-13.3 30 minutes ischaemia and 60 minutes recovery.

The inner segments at this stage were indistinguishable from those observed immediately after the period of ischaemia. Mitochondrial swelling was present with a decrease in the density of the mitochondrial matrix. Intracellular oedema and shortening of the inner segments were also featured.

5-13.4 30 minutes ischaemia and 240 minutes recovery.

The changes seen following 60 minutes recovery were no longer present. The inner segments appeared normal except for distension of the Golgi apparatus. This situation was identical to that seen following a similar recovery period from 15 minutes ischaemia.

5-13.5 60 minutes ischaemia and 60 minutes recovery.

The state of the inner segments remained similar to that seen immediately following the ischaemic episode. They were shortened and contained rounded mitochondria with disorganised cristae and an electron-translucent matrix. A few of the mitochondria were ruptured. The Golgi apparatus was often swollen (fig. 5-41).

5-13.6 60 minutes ischaemia and 240 minutes recovery.

With this recovery period considerable variation occurred in the appearance of the inner segments (fig. 5-43). There were signs of reorganisation in some inner segments while in others degenerative changes were evident. About half of the inner segments were long and slender and highly electron-dense while the remainder were short and swollen with a low electron density. The former contained many long mitochondria with numerous cristae and an electron-dense matrix (fig. 5-44). The cytoplasm was granular, highly electron-dense and contained the normal complement of cell organelles. The swollen inner segments possessed a cytoplasm of low electron density which contained rounded and distended mitochondria. These mitochondria had an electron-translucent matrix with small disorganised cristae. The other cell organelles could not be easily identified within the cytoplasm. At the terminal region of the swollen inner segments, there was frequently a portion of outer segment material, the discs of which were disorganised (fig. 5-49). A small proportion of these inner segments had ruptured cell membranes.

5-13.7 90 minutes ischaemia and 60 minutes recovery.

The inner segments were indistinguishable from those observed immediately after the period of ischaemia. Fragmentation of the inner segments was widespread and the fragments were often ruptured. The mitochondria remained swollen and frequently ruptured (fig. 5-46).

5-13.8 90 minutes ischaemia and 240 minutes recovery.

Following 4 hours recovery the inner segments were grossly abnormal (fig. 5-45). The majority were fragmented and possessed a cytoplasm of low electron density. The mitochondria within the fragments were round with few cristae and an electron-translucent matrix. Many of the mitochondria were ruptured. The other cell organelles were often difficult to distinguish. There were rare inner segments which were slender and had a high electron density (fig. 5-50).

5-13.9 120 minutes ischaemia and 60 minutes recovery.

The inner segments were totally disorganised with the majority being fragmented. Their appearance was similar to that seen immediately after the period of ischaemia.

5-13.10 120 minutes ischaemia and 240 minutes recovery.

With this longer period of recovery little change was apparent. The inner segments were grossly abnormal with fragments widely scattered within the subretinal space (fig. 5-40).

5-14 Electron microscopy of the external limiting membrane.

The junctions forming the external limiting membrane appeared to remain intact throughout the various recovery periods in spite of the severe damage observed in the visual cell inner segments following recovery from 90 and 120 minutes ischaemia (figs. 5-46 and 5-51). This so-called membrane was often interrupted by the ruptured membranes of the visual cells at the level of the external limiting membrane.

5-15 Electron microscopy of the outer nuclear layer.

5-15.1 15 minutes ischaemia and 60 minutes recovery.

The small focal dilations of the nuclear envelope seen immediately after the period of ischaemia were still present after 60 minutes recovery. The nuclei otherwise appeared normal.

5-15.2 15 minutes ischaemia and 240 minutes recovery.

The distensions of the nuclear envelope seen after the shorter period of recovery were still present (fig. 5-42).

5-15.3 30 minutes ischaemia and 60 minutes recovery.

The pyknotic changes evident immediately after the period of ischaemia remained following this post-ischaemic recovery period. The rounded nuclei were surrounded by mildly oedematous cytoplasm.

5-15.4 30 minutes ischaemia and 240 minutes recovery.

The nuclei appeared generally normal apart from limited distensions of the nuclear envelope. The nuclear appearance was similar to that seen after recovery from 15 minutes ischaemia (fig. 5-47). The pyknotic changes evident after the shorter recovery period were absent at this stage.

5-15.5 60 minutes ischaemia and 60 minutes recovery.

Pyknotic changes involving the rounding up of the nuclei and the condensation of the chromatin were present after this recovery period. This situation was similar to that seen immediately after the period of ischaemia.

5-15.6 60 minutes ischaemia and 240 minutes recovery.

Following this recovery period a wide spectrum of nuclear changes was evident (fig. 5-48). At one end of the spectrum the nuclei were similar to those seen after 4 hours recovery from 15 and 30 minutes ischaemia, although the nuclei were often slightly more electron-dense (fig. 5-49). These nuclei were frequently associated with the long slender electron-dense inner segments. At the other end of the spectrum the nuclei were round and the chromatin was usually a single electron-opaque mass which filled almost the entire nucleus (fig. 5-49). These circular nuclei were associated with the swollen and oedematous inner segments. The cytoplasm surrounding these nuclei was oedematous and contained floccular material of moderate electron density. The Müller cell cytoplasm surrounding the visual cell nuclei was oedematous having an electron density lower than in the control tissue.

5-15.7 90 minutes ischaemia and 60 minutes recovery.

The nuclei appeared similar to those seen immediately after the period of ischaemia. The cone nuclei remained better preserved than their rod counterparts, although on occasion there was a single cyst-like swelling of the nuclear envelope which contained a floccular material of moderate electron-density (fig. 5-46).

5-15.8 90 minutes ischaemia and 240 minutes recovery.

The majority of nuclei were in an advanced stage of pyknosis. At this stage there was a regional difference in the outer nuclear layer. In the peripheral retina the nuclei were rounded with prominent electron-dense chromatin masses. The perinuclear cytoplasm was oedematous and consisted of floccular material of moderate electron density. The receptor fibres were swollen and in many cases ruptured and the oedematous nature of the fibre cytoplasm was similar to that surrounding the nuclei (fig. 5-50). An occasional receptor of high electron density occurred. The Müller cell cytoplasm was electron-translucent and this gave prominence to the many fibrils within the cytoplasm. In the region of the visual streak, the visual cell nuclei were on the whole better preserved than in the peripheral retina. Although the surrounding Müller cell cytoplasm appeared to occupy a greater volume in the visual streak region (fig. 5-51). In both the visual streak and peripheral retina the cone nuclei were frequently pyknotic. This was the first appearance of changes in the cone nuclei. The affected nuclei were rounded and surrounded by oedematous cytoplasm with a low electron density (fig. 5-51).

5-15.9 120 minutes ischaemia and 60 minutes recovery.

The rod visual cell nuclei were severely pyknotic and remained similar to the nuclei seen immediately after the period of ischaemia. In addition a few nuclei were in a more advanced state of pyknosis. These nuclei were small and rounded, the perinuclear cytoplasm was oedematous. The cytoplasm was floccular with a low electron density and in many cases the cell membrane was ruptured.

5-15.10 120 minutes ischaemia and 240 minutes recovery.

There was no improvement in the state of the visual cell nuclei. Many nuclei were in a more advanced stage of pyknosis than the majority of nuclei after the shorter period of recovery. The pyknotic nuclei were similar to a few severely degenerate nuclei seen after 60 minutes recovery. At this

stage a regional difference existed, the nuclei of the visual streak were frequently better preserved than their counterparts in the peripheral retina. This was similar to the outer nuclear layer after 4 hours recovery from 90 minutes ischaemia.

5-16 Electron microscopy of the outer plexiform layer.

5-16.1 15 minutes ischaemia, 60 and 240 minutes recovery.

The outer plexiform layer appeared normal and was indistinguishable from the tissue seen immediately after the ischaemic episode.

5-16.2 30 minutes ischaemia, 60 and 240 minutes recovery.

At this stage the outer plexiform remained normal.

5-16.3 60 minutes ischaemia and 60 minutes recovery.

The receptor pedicles contained small randomly scattered vacuoles. The processes of the outer plexiform layer were mildly oedematous. This situation was little different from that seen immediately after the period of ischaemia.

5-16.4 60 minutes ischaemia and 240 minutes recovery.

Following this longer period of recovery, some of the receptor pedicles were degenerate while others were of normal appearance. The degenerative changes were evident in both the rod and cone pedicles (fig. 5-48). The degenerate pedicles were condensed and highly electron-dense (fig. 5-58), and often contained a few small electron-translucent vacuoles.

The swelling seen in the processes of the outer plexiform layer following the shorter period of recovery was no longer evident. The number of processes composing the layer appeared to be reduced compared with the control tissue.

5-16.5 90 minutes ischaemia and 60 minutes recovery.

In common with the other periods of ischaemia, this recovery period was associated with little or no change from the situation occurring immediately after the ischaemic episode. The rod pedicles were more

electron-dense than their control counterparts. The cone pedicles appeared unaffected. There was moderate distension of the processes of the outer plexiform layer.

5-16.6 90 minutes ischaemia and 240 minutes recovery.

The majority of the receptor pedicles were degenerate. The degeneration occurred in both the rod and cone pedicles. There were few relatively normal looking pedicles. The affected pedicles were shrunken and highly electron-dense, the ribbon synapse could still be identified. Small electron-transparent vacuoles were a feature of these abnormal pedicles (fig. 5-53). In the region of the visual streak the Müller cell cytoplasm adjacent to the pedicles was more oedematous than in the peripheral retina (figs. 5-53 and 5-59). The processes of the outer plexiform layer were no longer oedematous but were fewer than in the control tissue, this reduction was more marked in the region of the visual streak (fig. 5-53).

5-16.7 120 minutes ischaemia and 60 minutes recovery.

The receptor pedicles and the processes of the outer plexiform layer remained in a degenerate state similar to that seen immediately following the period of ischaemia.

5-16.8 120 minutes ischaemia and 240 minutes recovery.

This recovery period was associated with severe degeneration in almost all the receptor pedicles (fig. 5-53). The pedicles were shrunken and compressed and had a cytoplasm of high electron density. The number of processes were reduced and the cytoplasm of the radial pillars of the Müller cells was oedematous.

5-17 Electron microscopy of the inner nuclear layer.

5-17.1 15 minutes ischaemia, 60 and 240 minutes recovery.

There was no change from the situation observed immediately after the period of ischaemia with the nuclei and surrounding cytoplasm appearing normal.

5-17.2 30 minutes ischaemia, 60 and 240 minutes recovery.

The inner nuclear layer was normal in appearance following both these recovery periods. The limited focal separation of the nuclear membranes evident in some nuclei immediately after the ischaemic episode was not present following either of the recovery periods.

5-17.3 60 minutes ischaemia and 60 minutes recovery.

The nuclei were indistinguishable from those seen immediately following the period of ischaemia. There was a generalised swelling of the perinuclear cytoplasm in the neural cells of the layer. The Müller cells were of normal appearance (fig. 5-52).

5-17.4 60 minutes ischaemia and 240 minutes recovery.

The oedema evident after the shorter recovery period was no longer evident. The inner nuclear layer was generally of normal appearance (fig. 5-58), although there were occasional focal distensions of the nuclear envelope.

5-17.5 90 minutes ischaemia and 60 minutes recovery.

The oedematous changes present at this stage were often more severe than those seen immediately after this period of ischaemia. The oedema was frequently severe enough to result in rupture of the cell wall (figs. 5-55 and 5-50). The ruptured cells were generally sclerally situated and were either bipolar or horizontal cells. The Müller cells were not involved. In addition to the ruptured cell membranes, the nuclear envelope was also frequently ruptured (5-57). A few of the affected cells also had changes in their chromatin which was no longer uniform and had small electron-dense masses. On occasion the cytoplasm of the ruptured cell was associated with a vesicular body which was similar in some respects to a multivesicular body, although the limiting membrane was like that of a large coated vesicle (fig. 5-57). Such bodies were not found in relation to intact cells or in the control tissue.

5-17.6 90 minutes ischaemia and 240 minutes recovery.

This recovery period was associated with a considerable variation in the degree of degeneration evident in the inner nuclear layer. The peripheral retina (fig. 5-59) was in general less affected than the visual streak region (fig. 5-60). In the peripheral retina, the nuclei of the horizontal, bipolar and amacrine cells were rounded with a uniform chromatin of moderate electron density. The surrounding cytoplasm also had a moderate electron density with little evidence of oedema. A noticeable change was observed in the Müller cells. The nuclei were swollen and rounded with a moderate electron density. The Müller cell cytoplasm, however, appeared normal and had a higher electron density than the cytoplasm surrounding the processes of the outer plexiform and outer nuclear layers. In the area of the visual streak, some nuclei were similar to those in the periphery with a rounded outline and non-oedematous cytoplasm. The remaining nuclei were shrunken with prominent dense chromatin masses (fig. 5-60); the cytoplasm of these cells was oedematous and contained scattered vacuoles. The cell membranes and the nuclear envelope were frequently ruptured. The most advanced degenerative changes were seen in the horizontal, bipolar and amacrine cells, although it was often difficult to distinguish between these different cell types. The Müller cells were affected to a lesser extent, although with this long period of ischaemia, the nuclei were swollen and the cytoplasm oedematous with a low electron density. In addition there were occasional ruptures of the cell membranes.

5-17.7 120 minutes ischaemia and 60 minutes recovery.

In a similar fashion to 90 minutes ischaemia, the changes following 60 minutes recovery were more severe than the alterations occurring immediately after the period of ischaemia. Oedema was widespread and frequent ruptured cells were seen.

5-17.8 120 minutes ischaemia with 240 minutes recovery.

There was widespread degeneration throughout the inner nuclear layer, although it was more pronounced in the region of the visual streak. In the peripheral retina the degeneration was more advanced than that seen following 4 hours recovery from 90 minutes ischaemia.

5-18 Electron microscopy of the inner plexiform layer.

5-18.1 15 minutes ischaemia, 60 and 240 minutes recovery.

The inner plexiform layer retained the normal appearance seen immediately after the ischaemic insult.

5-18.2 30 minutes ischaemia and 60 minutes recovery.

Several of the processes of the inner plexiform layer were swollen with reduced neurofibrils and neurotubules. In some instances, the membranes of the processes were ruptured. The remaining processes appeared normal. This was identical to the situation seen immediately following the period of ischaemia.

5-18.3 30 minutes ischaemia and 240 minutes recovery.

There was little change from 60 minutes recovery with normal and abnormal processes occurring together. The former were more frequently found. Multivesicular bodies similar to those seen in the ruptured cells of the inner nuclear layer were also observed within some of the abnormal processes (fig. 5-61).

5-18.4 60 minutes ischaemia, 60 and 240 minutes recovery.

Following these two recovery periods the inner plexiform layers were similar in appearance. Normal and abnormal processes were present, the latter were more frequent. This was in contrast to the shorter period of ischaemia. The abnormal processes were similar to those seen following recovery from 30 minutes ischaemia. The cytoplasm was oedematous and contained reduced numbers of neurotubules and neurofibrils. Ruptures in the cell membrane of the processes were frequently seen (fig. 5-63). This situation was similar to that observed immediately following this period of ischaemia.

5-18.5 90 minutes ischaemia, 60 and 240 minutes ischaemia.

The appearance of the processes was similar following both the periods of recovery. The appearance was in turn indistinguishable from that seen immediately after the period of ischaemia. The majority of the processes were abnormal and were more severely affected than with the shorter periods of ischaemia. The cytoplasm was floccular with few or no neurotubules and neurofibrils. The membrane of the processes was frequently ruptured. In spite of the considerable disorganisation occurring in this layer, processes containing ribbon synapses could still be identified. The radial pillars of Müller cell cytoplasm generally possessed a granular appearance and had a low electron density (fig. 5-62). The appearance of the Müller cell cytoplasm was the only difference between the ischaemic and post-ischaemic tissue. Immediately following the ischaemic episode, the Müller cell cytoplasm had a higher electron density than the surrounding oedematous processes.

5-18.6 120 minutes ischaemia, 60 and 240 minutes recovery.

The processes of the inner plexiform layer following the two recovery periods were similar in appearance. These two periods of recovery were similar in appearance to that immediately following 120 minutes ischaemia, and identical to that seen after recovery from 90 minutes ischaemia. The majority of the processes were grossly swollen with a floccular cytoplasm and many of the processes were ruptured.

5-19 Electron microscopy of the ganglion cells.

5-19.1 15 minutes ischaemia, 60 and 240 minutes recovery.

The ganglion cells were indistinguishable from their control counterparts

5-19.2 30 minutes ischaemia, 60 and 240 minutes recovery.

The ganglion cells appeared normal following both these recovery periods. The focal distensions of the nuclear envelope seen immediately after the period of ischaemia were not evident during the post-ischaemic recovery phase.

5-19.3 60 minutes ischaemia, 60 and 240 minutes recovery.

The mild intracellular oedema evident in the ganglion cells immediately after the period of ischaemia remained following both these periods of recovery (fig. 5-63).

5-19.4 90 minutes ischaemia and 60 minutes recovery.

Severe intracellular oedema was present in the ganglion cells. The cell contents were often found as a mass adjacent to the nucleus. This was similar to the situation occurring immediately after the ischaemic episode.

5-19.5 90 minutes ischaemia and 240 minutes recovery.

The ganglion cells were condensed and more electron-dense than normal (fig. 5-64). Intracellular oedema was only present in a few cells. These cells were usually found in the peripheral retina. The cytoplasm of the condensed cells was granular and contained many free ribosomes and small cisternae of rough endoplasmic reticulum. The cell membranes were occasionally ruptured.

5-19.6 120 minutes ischaemia and 60 minutes recovery.

The ganglion cells remained in a similar state to those seen immediately after the period of ischaemia. Marked intracellular oedema was present in the ganglion cells.

5-19.7 120 minutes ischaemia and 240 minutes recovery.

The intracellular oedema evident previously was not present following 4 hours recovery. The cytoplasm was electron-dense, granular and rich in ribosomes. These cells were similar to those seen after an identical recovery period from 90 minutes ischaemia.

5-20 Electron microscopy of the nerve fibre layer and internal limiting membrane.

The Müller cell cytoplasm which surrounds the ganglion cells, the nerve fibres and extends to the internal limiting membrane was generally similar after both recovery periods to the situation prevailing immediately

after the various periods of ischaemia (fig. 5-56). However, after 4 hours recovery from 90 and 120 minutes ischaemia, the Müller cell cytoplasm contained shrunken profiles of smooth endoplasmic reticulum and had a lower electron density than in the other tissue (fig. 5-66).

The unmyelinated fibres of the nerve fibre layer often remained distended even after a 4 hour recovery period (fig. 5-65). This distension was largely confined to the larger fibres as there were many small normal looking fibres.

5-21 Electron microscopy of the myelinated nerve fibre zone.

The myelinated fibres of this layer generally appeared normal after 60 minutes recovery from the various periods of ischaemia. Although there were focal areas of disturbed myelin (fig. 5-67). In the fibres associated with the disturbed myelin, multivesicular bodies similar to those seen in the inner plexiform and inner nuclear layers were seen (fig. 5-67). The glial cells which were found amongst the nerve fibres and extended through the internal limiting membrane to envelop the extra-retinal blood vessels possessed distended mitochondria (figs. 5-67 and 5-69). The mitochondria of the blood vessels were also distended (fig. 5-69), although the remainder of the cell appeared normal.

Following 240 minutes recovery, there were still focal areas of myelin disturbance, but these were less pronounced than after the shorter recovery period. These disturbances were associated with the longer periods of ischaemia. In addition, in this latter tissue some of the nerves were of higher electron density than the others (fig. 5-⁶68). These nerves contained many dark staining inclusion bodies. Occasionally an unmyelinated nerve had a swelling containing many lightly staining vacuoles (fig. 5-68). After 4 hours recovery the mitochondrial swelling seen following the shorter recovery period was no longer evident in the glial cells or in the blood vessel endothelium.

5-22 Electron microscopy of the choroidal endothelium

In the course of a study into the effects of acute ischaemia on the structure of the retina, inclusion bodies were observed in the endothelium of some vessels of the choroid (figs. 5-70 and 5-71). These bodies possessed certain similarities to phagosomes contained in the retinal pigment epithelium. This led to a further investigation of the choroidal endothelium. Although the inclusion bodies were seen in one case immediately after the period of ischaemia, the bodies were predominantly found during the post-ischaemic phase.

The endothelium of the choroidal vessels appeared to be relatively resistant to ischaemic damage induced by high intracocular pressure. Immediately following the varying periods of ischaemia, an occasional myelin body was observed. The mitochondria were frequently distended with a decrease in the electron density of the matrix and a shortening of the cristae. There were also frequent lysosomal-like bodies. These were membrane-bound and contained a granular material of high density. In addition, there appeared to be a decrease in the number of pinocytic vesicles in the ischaemic endothelium, although no quantitative analysis was carried out. In general these features became more prominent with increasing durations of ischaemia. During the post-ischaemic recovery phase the endothelium rapidly regained a normal appearance although there was occasionally cytoplasmic clefting and the mitochondrial matrix generally had a higher electron density than normal.

In addition to the myelin bodies other inclusion bodies were evident in the endothelial cytoplasm (figs. 5-70 and 5-71). These were membrane-bound bodies 0.3-1.5 microns in diameter, containing organised membranous material. Apart from this material, the presumed phagosome contained discrete areas of granular material of high electron density (fig. 5-71). The endothelial phagosomes appeared similar to the phagosomes encountered

in the retinal pigment epithelium and particularly resembled in both size and organisation the phagosomes seen during the initial stages of the disposal and degradation of the terminal portions of the visual cells outer segments by the pigment epithelium.

The choroidal endothelium was the only location of the choroid in which these phagosomes containing lamellar material were found. They were absent from Bruch's membrane, the vessel lumen and choroidal histiocytes.

In the 30 eyes examined following periods of ischaemia and post-ischaemic recovery, endothelial phagosomes were found in six preparations. Of these six, one was from tissue immediately following the ischaemic episode and the remainder from various times during the post-ischaemic recovery phase (fig. 5-72).

5-23 Discussion.

This investigation shows that the rabbit retina was structurally able to withstand 15 minutes ischaemia. The only departure from normal after 4 hours post-ischaemic recovery was a mild disturbance of the outer segments. This disturbance was also seen after a similar recovery period from 30 minutes ischaemia. In addition abnormal processes were present in the inner plexiform layer. Apart from these two changes, the retina was relatively normal in appearance. The recovery pattern following 60, 90 and 120 minutes ischaemia indicated that the various layers of the retina appeared to possess different sensitivities to acute pressure-induced ischaemia. The retinal pigment epithelium and the Müller cells were the least sensitive while the visual cells were the most sensitive.

The retinal pigment epithelium shows a high resistance to ischaemia with the great majority of retinal pigment epithelial cells remaining intact even after 120 minutes ischaemia. This feature of the retinal pigment epithelium has also been demonstrated following choroidal ischaemia, where the pigment epithelium remained intact in spite of the complete destruction of

the visual cells (Gay, Golder and Smith, 1964, Golder and Gay 1967, Foulds, Lee and Taylor 1971, Hayreh and Baines 1972, Buettner, Machemer, Charles and Anderson 1973 and Anderson and Davis 1974). The retinal pigment epithelium showed signs of regeneration 4 hours after a period of 2 hours ischaemia. Many of the cells possessed mitochondria with an electron-dense matrix and wide cristae. Such mitochondria may be indicative of active cells and similar mitochondria can be seen in smooth muscle and synchronous insect flight muscles. Some of the round mitochondria with a matrix of high electron density appeared similar to those described by Grignolo, Orzalesi and Calabria (1966) in degenerating RPE cells following administration of sodium iodate. The mitochondria in the ischaemic tissue were thought to be in the initial stages of regeneration. The difference between the latter and those following sodium iodate poisoning may be explained on the basis that ischaemia was a temporary metabolic block while sodiumiodate was a more permanent metabolic block.

Although the great majority of the retinal pigment epithelial cells were intact and appeared viable, they may not have retained the ability to perform the functions associated with the normal cell. In the normal pigment epithelial cell many of its functions are reflected by its ultrastructural organisation and by studying this some idea of the functional capabilities of the post-ischaemic RPE may be gained from the organisation of the affected cells. The RPE was able to increase its phagocytic activity after the shorter periods of ischaemia, but not after the longer periods. This phagocytic activity appeared to be closely related to the degree of damage to the outer segments as well as the pigment epithelium and, in turn, to the duration of ischaemia and period of post-ischaemic recovery. Short periods of ischaemia caused the outer segments to fragment and swell, although much of the structural uniformity present in the control tissue was still evident. The longer periods of ischaemia (60, 90 and 120 minutes) caused further

fragmentation along with disruption and disintegration of the discs themselves. This structural disorganisation was thought to account for the apparent preponderance of stage 2 phagosomes observed during the recovery phase from 60 minutes ischaemia for stage 1 and 2 were probably confused because the RPE had engulfed material that was already structurally altered. After 15 minutes ischaemia, a moderate increase in the number of phagosomes occurred while after 30 minutes ischaemia a ^{lower} ~~higher~~ increase in the number of phagosomes was apparent. The changes were generally more marked after 4 hours recovery. Following these periods of ischaemia, the RPE was able to increase its rate of phagocytosis three-fold. If the assumption was correct that after recovery from 60 minutes ischaemia the so-called stage 2 phagosomes comprised both stages 1 and 2 then the phagocytic capacity of the cells was less after 1 hour of ischaemia than in those cells investigated after the shorter periods of ischaemia. After 90 minutes ischaemia, no increase in the phagocytic activity was evident in the pigment epithelium. This then was evidence that periods of ischaemia longer than 30 minutes may inhibit the ability of the RPE to engulf extra outer segment material. The increases in phagocytic activity that did occur were more marked in the peripheral retina and may suggest that under normal circumstances, cells of the central RPE were nearer the upper limit of phagocytic capacity than the cells in the periphery, although there are other interpretations (see 3-3.1).

Another important function of the RPE is in the transport of fluid and material from the choriocapillaris. The basal region of the cell is modified for this purpose by virtue of its infoldings and adjacent mitochondria. These infoldings were markedly affected by ischaemia of 90 or 120 minutes duration. Although even after a recovery period of 4 hours the cells appeared viable, they no longer possessed the heavily infolded basal cell wall and this suggested that their ability to transport fluid may have been severely reduced.

The retinal pigment epithelium also acts as a barrier to diffusion of materials from the choriocapillaris as well as the subretinal space. The apical junctional complexes are thought to be responsible for this barrier, in addition the gap junctions are thought to mediate electrical coupling between adjacent RPE cells. In the majority of cells, the junctions appear ultrastructurally intact, although this does not signify functional integrity. An investigation using tracer substances such as horse-radish peroxidase, ferritin and colloidal carbon would be helpful in this instance. In a few cases where the basal cell wall was ruptured, the gap junctions could not be identified and this may have affected ion flux between adjacent cells as well as chorio-retinal diffusion. The cells adjacent to these ruptured cells had finger-like projections which extended along Bruch's membrane. This lateral spreading of the intact cells may have been ^{the} initial reaction of the RPE to plug the gap left by the ruptured cell and maintain a complete covering of intact cells over Bruch's membrane.

The ruptured basal cell membrane may also be a route for the passage of outer segment material into the choroid. The presence of phagosomes in the choroidal endothelium was an unexpected finding, although their presence was open to much speculation. A similarity did exist between these endothelial phagosomes and those of the retinal pigment epithelium and the contents may have been of visual cell origin. If this was so, the material in the phagosomes must have reached the choroidal endothelium either as disrupted outer segment material or as partly digested phagosomes from the pigment epithelium. In either case, one must postulate a trans-pigment epithelial route to the choroidal vessels, for even after lengthy periods of ischaemia, the apical surface of the pigment epithelium formed an intact layer over Bruch's membrane throughout the experiments. The ruptured basement membrane may not have been the only possible route for the passage of material into the choroid. Partly digested phagosomes may also be able to pass out of intact

pigment epithelial cells as Hogan (1971) has described their presence in Bruch's membrane in the human eye. The route by which the material entered the choroid remains speculative as no such material was observed in either Bruch's membrane or in the lumen of the blood vessels. However, the small chance of observing material in this latter site must have been further reduced by the use of intra-arterial perfusion during the process of fixation.

The vascular endothelium outside the reticulo-endothelial system has been shown to be capable of phagocytosis, although this does not occur readily. Cotran (1965) has demonstrated in rats and mice that following repeated injections of colloidal carbon phagocytosis was evident in the endothelium of small myocardial vessels in the endocardium, in the pulmonary capillary endothelium, in the aorta and in glomerular and peritubular capillary endothelium. In the eye, the non-vascular endothelium lining the trabecular beams underlying Schlemm's canal has been shown capable of considerable phagocytic activity (Grierson and Lee, 1973).

Under normal circumstances, the choroidal endothelium does not appear to be phagocytically active. Ischaemia induced by high intraocular pressure may have been a sufficient stimulus to expose a latent phagocytic ability of the choroidal endothelium. This route for the removal of outer segment debris must have accounted for a small amount of the debris compared with the removal of similar material by macrophages and the retinal pigment epithelium.

An interesting feature of the post-ischaemic outer retina was the absence of macrophages in spite of the large amounts of debris remaining in the subretinal space during the recovery phase from the longer periods of ischaemia. The retinal pigment epithelium under these conditions appears to act as an auxiliary macrophage. The fate of the macrophages seen in the ischaemic tissue is not known. They may have reverted to pigment epithelium (assuming their origin was the RPE) or have passed into the general circulation. No evidence of either event was seen in this study.

The visual cells appeared to be the least resistant of any of the retinal cells to ischaemia. Following recovery from 15 and 30 minutes ischaemia, there were limited changes in the outer segments, outer nuclear layer and in the Golgi apparatus of the myoid region of the inner segments. 4 hours after the ischaemic episode the cells appeared viable and the changes seen were thought likely to disappear with longer periods of recovery. However, after 60 minutes ischaemia, some cells were evidently degenerate and would not be expected to recover. Following 90 and 120 minutes ischaemia the degeneration in the visual cell was severe and so widespread that few cells would have had the ability to recover. To determine more precisely the post-ischaemic recovery process in the rabbit retina, longer recovery periods need to be studied. The visual cells would appear from this study to be capable of withstanding up to 30 minutes ischaemia. Sixty minutes ischaemia produced irreversible changes in some visual cells as evidenced by the appearance immediately after this period of ischaemia of swollen and ruptured inner segments, distended fragments of outer segment material and advanced pyknotic changes in the visual cell nuclei. Degenerate receptor pedicles were prominent 4 hours after ischaemia, although immediately after the period of ischaemia there were few degenerative signs present. It may therefore be difficult to assess the degree of damage in the pedicles by their ultrastructural appearance immediately after the period of ischaemia. Periods of ischaemia longer than 60 minutes were associated with more severe and probably irreversible changes. In spite of the further appearance of damage to the visual cells during the recovery phase there seemed to be some reorganisation in the outer segments. Following 4 hours recovery from 60, 90 and 120 minutes ischaemia, there were many portions of outer segments containing well-ordered stacks of discs. After 60 minutes ischaemia, many of these portions were in the form of relatively normal outer segments, while after 90 minutes ischaemia, although portions of outer segment material were

often large, few intact outer segments were seen. Following recovery from 120 minutes ischaemia there were no intact outer segments and the portions of outer segment material were smaller and fewer. Cohen (1971) has shown that the outer segments act as relatively good osmometers. The above results may suggest that the ionic environment of the subretinal space was not too far removed from normal. If this were the case, the relatively intact retinal pigment epithelium may have continued to exert a considerable influence on the ionic environment of the subretinal space in spite of the ischaemic insult. The inner segment of the visual cells were often grossly degenerate and would be unlikely to exert much influence on the ion balance in this region. Another feature that indicates that the ionic environment was more normal during the post-ischaemic phase than immediately after the period of ischaemia was the absence of retinal folds in the post-ischaemic tissue.

The changes occurring in the visual cells were generally uniform throughout the retina. However, following recovery from 90 and 120 minutes ischaemia, the outer nuclear layer was frequently better preserved in the area of the visual streak as compared with the peripheral retina. The underlying reason for this regional variation was not understood although it may be related to the better developed choroid in the visual streak. If this were so, one might have expected the inner and outer segments to be better preserved as well, but this was not so.

The inner retina was better preserved than the outer retina. This may have been related to the fact that the Müller cell cytoplasm in the latter region was prominent with a high glycogen content. Weiss (1972) however showed that it was not the amount of glycogen present, but the ability to metabolise it that was important. This ability rapidly fails following 60 minutes ischaemia and does not return to normal even with long periods of post-ischaemic recovery. It was after this period of ischaemia that degenerative changes were seen in the inner retina during the recovery phase.

In the inner nuclear layer, a regional variation was again evident during the recovery phase from 90 and 120 minutes ischaemia. In the area of the visual streak the nuclei were in a more advanced stage of pyknosis than in the peripheral retina. The underlying reason for this regional variation was not known.

The neural elements of the inner nuclear layer were more readily affected than the Müller cells. This was similar to the findings immediately after the period of ischaemia. Following the recovery phase from 90 and 120 minutes ischaemia there was a marked reduction in the number of processes in the outer plexiform layer. This reduction coincided with severe degeneration in the inner nuclear layer. There was a noticeable paucity of transverse horizontal fibres in the outer plexiform layer, although the horizontal cells did not appear more degenerate than the other neural cells.

The inner plexiform layer was very susceptible to ischaemic damage as evidenced by the ruptured processes during recovery from 30 minutes ischaemia. There was no apparent decrease in the number of processes in this layer after the longer recovery periods as was the case in the outer plexiform layer.

In several of the ruptured cells of the inner nuclear layer and the processes of the inner plexiform layer a type of multivesicular body was found. This was only apparent in damaged cells. The significance of this body was not known although it was indicative of severely damaged cells.

The ganglion cells appeared relatively resistant to ischaemia. This finding departed from many other studies which have shown that the ganglion cells were sensitive to increases in intraocular pressure. Flocks, Tsukahara and Miller (1959), Kupfer (1962) and De Carvalho (1962) have shown that the ganglion cells in the rabbit retina readily become degenerate following long-term elevations of intraocular pressure. The difference between these studies and the present may be in the difference between chronic and acute elevations

of intraocular pressure. In animals with a dual circulation, acute rises in intraocular pressure resulted in rapid degeneration of the ganglion cells (Smith and Baird, 1952, Reinecke, Kuwabara, Cogan and Weis 1962, and Anderson and Davis 1975). In the rat retina, irreversible changes in the ganglion cells occurred after 20 minutes acute ischaemia. However, Reinecke et al (1962) showed in cats that 90 minutes ischaemia was necessary before changes were evident in the ganglion cells. In this present study, the ganglion cells were apparently able to withstand up to 2 hours of ischaemia. The surrounding Müller cell cytoplasm with its high glycogen content may act as a protective coating although the Müller cells' ability to utilise this material must be impaired (Weiss 1972).

Few ultrastructural studies have been undertaken on the pattern of post-ischaemic recovery in tissues. Bassi and Bernelli-Zazzera (1964) describe the changes in rat liver and show that up to 60 minutes ischaemia was compatible with a return to normality. They found no specific lesion which was related to the death of the liver cells subjected to ischaemia. The limit of irreversibility was reached through a progressive deterioration of different cellular structures and death appeared as the outcome of many defects in subcellular organisation that had passed the stage of compensatory repair. Webster and Ames (1965) describe the pattern of ultrastructural recovery following anoxia in isolated rabbit retinae. They found that longer than 20 minutes anoxia was not compatible with structural recovery in the visual cells. In addition to degenerative changes in the visual cells, there was marked oedema in the inner retina. They concluded that the irreversible changes were linked with the appearance of ruptured cell and mitochondrial membranes. It is difficult to draw parallels between this study (Webster and Ames 1965) and the present, because in the former the RPE was not present and it is thought that it plays a significant role in the maintenance of the outer retina and especially the visual cells.



FIG.5-1 Light micrograph of the peripheral retina(15 minutes ischaemia,60 minutes recovery),apart from the mild disturbance of the outer segments of the visual cells the retina appears normal. (550 X)

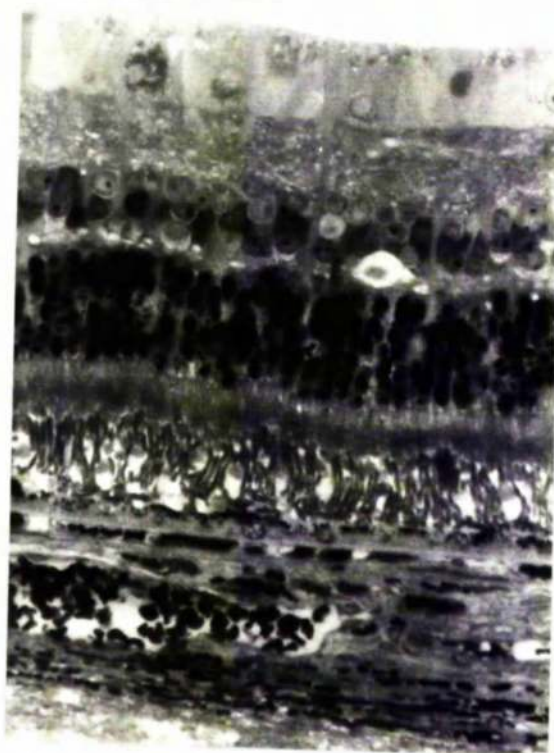


FIG.5-2 Light micrograph of the peripheral retina(30 minutes ischaemia,60 minutes recovery),the retina appears relatively normal apart from the disturbed outer segments of the visual cells.(550 X)



FIG.5-3 Light micrograph of the visual streak region(60 minutes ischaemia,60 minutes recovery),degenerative changes are evident throughout the retina but are more pronounced in the outer retina.(550 X)

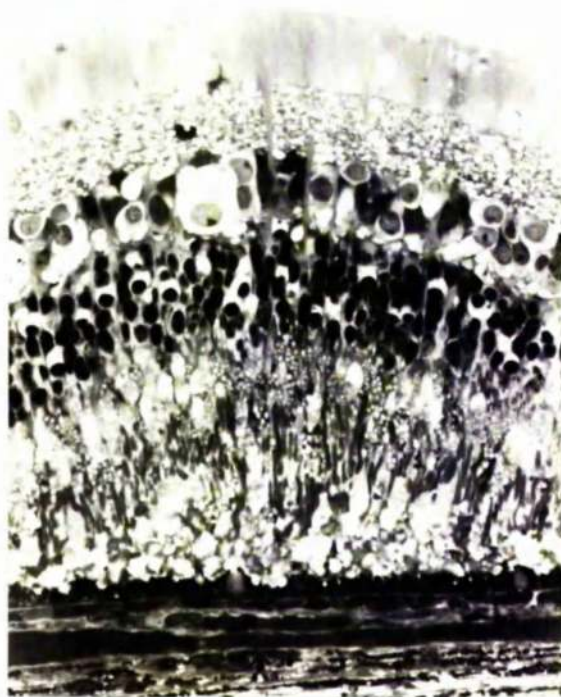


FIG.5-4 Light micrograph of the peripheral retina(90 minutes ischaemia,60 minutes recovery),degenerative changes occur throughout the retina but are more marked in the outer retina.(550 X)



FIG.5-5 Light micrograph of the retina underlying the bands of myelinated nerve fibres(120 minutes ischaemia,60 minutes recovery),the inner and outer segments are fragmented and pyknotic changes are seen in the outer and inner nuclear layers.(550 X)



FIG.5-6 Light micrograph of the peripheral retina(90 minutes ischaemia,60 minutes recovery),following the longer periods of ischaemia retino-schisis is sometimes a feature of the retina.The split occurs in the outer nuclear layer adjacent to the external limiting membrane. (550 -X)

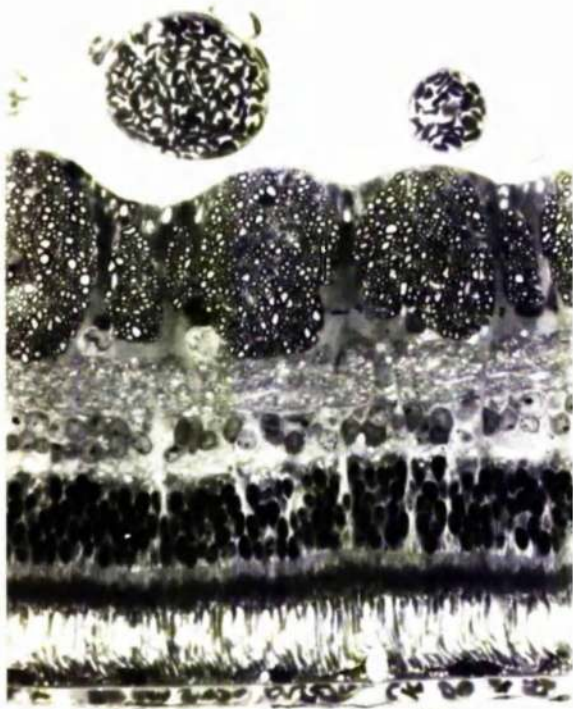


FIG.5-7 Light micrograph of the horizontal nerve fibre zone(15 minutes ischaemia, 240 minutes recovery),the retina appears normal apart from a mild disturbance of the outer segments of the visual cells.(550 X)

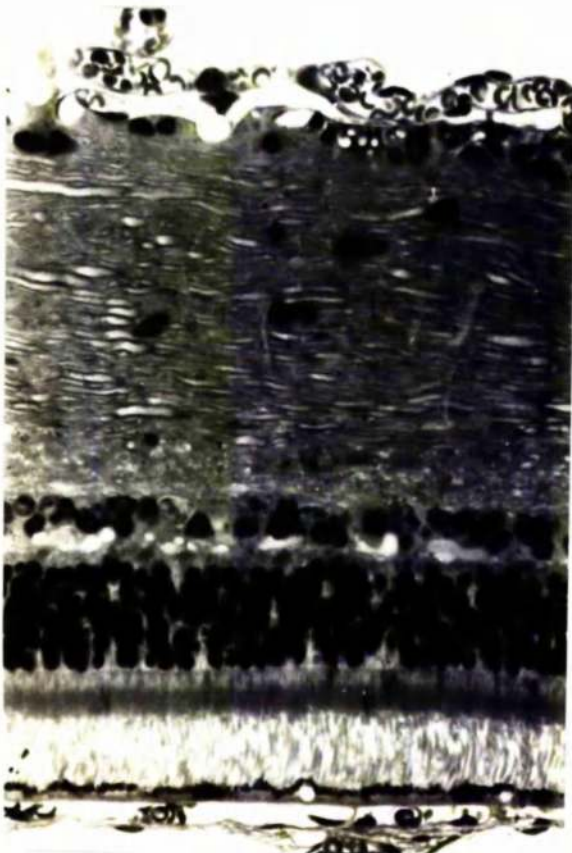


FIG.5-8 Light micrograph of the horizontal nerve fibre zone(30 minutes ischaemia, 240 minutes recovery),the retina appears normal apart from a mild disturbance of the outer segments of the visual cells.(550 X)

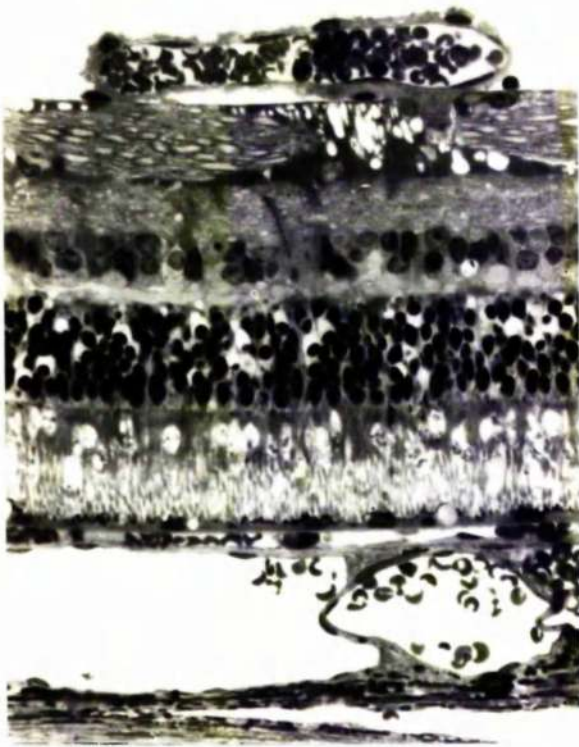


FIG.5-9 Light micrograph of the horizontal nerve fibre zone(60 minutes ischaemia, 240 minutes recovery),many of the visual cell nuclei are pyknotic and some inner segments are grossly swollen. The inner retina appears relatively normal.(550 X)

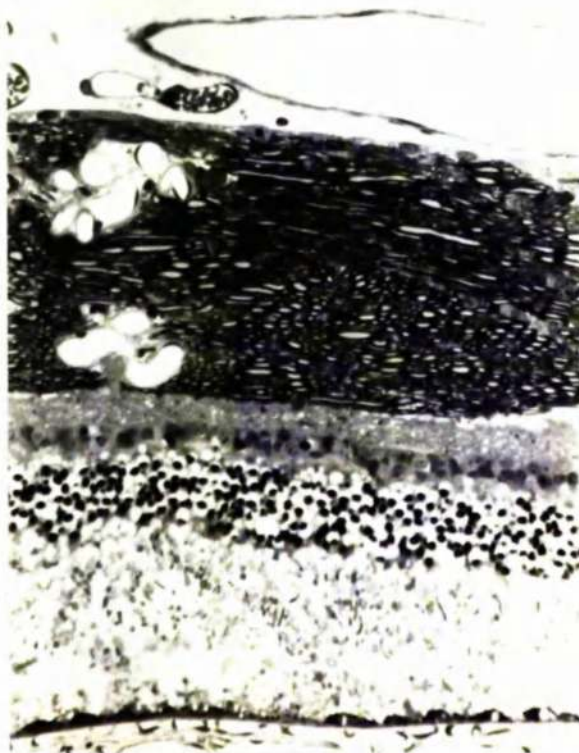


FIG.5-10 Light micrograph of the horizontal nerve fibre zone(120 minutes ischaemia, 240 minutes recovery),the visual cells are grossly degenerate and some pyknotic changes are evident in the inner nuclear layer.(550 X)

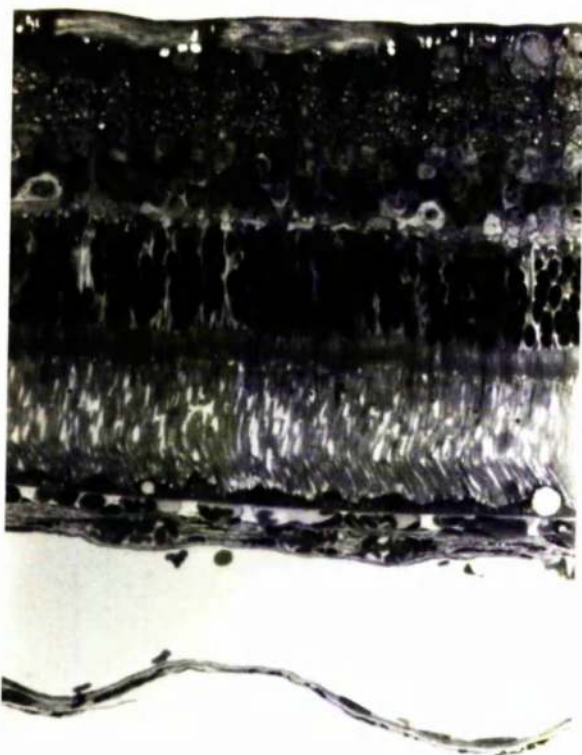


FIG.5-II Light micrograph of the visual streak region(15 minutes ischaemia,240 minutes recovery),the retina appears normal except for a mild disorganisation in the outer segments of the visual cells. (550 X)



FIG.5-I2 Light micrograph of the visual streak region(90 minutes ischaemia,240 minutes recovery),the visual cells are degenerate and pyknotic nuclei occur in the inner nuclear layer.(550 X)

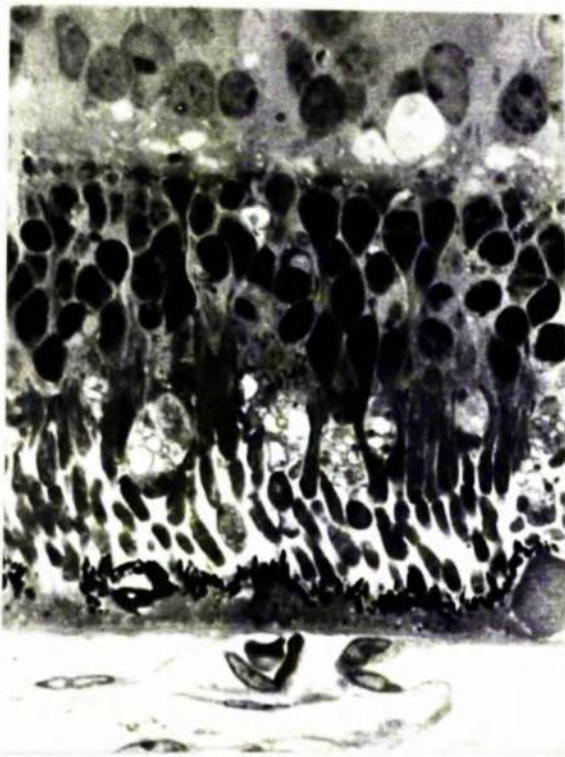


FIG.5-13 Light micrograph of the outer retina(60 minutes ischaemia,240 minutes recovery) normal and abnormal visual cells occur together.The pigment epithelium appears normal. (1,500 X)

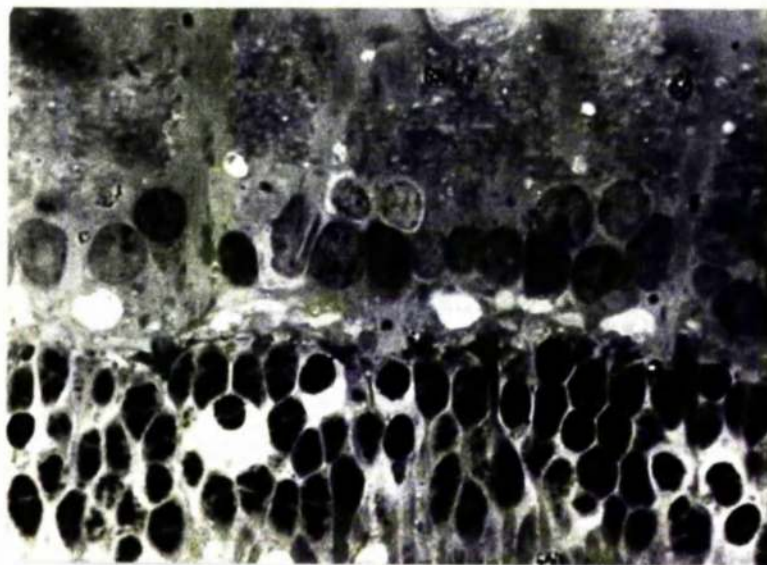


FIG.5-14 Light micrograph of the inner nuclear layer(60 minutes, ischaemia,240 minutes recovery),the nuclei are rounded but have a normal staining reaction.(1,500 X)



FIG.5-15 Light micrograph of the outer retina(90 minutes ischaemia, 240 minutes recovery), the pigment epithelium is undulating and the pigment granules are unevenly dispersed in an intensely staining cytoplasm.(1,500 X)



FIG.5-16 Light micrograph of the visual cells(90 minutes ischaemia, 240 minutes recovery), the inner and outer segments are fragmented and swollen. The visual cell nuclei are grossly pyknotic.(1,500 X)

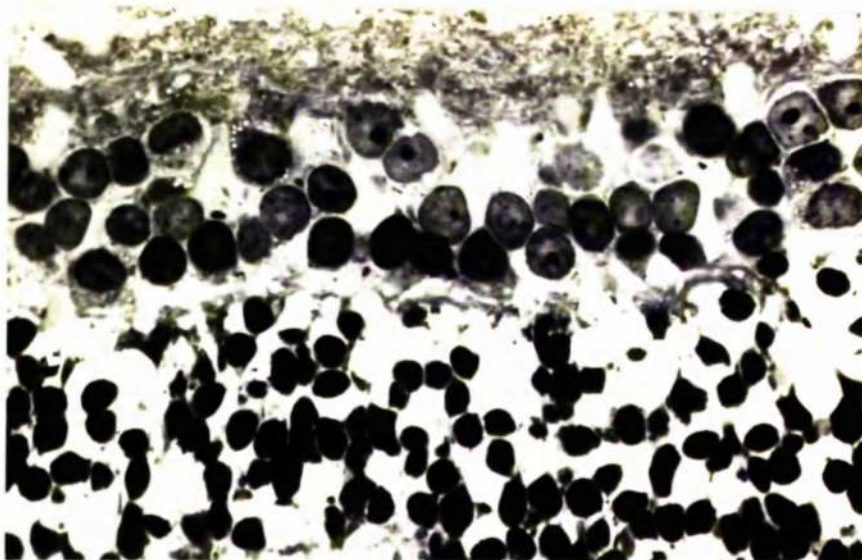


FIG.5-17 Light micrograph of the inner and outer nuclear layers in the peripheral retina(90 minutes ischaemia,240 minutes recovery), severe pyknotic changes are evident in the outer nuclear layer while in the inner nuclear layer the nuclei are rounded and lie in oedematous cytoplasm.(I,500 X)

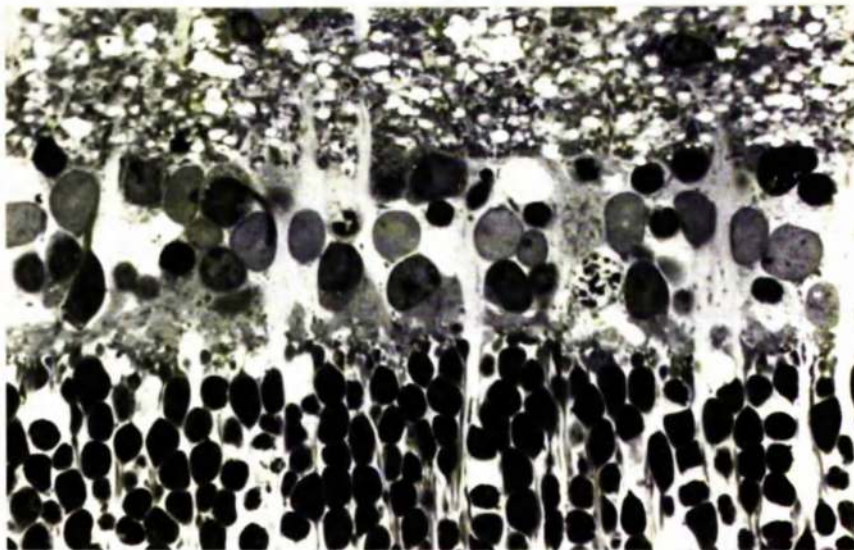


FIG.5-18 Light micrograph of the inner and outer nuclear layers in the region of the visual streak(90 minutes ischaemia,240 minutes recovery),advanced pyknotic changes are evident in the inner nuclear layer.The outer nuclear layer is less affected than in the peripheral retina.(I,500 X)



FIG.5-19 Electron micrograph of the pigment epithelium(30 minutes ischaemia,60 minutes recovery),the cell is little affected except for limited mitochondrial swelling.(14,000 X)



FIG.5-20 Electron micrograph of the pigment epithelium(120 minutes ischaemia,60 minutes recovery),the mitochondria(M) are abnormal and the smooth endoplasmic reticulum forms an amorphous mass amongst which is found swollen cisternae of rough endoplasmic reticulum and vacuoles.(14,000 X)



FIG.5-2I Electron micrograph of the pigment epithelium(30 minutes ischaemia,240 minutes recovery),phagosomes(P) in the early stages of degradation are often prominent in the cytoplasm.The processes of the apical surface show considerable disturbance.(16,000 X)



FIG. 5-22 Electron micrograph of the basal region of the pigment epithelium (90 minutes ischaemia, 240 minutes recovery), the basal infoldings are either reduced or absent, the mitochondria (M) are abnormal and the smooth endoplasmic reticulum (S) is shrunken. (30,000 X)



FIG. 5-23 Electron micrograph of the basal region of the pigment epithelium (90 minutes ischaemia, 240 minutes recovery), in spite of the ruptured cell membrane (arrow) the zonulae adherentes appear intact although the gap junction can not be identified. The adjacent intact cell has a finger like projection extending along the inner surface of Bruch's membrane. (20,000 X)

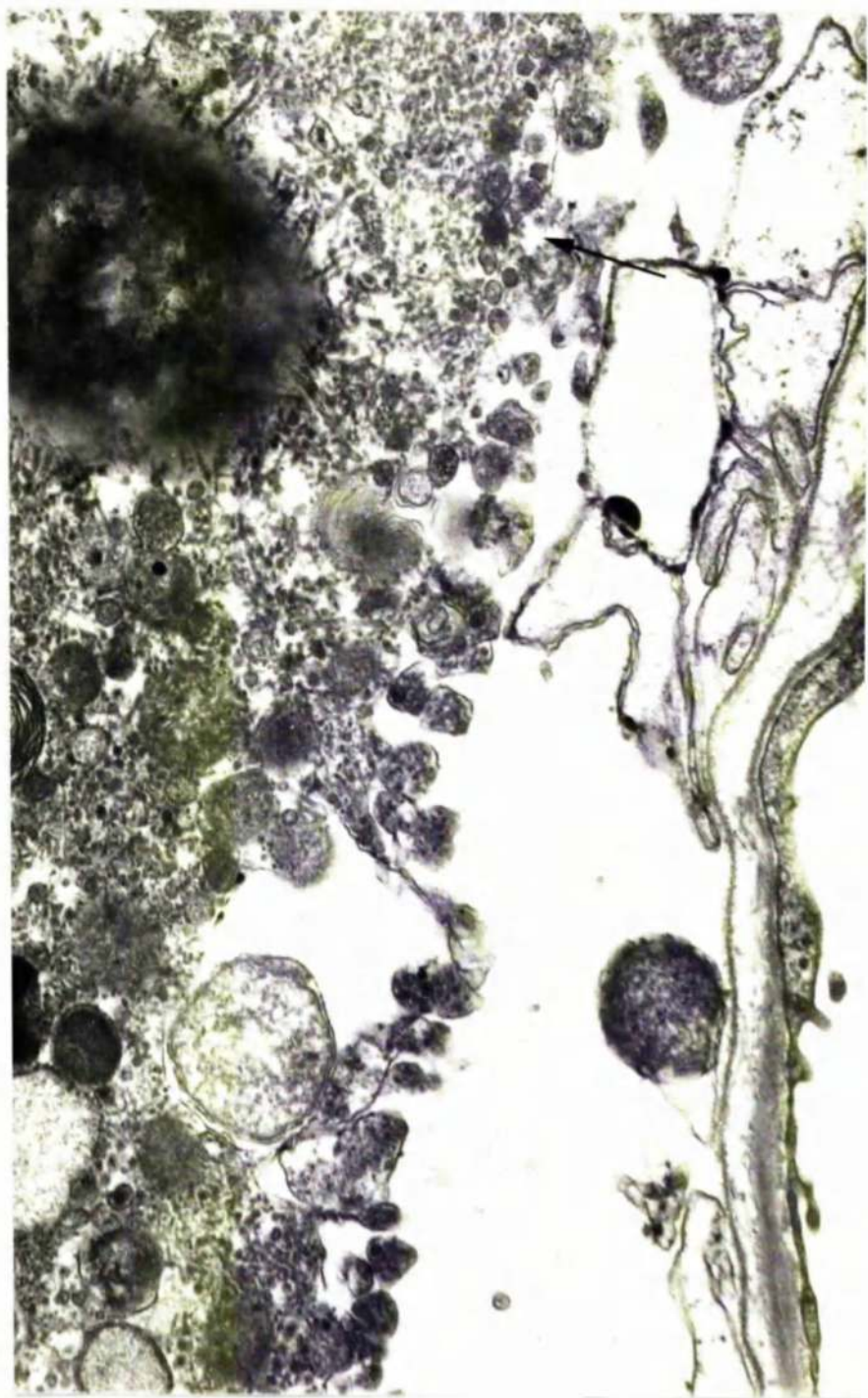


FIG.5-24 Electron micrograph of the basal region of the pigment epithelium(90 minutes ischaemia, 240 minutes recovery), the cell membrane is ruptured(arrow) and the cell contents are exposed to Bruch's membrane. The smooth endoplasmic reticulum forms a reticular mass and the rough endoplasmic reticulum is swollen. (20,000 X)



FIG.5-25 Electron micrograph of the pigment epithelium(90 minutes ischaemia,240 minutes recovery),following the longer periods of ischaemia the cells can become attenuated so that the distance between the sub-retinal space and Bruch's membrane is as little as 1 micron, such an area of attenuation is shown above.(16,000 X)

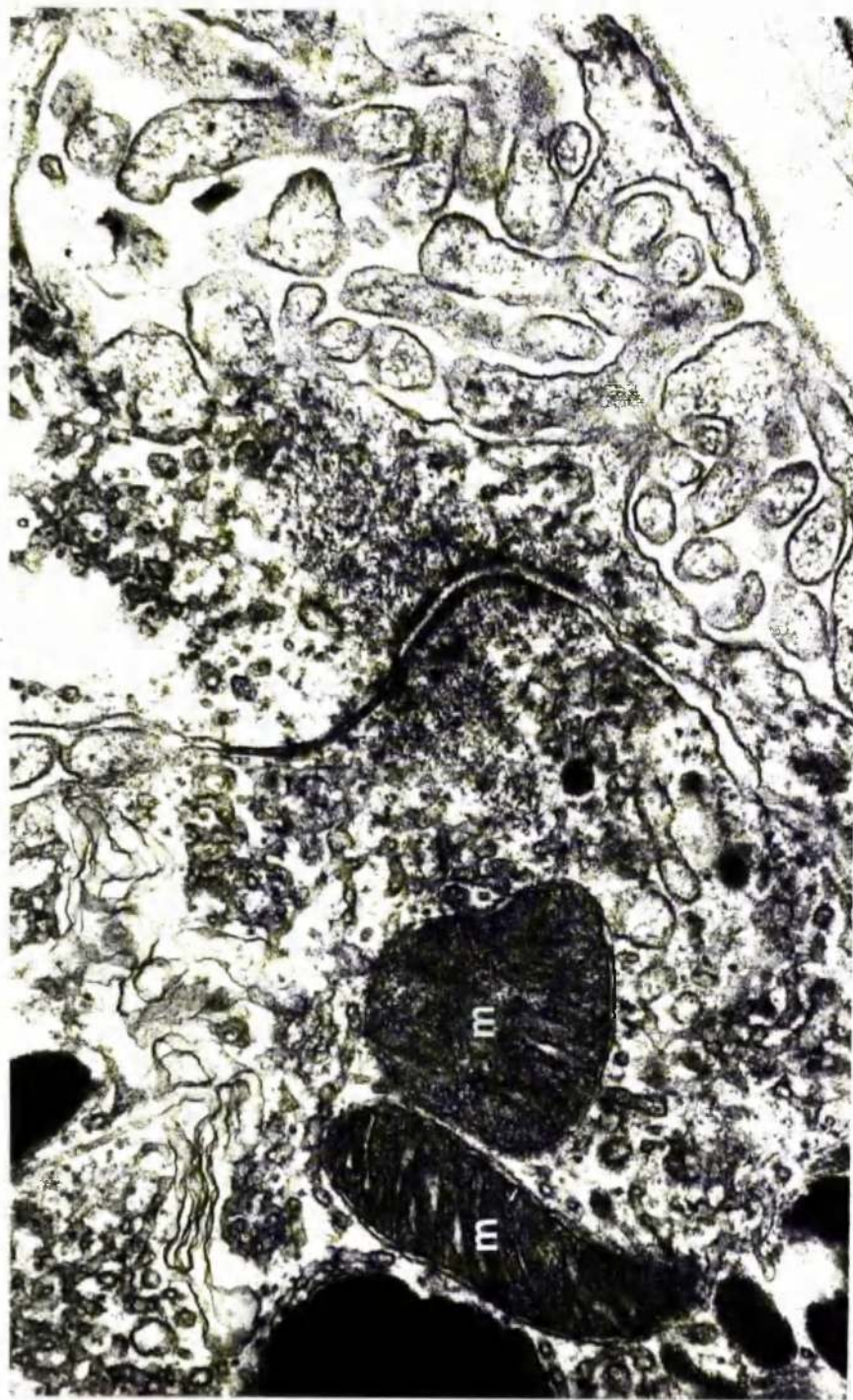


FIG. 5-26 Electron micrograph of the retinal pigment epithelium (120 minutes ischaemia, 240 minutes recovery), the junctional complex appears normal. The mitochondria (M) have a highly electron dense matrix and prominent cristae. (30,000 X)

PERIOD OF ISCHAEMIA (MINUTES)

a)	15				30				60				90			
	V	P	V	P	V	P	V	P	V	P	V	P	V	P	V	P
Stage																
1	46	49	57	73	91	105	86	84	49	31	38	38	47	24	38	33
2	125	116	144	139	133	112	114	110	251	234	208	212	111	68	126	96
3	157	124	169	157	189	172	135	147	182	162	165	143	125	89	133	106
4	219	185	242	214	213	201	177	186	223	184	205	186	194	137	217	145
5	304	248	330	273	324	268	287	238	364	256	289	231	249	192	272	214
Animal key	9		10		11		12		13		14		15		16	

FIG.5-27 Table showing the number of phagosomes occurring at each stage of degradation after 60 minutes recovery from the various periods of ischaemia in the visual streak(V) and in the peripheral retina(P). Animals 9-16.

PERIOD OF ISCHAEMIA (MINUTES)

b)	15				30				60				90			
	V	P	V	P	V	P	V	P	V	P	V	P	V	P	V	P
Stage																
1	5.6	6.8	6.1	8.5	9.9	12.2	11.0	11.0	4.9	3.5	4.3	4.7	6.5	4.5	4.6	5.6
2	14.7	10.1	15.3	16.1	14.3	13.1	14.6	14.4	24.9	28.6	23.3	26.2	15.3	16.6	16.1	16.2
3	18.4	17.2	17.9	18.4	18.2	20.0	17.3	19.2	18.0	18.4	18.7	17.7	17.2	18.5	17.0	17.8
4	25.7	25.6	25.7	25.0	22.9	23.4	22.7	24.3	22.1	22.1	23.2	23.0	26.7	25.8	27.7	24.4
5	35.8	34.3	35.0	31.9	34.8	31.2	34.4	31.1	30.1	29.4	30.5	28.5	34.3	36.2	34.7	28.0
Animal key	9		10		11		12		13		14		15		16	

FIG.5-28 Table showing the percentage distribution of the phagosome stages after 60 minutes recovery from the various periods of ischaemia in the visual streak(V) and in the peripheral retina(P). Animals 9-16.

a)

PERIOD OF ISCHAEMIA (MINUTES)

Stage	15				30				60				90			
	V	P	V	P	V	P	V	P	V	P	V	P	V	P	V	P
1	68	69	48	60	122	148	126	98	54	38	35	28	53	43	37	30
2	162	183	137	148	213	220	152	196	227	204	199	190	86	73	67	88
3	177	132	138	119	134	108	118	99	133	102	115	79	174	121	117	103
4	239	186	203	163	198	142	167	134	204	183	185	102	215	162	171	135
5	298	251	256	188	277	249	245	206	327	274	267	224	288	224	205	177
Animal key	17		18		19		20		21		22		23		24	

FIG.5-29 Table showing the number of phagosomes occurring at each stage of degradation after 240 minutes recovery from the various periods of ischaemia in the visual streak(V) and peripheral retina (P).Animals I7-24

PERIOD OF ISCHAEMIA (MINUTES)

b)

Stage	15				30				60				90			
	V	P	V	P	V	P	V	P	V	P	V	P	V	P	V	P
1	7.2	8.4	6.1	8.8	13.0	18.0	14.6	13.4	5.7	4.9	4.3	4.1	6.5	5.9	8.2	5.8
2	17.2	22.3	17.5	21.8	22.6	25.1	18.9	26.7	24.0	25.4	24.2	27.8	10.5	11.7	11.2	13.3
3	18.6	16.1	17.6	17.6	14.2	12.3	14.4	13.5	14.1	12.7	14.0	11.6	21.3	19.4	19.6	20.1
4	25.3	22.7	25.0	24.0	20.8	16.2	20.7	18.3	31.6	22.8	22.5	23.7	28.3	26.0	28.6	26.3
5	31.6	30.6	32.7	27.7	29.4	28.4	30.4	28.1	34.6	34.2	35.0	32.8	35.3	36.0	34.3	34.5
Animal key	17		18		19		20		21		22		23		24	

FIG.5-30 Table showing the percentage distribution of the various phagosome stages after 240 minutes recovery from the various periods of ischaemia in the visual streak(V) and peripheral retina(P).Animals I7-24

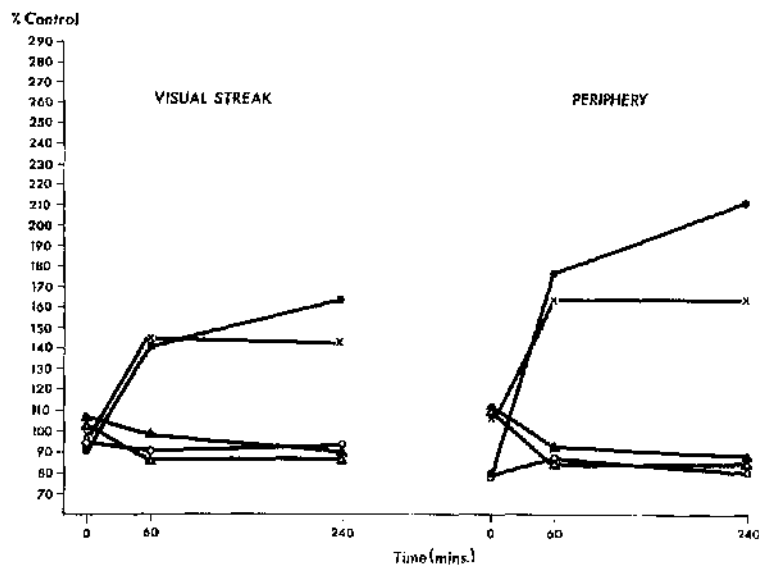


FIG.5-31 Graph showing the average distribution of the five phagosome stages in the visual streak and periphery of the test eyes compared to the distribution in similar regions of the corresponding control eyes during the post-ischaemia recovery phase from 15 minutes ischaemia. Increases occur in stages I and 2 which are more pronounced in the periphery. ● Stage I; x Stage 2; Δ Stage 3; ○ Stage 4; ▲ Stage 5.

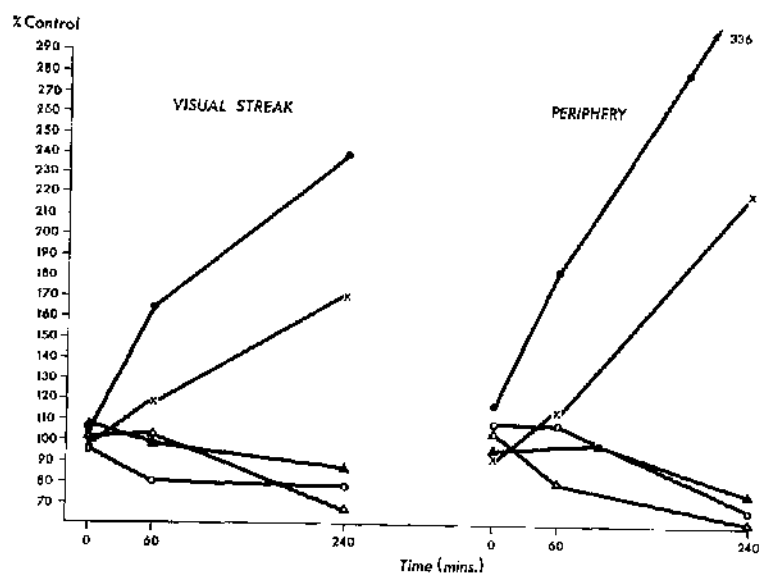


FIG.5-32 Graph showing the average distribution of the five phagosome stages in the visual streak and periphery of the test eyes compared to the distribution in similar regions of the corresponding control eyes during the post-ischaemia recovery phase from 30 minutes ischaemia, the increases are again limited to stages I and 2 although they were more marked in the periphery compared with changes after the shorter period of ischaemia. ● Stage I; x Stage 2; Δ Stage 3; ○ Stage 4; ▲ Stage 5.

▲ Stage 5.

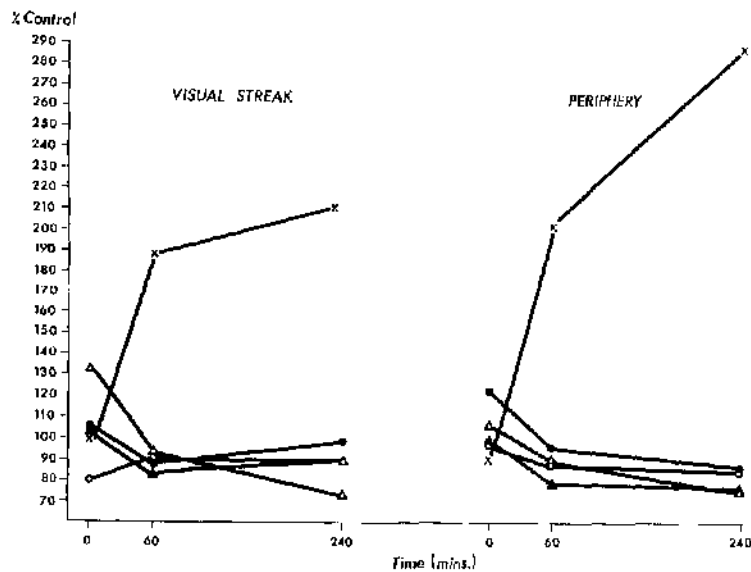


FIG.5-33 Graph showing the average distribution of the five phagosome stages in the visual streak and periphery of the test eyes compared to the distribution in similar regions of the corresponding control eyes during the post-ischaemia phase after 60 minutes ischaemia, an increase in stage 2 only was observed and is more marked in the periphery. ● Stage 1; X Stage 2; Δ Stage 3; ○ Stage 4; ▲ Stage 5.

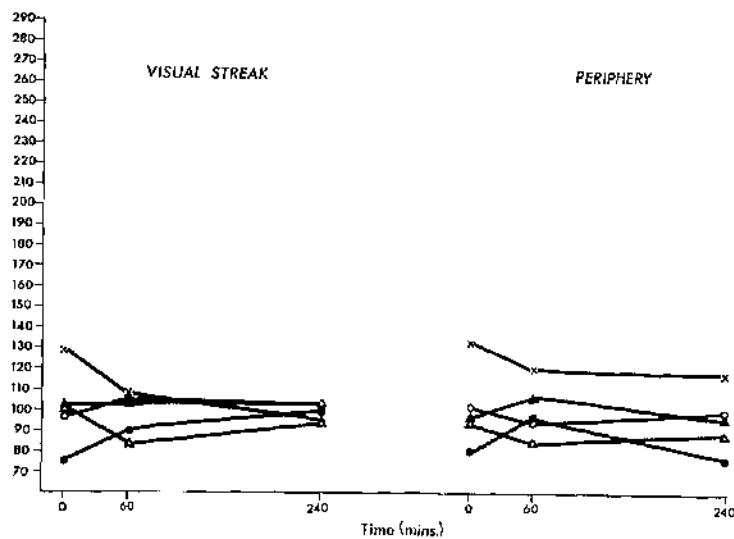


FIG.5-34 Graph showing the average distribution of the five phagosome stages in the test eyes (visual streak and periphery) compared to the distribution in similar regions in the corresponding control eyes during the post-ischaemia phase after 90 minutes ischaemia, no increases in any of the five stage is seen. ● Stage 1; X Stage 2; Δ Stage 3; ○ Stage 4; ▲ Stage 5.



FIG.5-35 Electron micrograph of the outer segments(30 minutes ischaemia,60 minutes recovery),the terminal portions of the outer segments(OS) are often disturbed while the proximal portions are relatively normal.(13,000 X)



FIG.5-36 Electron micrograph of the outer segments(30 minutes ischaemia,60 minutes recovery),in some areas of the outer segments there are focal disturbances of the discs which are associated with the rupture of the cell membrane.(13,000 X)

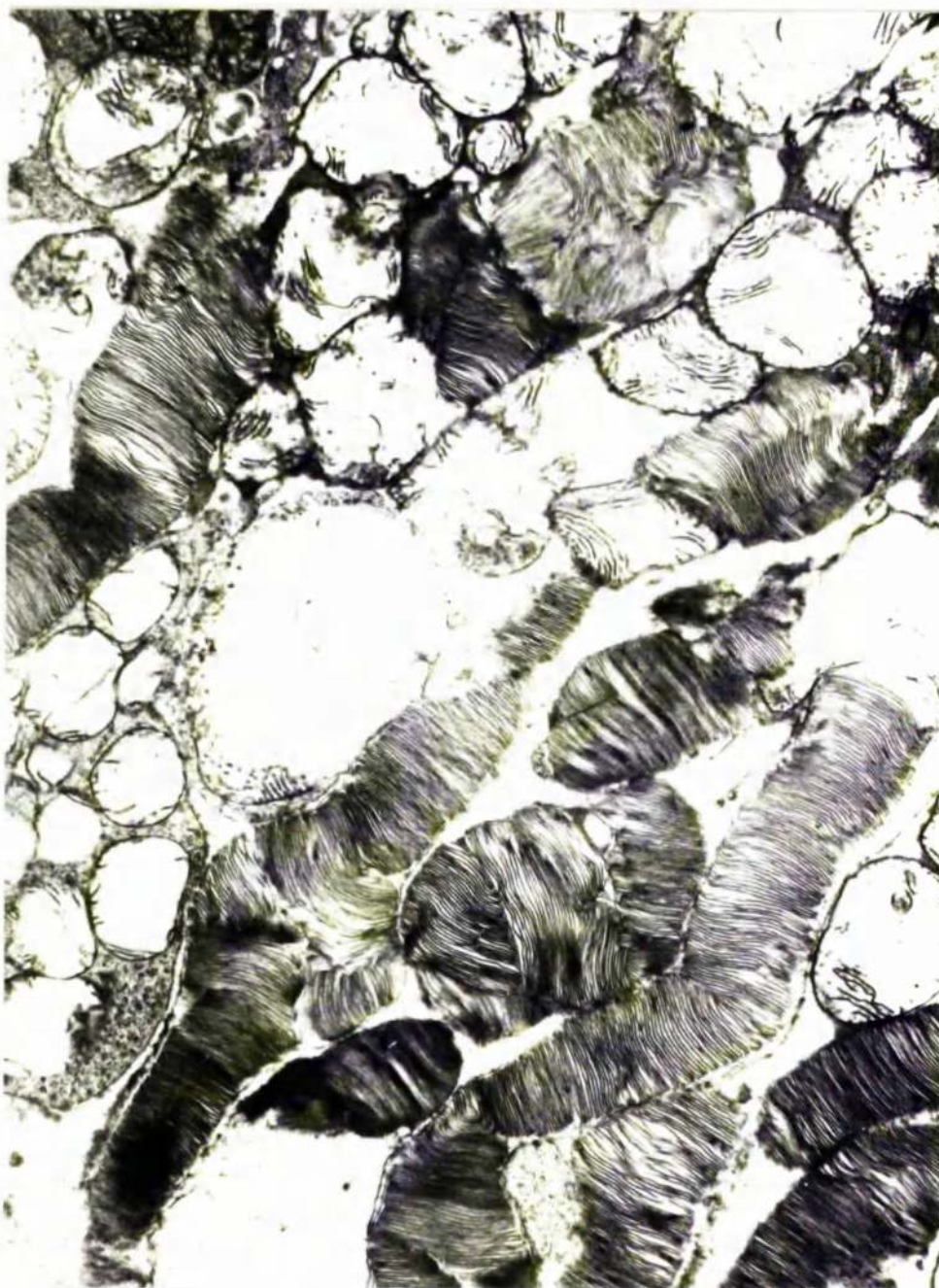


FIG.5-37 Electron micrograph of the outer segments(90 minutes ischaemia,60 minutes recovery),the inner and outer segments are fragmented.The mitochondria of the inner segment fragments are distended with a matrix of low electron density.(9,100 X)



FIG. 5-38 Electron micrograph of the outer segments (15 minutes ischaemia, 240 minutes recovery), the outer segments are intact but the terminal portions are frequently disturbed. (12,000 X)

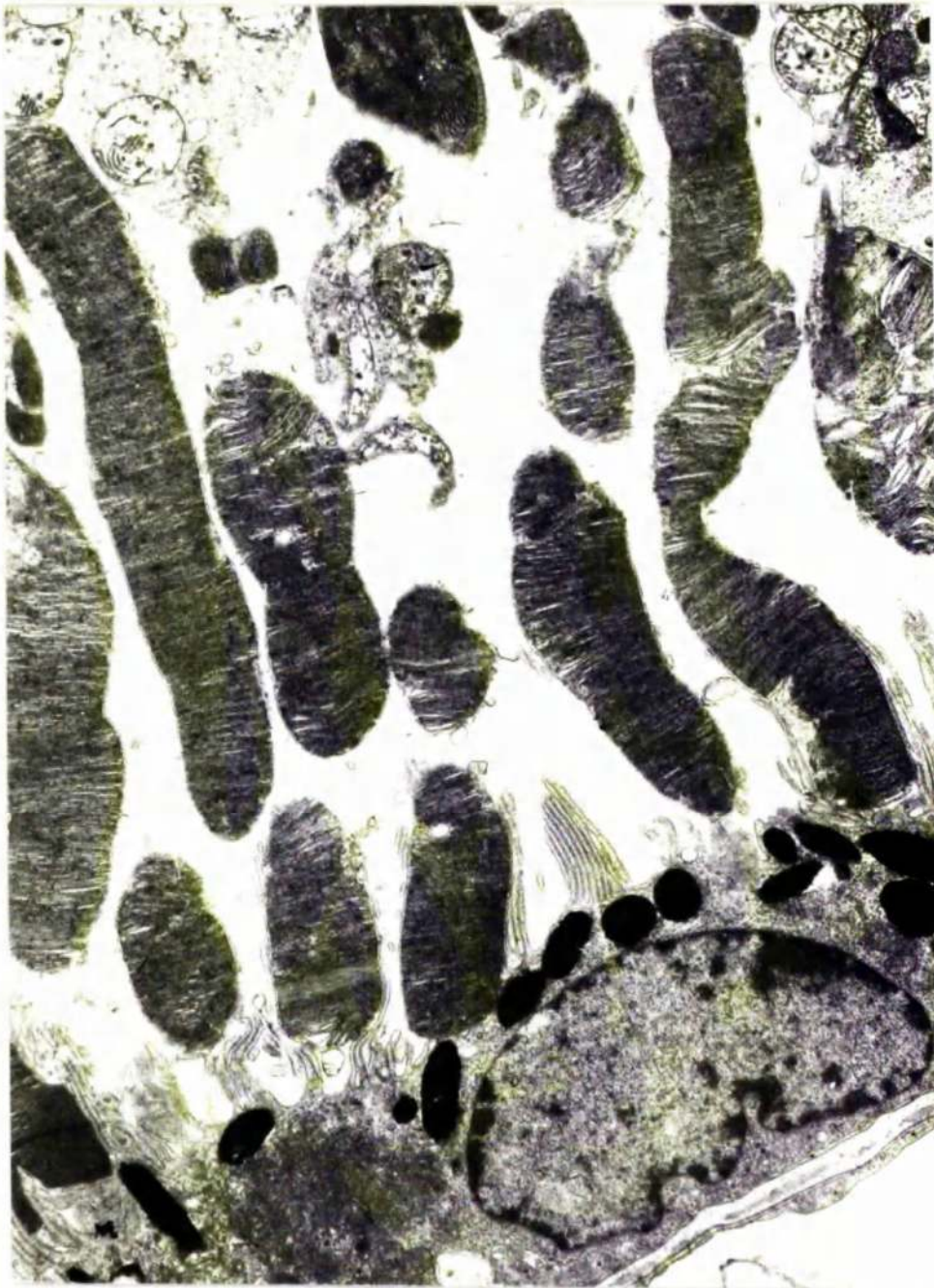


FIG.5-39 Electron micrograph of the outer segments(60 minutes ischaemia,240 minutes recovery),intact outer segments occur amongst many fragments containing relatively normal discs.The intact outer segments often contain focal areas of disruption.(9,000 X)



FIG. 5-40 Electron micrograph of the outer segments (120 minutes ischemia, 240 minutes recovery) the outer segments are grossly abnormal although small portions of relatively normal discs occur. Fragments of inner segment material also occur. (8,000 X)

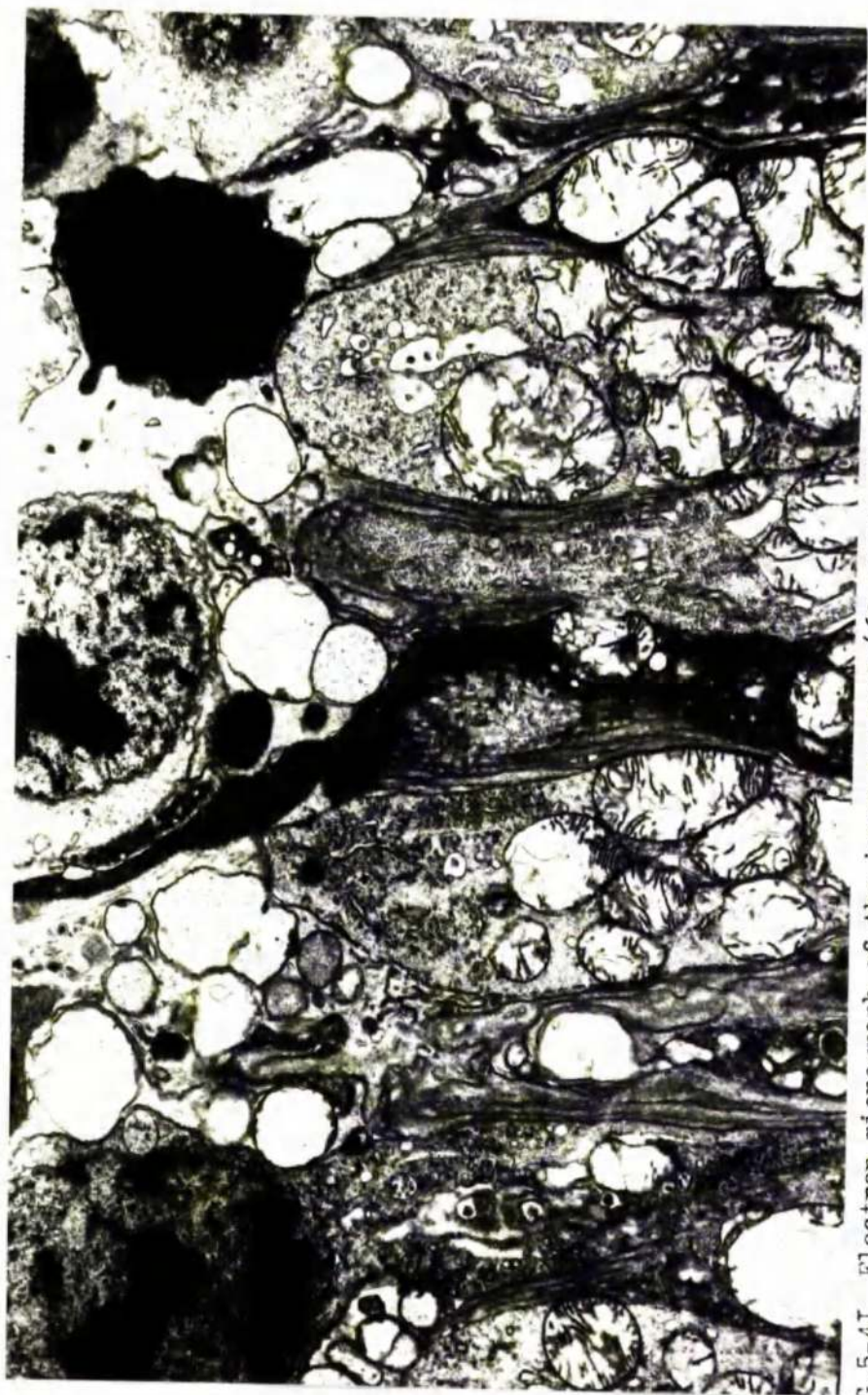


FIG. 5-4I Electron micrograph of the inner segments (60 minutes ischaemia, 60 minutes recovery), the inner segments are shortened and contain swollen and ruptured mitochondria. (16,000 X)



FIG.5-42 Electron micrograph of the inner segments(15 minutes ischaemia,240 minutes recovery),the inner segments appear normal apart from a distended Golgi apparatus(G).There is also a focal swelling of the nuclear envelope of the visual cell nuclei(N). (9,000 X)



FIG.5-43 Electron micrograph of the outer retina(60 minutes ischaemia,240 minutes recovery)
the retinal pigment epithelium is relatively normal apart from some condensation of the
smooth endoplasmic reticulum.The visual cells appear to be either swollen and oedematous
or electron dense with intact outer segments.(4,500 X)

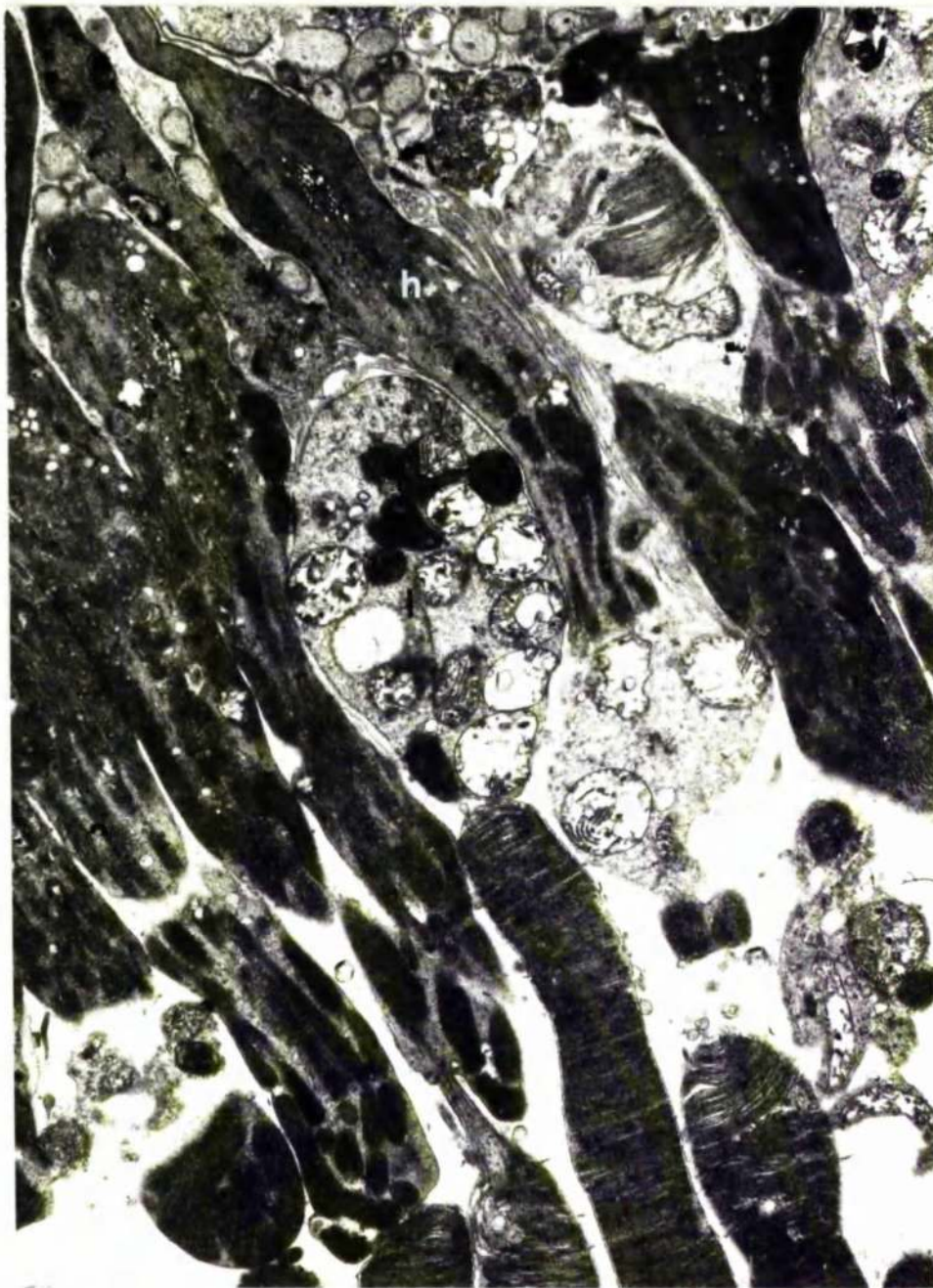


FIG.5-44 Electron micrograph of the inner segments(60 minutes ischaemia,240 minutes recovery),the cytoplasm of some of the inner segments has a high electron density (H) while in others the cytoplasm has a low electron density(L).(9,000 X)

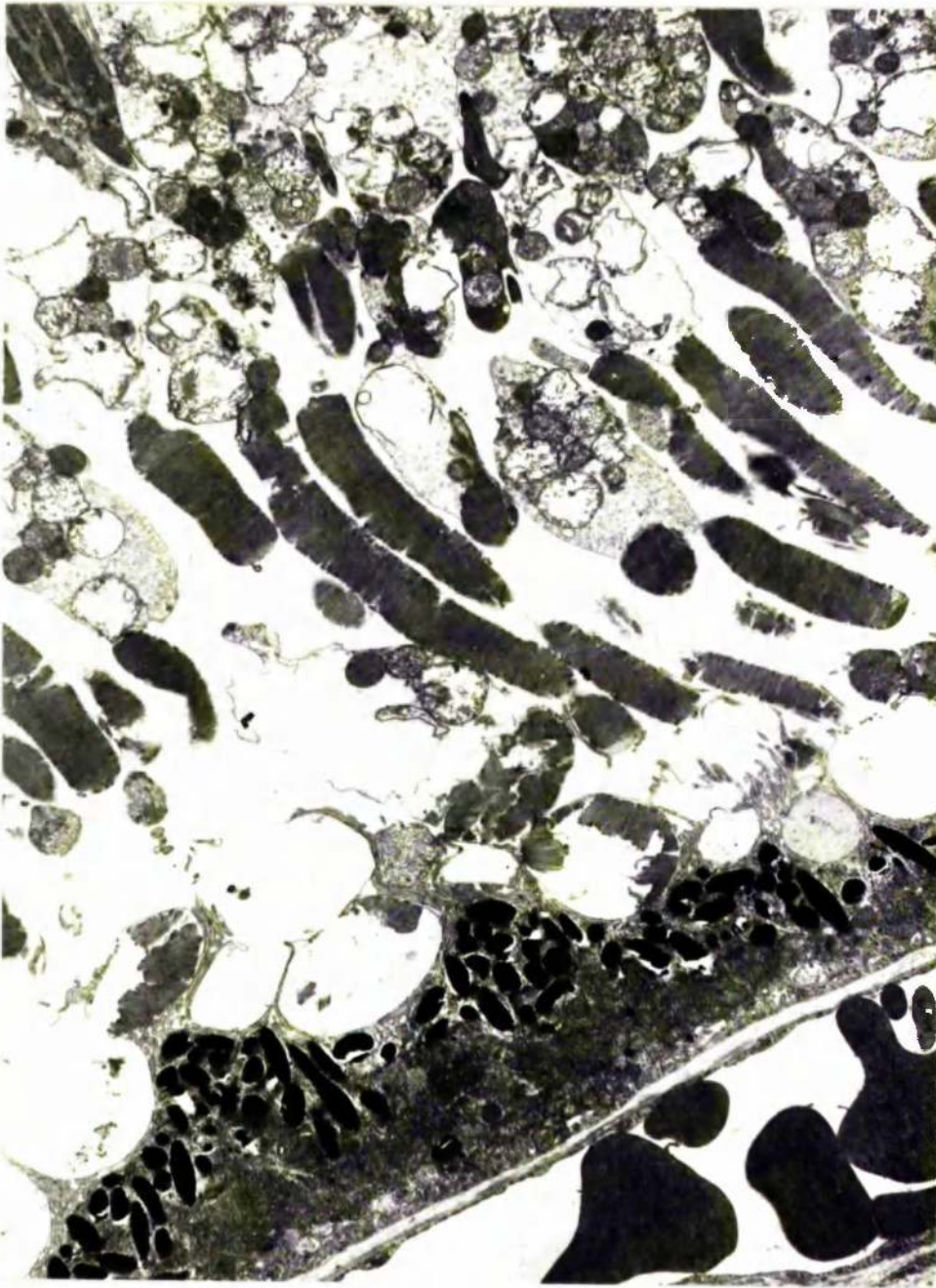


FIG.5-45 Electron micrograph of the outer retina(90 minutes ischaemia,240 minutes recovery),the pigment epithelium contains condensed smooth endoplasmic reticulum,the apical surface is undulating and the pigment granules are unevenly distributed.The inner and outer segments of the visual cells are grossly degenerate.
(7,000 X)

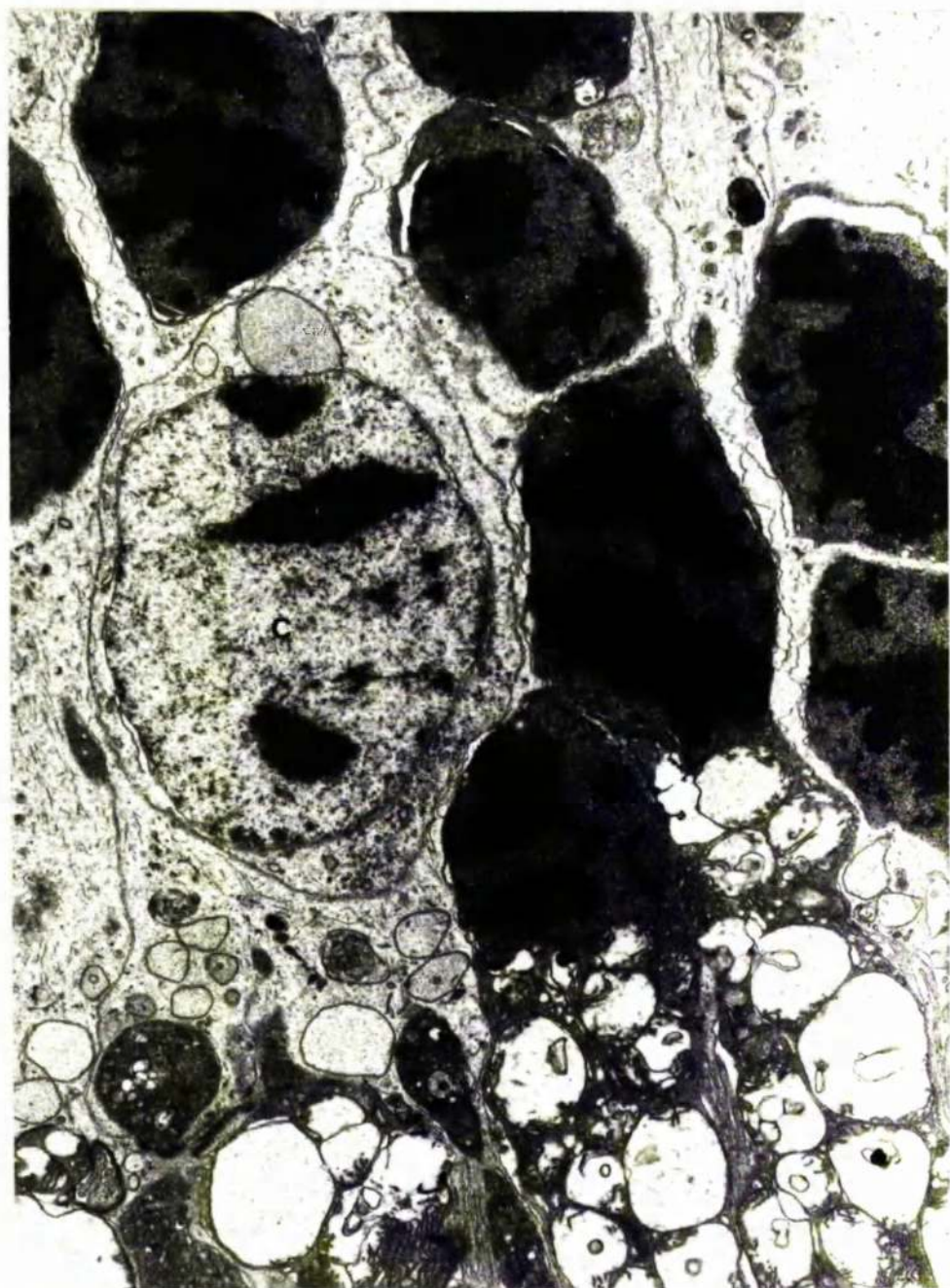


FIG.5-46 Electron micrograph of the outer aspect of the outer nuclear layer(90 minutes ischaemia,60 minutes recovery),the cone nucleus(C) has a single cyst like swelling of the nuclear envelope, the nucleus is otherwise relatively normal in appearance.(II,000 X)

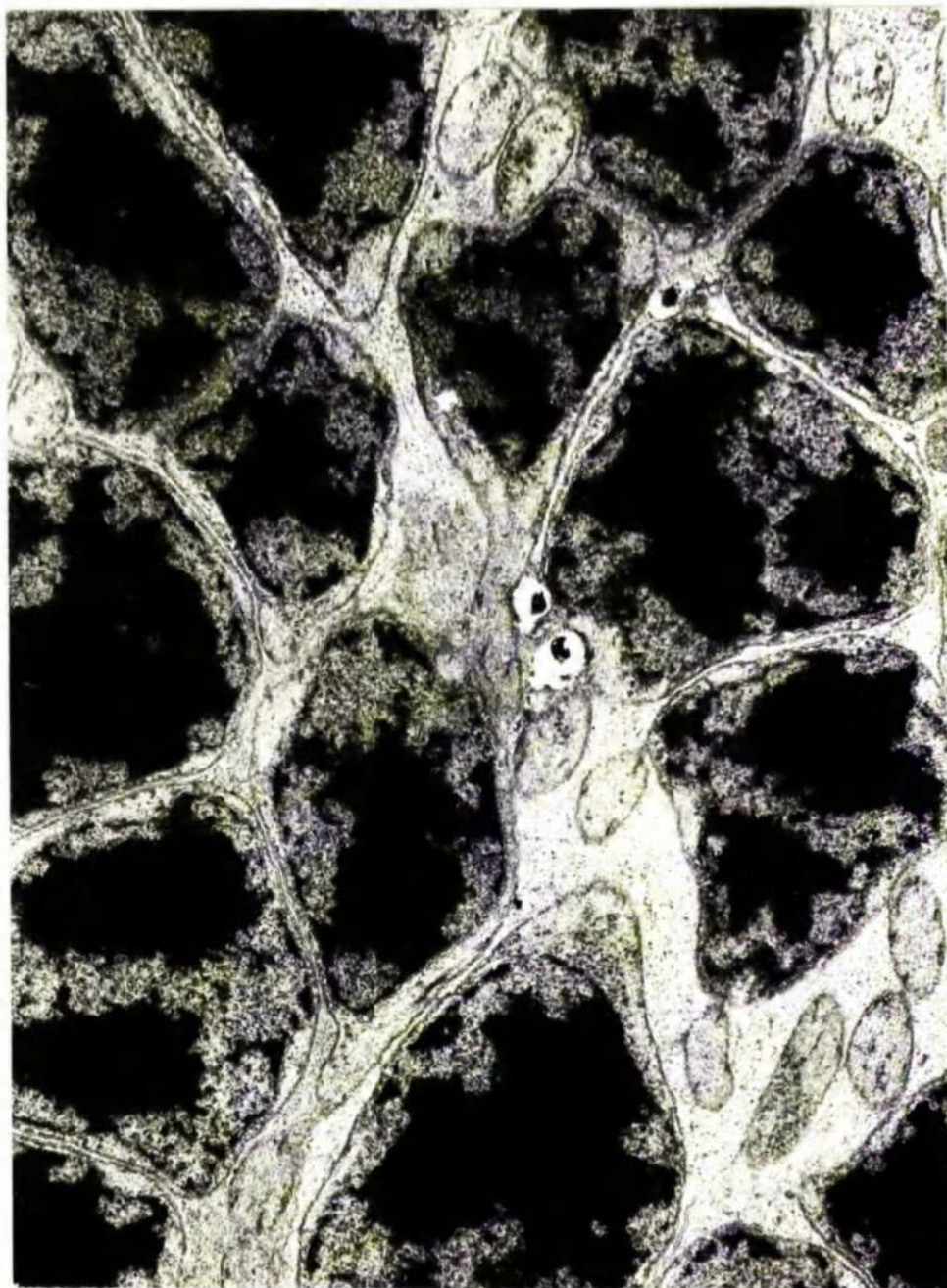


FIG.5-47 Electron micrograph of the outer nuclear layer(90 minutes ischaemia,240 minutes recovery),the nuclei appear normal apart from focal swellings of the nuclei envelope.(11,000 X)

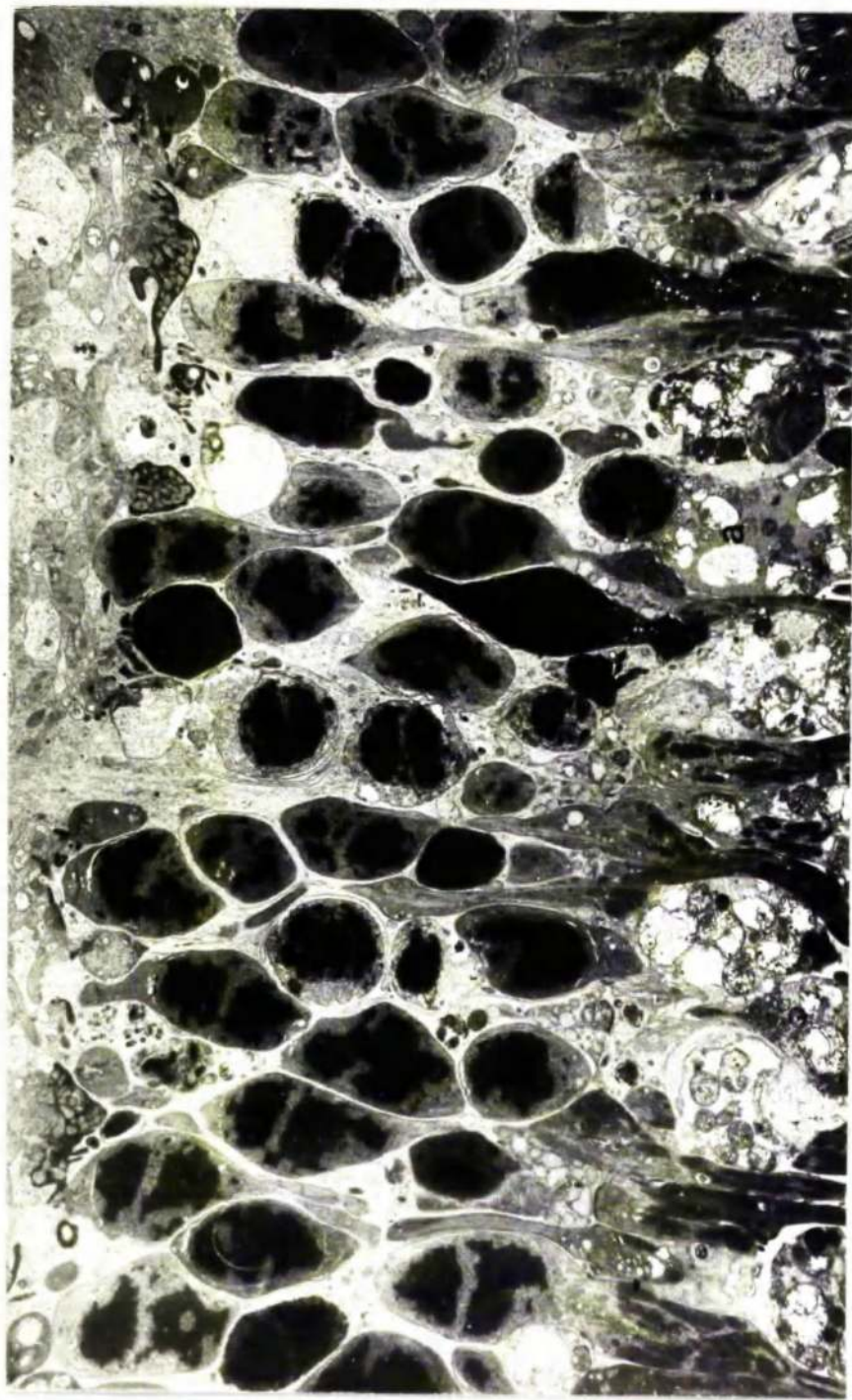


FIG. 5-48 Electron micrograph of the inner segments and outer nuclear layer (60 minutes ischaemia, 240 minutes recovery), some of the inner and outer segments are grossly abnormal (Δ) these are associated with round electron dense nuclei, while other inner segments are relatively normal apart from a marked electron density and are associated with nuclei of normal appearance. In the outer plexiform layer both normal and abnormal receptor pedicles are found. (4,500 X)

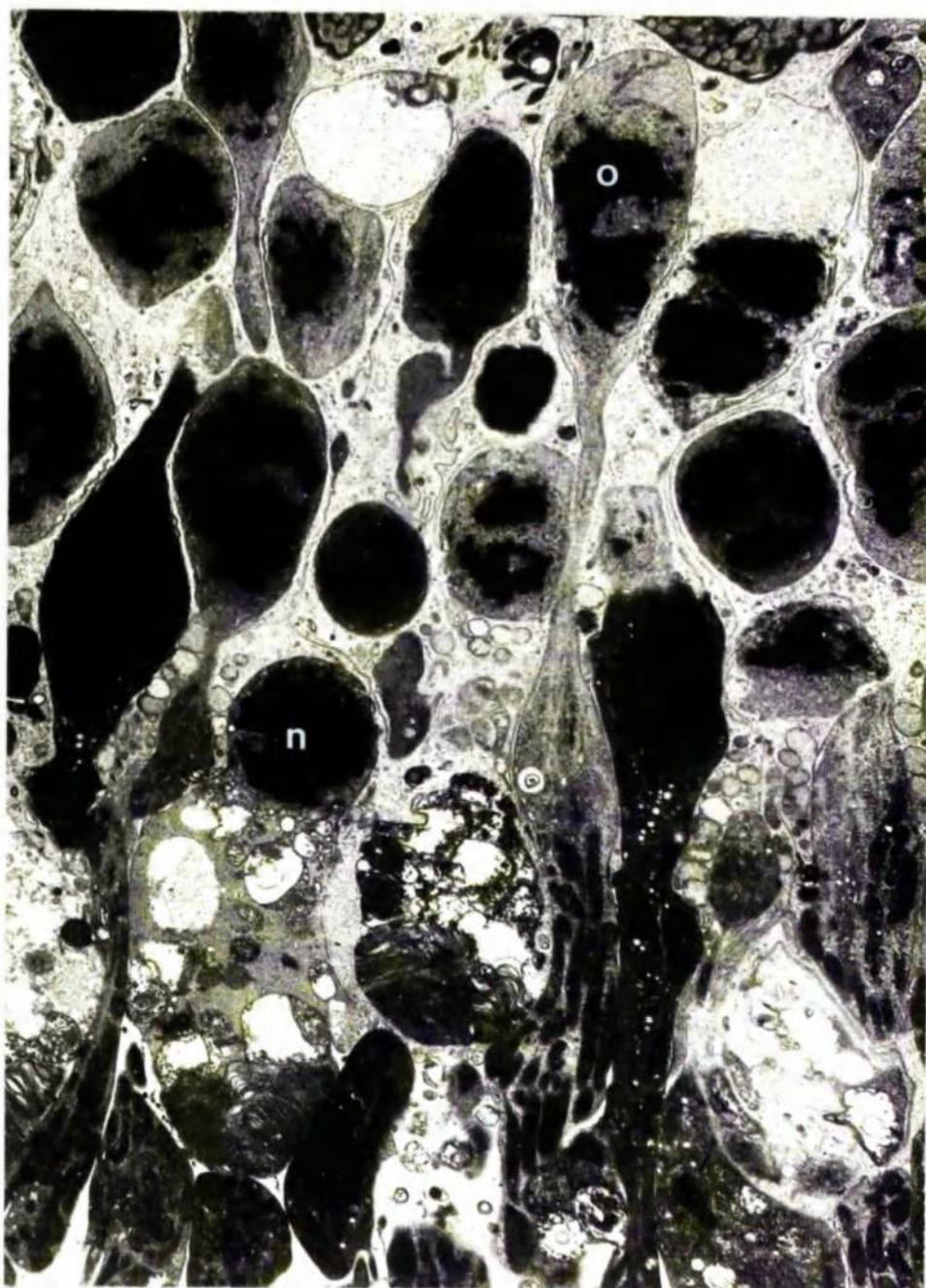


FIG.5-49 Electron micrograph of the visual cells(60 minutes ischaemia,240 minutes recovery),the rounded nucleus(N) is associated with a swollen abnormal inner segment,the nucleus(O) is relatively normal and is associated with a-comperatively normal inner segment.(9,000 X)

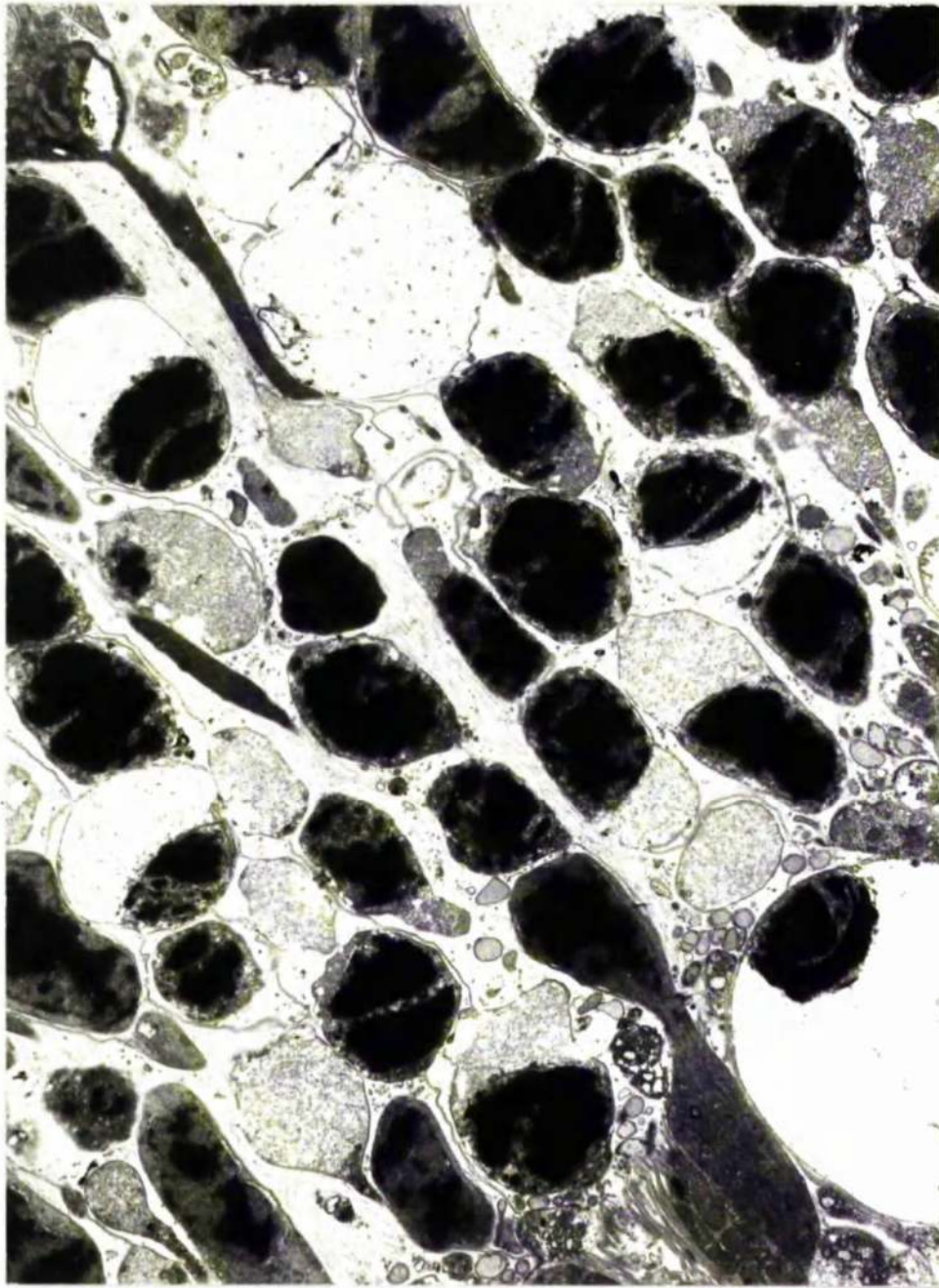


FIG.5-50 Electron micrograph of the outer nuclear layer(90 minutes ischaemia,240 minutes recovery),the majority of the nuclei are abnormal with oedematous perinuclear cytoplasm.(9,000 X)

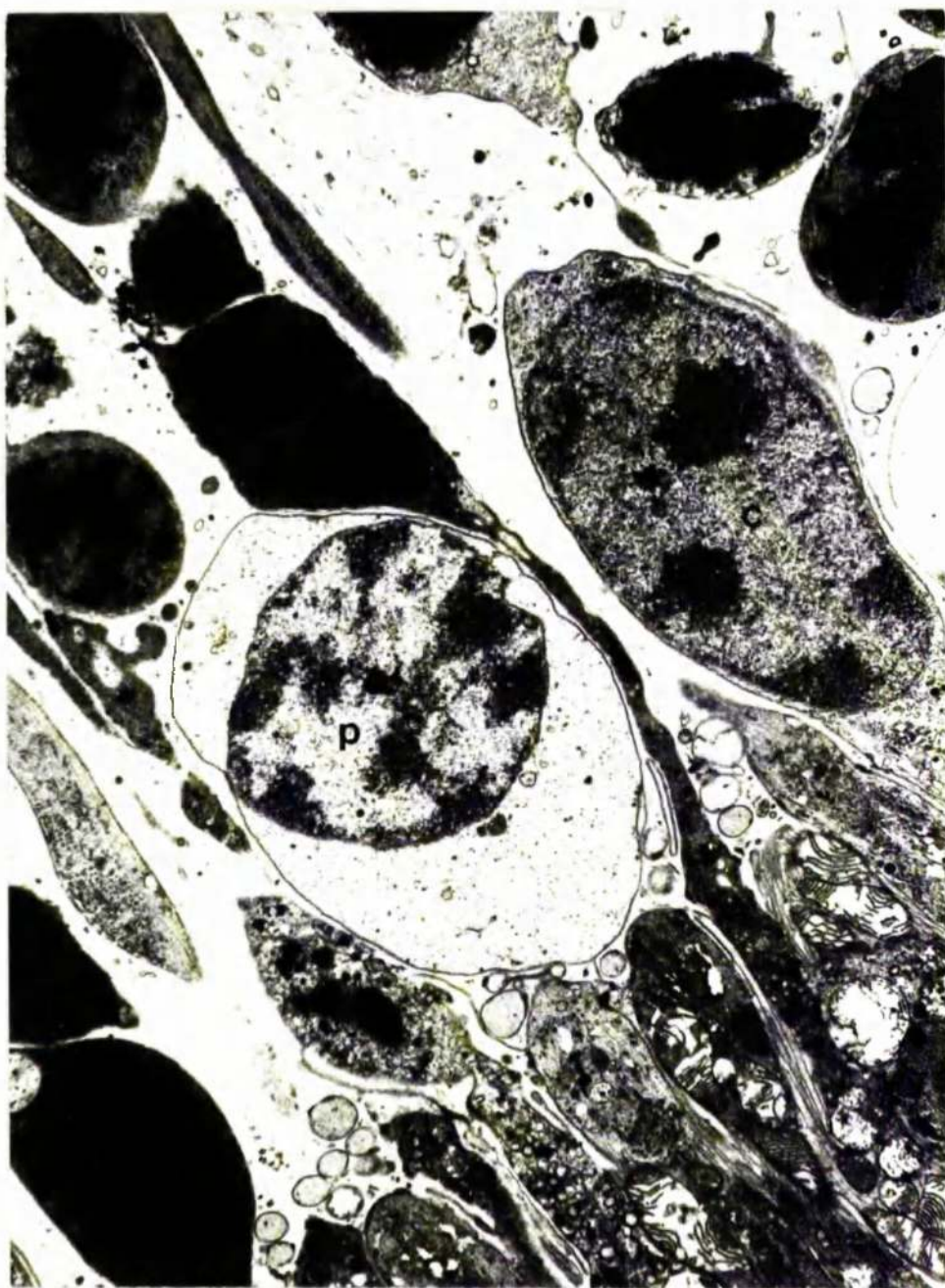


FIG.5-5I Electron micrograph of the outer aspect of the outer nuclear layer(90 minutes ischaemia,240 minutes recovery), showing a relatively normal cone nucleus(C) adjacent to one which is pyknotic(P).(12,000 X)



FIG.5-52 Electron micrograph of the outer plexiform layer(60 minutes ischaemia.60 minutes recovery),the cedematous changes in the outer plexiform layer and the inner nuclear layer are similar to those seen immediately after the period of ischaemia.(10,000 X)

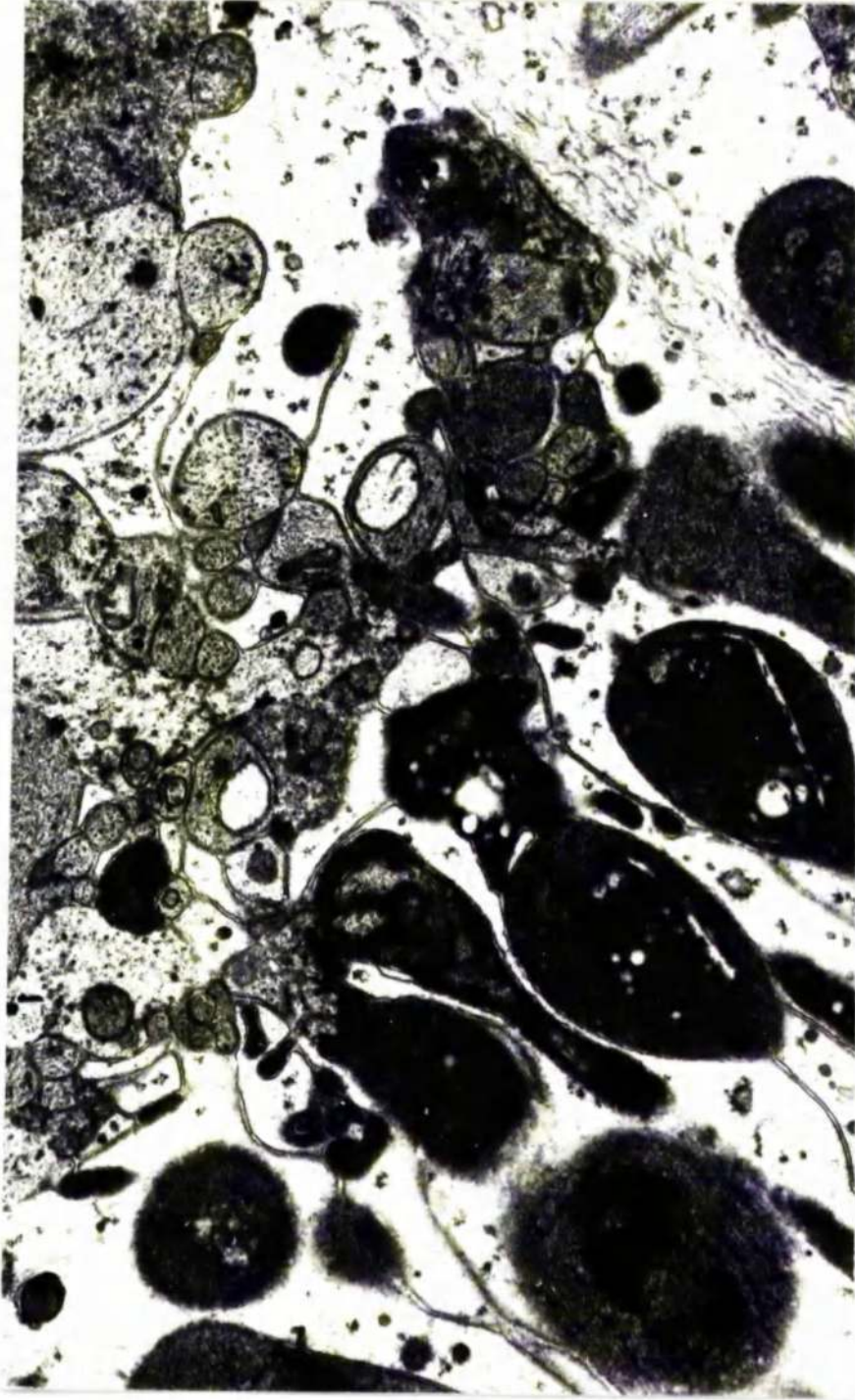


FIG. 5-53 Electron micrograph of the outer plexiform layer (90 minutes ischaemia, 240 minutes recovery), the receptor pedicles are condensed and highly electron dense. The processes in the outer plexiform layer are reduced in number. The Müller cell cytoplasm surrounding the processes and the pedicles is oedematous. (13,000 X)



FIG. 5-54 Electron micrograph of the receptor pedicles (120 minutes ischemia, 240 minutes recovery), both the rod (R) and cone (C) pedicles are shrunken and electron dense. Advanced pyknotic changes are evident in some nuclei of the visual cells. (12,000 X)

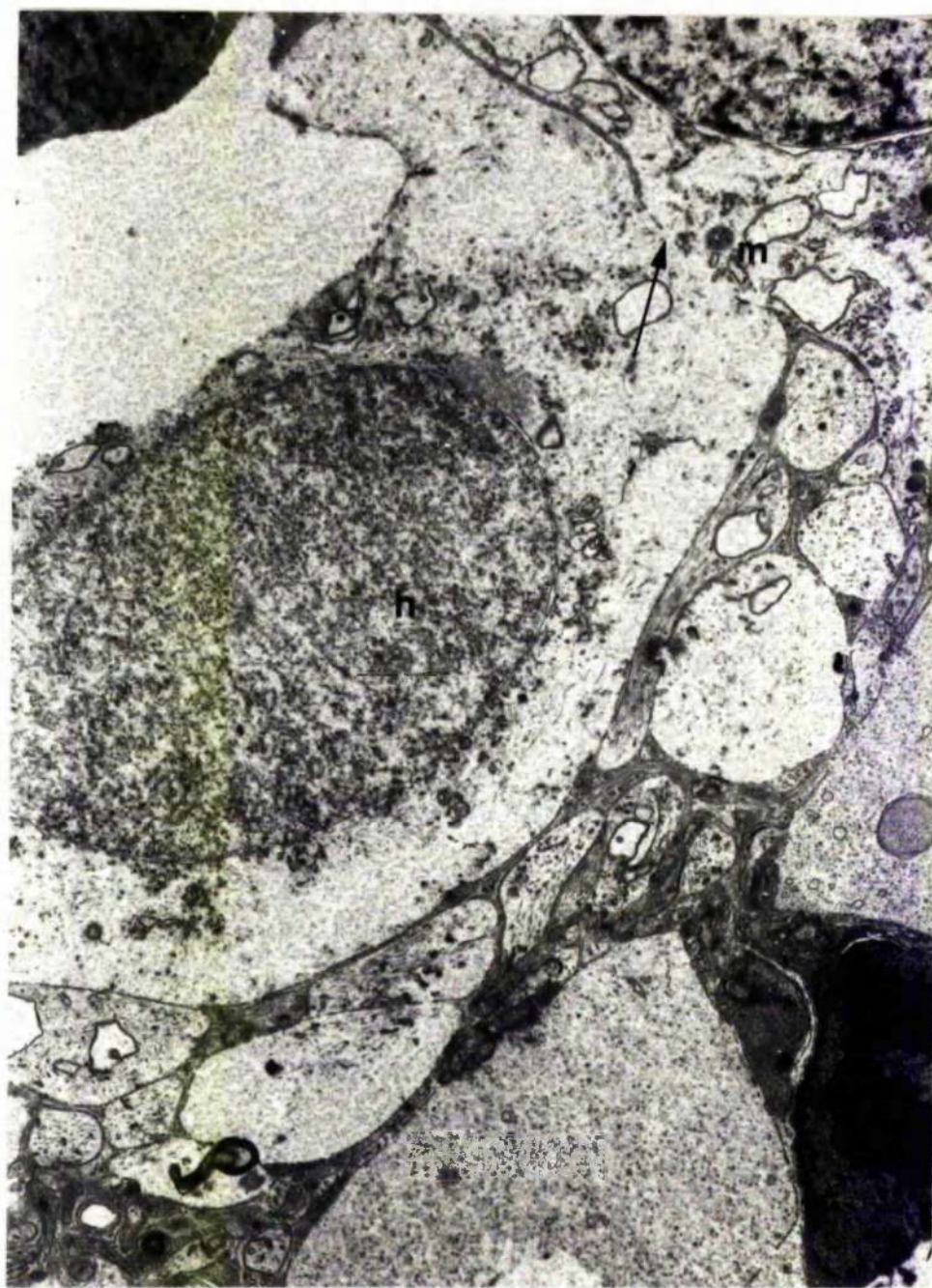


FIG.5-55 Electron micrograph of the outer aspect of the inner nuclear layer(90 minutes ischaemia,60 minutes recovery),the horizontal cell(H) has a ruptured cell membrane(arrow) and the cytoplasm is oedematous.A multivesicular like body occurs in the cytoplasm(M). (12,000 X)

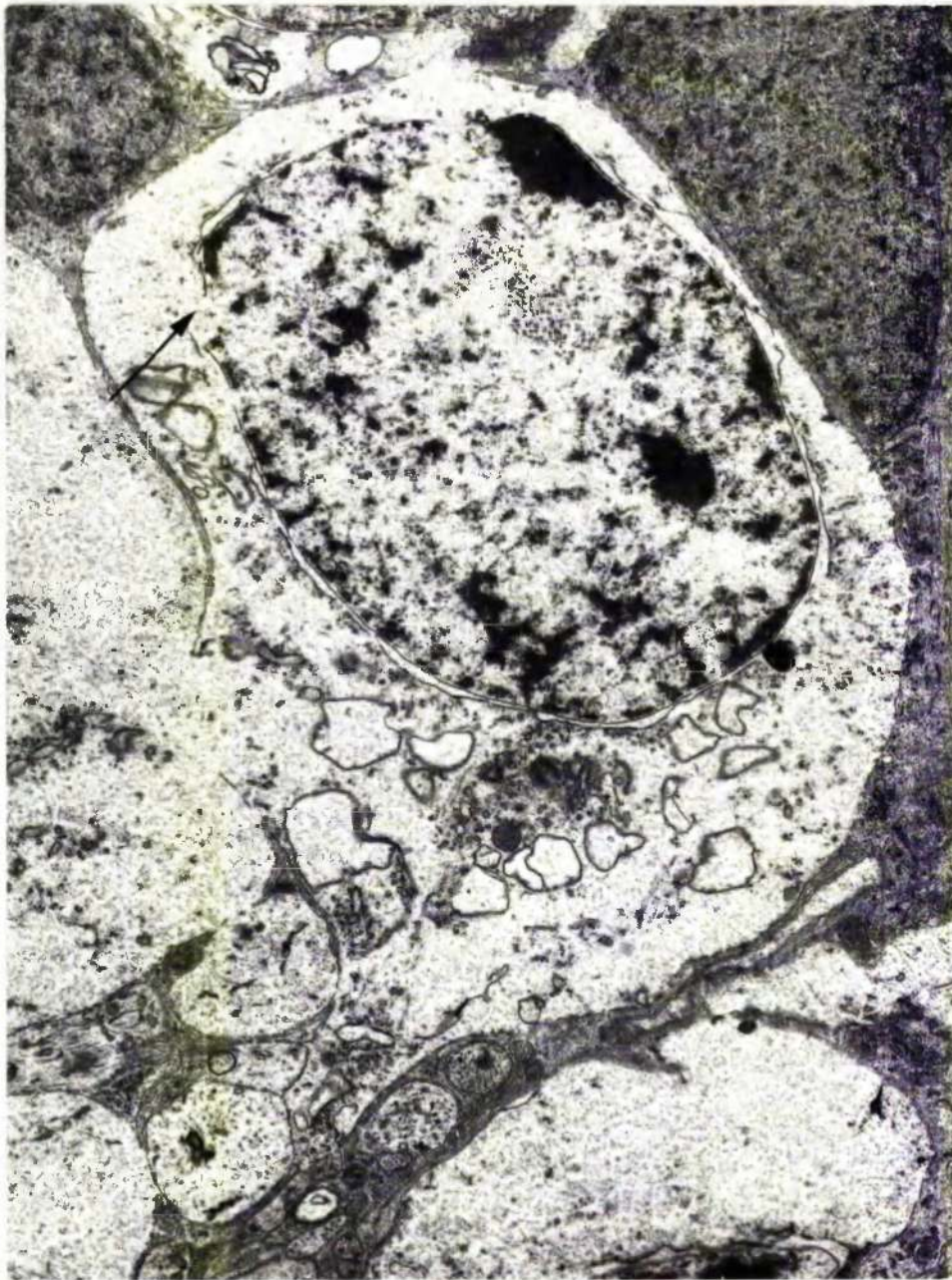


FIG.5-56 Electron micrograph of a bipolar cell(90 minutes ischaemia, 60 minutes recovery), the cell is adjacent to the ruptured cell shown in the previous figure(Fig.5-55) and it to has a ruptured cell membrane and oedematous cytoplasm. The membranes of the nuclear envelope are also ruptured(arrow).(12,000 X)

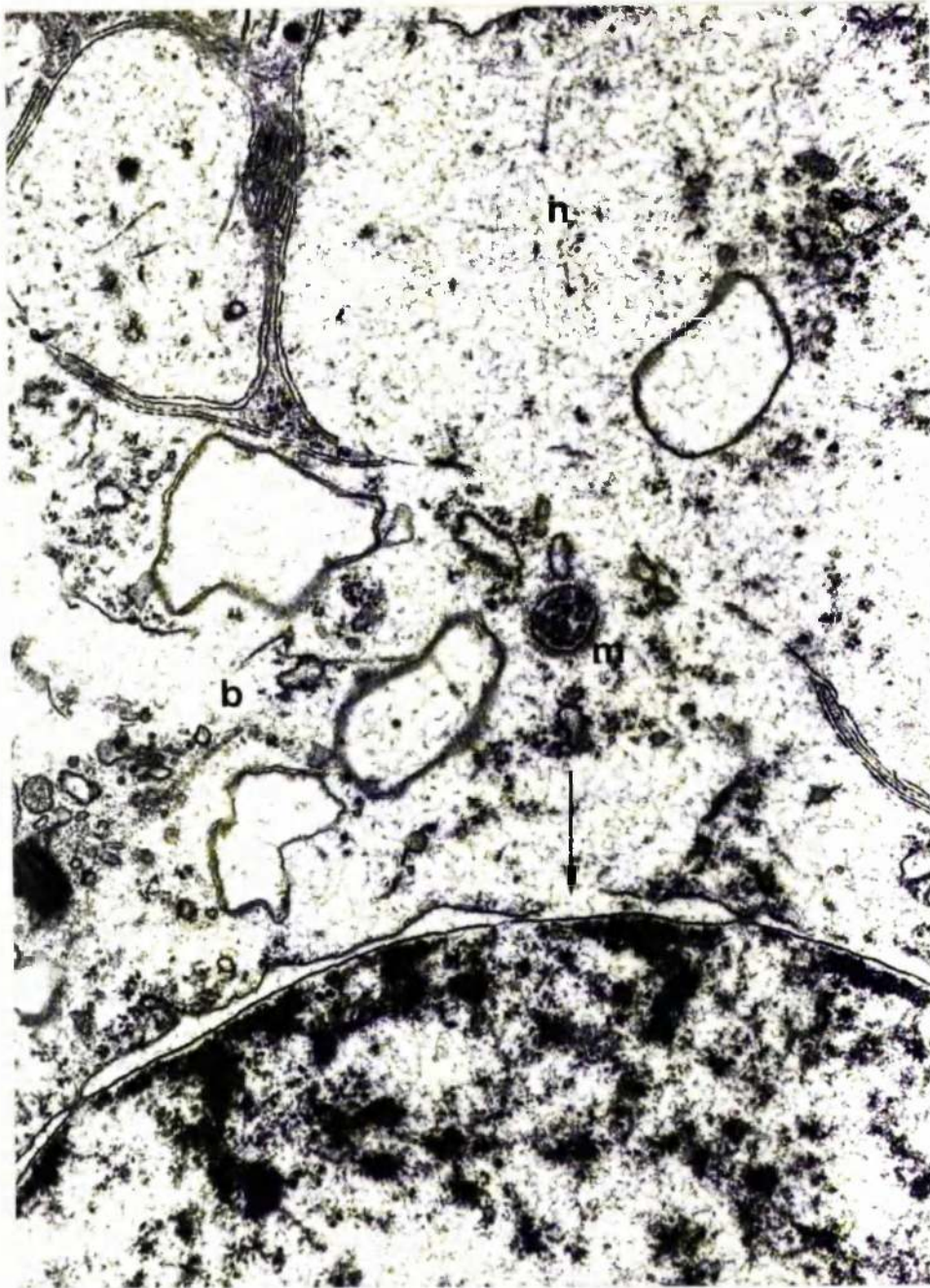


FIG.5-57 Electron micrograph of the region of the ruptured cell membranes shown in the two previous figures(90 minutes ischaemia, 60 minutes recovery),the bipolar cell(B) and the horizontal cell (H) are indistinguishable in the region of the rupture.The nuclear envelope of the bipolar cell nucleus is also ruptured(arrow).A multivesicular like body(M) can be seen in the cytoplasm.(30,000 X)

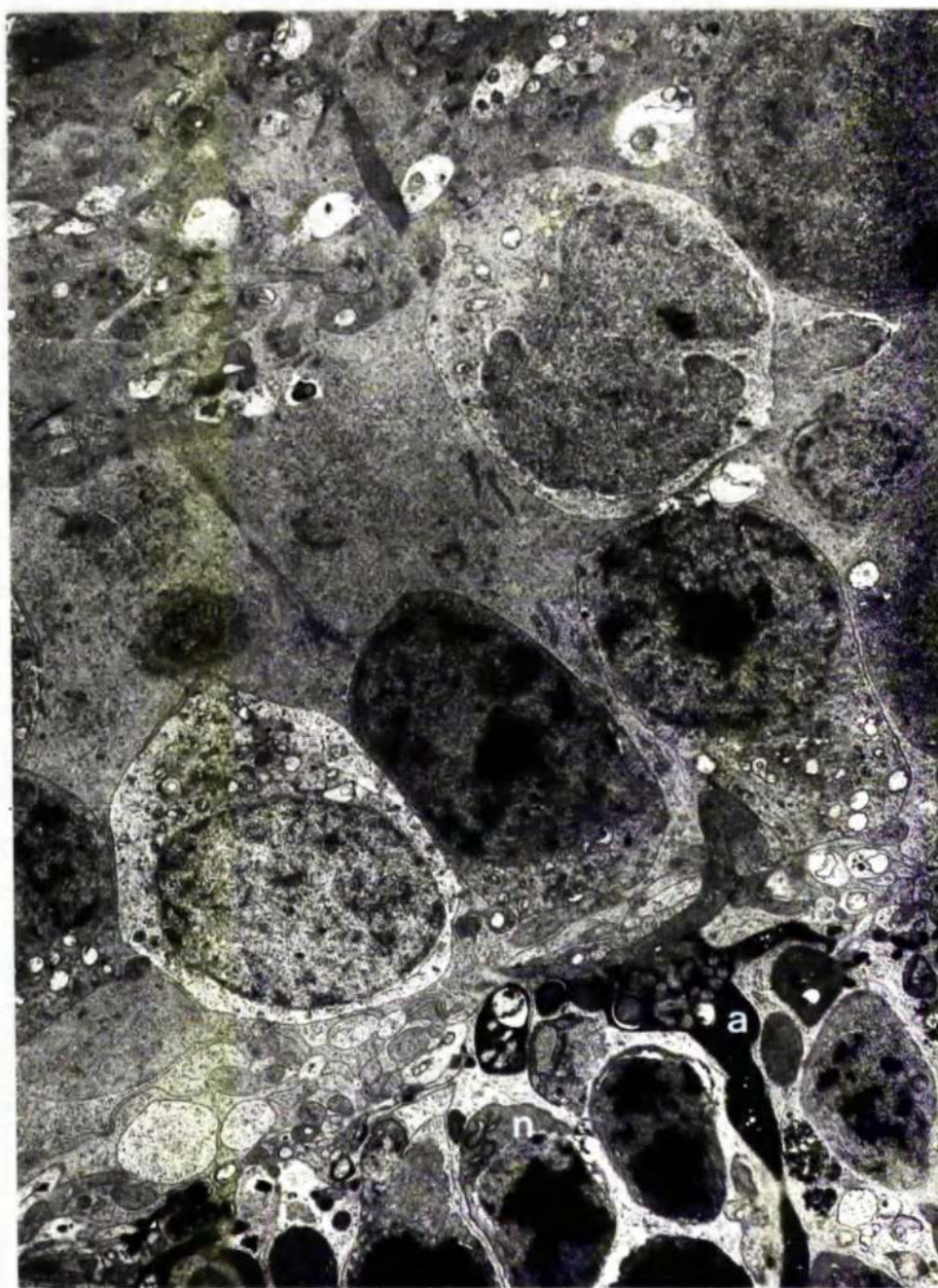


FIG.5-58 Electron micrograph of the inner nuclear layer(60 minutes ischaemia,240 minutes recovery),the nuclei of the layer appear relatively normal,however in the outer plexiform layer both normal (N) and abnormal(A) receptor pedicles occur.(7,000 X)

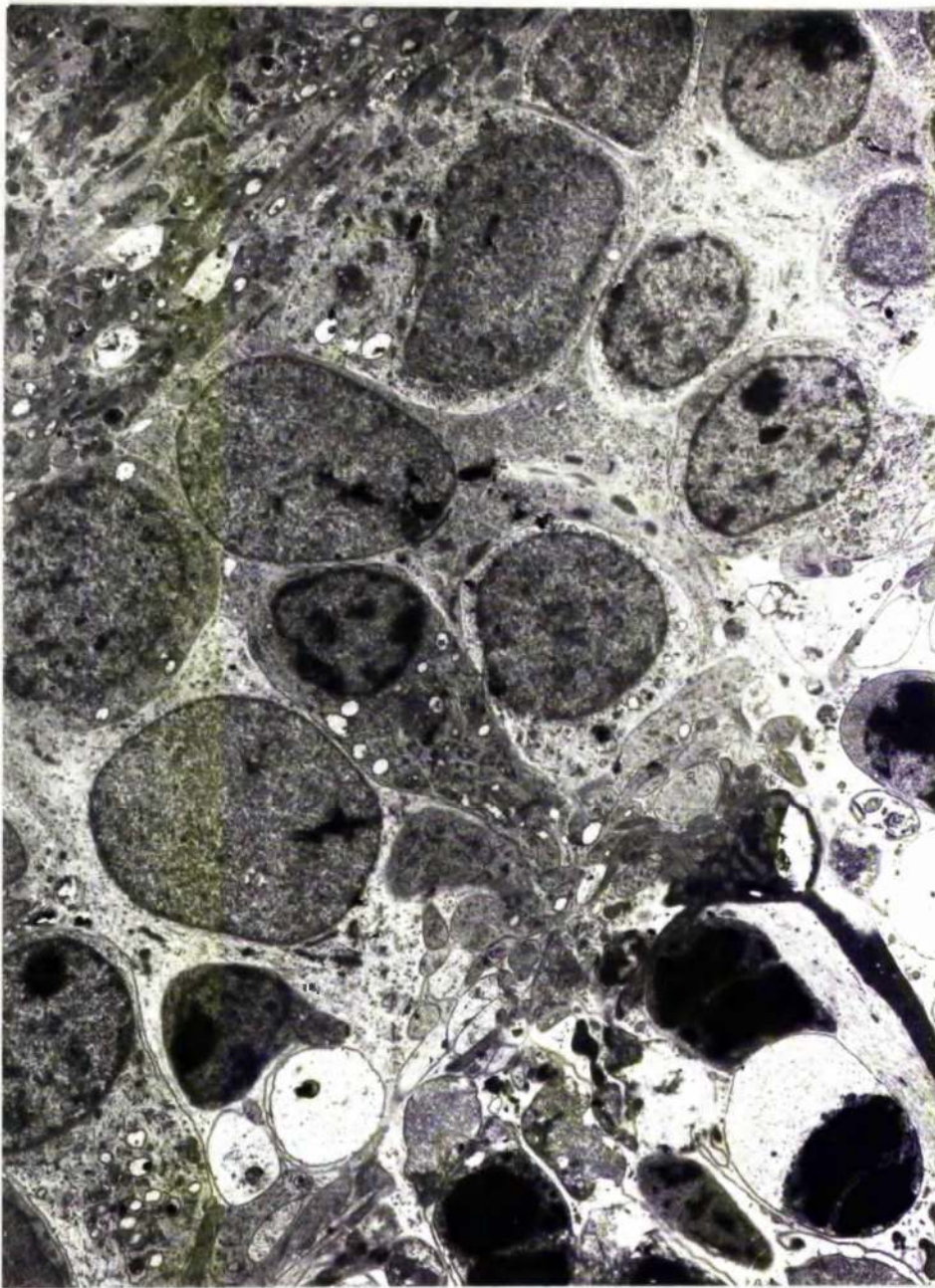


FIG.5-59 Electron micrograph of the inner nuclear layer(peripheral retina,90 minutes ischaemia,240 minutes recovery),many of the nuclei including those of the Muller cells are rounded and have a lower electron density than normal.(7,000 X)

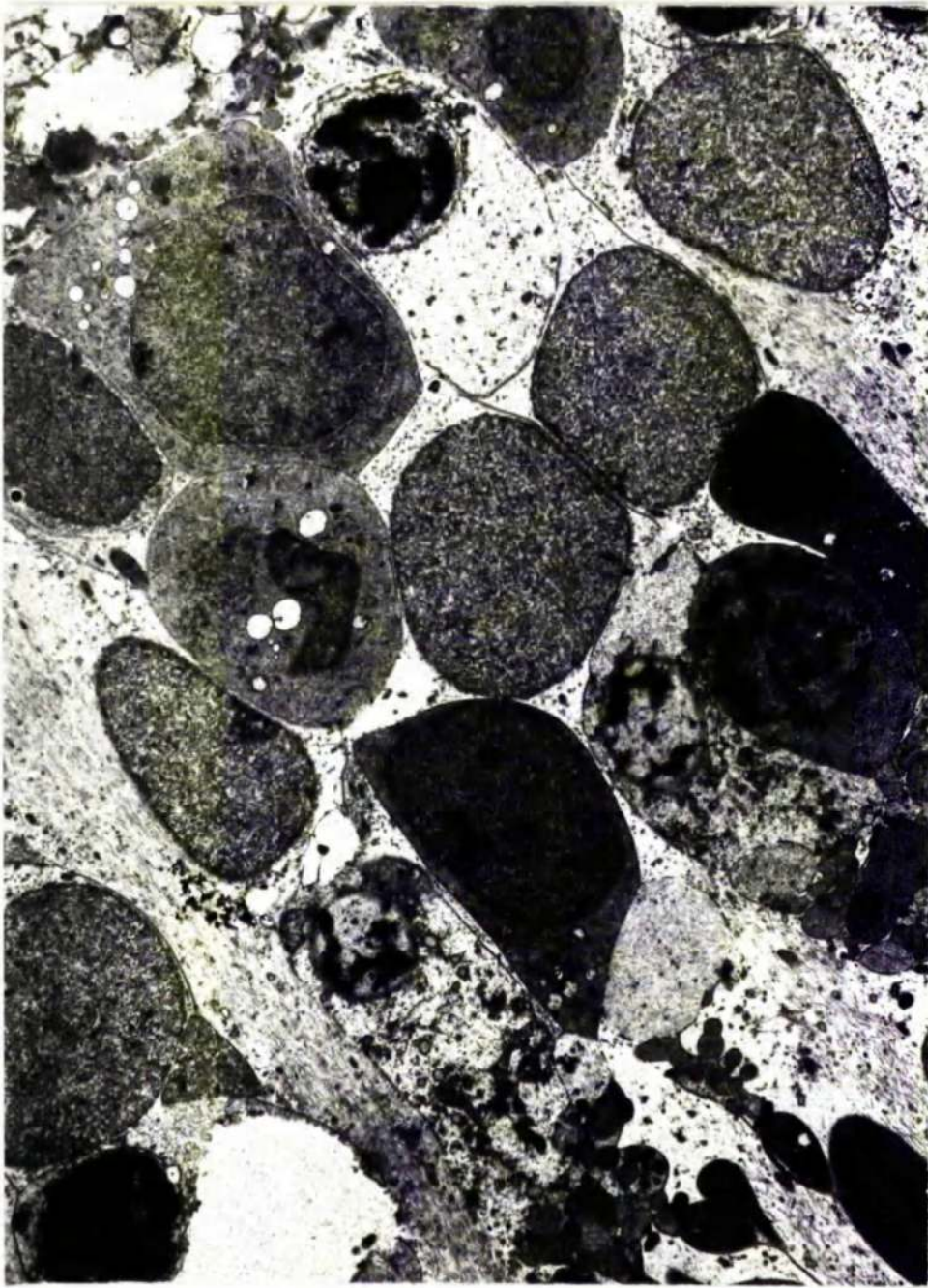


FIG.5-60 Electron micrograph of the inner nuclear layer(visual streak,90 minutes ischaemia,240 minutes recovery),advanced pyknotic changes are evident in the nuclei of the layer with the exception of the Muller cell nuclei.The Muller cell nuclei are rounded and have a low electron density.The outer plexiform layer is greatly reduced and the Muller cell cytoplasm is oedematous.(7,000 X)

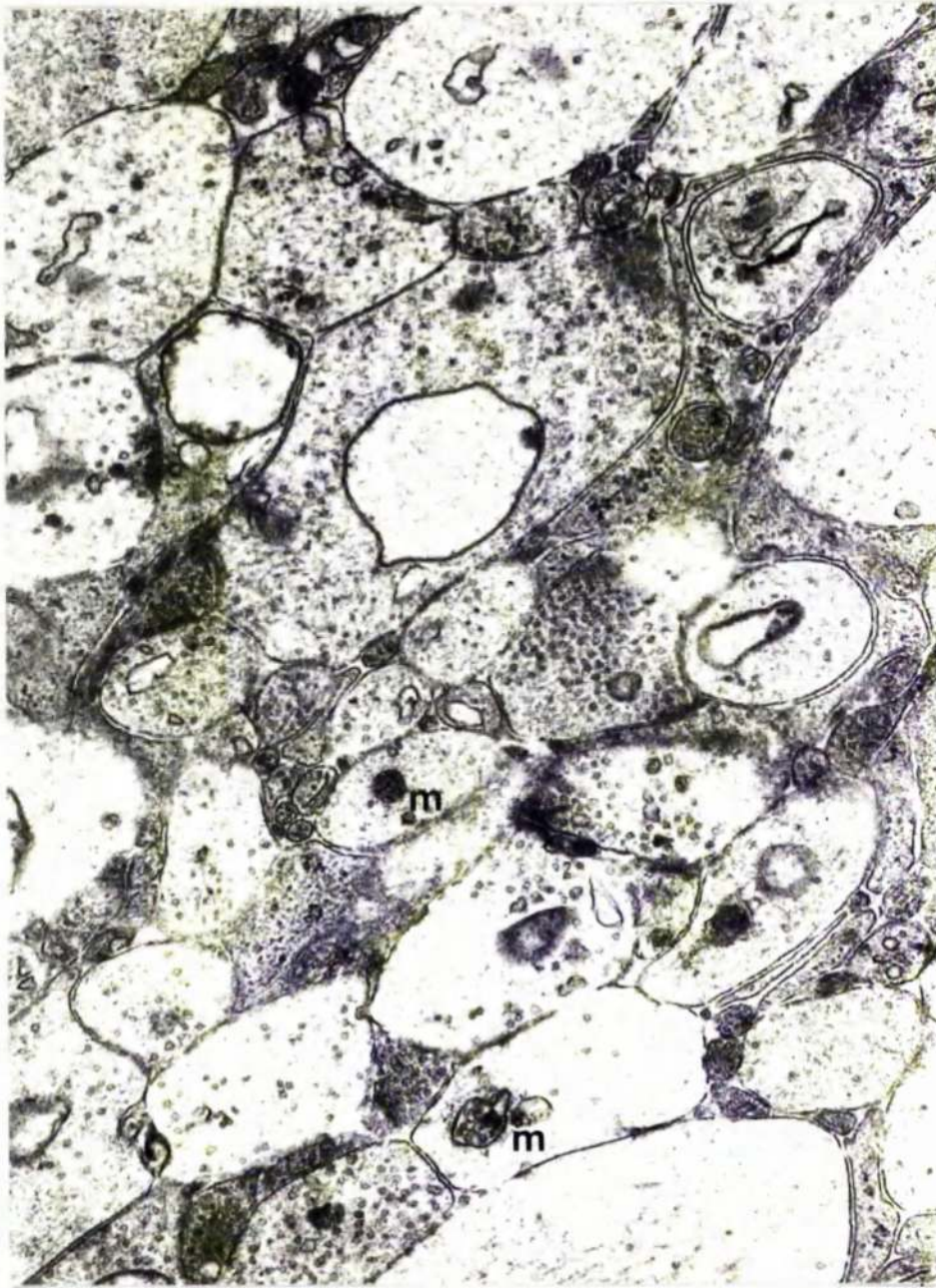


FIG.5-6I Electron micrograph of the inner plexiform layer(30 minutes ischaemia,240 minutes recovery),ruptured cell processes are common and multivesicular like bodies(m) are found within some of these ruptured processes.(19,000 X)

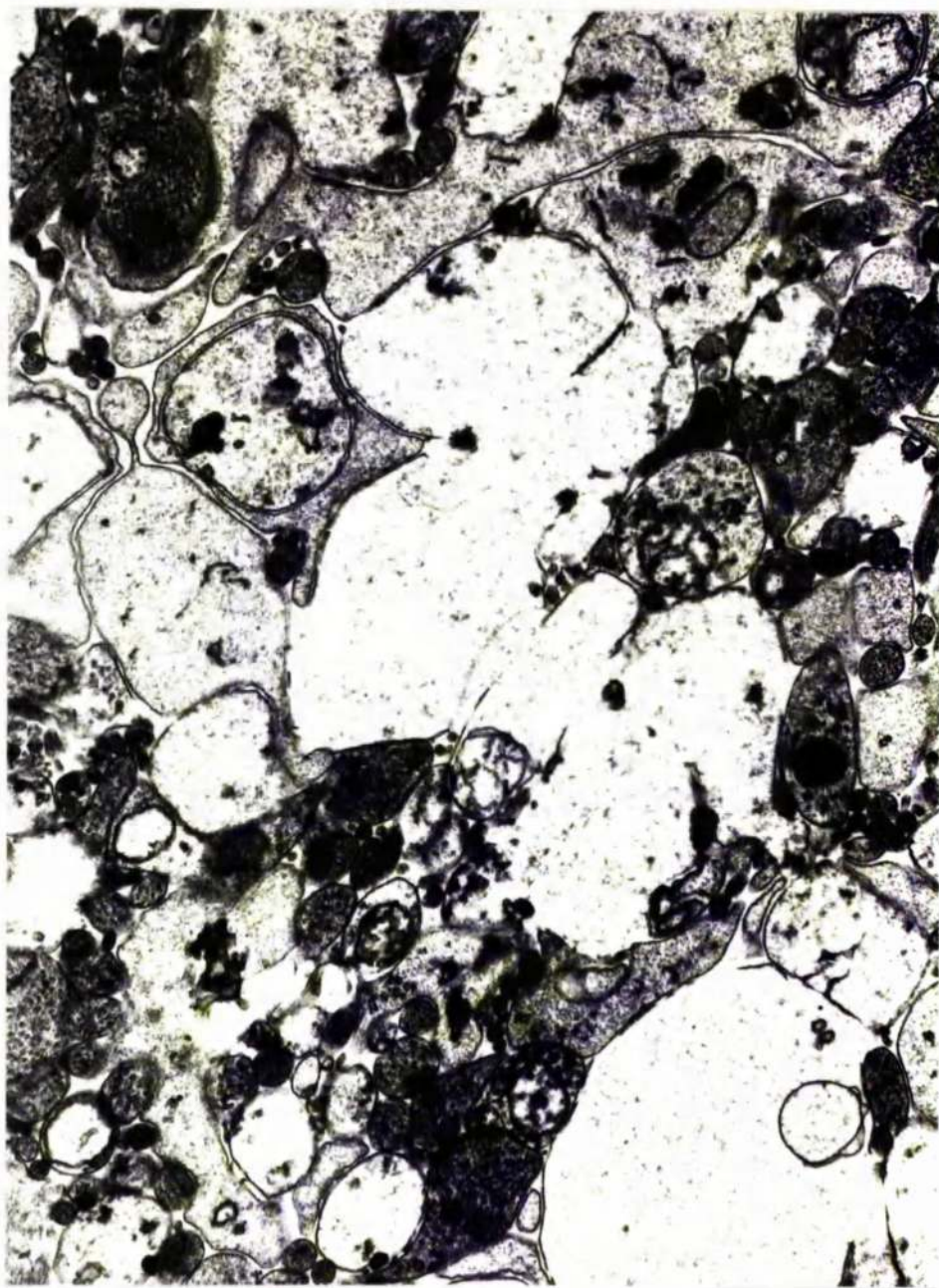


FIG.5-62 Electron micrograph of the inner ~~nuclear~~^{plexiform} layer(90 minutes ischaemia, 240 minutes recovery), many of the processes are ruptured although the occasional ribbon synapse(R) can still be identified. (12,000 X)



FIG.5-63 Electron micrograph of the inner aspect of the inner plexiform layer(60 minutes ischaemia,240 minutes recovery),the processes of the inner plexiform layer are oedematous as is the cytoplasm of the ganglion cell(G).The Muller cell cytoplasm however is comparatively normal.(12,000 X)

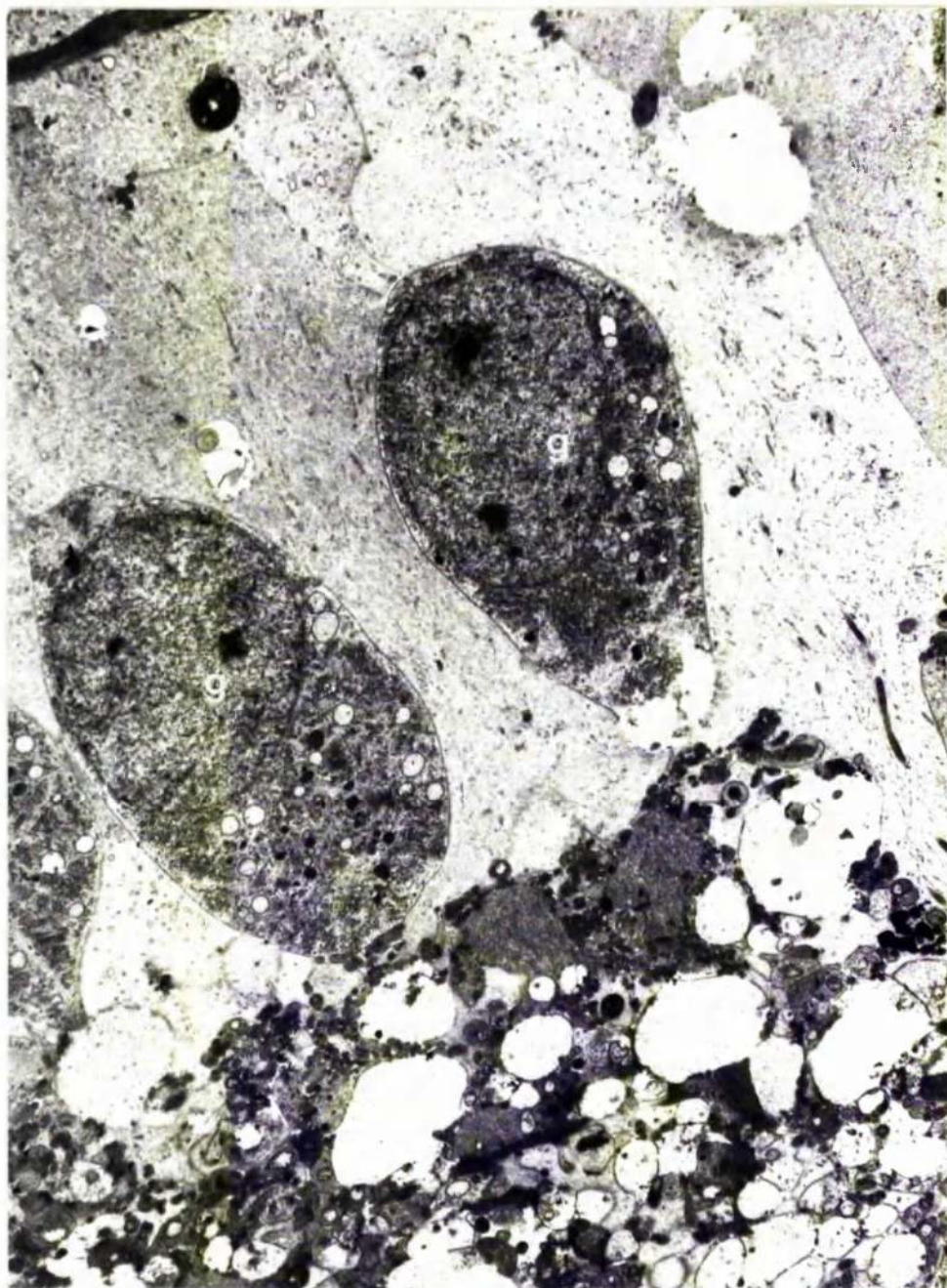


FIG.5-64 Electron micrograph of the ganglion cell layer(90 minutes ischaemia,240 minutes recovery),the cytoplasm of the ganglion cells (G) is condensed and more electron dense than normal.The processes of the inner plexiform layer are severely degenerate with many of the processes being ruptured.The Muller cell cytoplasm surrounding the ganglion cells has a lower electron density than normal.(10,000 X)

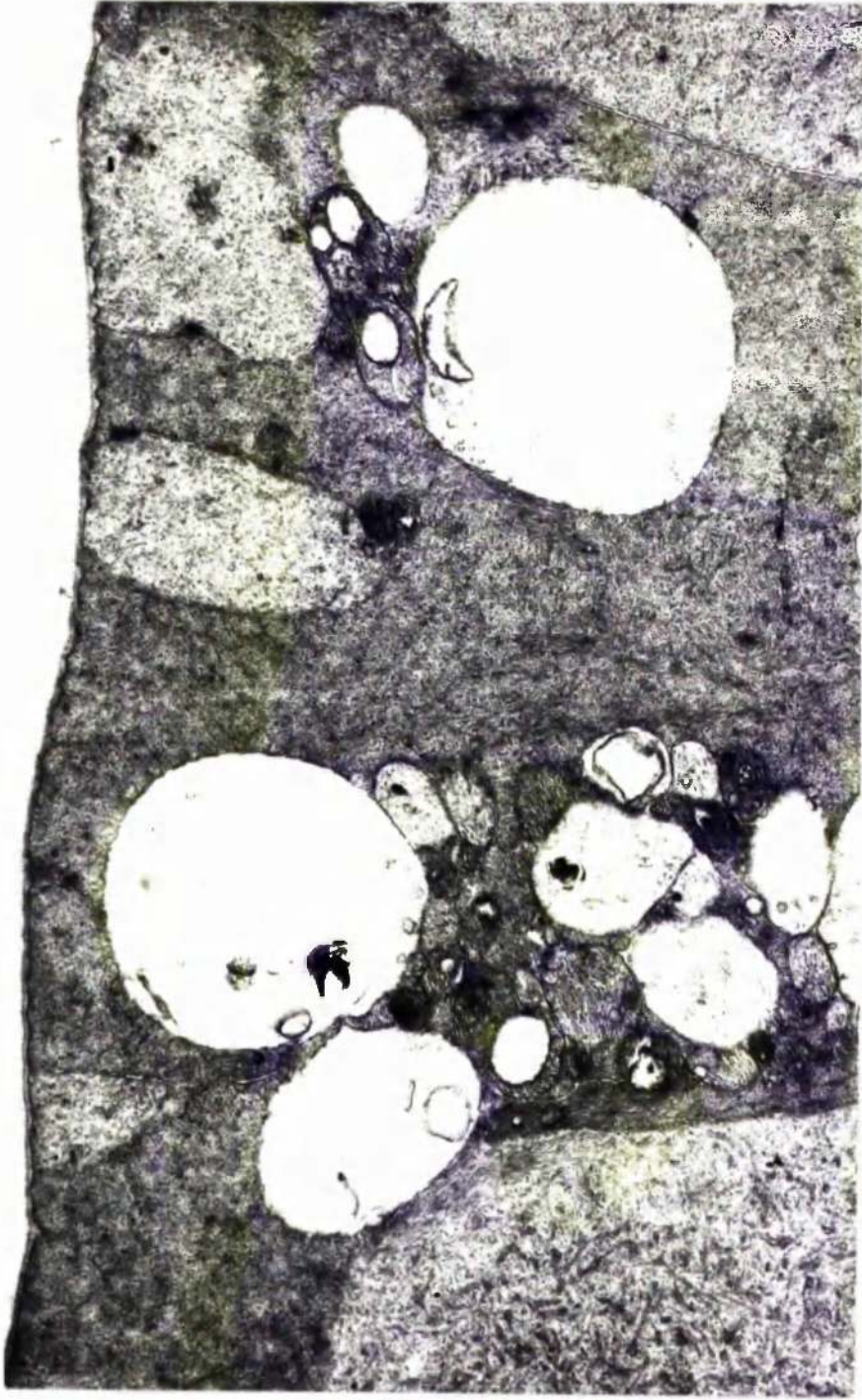


FIG. 5-65 Electron micrograph of the internal limiting membrane (60 minutes ischaemia, 240 minutes recovery), the unmyelinated nerve fibres of the nerve fibre zone of the peripheral retina are frequently cedematous especially the larger nerve fibres. (16,000 X)



FIG.5-66 Electron micrograph of the Muller cell cytoplasm at the level of the ganglion cells(90 minutes ischaemia,240 minutes recovery),the tubules of smooth endoplasmic reticulum(S) are swollen and the cytoplasm has a more granular appearance than normal.The adjacent ganglion cell cytoplasm(G) contains many free ribosomes.
(30,000 X)

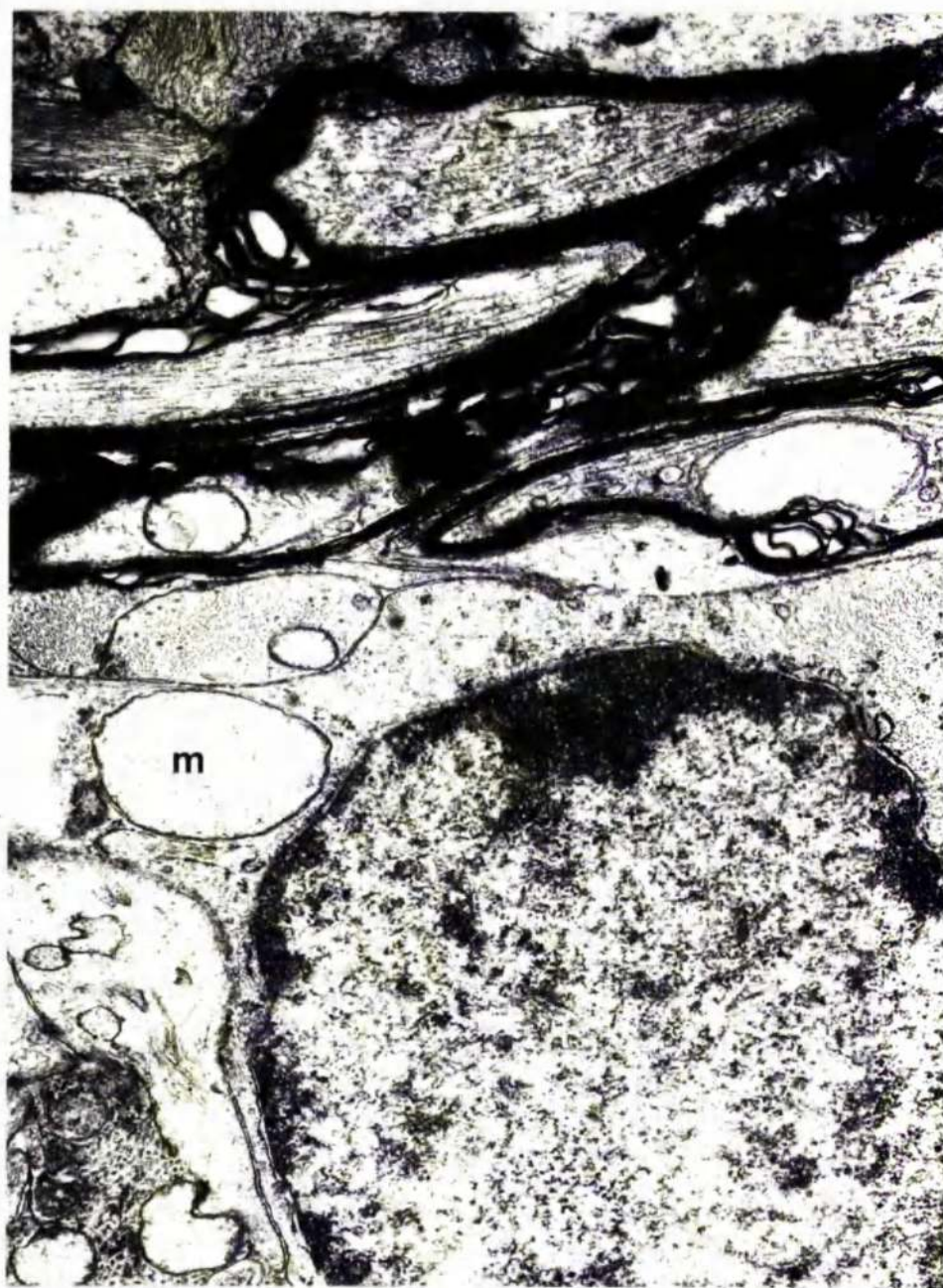


FIG.5-67 Electron micrograph of the horizontal nerve fibre zone (90 minutes ischaemia, 60 minutes recovery), the myelin sheath is often disturbed. The astrocytes which are found in this region often contain swollen mitochondria(M). (16,000 X)



FIG.5-68 Electron micrograph of the horizontal nerve fibre zone(90 minutes ischaemia,240 minutes recovery),many of the myelinated fibres appear normal,however the occasional fibre appears electron dense and contains electron dense particles.(14,000 X)

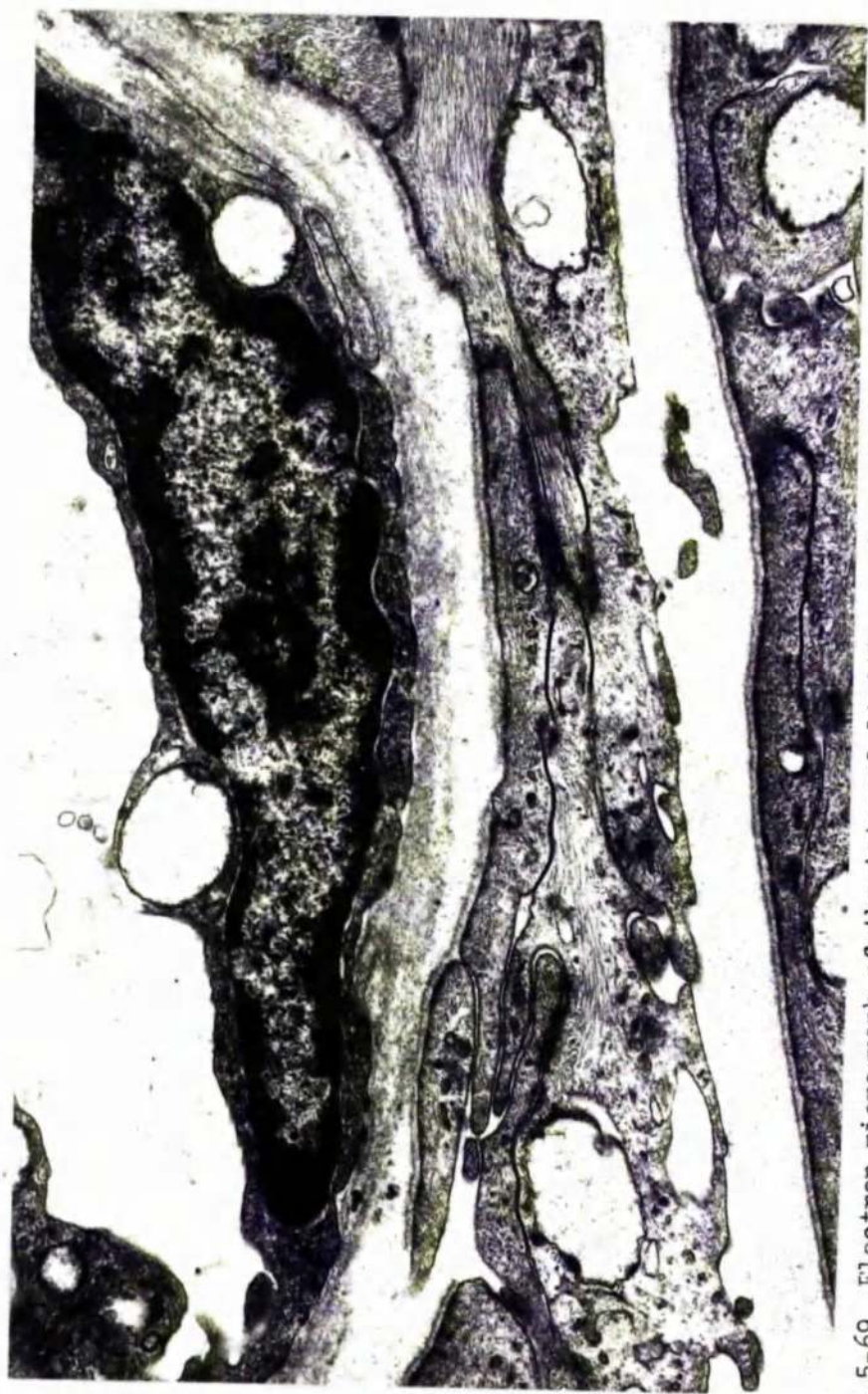


FIG.5-69 Electron micrograph of the internal limiting membrane in the region of the horizontal myelinated nerve fibre zone. (60 minutes ischaemia, 60 minutes recovery) A retinal blood vessel lies above the internal limiting membrane and the extra-retinal glial cells. Mitochondrial distension is a prominent feature of this region. (16,000 X)



FIG.5-70 Electron micrograph of a choroidal vessel(15 minutes ischaemia,60 minutes recovery),showing phagosomes within the cytoplasm of the endothelial wall.(15,000 X)



FIG.5-7I Electron micrograph of the vascular endothelium of a choroidal vessel(60 minutes ischaemia,240 minutes recovery),the endothelium contains a membrane bound vacuole containing organised membrane like material.(35,000 X)

		Minutes recovery		
		0	60	240
Minutes	15	0	1	0
	30	1	1	0
	60	0	1	1
	90	0	0	1
Ischaemia	120	0	0	0

FIG.5-72 Table showing the distribution of the six preparations in which probable endothelial phagosomes were found.

Chapter 6 - The Pattern of Functional Recovery

Following periods of Ischaemia.

6-1 Introduction.

This chapter describes the functional recovery of the rabbit retina following 15-120 minutes acute total pressure-induced ischaemia. Retinal function was investigated by electroretinography under scotopic conditions. Electroretinography is a recognised measure of retinal function and is a method for producing a transient potential change from the outer retina by means of a brief flash of light. The electrical response has a characteristic wave form which is an algebraic sum of several components. The components of the ERG in the order of appearance have been designated as follows, the 'a' wave (Granit's pIII component or later receptor potential), the 'b' wave (Granit's pII component), the 'n' wave (post-'b' negativity) and the 'c' wave (Granit's pI component). The 'a' wave is thought to arise from the visual cells and the 'b' wave from the Müller cells under ionic influence from the bipolar cells in the inner nuclear layer. The ERG is a convenient measure of retinal function although it has its limitations. The ERG only provides information up to the level of the bipolar cells. No information concerning the function of the ganglion cells is gained. In addition, the ERG is a mass response, reflecting the overall activity of the retina which may mask variations throughout the retina.

6-2 Dark Adaptation.

ERGs were recorded under scotopic conditions, this provided stable recording conditions without the possible additive effects of light and ischaemia. In addition under these conditions the ERG has a high signal to noise ratio.

On completion of the operative procedures, the animals were light adapted for 2 minutes (30 cps, $3.3 \text{ mJoules/cm}^2/\text{sec}$). Following this common state of light adaptation, the animals required up to 2 hours adaptation to reach the fully dark adapted state (fig. 6-1) after which time the ERG remained stable.

The course of dark adaptation was followed up to 4 hours in 6 control animals (fig. 6-2). In each of these experimental animals dark adaptation followed an identical pattern. Immediately after light adaptation the ERG comprised a small 'a' and 'b' wave. The 'n' wave appeared after 4-10 minutes. During the subsequent 7-100 minutes the 'b' wave continued to increase in amplitude. The 'a' and 'n' waves remained constant in amplitude following 30-60 minutes dark adaptation. The 'c' wave appeared after 30 minutes, although it was erratic in its presence (fig. 6-1). The recordings from both eyes of each animal were similar in respect of amplitude and rate of dark adaptation, (fig. 6-3).

6-3 Quantitation of the electroretinogram.

The fully dark adapted ERG had a characteristic wave form (fig. 6-1). To obtain both the whole signal and the latencies of the initial potential changes, ERGs were recorded at different sweep speeds (0.1 or 0.2 sec/div and 20 msec/div). The amplitudes and latencies of the negative and positive deflections were measured according to the way set out in figure 6-4. The amplitudes of the 'a', 'n' and 'c' waves were measured from the intersect of a perpendicular line from the peak of the 'b' wave to a line drawn between the troughs of the 'a' and 'n' waves. This was thought to be the best expression of the 'b' wave amplitude in these particular experiments. The main reason for this was that during the recovery phase in the ischaemic eye, there was frequently a marked negativity in the ERG which often resulted in the 'b' wave remaining below the iso-electric line (fig. 6-18). This way of measuring the 'b' wave corresponds roughly to the 'b' wave which Karpe (1945) measured from the trough of the 'a' wave to the peak of the 'b' wave. The absolute latency was measured from the stimulus onset to the onset of the 'a' wave. The peak latencies were measured from the stimulus onset to the intersect of a perpendicular line from the peak of the particular wave to the iso-electric line.

During the recovery phase the amplitude of the individual ERG components in the ischaemic eye were expressed as a ratio of their counterpart in the control eye for each recording. The ratio was then corrected for any differences between the individual components of the fully dark adapted ERG of the left and right eye of each animal prior to the induction of ischaemia. The use of this ratio was thought to minimise variance from factors such as altered metabolism from the length of ischaemia, temperature, blood sugar level and so on.

6-4 The ERG during acute total ocular ischaemia.

In all cases, elevation of the intraocular pressure above systolic arterial blood pressure led to a rapid abolition of the ERG (fig. 6-6). In general, the ERG was extinguished within 7 minutes. The 'c' wave was the first component to go and usually disappeared within 4 minutes of the onset of ischaemia. During the first few minutes of ischaemia, the amplitude of the 'b' wave rapidly decreased and became unrecordable within 5 minutes. The 'a' wave was more resistant than either the 'c' wave or the 'b' wave, but after 7 minutes of ischaemia on average it too disappeared and during the remaining period of ischaemia, no ERG was recordable from the eye with raised intraocular pressure.

6-5 The pattern of post-ischaemic recovery of the ERG.

Following restoration of the circulation to the blind eye, some recovery of the ERG was found in all eyes made ischaemic for up to 120 minutes, although after longer periods of ischaemia, recovery of the ERG was delayed and incomplete. The various components of the ERG behaved differently during the post-ischaemic recovery phase and will be considered separately.

6-5.1 Post-ischaemic recovery of the 'a' wave.

The 'a' wave was the first component to return after restoration of the circulation. Following 15 and 30 minutes of ischaemia recovery of the 'a'

wave had started within 5 minutes on average and was often present within 1 minute. Following 60 or 90 minutes of ischaemia, the 'a' wave had started 5-10 minutes after restoration of the ocular circulation. Following 120 minutes of ischaemia the appearance of the 'a' wave was erratic, but was generally present within 25 minutes. During the later recovery phase, prominent 'a' waves occurred following 15, 30 and 60 minutes of ischaemia (figs. 6-7, 6-8 and 6-9) while after 90 minutes and 120 minutes of ischaemia, the 'a' wave was less marked (figs. 6-10 and 6-11).

A quantitative analysis showed the the 'a' wave quickly returned to normal values following 15 and 30 minutes of ischaemia (fig. 6-12). After 15 minutes of ischaemia the 'a' wave was initially large ($71.9\% \pm 37.6$ after 5 minutes recovery) and returned to normal within 30 minutes. While after 30 minutes of ischaemia 'a' wave recovery was $37.9\% \pm 27.1$ after 5 minutes and was fully recovered within 45 minutes. Recovery from 60 minutes of ischaemia was slower and incomplete compared with the shorter periods of ischaemia after 5 minutes of recovery, the 'a' wave recovery was only $16.8\% \pm 15.3$. Maximum recovery of the 'a' wave occurred after 60-90 minutes and was 60-80% of the fellow eye. The 'a' wave after 90 minutes of ischaemia was also initially small ($20.7\% \pm 14.1$ after 5 minutes) and recovered slowly to about 50% after 100-120 minutes and thereafter remained constant. No quantitative analysis was carried out on the animals subjected to 120 minutes of ischaemia. However, it could be seen from the records that the 'a' wave appeared within 25 minutes and was generally smaller than with 90 minutes ischaemia.

While a considerable variation occurred in the amplitude of the 'a' wave, the peak latency of the wave form appeared to alter little from that of the control eye following periods of ischaemia up to 60 minutes (fig. 6-14). During the recovery phase following 90 and 120 minutes of ischaemia, the absolute latency of the 'a' wave was similar to that of the control eye while the peak latency was of longer duration (fig. 6-14). It was often difficult

to determine the peak of the 'a' wave especially after 120 minutes of ischaemia because of the extended slope of the wave form.

A problem with the reliable measurement of the 'a' wave was its small amplitude in relation to the background activity. This led to a large variance (fig. 6-13). However, with the number of animals used the trend could be well established (fig. 6-12).

There were two circumstances in which the 'a' wave was seen in isolation. The first of these occurred after the restoration of the circulation following the shorter periods of ischaemia (15-60 minutes of ischaemia). In this case, the isolated 'a' wave appeared before the presence of a prominent 'b' wave (fig. 6-15). The second circumstance occurred following 90 and 120 minutes ischaemia where the appearance of the 'b' wave was delayed or in some cases absent. In this case the solitary 'a' wave formed the leading edge of a shallow negative trough (exposed pIII component) (fig. 6-15).

6-5.2 Post-ischaemic recovery of the 'b' wave.

After periods of ischaemia of 15, 30 or 60 minutes, a recordable 'b' wave appears within 5 minutes of the restoration of the ocular circulation. After 90 minutes of ischaemia, recovery of the 'b' wave can be seen some 15-20 minutes after restoration of the circulation, while after 120 minutes of ischaemia, the appearance of a recordable 'b' wave may be delayed for as long as 45 minutes (figs. 6-7 to 6-11).

A quantitative analysis was possible with all five periods of ischaemia (fig. 6-16). Following 15 minutes of ischaemia, the 'b' wave amplitude was initially large ($46.4\% \pm 8.8$ after 5 minutes) and grew rapidly and reached near normal values after 70 minutes ($90.4\% \pm 6.7$). Following 30 minutes of ischaemia, 'b' wave recovery after 5 minutes was $27.1\% \pm 6.8$. The 'b' wave amplitude increased quickly and became supernormal after 70-80 minutes. Maximum recovery (120-150%) occurred after 160-170 minutes and thereafter

remained at this level. After 60 minutes ischaemia, the 'b' wave amplitude was initially low ($6.3\% \pm 4.2$ after 5 minutes) and recovery was slower and less complete than with the shorter periods of ischaemia. The maximum recovery (50-70%) occurred after 120-130 minutes after the restoration of the circulation and thereafter remained at this level for the rest of the experiment. The appearance of the 'b' wave following the return of the ocular circulation after 90 minutes of ischaemia was delayed in some cases up to 20 minutes. The average 'b' wave recovery was $4.1\% \pm 4.8$ after 5 minutes, the subsequent increase in amplitude was slow and revealed its maximum value (20-50%) after 100-120 minutes. After 120 minutes of ischaemia, there was a long delay (not less than 20 minutes and up to 45 minutes) before the 'b' wave appeared. The appearance of the 'b' wave was transitory, being absent in all animals after 180 minutes. With the two longer periods of ischaemia (90 and 120 minutes) the 'b' wave was often small and failed to rise above the iso-electric line (fig. 6-18).

The variance of the 'b' wave amplitudes was smaller than that of the 'a' wave (fig. 6-17). Following all the periods of ischaemia (with the exception of 120 minutes ischaemia) recovery was greater after 4 hours than after only 1 hour. The difference between the two recovery periods was most marked after 30 minutes ischaemia.

The peak latency of the 'b' wave during the recovery phase from 15-60 minutes of ischaemia was similar to that of the control eye (fig. 6-19). Following 90 and 120 minutes of ischaemia, the peak latency of the 'b' wave was longer. Although the exact peak of the 'b' wave was difficult to determine because of the rounded nature of the wave form (fig. 6-19).

6-5.3 Post-ischaemic recovery of the 'n' wave.

A feature of the ERG during recovery from ischaemia was the occurrence of a marked post-'b' wave negativity. A quantitative analysis showed that following 15 and 30 minutes of ischaemia, the amplitude of the

post 'b' wave negativity was in order of 50% of the control value after 5-10 minutes. The 'n' wave grew rapidly and became hypernormal within 40 minutes and thereafter remained relatively stable (fig. 6-20). The increase in amplitude was more rapid and marked following 30 minutes of ischaemia. Following 60 minutes of ischaemia, the mean 'n' wave amplitude was initially small (23% after 5-10 minutes) and grew rapidly. The 'n' wave became similar to that in the control eye after 20-30 minutes recovery. The variance of the 'n' wave was large following these three shorter periods of ischaemia (fig. 6-21). Quantitative analyses were not carried out on tissue made ischaemic for 90 and 120 minutes. During the recovery phase from the latter periods of ischaemia, the 'n' wave was very variable and erratic in appearance although in a few cases, there was a very marked negativity (fig. 6-10).

6-5.4 Post-ischaemic recovery of the 'c' wave.

With the techniques used the 'c' wave of the ERG was found to be more variable than the 'a' or 'b' waves. It was however notable that after ischaemia, the 'c' wave was often of larger amplitude than in the pre-ischaemic ERG. A 'c' wave of normal or supernormal value often appeared when both the 'a' and 'b' waves were relatively small (figs. 6-8 and 6-9) even after the longer periods of ischaemia.

6-6 DISCUSSION.

The method used for inducing ischaemia in the rabbit eye undoubtedly interrupted both the retinal and choroidal circulations. Although the effect of loss of the choroidal circulation in the rabbit would be more marked than of the retinal circulation owing to the vestigial nature of the retinal blood supply in this species (Michelson, 1954). The findings of Fujino and Hamasaki (1967) support the view that the changes in the ERG resulting from high intraocular pressure were due to ischaemia and not directly related to the raised intraocular pressure.

Recovery of the ERG after ischaemia is thought to be influenced by temperature (Winkler 1972) and by retinal glycogen levels (Vassileva and Dubov 1976). Care was taken in the present study to keep the body temperature normal and only healthy preparations maintaining a normal blood pressure were accepted. The use of the ratio of the individual ERG components in the ischaemic eye to their counterparts in the control eye for each recording of the ERG was thought to minimise variance from factors such as altered metabolism from the length of anaesthesia, temperature and so on. However, one drawback to the use of this ratio was an increase in amplitude of the 'b' wave in the control eye during the ischaemic and post-ischaemic phases (fig. 6-5). This increase in amplitude occurred shortly after induction of ischaemia and was similar with all periods of ischaemia (up to 40%), except with 30 minutes ischaemia where the increase was more marked (up to 80%). The underlying reasons for this increase are ^{not} known although it may be mediated via either a humoral or nervous mechanism. However, there is no general agreement as to whether mammals, including rabbits, possess centrifugal fibres in the retina (Winkler 1972). Centrifugal fibres would be necessary for such a nervous pathway. For the purposes of this study the mechanism involved was assumed to be bilateral. If, however, the effect is unilateral, the ratio of the test and control eyes would be invalidated. In this case, the increase in the 'b' wave during the post-ischaemic recovery phase would be more pronounced.

The abolition of the ERG within 7 minutes of total intraocular ischaemia compares with published work and the loss of the 'c' wave, 'b' wave and 'a' wave in that order confirms the findings of Granit (1933) and many others, although at variance with the results reported by Arden and Greaves (1956). The difference may be in the stimulus intensity used, for the 'a' and 'c' waves require a high stimulus while the 'b' wave due to convergence, can be elicited at relatively low stimulus intensities (Granit 1933). With

stimuli of relatively low intensity, the 'a' wave might well appear to be more sensitive to ischaemia than the 'b' wave, with the small 'a' wave being rapidly lost amongst the background activity leaving a reduced 'b' wave. While with high stimulus intensities the 'a' wave would be larger and less liable to be lost amongst the background activity before the loss of the 'b' wave.

Interpretation of the findings during recovery from ischaemia was difficult. In general, the more prolonged the period of ischaemia, the more severely affected was the 'b' wave, both as regards the rate of recovery and the completeness of recovery. In contrast, even after lengthy periods of ischaemia, there was a rapid return of the 'a' wave and often the occurrence of a supernormal 'c' wave. When the 'b' wave was reduced or absent the light stimulus may have evoked a potential change which was almost certainly an exposed pIII component. A similar negative potential has been described by Fujino and Hamasaki (1965) following occlusion of the retinal circulation in monkeys leaving the outer retina (the visual cells and RPE) nourished from the choroidal circulation.

The pattern of recovery of the ERG after ischaemia, in relation to the 'a' and 'b' waves was the reverse of the sequence observed following the onset of ischaemia. The earlier affected and presumably more sensitive component, the 'b' wave was last to recover, while the more resistant component, the 'a' wave, was the first to appear during the recovery phase.

There is good evidence that the 'a' wave (or the negativity of the pIII component which is exposed by abolition of the pI and pII components) is generated in the receptor cells (Brown and Wiesel 1961, Brown and Watanabe 1961, Arden and Brown 1965, Brown 1968 and Penn and Hagins 1969) and that the 'c' wave is generated in the retinal pigment epithelium (Noell 1954, Heck and Lapst 1957 and Steinberg, Schmidt and Brown 1970). It appears likely that the 'b' wave is generated in the inner nuclear layer, probably by the Müller

cells, although it closely parallels neural activity in the bipolar cells (Werblin and Dowling 1969 and Miller 1973). As the 'a' and 'c' waves returned more promptly than the 'b' wave after even lengthy periods of ischaemia, it would appear either that the pigment epithelium and the receptor cells were more resistant to ischaemic damage than the mid-retina, or that in the rabbit with its predominantly choroidal blood supply recovery of the tissues adjacent to the choroid occurred first when the choroidal circulation was restored.

A feature of the recovery phase from the shorter periods of ischaemia (15 and 30 minutes) was the presence of supernormal negative components ('a' and 'n' waves) and following 30 minutes of ischaemia a greatly enhanced 'b' wave. An enhanced 'c' wave was also seen even after the longer ischaemic episodes. A supernormal 'c' wave can occur following disturbance of the choroidal circulation (Fujino and Hamasaki 1965). The increased 'b' wave following 30 minutes ischaemia is reminiscent of the supernormal 'b' wave found after mild hypoxia in the cat by Van de Bos (1969) and in humans by Henkes (1954) and following small rises in intraocular pressure in humans (Vanysek, Hrachovina, Anton and Moster 1968).

From the results of the experiments reported, we should expect that the pigment epithelium and the retinal receptors would show histological evidence of a return to normality during the post-ischaemic phase, even after lengthy periods of ischaemia, whereas the neural elements or glial cells of the retina might well show more lasting or even permanent damage.

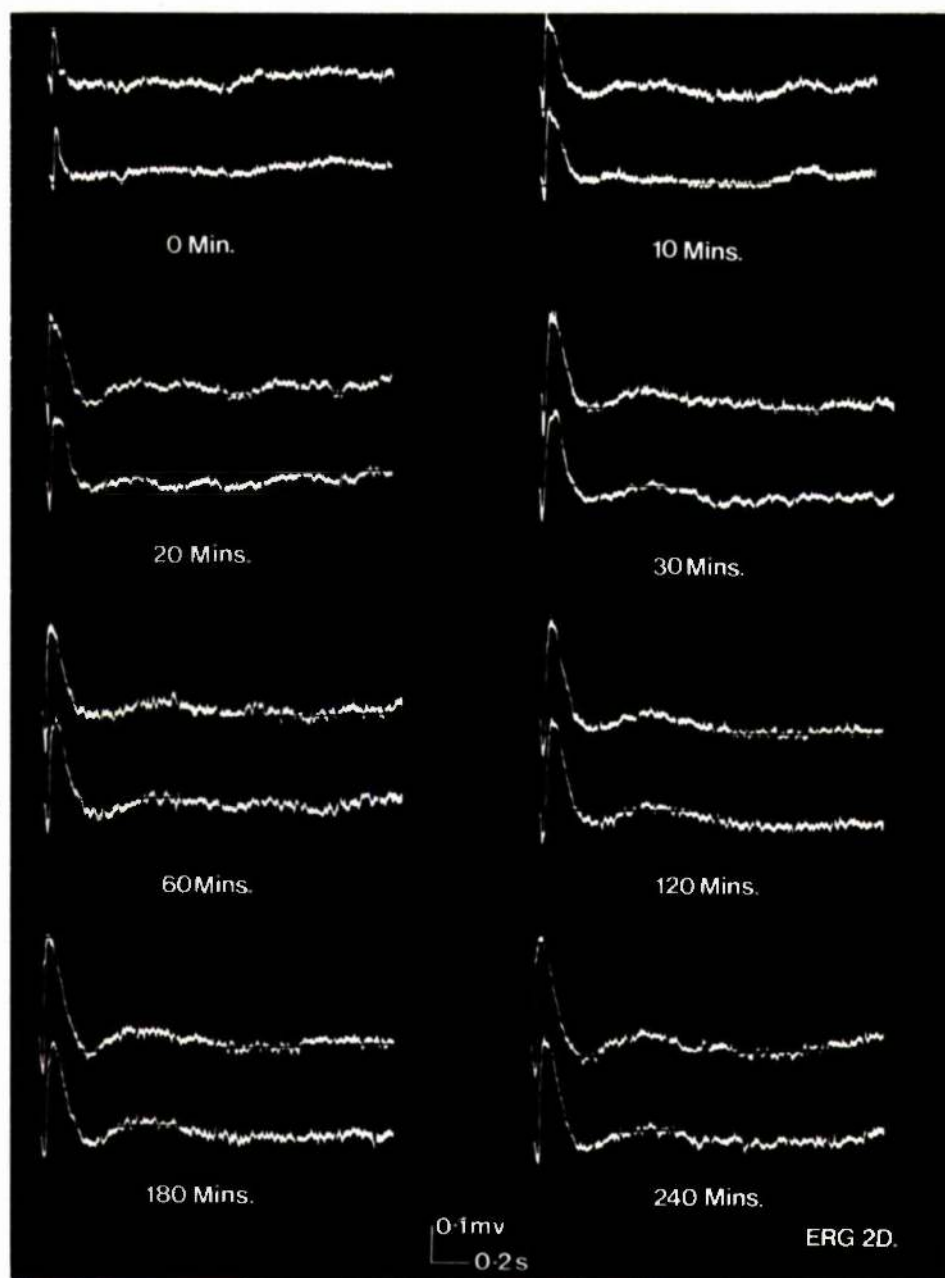


FIG.6-I ERGs recorded from each eye of a control animal at various intervals during the course of dark adaptation. All the components of the ERG become larger after the onset of dark adaptation. The ERG remains unchanged after 120 minutes dark adaptation.

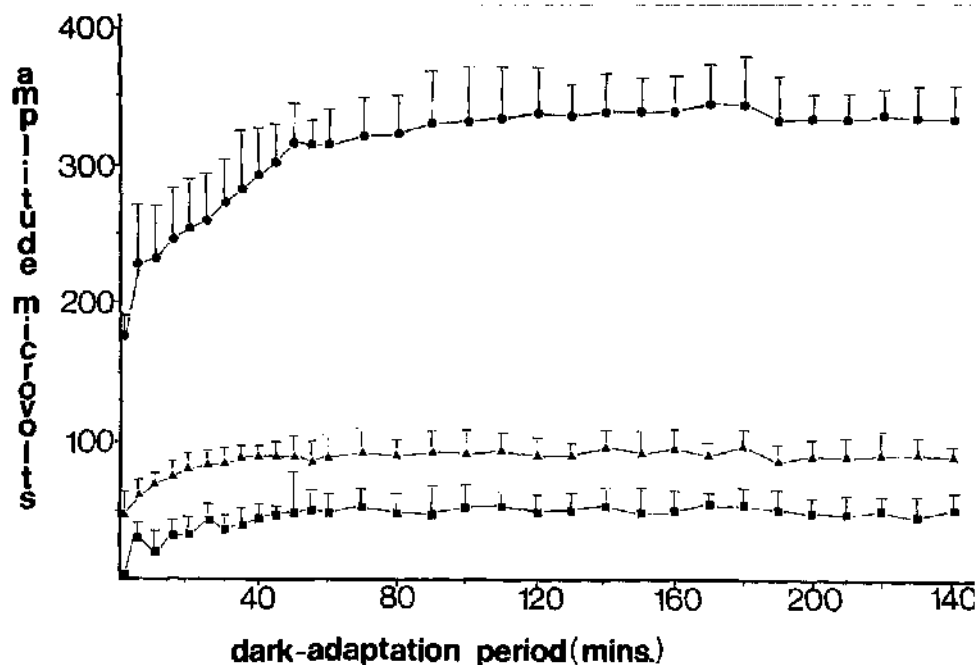


FIG.6-2 Graph of the dark adaptation curves of the 'a', 'b' and 'n' waves of the ERGs recorded from each eye of the control animals. Each curve represents the mean values of the ERG components measured at each point in the course of dark adaptation, the error bars represent the standard deviation of the particular point. (▲; 'a' wave, ●; 'b' wave, ■; 'n' wave.) The 'b' wave adapts after 80-100 minutes while the 'a' and 'n' waves adapt after 30-60 minutes.

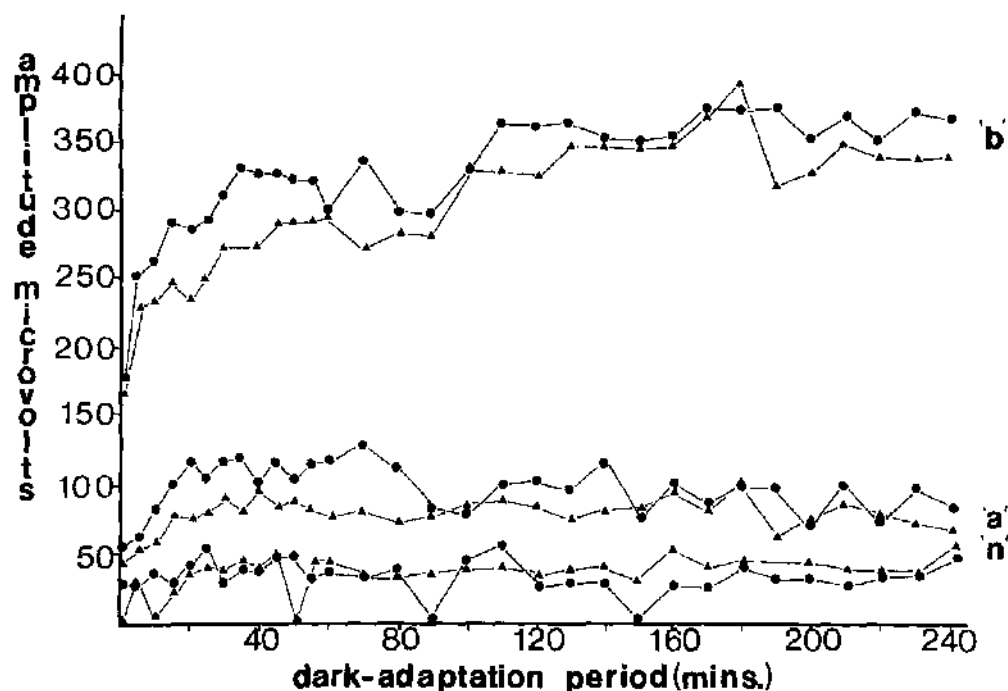


FIG.6-3 Graph of the ERG components recorded from each eye of one control animal during the course of dark adaptation. The recordings from each eye are similar to one another. ●; the left eye, ▲; the right eye.

key
 latency
 ----- amplitude

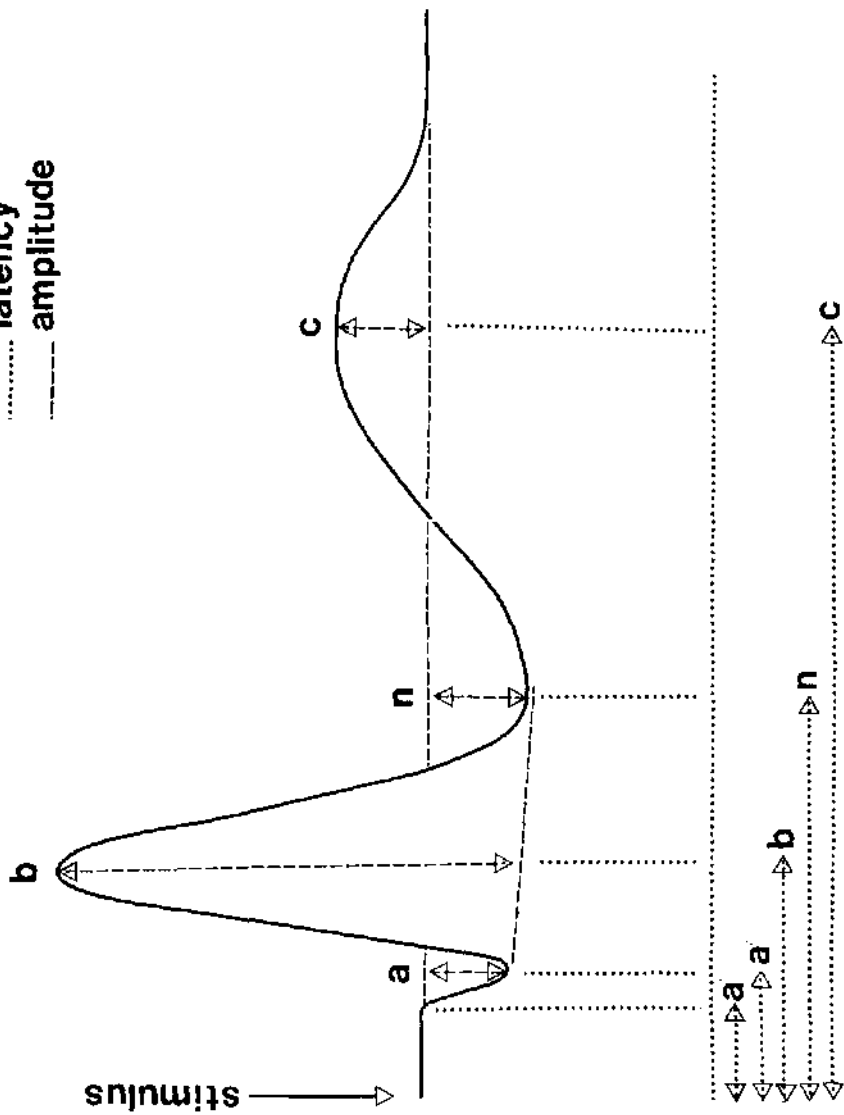


FIG.6-4 Diagram illustrating the points at which the amplitudes and latencies of the various components of the ERG. were measured.

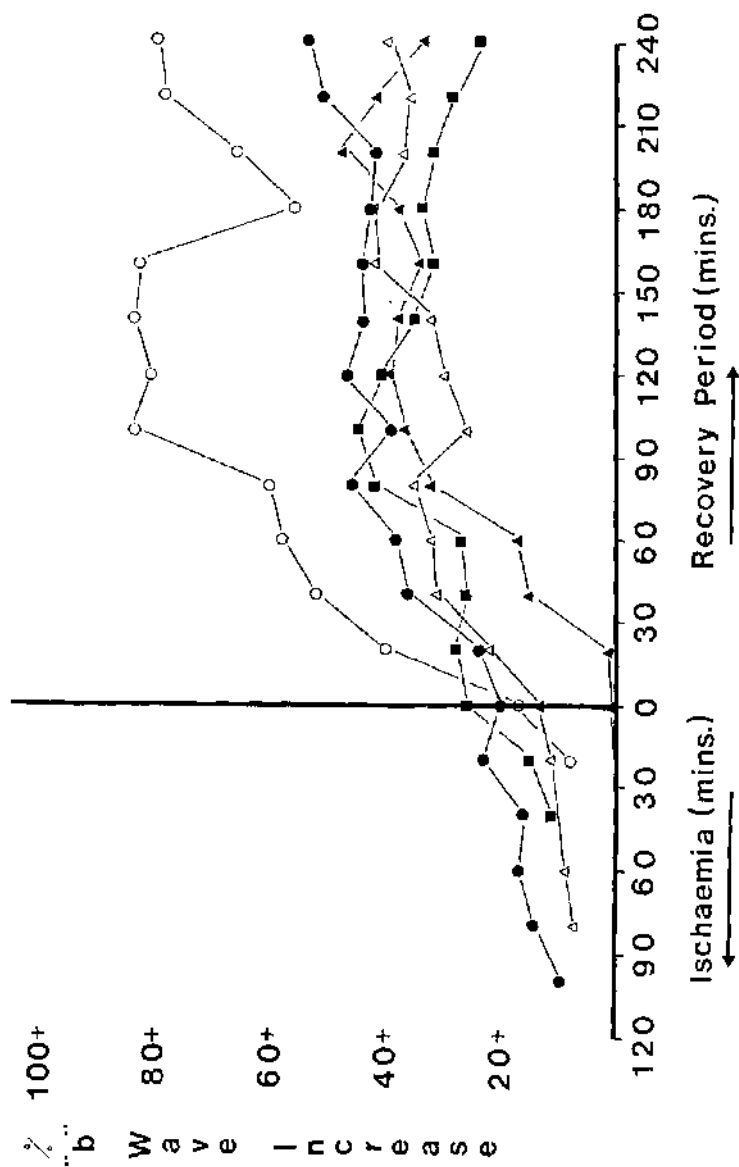


FIG.6-5 Graph showing the % increase in the 'b' wave amplitude in the control eyes after the induction of ischaemia in the contralateral eye. The increases in the 'b' wave amplitude is similar with all the periods of ischaemia except for 30 minutes ischaemia where the increase is more pronounced. ▲ ;15 minutes, ○ ;30 minutes, ■ ;60 minutes, △ ;90 minutes, ● ;120 minutes ischaemia.

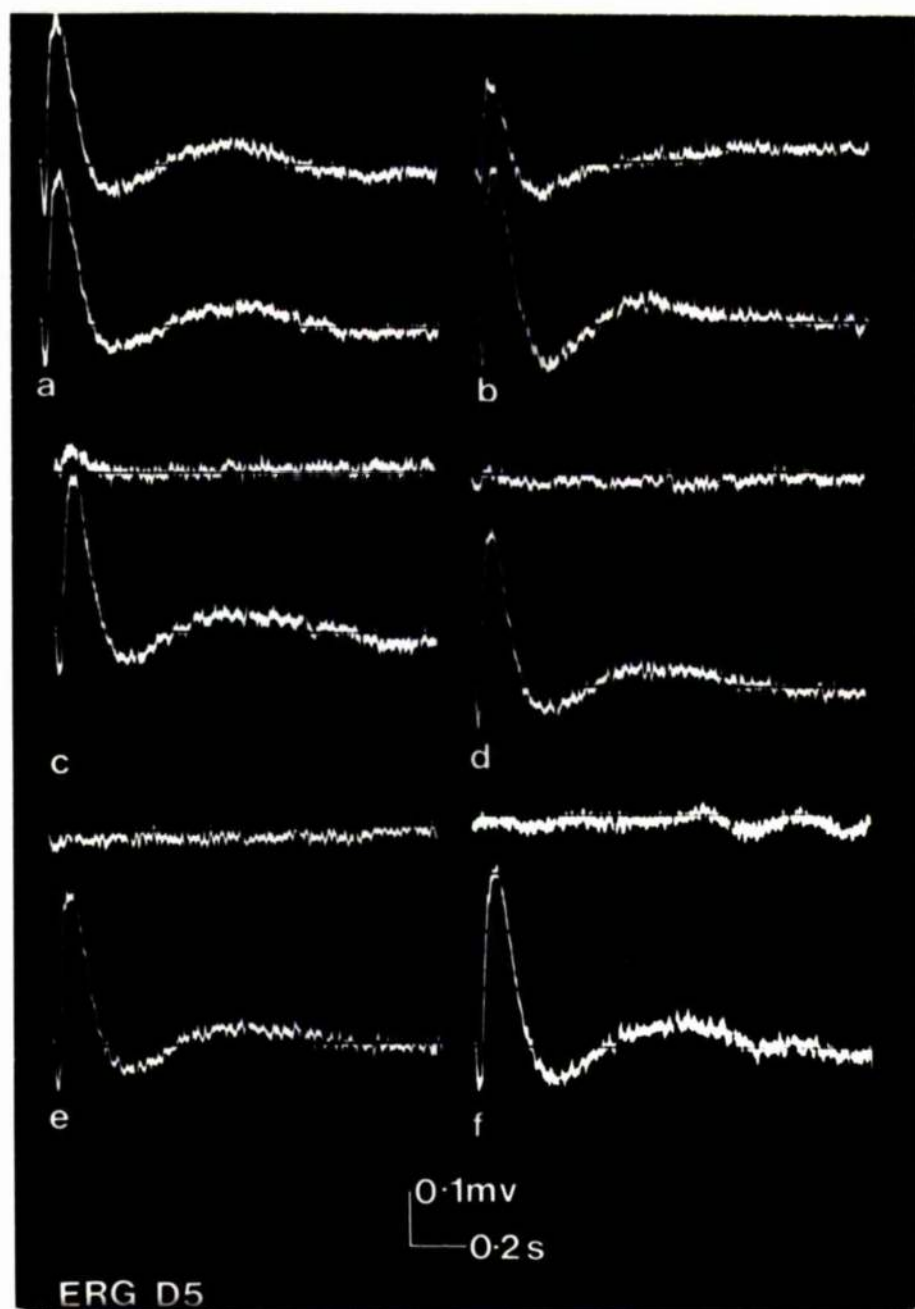


FIG.6-6 ERGs recorded from both eyes of one animal immediately before and after the induction of ischaemia in one eye(upper trace), the other eye remaining as the control.The 'c' wave disappears rapidly (b) and the 'b' wave amplitude decreases quickly(b and c) and disappears before the 'a' wave is lost.The ERG is extinguished within 7 minutes.(f) a)-Pre-ishaemia;b)- 1 minute of ischaemia;c)- 2 minutes of ischaemia;d)- 3 minutes of ischaemia;e)- 5 minutes of ischaemia;f)- 7 minutes of ischaemia.

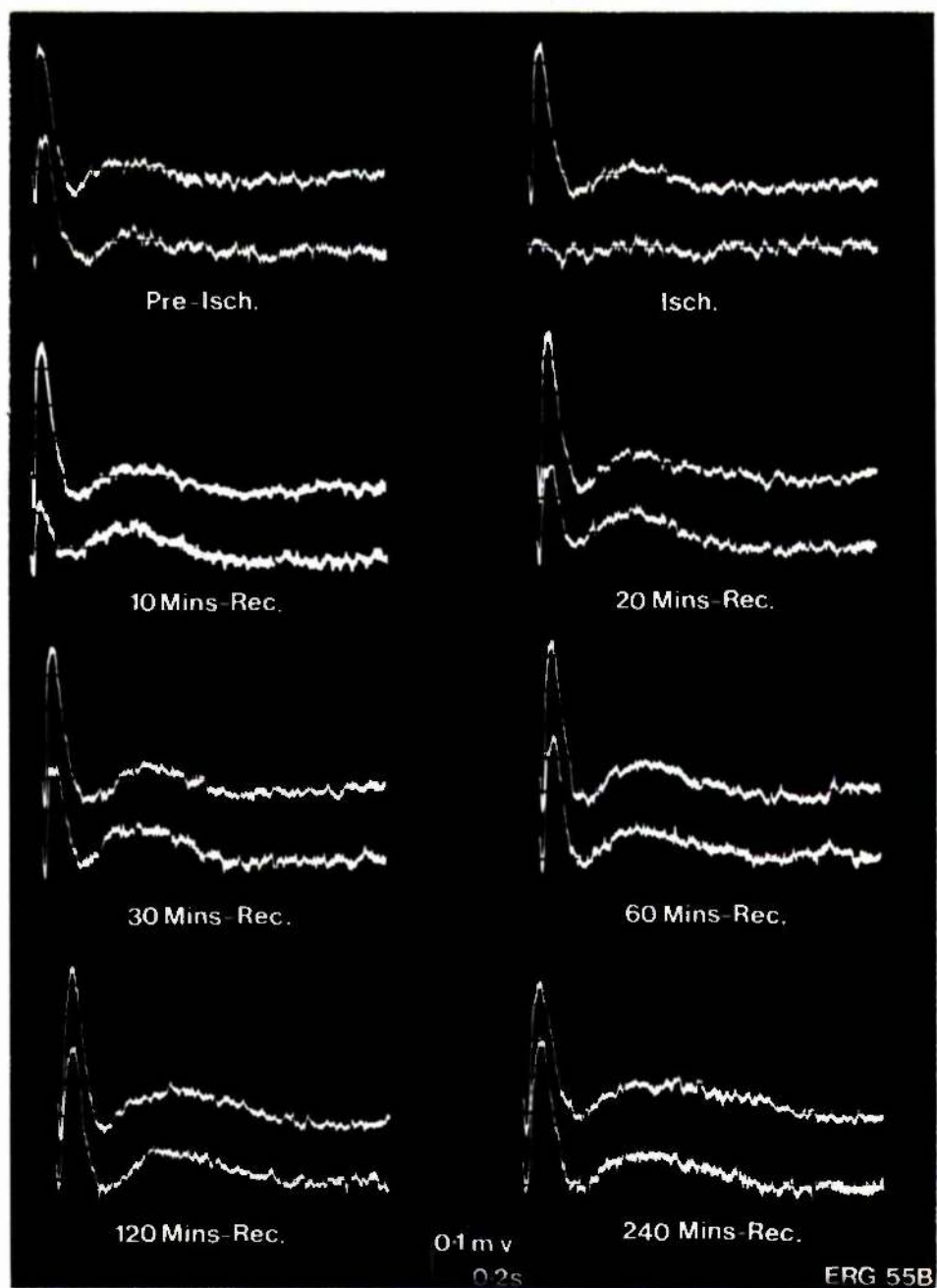


FIG.6-7 ERGs recorded from both eyes of one animal before,during and after 15 minutes of induced ischaemia in one eye(lower trace). The ERG rapidly returns to normal during the recovery phase.



FIG.6-8 ERGs recorded from both eyes of one animal before, during and after 30 minutes of induced ischaemia in one eye (upper trace). The ERG rapidly returns and the 'b' wave becomes supernormal.

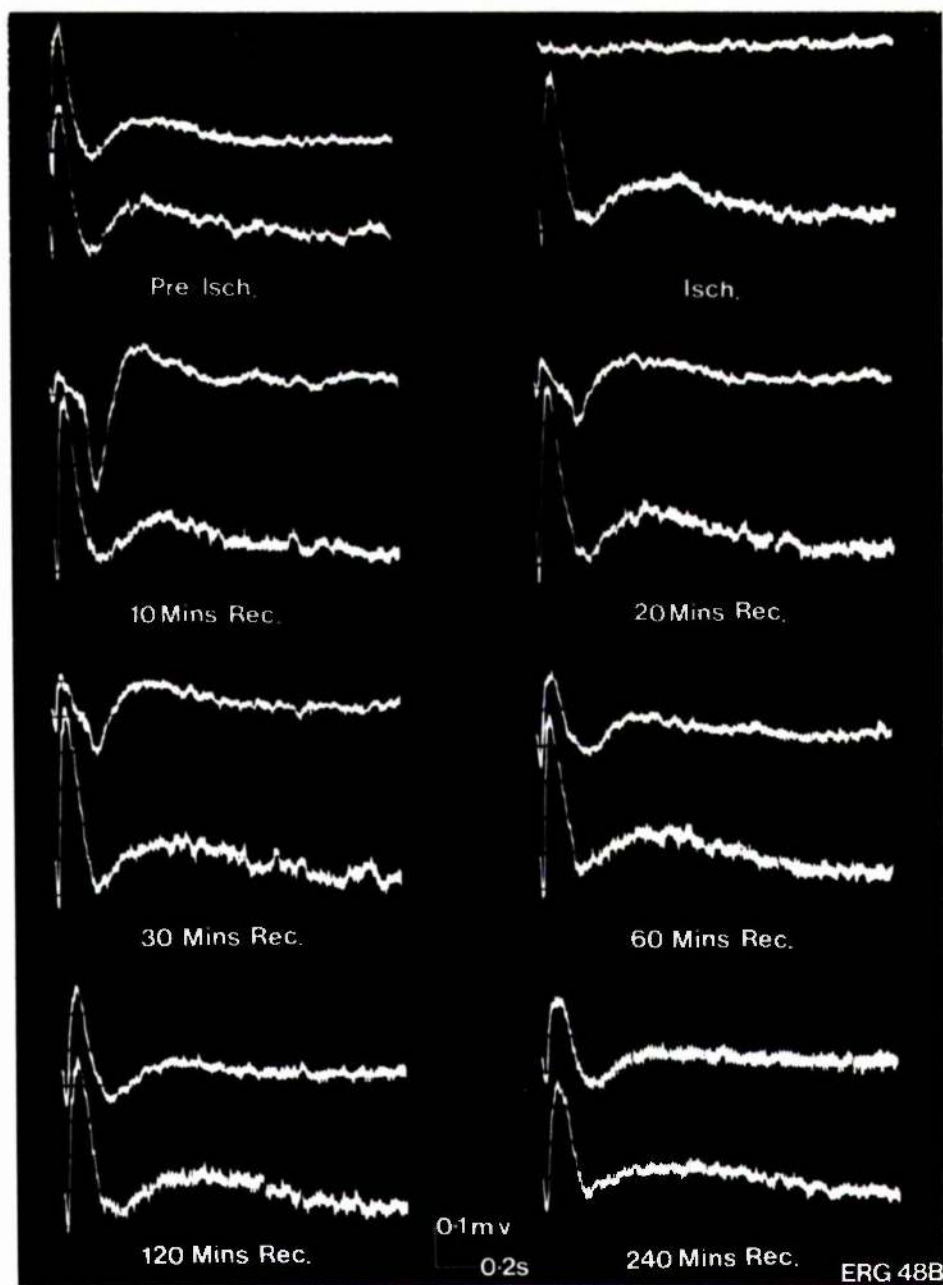


FIG.6-9 ERGs recorded from both eyes of one animal before, during and after 60 minutes of induced ischaemia in one eye (upper trace). The post-ischaemic phase is marked by an increase in the amplitudes of the negative components and the 'c' wave. There is an incomplete recovery of the 'b' wave.

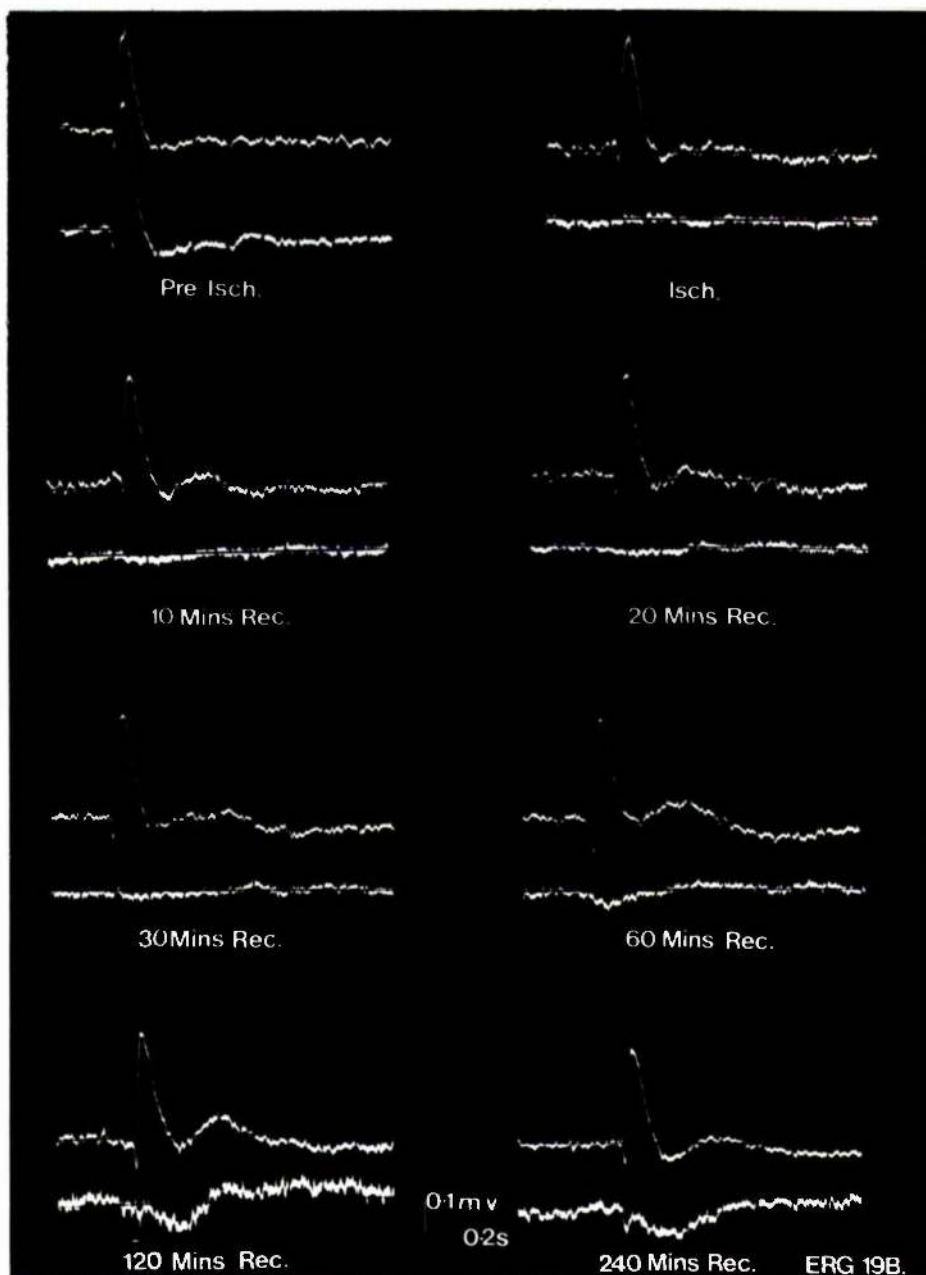


FIG.6-10 ERGs recorded from both eyes of one animal before,during and after 90 minutes of induced ischaemia in one eye(lower trace). The post-ischaemic recovery phase is characterised by marked negativity of the ERG and a very incomplete recovery of the 'b' wave.

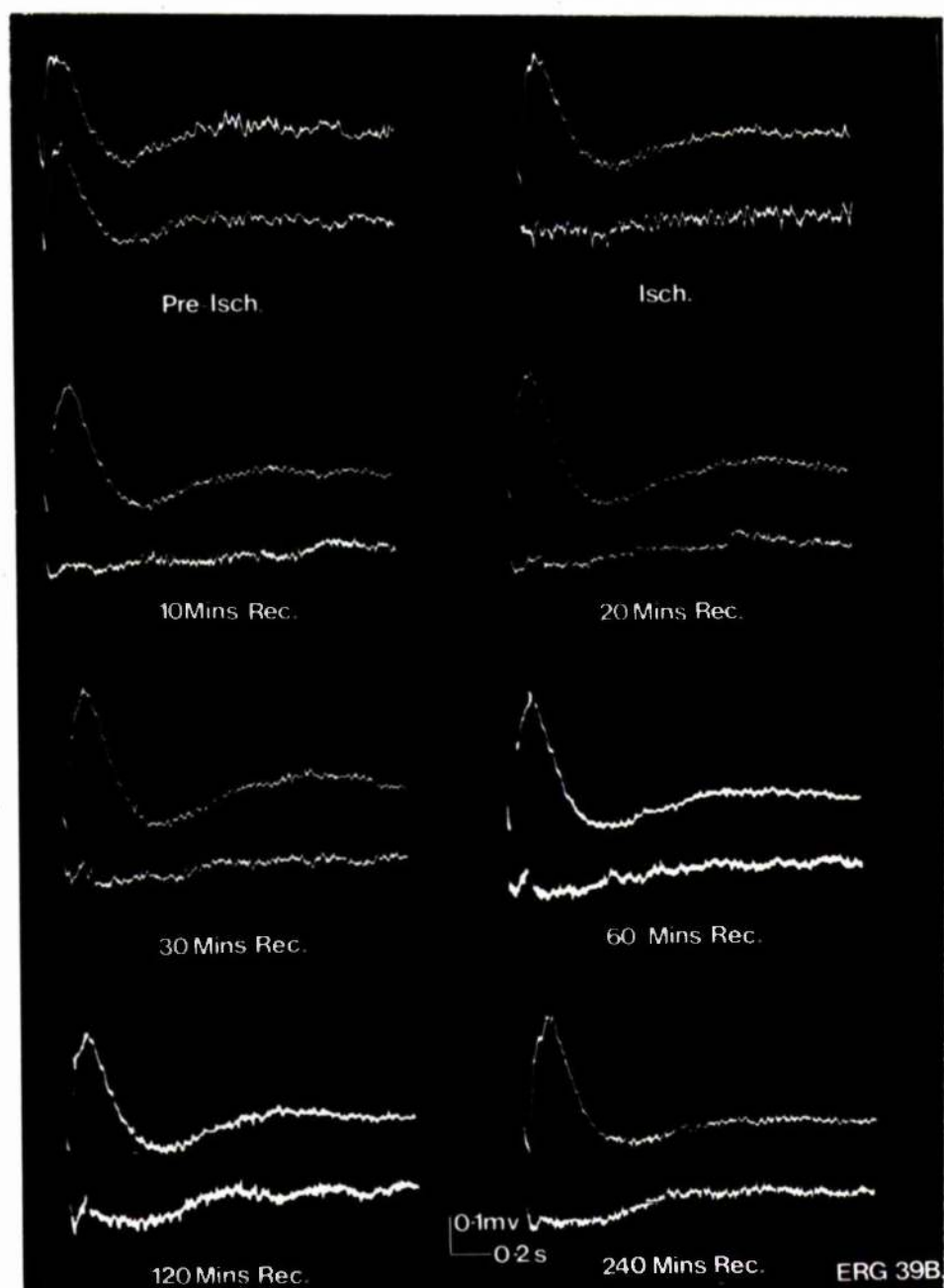


FIG.6-II ERGs recorded from both eyes of one animal before, during and after 120 minutes of induced ischaemia in one eye(lower trace). During the recovery phase there is only a small negative deflection and a greatly reduced 'b' wave that does not reach the iso-electric line.

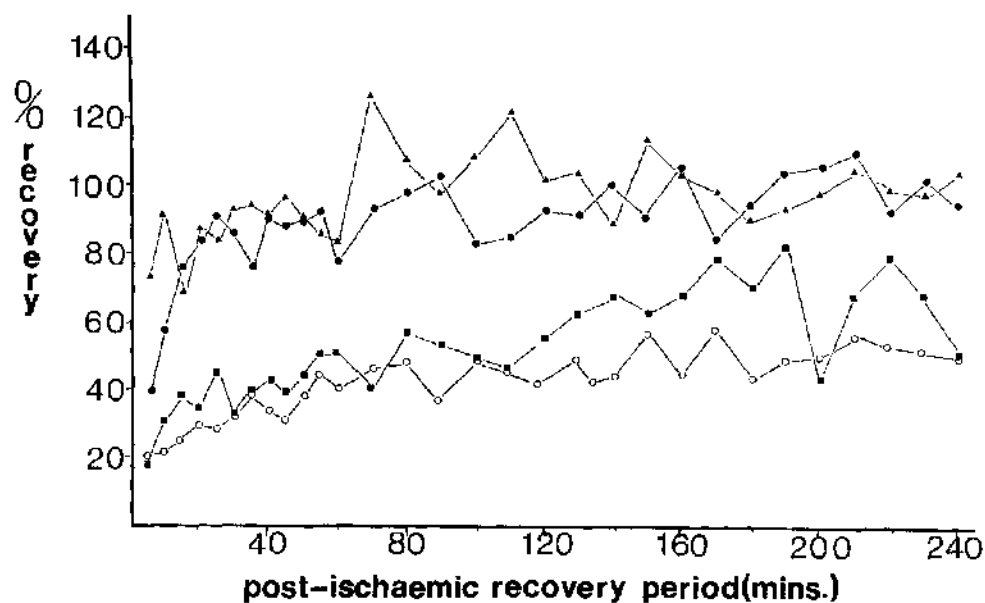


FIG.6-I2 Graph showing the mean values for the 'a' wave during the post-ischaemic recovery phase from 15(Δ), 30(\bullet), 60(\blacksquare) and 90 (\circ) minutes ischaemia. There is almost a complete recovery after 15 and 30 minutes ischaemia, limited recovery occurs after 60 and 90 minutes ischaemia.

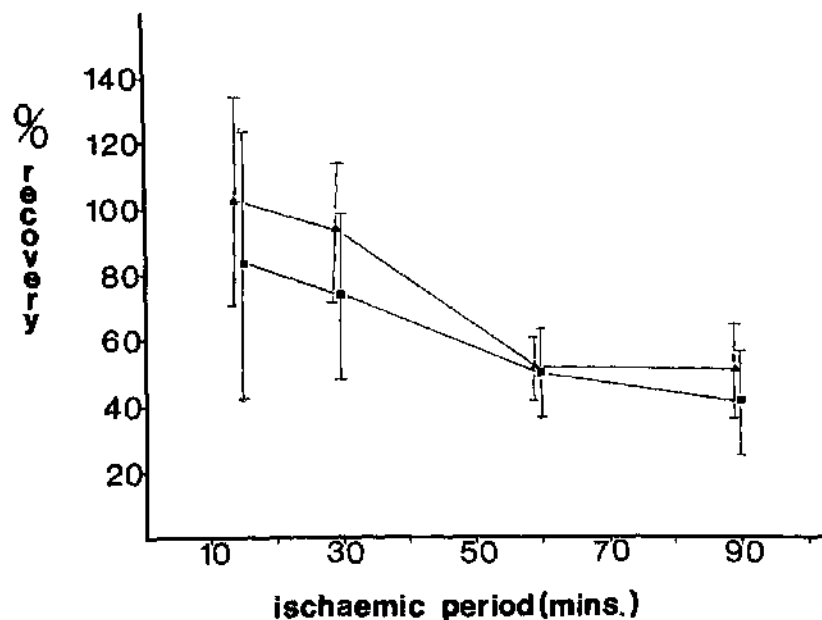


FIG.6-I3 Graph showing the mean value and standard deviation of 'a' wave recovery 60 minutes(\blacksquare) and 240 minutes(\blacktriangle) after the cessation of the induced ischaemia. The 'a' wave recovery becomes less with the longer periods of ischaemia although the standard deviation is often large.

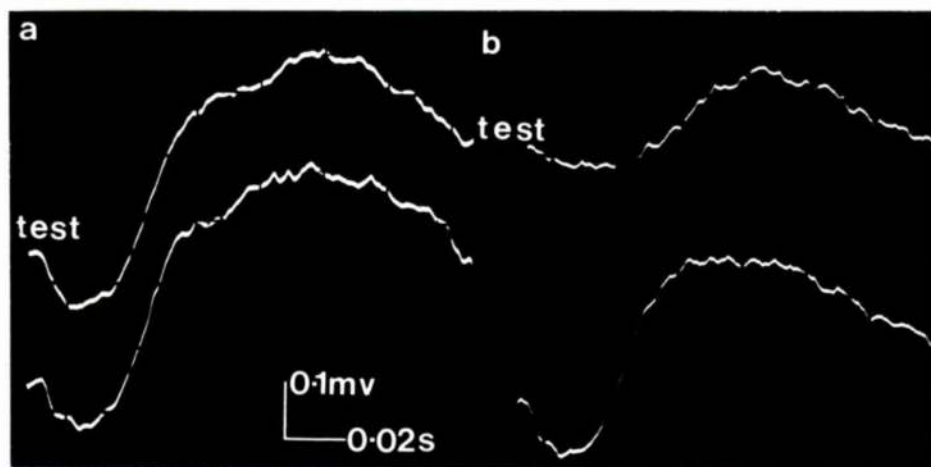


FIG.6-14 ERGs showing the latency of the 'a' wave following;a) 60 minutes ischaemia and 180 minutes recovery and b) 90 minutes ischaemia and 180 minutes recovery.A change in the peak latency is apparent during the post-ischaemic recovery phase from 90 minutes ischaemia.

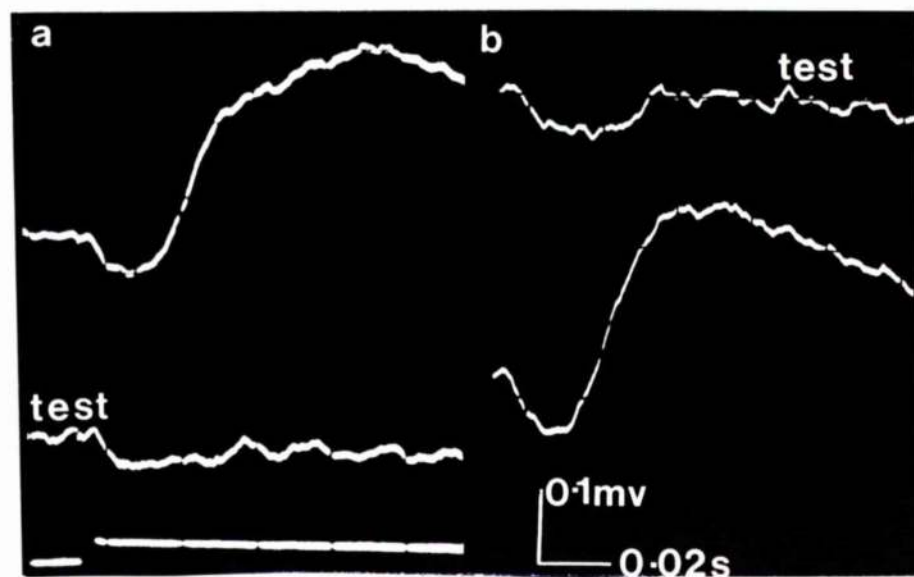


FIG.6-15 ERGs showing isolated 'a' waves following;a) 15 minutes ischaemia and 3 minutes recovery and b) 90 minutes ischaemia and 30 minutes recovery.After short periods of ischaemia the 'a' wave appears before the return of the 'b' wave while after longer periods of ischaemia the 'a' wave is often isolated due to the absence or delay of 'b' wave recovery.

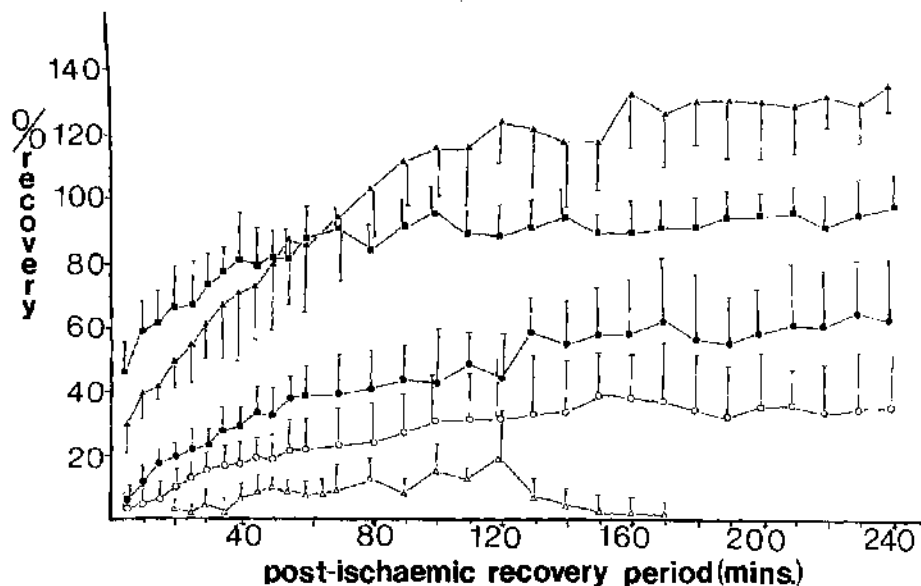


FIG.6-16 Graph showing the mean values and standard deviations for the 'b' wave during the post-ischaemic recovery phase from 15(■), 30(▲), 60(●), 90(○) and 120(△) minutes ischaemia. The 'b' wave rapidly returns to normal after 15 and 30 minutes ischaemia and becomes supernormal after the latter period. Following the longer periods of ischaemia the recovery is less complete.

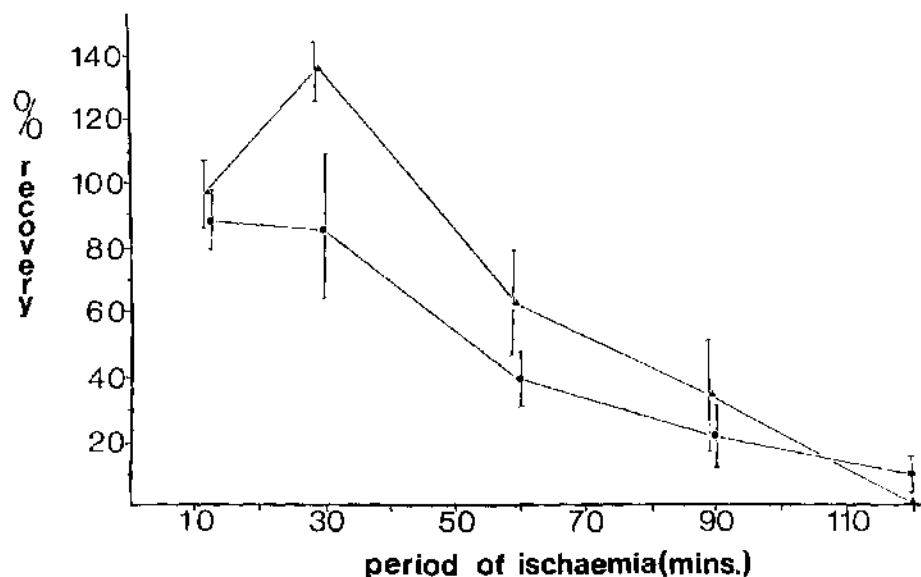


FIG.6-17 Graph showing the mean value and standard deviation of 'b' wave recovery 60 minutes(●) and 240 minutes(▲) after the cessation of the induced ischaemia. Periods of ischaemia longer than 30 minutes results in a diminished 'b' wave after both 60 and 240 minutes recovery.

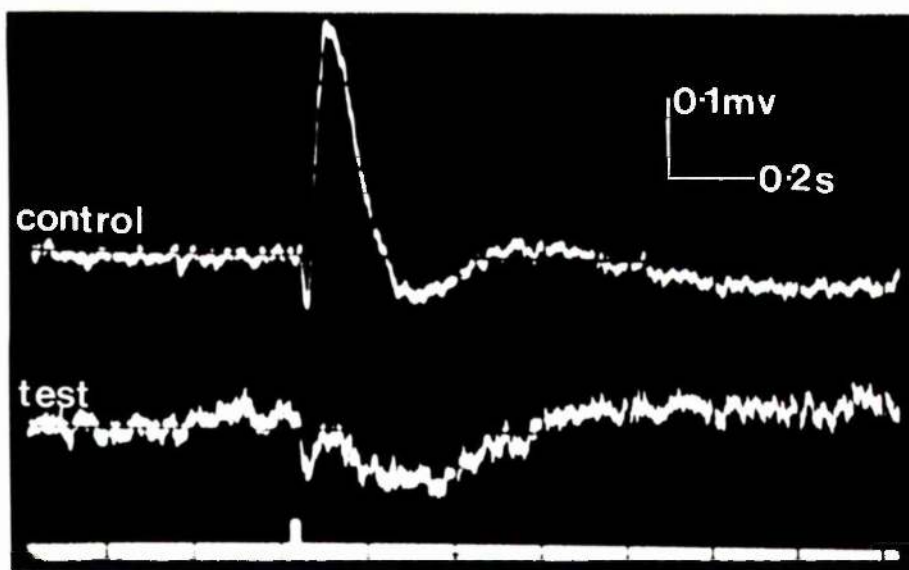


FIG.6-18 ERGs showing a pronounced negativity and a failure of the 'b' wave to rise above the iso-electric line.(90 minutes ischaemia and 160 minutes recovery.)

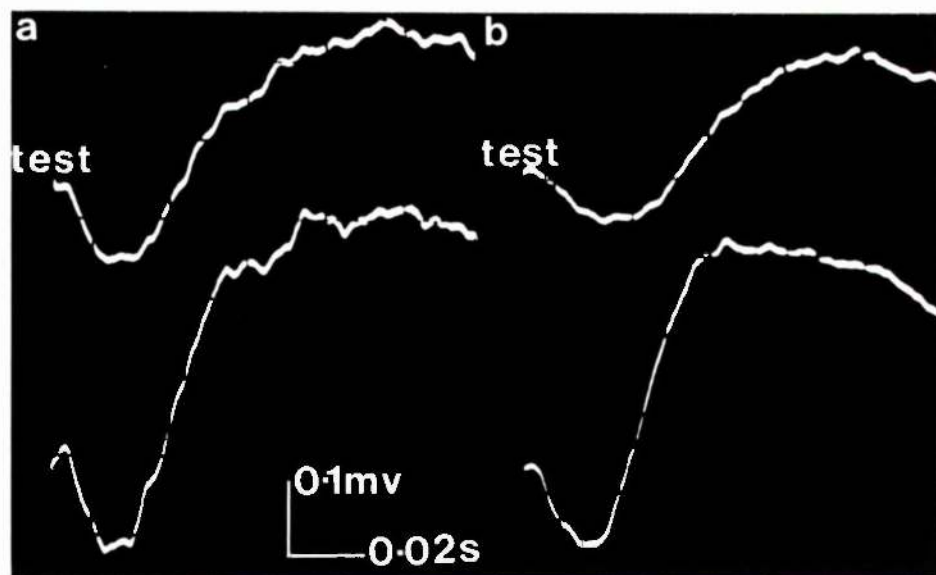


FIG.6-19 ERGs showing the peak latency of the 'b' wave following; a) 15 minutes ischaemia and 240 minutes recovery and b) 90 minutes ischaemia and 240 minutes recovery. Following recovery from 15 minutes ischaemia the control and test eyes are similar while after 90 minutes ischaemia the peak latency is increased.

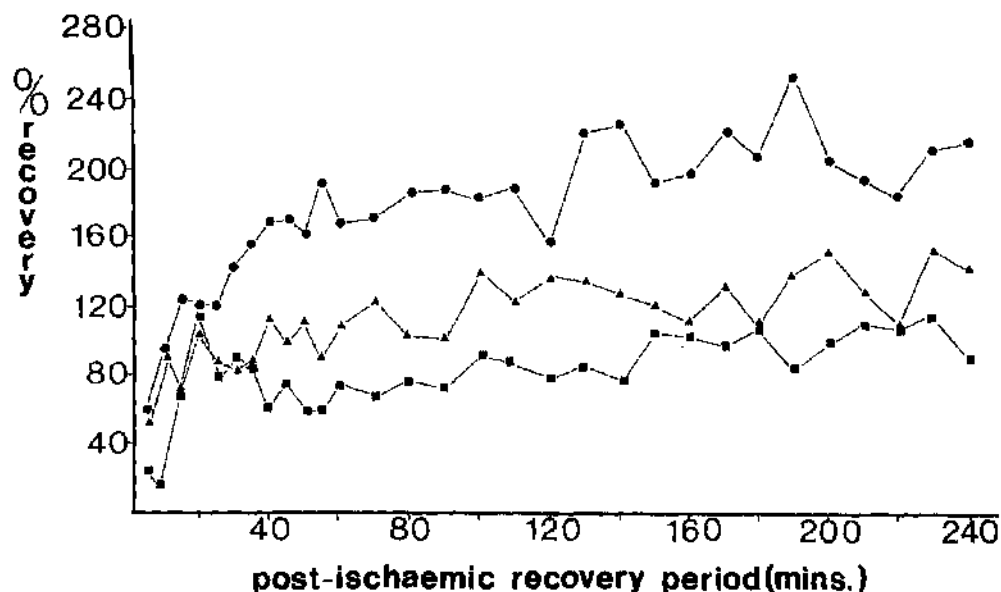


FIG.6-20 Graph showing the mean values for the 'n' wave during the post-ischaemic recovery phase from 15(Δ), 30(\bullet) and 60(\blacksquare) minutes ischaemia. The 'n' wave returns to normal after 15 and 30 minutes ischaemia and becomes supernormal after the latter period, following 60 minutes ischaemia the recovery is less complete.

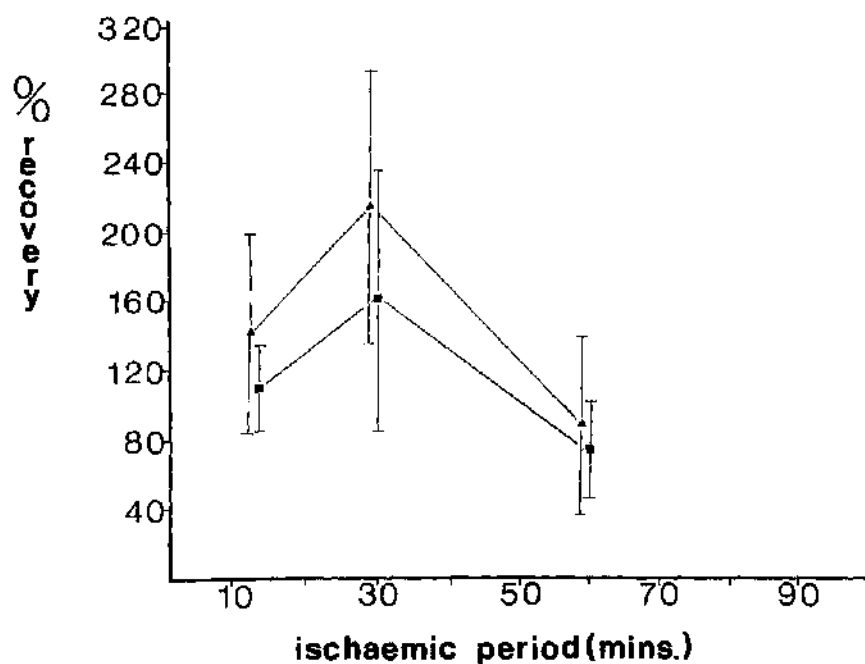


FIG.6-21 Graph showing the mean value and standard deviation of 'n' wave recovery 60 minutes(\blacksquare) and 240 minutes(Δ) after the cessation of the induced ischaemia. The 'n' produces considerable variation although the trend shows the 'n' wave decreasing with periods of ischaemia longer than 30 minutes.

Chapter 7 - Discussion.

Chapter 7.

This thesis reports the changes⁵ occurring ~~in~~ⁱⁿ the rabbit retina during and after varying periods of total acute ischaemia induced by high intraocular pressures. The changes observed appeared to have arisen from the effects of ischaemia rather than any mechanical effects of the high intraocular pressures employed. This view was supported by the similar ultrastructural changes occurring in the pressure-induced ischaemic tissue and non-pressure-induced ischaemic tissue (post-mortem). This was in addition to the functional finding of Fujino and Hamasaki (1967) who showed that the changes in the ERG resulting from high intraocular pressure were due to ischaemia and not directly related to the raised intraocular pressure.

The rabbit retina as a whole could withstand up to 30 minutes ischaemia and return to near normality within 4 hours. This period of ischaemia was some 3-6 times longer than the ischaemic tolerance of the brain from which the eye is embryologically derived. However, the ischaemic tolerance of the eye was similar to that of some other tissues of the body such as the liver (Oudea 1963, Trump, Goldblatt and Stowell 1962 and Bassi and Bernelli-Zazzera 1964) and heart (Bryant, Thomas and O'Neal 1958).

While the retina as a whole was able to withstand 30 minutes ischaemia, the individual cell types of the retina possessed differing tolerance to ischaemia. Structurally the RPE and the Müller cells were the most resistant while the visual cells were least resistant to ischaemia. The neural components of the inner retina showed an intermediate sensitivity to ischaemia. On the basis of the histological findings, one could postulate the possible functional findings from electrophysiology. One would expect a marked effect on the 'a' wave with a relative sparing of the 'b' and 'c' waves.

The functional study by electroretinography revealed that the 'b' wave was readily affected by ischaemic insults. In general, the more

prolonged the ischaemic episode, the slower was the rate and extent of 'b' wave recovery. In contrast, even after lengthy periods of ischaemia there was a rapid return of the 'a' and 'c' waves. On this basis, one would predict that the RPE and the visual cells would return to structural normality during post-ischaemic recovery while severe or permanent damage would be expected in the inner retina.

A comparison of the predicted and actual findings revealed several differences. The main discrepancy involved the 'a' wave of the electroretinogram and the ultrastructure of the visual cells. In spite of the severe damage observed in the visual cells during the post-ischaemic recovery phase, the 'a' wave could still be elicited by a flash of light.

The disappointing correlation between the individual components of the ERG and the histology of the cells from which the components were thought to arise was not surprising. The ERG is an algebraic sum of the various components and as such each component depends to some extent on the others for its expression. A better indication of the structural integrity of the retina was the overall wave form of the ERG. A marked negativity with reduced positive components was indicative of a severely damaged retina. This was in agreement with many clinical studies especially those of Karpe (1945) which showed that the latter type of ERG was associated with a poor prognosis for visual recovery following ocular vascular insufficiency in humans.

The RPE showed a remarkable structural resistance to ischaemia, tolerating up to 60 minutes of ischaemia and returning to near normality within 4 hours. It was only after 90 and 120 minutes of ischaemia that the RPE lost many of the characteristics associated with normal RPE cells. The basal infoldings were reduced or absent, the mitochondria were abnormal and the smooth endoplasmic reticulum shrunken. In spite of these changes, some cells were thought to be viable in view of the presence of small mitochondria

with an electron-dense matrix. Such mitochondria were thought to be indicative of active cells. The RPE may survive as a cell layer following lengthy periods of ischaemia, but whether it can function in a normal fashion remains open to question. Unfortunately the 'c' wave which was thought to arise from the RPE could not be used as a reliable guide to RPE function. This was because of its erratic appearance arising from the characteristics of the light source used to elicit the ERG and the AC coupling technique used to record the ERG. It was noted, however, that a 'c' wave was sometimes present during the recovery phase from 120 minutes ischaemia. One function of the RPE that could be easily identified and quantified was the removal and degradation of outer segment material. An analysis of the phagocytic activity of the RPE following ischaemia revealed that the RPE could increase its phagocytic activity following periods of ischaemia up to 60 minutes. There was no increase after 90 minutes and it was often this period that marked changes occurred in the ultrastructure of the RPE cells.

The phagocytic removal of outer segment debris by the RPE following the restoration of the ocular circulation appeared to be the main route for the removal of the outer segment material during the recovery phase. This was in contrast to the situation occurring during the ischaemic episode where the macrophages in the subretinal space appeared to be the main mechanism for the disposal of the membrane debris. The macrophages were a prominent feature of ischaemic retinal tissue and were thought to arise from the RPE.

The limiting factor for the visual recovery following ocular ischaemia in the rabbit appeared to be the extent of the damage to the visual cells. The receptor cells are the initial cells of the visual pathway converting light into nervous energy. Damage to these cells must affect the nervous activity of the remaining cells of the visual pathway.

Irreversible damage appeared to occur in some visual cells after 60 minutes ischaemia. It was interesting to note that the 'a' wave which was thought to arise from the visual cells (Penn and Hagins 1969) was not greatly reduced following 4 hours recovery from 90 and 120 minutes of ischaemia. With these latter periods of ischaemia there was considerable disruption of the visual cells, especially at the level of the inner and outer segments. How the 'a' wave was generated under these circumstances was unknown. It was thought that both the inner and outer segments were necessary for the production of the 'a' wave (Hagins 1972). The model suggested by Hagins (1972) proposes that in the visual cells, a continuous "dark current" exists which is carried by sodium ions. The current enters passively through the membrane of the outer segment and exits from the inner segments where a sodium pump mechanism is thought to occur. The model in addition proposes that calcium ions are involved in the receptor transducer mechanism. In the dark the calcium ions are thought to be actively taken up from the cytoplasm by the disc giving a low cytoplasmic concentration of calcium ions. Following exposure to light, the bleaching of the photopigment produces permeability changes in the disc membrane which allows the calcium ions into the cytoplasm. The calcium ions then act on the cell membrane to decrease its permeability to sodium ions which interrupts the "dark current". The 'a' wave or late receptor potential which is a hyperpolarising potential apparently arises from the increase in the resistance of the receptor membrane to the passage of sodium ions (Toyoda, Nosaki and Tomita 1969). It was conceivable that the exchange of ions responsible for the generation of the 'a' wave could occur in disrupted inner and outer segments following single and temporally well separated stimuli as were used in this study. This presentation of the light stimulus may not have been too demanding on the membrane systems remaining in the disorganised inner and outer segments. However, constant light or rapidly repeated stimuli may lead to a breakdown

of the system. This could also be true of the processes involved in the bleaching and regeneration of the photopigments. The small number of flashes employed in this study may not have altered the level of unbleached photopigments to a great extent. The effect of light during and after periods of acute ischaemia warrants further attention. In spite of the retention of the 'a' wave, the visual cells may not function in a similar way to those of the normal eye. One would expect that the visual acuity and the directional sensitivity of the retina (Stiles-Crawford effect) to be adversely affected as a result of the unordered arrangement of the outer segments.

Correlation of the structural and functional changes in the inner nuclear layer was difficult. Structurally, the neural elements of the inner nuclear layer exhibited an intermediate tolerance to ischaemia, between that of the visual cells and the retinal pigment epithelium. The neural cells of the inner nuclear layer, the horizontal, the bipolar and the amacrine cells appeared to tolerate 60 minutes of ischaemia and return to normality within 4 hours. However, after a similar recovery period, 90 minutes of ischaemia was associated with marked pyknotic changes in the visual streak region with relative sparing of the peripheral retina. Following 4 hours recovery from 120 minutes of ischaemia degenerative changes were widespread throughout the inner nuclear layer. The pyknotic changes were thought to be irreversible in many cases and affected all three types of neural cells. The Müller cells however appeared relatively insensitive to ischaemia with mild oedema present only after 90 and 120 minutes of ischaemia. The majority of these cells appeared viable and would be expected to return to normality with longer recovery periods. The 'b' wave of the ERG is generally thought to arise from the inner nuclear layer and to provide a measure of the functional state of this layer. Following the restoration of the ocular circulation, the 'b' wave returned to normal values within 4 hours after 15 and 30 minutes ischaemia, in the latter case a supernormal 'b' wave occurred. During the recovery phase

from the longer periods of ischaemia, there was only a partial return of the 'b' wave. The longer the period of ischaemia, the more adversely affected was the recovery of the 'b' wave in respect of the extent and rate of recovery. The 'b' wave has been shown to arise from the Müller cells (Miller and Dowling 1970) under ionic influence of the other cells in the inner nuclear layer. It would appear that the initial changes in the 'b' wave may have been related to changes in the neural cells rather than the Müller cells. The difficulty in correlating the structural and functional findings arose from the fact that the specific nature of the structural results could not be easily related to the unspecific nature of the electrophysiological findings. The 'b' wave arises from the Müller cells which are not part of the visual pathway, and the ionic influences which trigger the 'b' wave could come from a variety of cells because of the extensive ramifications of the Müller cell cytoplasm. As well as changes in the 'b' wave of the test eye there were unexplained increases in the amplitude of the 'b' wave in the control eye. The amplitude increased following induction of ischaemia in the contralateral eye. The factors involved in this increase warrant further investigation.

The functional state of the ganglion cells during and after periods of ischaemia could not be determined as the activity of the ganglion cells was not reflected in the potential changes of the ERG (Winkler 1972). This aspect of the study remains undetermined although structurally the ganglion cells appeared to tolerate the effects of ischaemia well. However, a critical factor in ganglion cell function may be axonal flow which is not obvious with electron microscopy, unless special techniques are employed. Periods of raised intraocular pressure in monkeys have been shown to affect axonal flow in ganglion cell axons (Anderson and Hendrickson 1974 and Levy and Adams 1975) and also their function as measured by visually evoked responses (Levy and Adams 1975).

It can be seen from this thesis that full recovery of the electroretinogram followed 30 minutes of induced ocular ischaemia but two hours of induced ischaemia was associated with a limited recovery of function as measured by electroretinography. The ischaemic episodes caused damage to the outer layers of the retina preferentially, and changes were still in evidence in those eyes recovering a normal electroretinogram. The correlation between electroretinography and the electron microscopy appearance of the tissue was generally poor.

References.

AMALRIC, P.

1971 Mod. Probl. Ophthalm. 9, 68-77
Triangular shaped choroidal alterations.

ANDERSON, D.R. and DAVIS, E.B.

1974 Arch. Ophthalm. 92, 422-426
Retina and optic nerve after posterior ciliary artery occlusion.

ANDERSON, D.R. and DAVIS, E.B.

1975 Arch. Ophthalm. 93, 267-274
Sensitivities of ocular tissues to acute pressure-induced ischaemia.

ANDERSON, D.R. and HENDRICKSON, A.

1974 Invest. Ophthalm. 13, 771-783
Effect of intraocular pressure on rapid axoplasmic transport in monkey optic nerve.

ARDEN, G.B. and BROWN, K.T.

1965 J. Physiol. 176, 429-461
Some properties of components of the cat electroretinogram revealed by local recording under oil.

ARDEN, G.B. and GREAVES, D.P.

1956 J. Physiol. 133, 266-274
The reversible alterations of the electroretinogram of the rabbit after occlusion of the retinal circulation.

ASHTON, N., DOLLERY, C.T., HENKIND, P., HILL, D.W., PATERSON, J.W.,
RAMALHO, P.S., and SHAKIB, M.

1966 Brit. J. Ophthalm. 50, 281-384
Focal retinal ischaemia.

BAIRATI, A. and ORZALESI, N.

1963 J. Ultrastruc. Res. 9, 484-496
The ultrastructure of the pigment epithelium and of the photoreceptor-pigment epithelium junction in the human retina.

BASSI, M., BERNELLI-ZAZZERA, A. and CASSI, E.

1960 J. Path. Bact. 79, 179-183
Electron microscopy of rat liver cells in hypoxia.

BASSI, M. and BERNELLI-ZAZZERA, A.

1964 Exp. Mol. Path. 3, 332-350
Ultrastructural cytoplasmic changes of liver cells after reversible and irreversible ischaemia.

BECKER, B. and POST, L.T.

1951 Am. J. Ophthalm. 34, 677-686
Retinal vein occlusion.

BERKOWITZ, L.R., FIORELLO, O., KRUGER, L. and MAXWELL, D.S.

1968 J. Histochem. and Cytochem. 16, 808-814
Selective staining of nervous tissue for light microscopy following preparation for electron microscopy.

BERNSTEIN, M.H.

1961 In "The Structure of the Eye" Ed. Smelser, G. Academic Press. London and New York.

Functional architecture of the retinal epithelium.

BERNSTEIN, M.H. and HOLLENBERG, M.F.

1965 In "The Structure of the Eye" Ed. Rohen, E.W. Schauttauer Verlag Stuttgart
Movement of electron opaque markers through capillaries of the retina.

BOCK, J., BOMSCHEIN, H. and HOMMER, K.

1964 Graefe Arch. Ophthalm. 167, 276-283

Die wiederbelebungzeit der menschlichen netzhaut.

BORNSCHEIN, H.

1959 Arch. ges. Physiol. 270, 184-194

Der einfluss der reizfrequenze auf die uberlebenszeit des skotopischen ERG.

BORNSCHEIN, H. and ZWAIVER, A.

1952 Graefe Arch. Ophthalm. 152, 527-536

Das elektroretinogramm des kaninchens bei experimenteller erhöhung des
intraocularen druckes.

VAN de BOS, G.G.

1969 J. Physiol. (Paris) 60, 199-216

L'electroretinogramme du chat en cas d'hypoxie.

BROWN, K.T.

1968 Vision Res. 8, 633-677

The ERG its components and their origins.

BROWN, K.T. and WATANABE, K.

1962 Nature 193, 958-960

Isolation and identification of a receptor potential from the pure cone fovea
of the monkey retina.

BROWN, K.T. and WIESEL, T.N.

1961 J. Physiol. 158, 257-280.

Localisation of origins of electroretinogram components by intraretinal
recording in the intact cat eye.

BRYANT, R.E., THOMAS, W.A. and O'NEAL, R.M.

1958 Circul. Res. 6, 699-709

An electron microscopic study of the myocardial ischaemia in the rat.

BUETTNER, H., MACHEMER, R., CHARLES, S. and ANDERSON, D.R.

1973 Am. J. Ophthalm. 75, 943-952

Experimental deprivation of choroidal blood flow.

BURIAN, H.M.

1953 Arch. Ophthalm. 49, 241-256

Electroretinography and its clinical application.

CAMPBELL, F.P.

1961 Arch. Ophthalm. 65, 26-34

Retinal vein occlusion. An experimental study.

- CARR, I.
1973 In "The Macrophage - A review of ultrastructure and function"
Academic Press. London and New York.
- DE CARVALHO, C.A.
1962 Arch. Ophthalm. 67, 123-127
Histopathology of retina and optic nerve with experimental glaucoma.
- CAULFIELD, J. and KLIONSKY, B.
1959 Am. J. Path. 35, 489-523
Myocardial ischaemia and early infarction - an electron microscopic study.
- CHANDRA, S. and SKELTON, F.R.
1964 Stain Techn. 39, 107-110
Staining juxtaglomerular cell granules with toluidine blue or with basic fuchsin for light microscopy after epon embedding.
- COHEN, A.I.
1965 Nature 205, 1222-1223
A possible cytological basis for the 'R' membrane in the vertebrate eye.
- COHEN, A.I.
1971 J. Cell Biol. 48, 547-565
Electron microscopic observations on form changes in photoreceptor outer segments and their saccules in response to osmotic stress.
- COLLIER, R.H.
1967 Arch. Ophthalm. 77, 683-692
Experimental embolic ischaemia of the choroid.
- COTRAN, R.S.
1965 J. Exp. Mol. Path. 4, 217-231
Endothelial phagocytosis. An electron microscopic study.
- DAVIS, F.A.
1929 Trans. Am. Ophthalm. Soc. 24, 401-441
The anatomy and histology of the eye and orbit of the rabbit
- DAVIS, R.J. and ARNOTT, G.P.
1955 Am. J. Ophthalm. 40, 71-76
An experimental study of the electroretinogram.
- DEWAR, J. and MCKENDRICK, J.G.
1873 Trans. Roy. Soc. Edin. 27, 141-166
On the physiological action of light.
- DUKE-ELDER
1967 In "System of Ophthalmology" Vol. X. Diseases of the retina.
H. Kimpton - London.
- EDMUND, J. and JENSEN, S.F.
1967 Acta Ophthalmol. 45, 601-609
ERG in temporal arteritis.

EINTHOVEN and JOLLY, W.A.

1908 Quart. J. Exper. Physiol. 1, 343-416

The form and magnitude of the electrical response of the eye to stimulation by light at various intensities.

FEDER, N. and O'BRIEN, T.P.

1968 Am. J. Bot. 55, 123-142

Plant microtechnique some principles and new methods.

FLOCKS, M., TSUKAHARA, I. and MILLER, J.

1959 Am. J. Ophthal. 48, 11-18

Mechanically-induced glaucoma in animals.

FOULDS, W.S., LEE, W.R. and TAYLOR, W.O.G.

1971 Trans. Ophthal. Soc. U.K. 91, 323-341

Clinical and pathological aspects of choroidal ischaemia.

FRIEDMAN, E. and KUWABARA, T.

1968 Arch. Ophthal. 80, 265-279

The retinal pigment epithelium. IV The damaging effects of radiant energy.

FUJINO, T., CURTIN, V.T. and NORTON, E.W.D.

1968 Trans. Am. Ophthal. Soc. 66, 318-329

Experimental central retinal vein occlusion. A comparison of intraocular and extraocular occlusion.

FUJINO, T. and HAMASAKI, D.I.

1965 J. Physiol. 180, 837-845

The effect of occluding the retinal and choroidal circulations on the electroretinogram of monkeys.

FUJINO, T. and HAMASAKI, D.I.

1967 Arch. Ophthal. 78, 757-765

Effect of intraocular pressure on the electroretinogram.

GAY, A.J., GOLDBER, H. and SMITH, M.

1964 Invest. Ophthal. 3, 647-656.

Chorioretinal vascular occlusions with latex spheres.

GERSTLE, C.L., ANDERSON, D.R. and HAMASAKI, D.I.

1973 Arch. Ophthal. 90, 121-124.

Pressure effect on ERG and optic nerve conduction of visual impulse.

GLOOR, B.P.

1969 Graefes Arch. Klein. exp. Ophthalmol., 179, 105-117.

Phagocytotische aktivitat des pigment epithels nach licht coagulation.

Zur frage der her kunft von makrophagen in der retina.

GAY, A.J., GOLDBER, H. and SMITH, M.

1964 Invest. Ophthal. 3, 647-656

Chorioretinal vascular occlusions with latex spheres.

GOLDBER, H. and GAY, A.J.

1967 Invest. Ophthal. 6, 51-58

Chorioretinal vascular occlusions with latex microspheres (A long-term study).

Part II.

GOTCH, F.

1903 J. Physiol. 29, 388-410

The time relations of the photo-electric changes in the eyeball of the frog.

GRANIT, R.

1933 J. Physiol. (Lond.) 77, 207-239

The components of the retinal action potential in mammals and their relation to the discharge in the optic nerve.

GRIERSON, I. and LEE, W.R.

1973 Brit. J. Ophthalm. 57, 400-415

Erythrocyte phagocytosis in the human trabecular meshwork.

GRIGNOLO, A., ORZALESI, N. and CALABRIA, G.A.

1966 Eye Res. 5, 86-97

Studies on the fine structure and the rhodopsin cycle of the rabbit retina in experimental degeneration induced by sodium iodate.

GRIMELY, P.M.

1964 Stain Techn. 39, 229-233

A tribasic stain for thin sections of plastic embedded OsO_4 fixed tissues.

GRIMELY, P.M., ALBRECHT, J.M. and MICHELITCH, H.J.

1965 Stain Techn. 40, 357-366.

A tribasic stain for thin sections of plastic embedded O SO_4 fixed tissues.

HADDOW, A. and LEXTON, W.A.

1946 Nature 157, 500-503

Influence of carbonic esters (Urethanes) on experimental animal tumours.

HAGER, H., HIRSCHBERGER, W., and SCHOLZ, W.

1960 Aerospace Med. 31, 379-387

Electron microscopic changes in brain tissue of Syrian hamsters following acute anoxia.

HAGINS, W.A.

1972 Ann. Rev. Biophys. Bioengineer. 1, 131-158

The visual process excitatory mechanisms in the primary receptor cells.

HAPBURN, M.L.

1935 Trans. Ophthalm. Soc. U.K. 55, 434-477

The role played by the pigment and visual fields in the diagnosis of diseases of the fundus.

HAYREH, S.S.

1965 Brit. J. Ophthalm. 49, 626-639

Occlusion of the central retinal vessels.

HAYREH, S.S.

1969 Brit. J. Ophthalm. 53, 721-748

Blood supply of the optic nerve head and its role in optic atrophy, glaucoma and oedema of the optic disc.

HAYREH, S.S.

1971 Trans. Ophthalm. Soc. U.K. 91, 291-303
Posterior ciliary arterial occlusive disorders.

HAYREH, S.S. and BAINES, J.A.B.

1972 Brit. J. Ophthalm. 56, 736-753
Occlusion of the posterior ciliary artery II chorioretinal lesion.

HENKES, H.E.

1953 Arch. Ophthalm. 49, 190-201
Electroretinogram in circulatory disturbances of the retina. I

HENKES, H.E.

1954 Arch. Ophthalm. 51, 42-66
Electroretinogram in circulatory disturbances of the retina. II

HILL, D.W., REES, D.M. and YOUNG, S.

1973 Exp. Eye Res. 16, 475-485
Acute graded ocular ischaemia by arterial compression in the cat.

HOEFFERT, L.L.

1968 Stain Techn. 43, 145-151
Polychromatic stains for thin sections of Beta embedded in epoxy resin.

HOGAN, M.J.

1971 Trans. Am. Acad. Ophthalm. and Otol. 76, 64-80
Role of the retinal pigment epithelium in macular disease.

HOLMGREN, F. (cited by Einthoven and Jolly, 1908).

1865 Upsala Lakaref, Förh, 177-191
Method att objectivera effecten au ljusintyck pa retina.

HORSTEN, G.P.M. and WINKELMAN, J.E.

1957 Am. Arch. Ophthalm. 57, 557-565
Effect of temporary occlusion of the aorta on the electroretinogram.

HUBER, J.D., PARKER, F. and ODLAND, G.F.

1968 Stain techn. 43, 83-87
A basic fuchsin and alkalized methylene blue rapid stain for epoxy-embedded tissue.

ISHIKAWA, Y., UGA, S. and IKUI, H.

1973 J. Electron Microscop. 22, 273-275
The cell division of the pigment epithelium in the repairing retina after photocoagulation.

ISHIKAWA, Y. and IKUI, H.

1974 Jap. J. Ophthalm. 18, 334-349
Electron microscopic studies on retinal repair in the monkey after Xenon photocoagulation. I Cellular responses in the early stages of repair.

KOHNER, E.M., DOLLERY, C.T., SHAKIB, M., HENKIN, D.P., PATERSON, J.W.,
do OLIVEIRA, L.N.F. and BULPITT, C.J.

1970 Am. J. Ophthalm. 69, 778-825
Experimental retinal branch vein occlusion.

KARLBERG, B., HEDIN, A. and BJORNBERG, K.

1968 Acta Ophthalmol. 46, 742-748

Electroretinography during short-term intraocular tension rise.

KARPE, G.

1945 Acta Ophthalmol. 24, 1-118 (Suppl.)

The basis of clinical electroretinography.

KOHNER, E.M., DOLLERY, C.T., SHAKIB, M., HENKIND, P., PATERSON, J.W.,

de OLIVEIRA, L.N.F. and BULPITT, C.J.

1970 Am. J. Ophthalmol. 69, 778-825

Experimental retinal branch vein occlusion.

KROJL, A.J.

1968 Arch. Ophthalmol. 79, 453-469

Experimental central retinal artery occlusion.

KUPFER, C.

1962 Invest. Ophthalmol. 1, 474-479

Studies of intraocular pressure. II. The histopathology of experimentally increased intraocular pressure in the rabbit.

KUWABARA, T.

1975 Invest. Ophthalmol. 14, 457-467

Cytologic changes of the retinal and pigment epithelium during hibernation.

KUWABARA, T. and COGAN, D.G.

1961 Arch. Ophthalmol. 66, 680-688

Retinal Glycogen.

LEE, J.C. and HOPPER, J.

1965 Stain Techn. 40, 37-40

Basic fuchsin crystal violet, a rapid staining sequence for juxtaglomerular cells embedded in epoxy resins.

LEVINE, S. and PAYAN, H.

1966 Exp. Neurology 16, 255-262

Effects of ischaemia and other procedures on the brain and retina of the Gerbil (*Meriones unguiculatus*).

LEVY, N.S. and ADAMS, C.K.

1975 Invest. Ophthalmol. 14, 91-97

Slow axonal protein transport and visual function following retinal and optic nerve ischaemia.

LINCOFF, H. and KREISSIG, I.

1971 Am. J. Ophthalmol. 71, 674-689

The mechanism of the cryosurgical adhesions. IV. Electron microscopy.

MCLEOD, D. and HAYREH, S.S.

1972 Brit. J. Ophthalmol. 56, 765-769

Occlusion of posterior ciliary artery. IV. Electroretinographic studies.

MAGALHAES, MM. and COIMBRA, A.

1972 J. Ultrastruct. Res. 39, 310-326

The rabbit retina Müller cell. A fine structural and cytochemical study.

MARSHALL J., FAUKHAUSER, F., LOTMAR, W. and ROULIER, A.

1971 Graefes Arch. klein Exp. Ophthalmol. 182, 154-169.

Pathology of short pulse retinal photocoagulation using the Goldmann contact lens.

MARTIN, J.H., LYNN, J.A. and NICKEY, W.M.

1966 Am. J. Clin. Path. 46, 250-251

A rapid polychrome stain for epoxy-embedded tissue.

NICHOLSON, I.C.

1954 In "Retinal circulation in man and animals".

Charles C. Thomas Springfield.

MILLER, R.F.

1973 J. Neurophysiol. 36, 28-38

Role of K^+ in generation of b-wave of electroretinogram.

MILLER, R.F. and DOWLING, J.E.

1970 J. Neurophysiol. 33, 323-341

Intracellular responses of the Müller (glial) cells of mud puppy retina: their relation to b-wave of the electroretinogram.

MOORE, R.D., MUMAW, V. and SCHÖENBERG, M.D.

1960 J. Ultrastruct. Res. 4, 113-116

Optical microscopy of ultrathin tissue sections.

NICHOLS, J.V.V.

1938 Brit. J. Ophthalm. 22, 672-687

Effect of section of ciliary arteries in the rabbit.

NOELL, W.K.

1951 J. Applied physiol. 3, 489-500

Site of asphyxial block in mammalian retinae.

NOELL, W.K.

1952 Am. J. Ophthalm. 35, 126-133

Electrophysiologic study of the retina during metabolic impairment.

NOELL, W.K.

1954 Am. J. Ophthalm. 38, 78-90

The origin of the electroretinogram.

NOELL, W.K. and CHINN, R.I.

1950 Am. J. Physiol. 161, 573-590

Failure of the visual pathway during anoxia.

ORZALESI, N., GRIGNOLO, A. and CALABRIA, G.A.

1967 Exp. Eye Res. 6, 165-170

Experimental degeneration of the rabbit retina induced by sodium fluoride.

OUDEA, P.R.

1963 Lab. Invest. 12, 386-394

Anoxic changes of liver cells.

- PALLI, E.
1958 Acta Ophthalmol. 36, 208-243
The ocular crisis of the temporal arteritis syndrome.
- PAPST, W. and HECK, J.
1957 Graefes Arch. Ophthalmol. 159, 52.
Der erholungsverlauf des elektroretinogramms nach intraoculaner ischämie und seine beeinflussung durch hypoglykämie.
- PENN, R.D. and HAGINS, W.A.
1969 Nature 223, 201-205
Signal transmission along retinal rods and the origin of the electroretinographic a-wave.
- PEYMAN, G.A. and BOK, D.
1972 Invest. Ophthalmol. 11, 35-45
Peroxidase diffusion in the normal and laser coagulated primate retina.
- PEYMAN, G.A., SPITZNAS, M. and STRAATSMA, B.R.
1971 Invest. Ophthalmol. 10, 181-189
Peroxidase diffusion in the normal and photocoagulated retina.
- POPP, C.
1955 Graefes Arch. Ophthalmol. 156, 395-
Die retinafunktion nach intraoculaner ischämie.
- REINECKE, R.D., KUWABARA, T., COGAN, D.G. and WEIS, D.R.
1962 Arch. Ophthalmol. 67, 470-475
Retinal vascular patterns. Part V. Experimental ischaemia of the cat eye.
- REVEL, J.P., YEE, A.G. and HUDSPETH, A.J.
1971 Proc. Nat. Acad. Sci. 68, 2924-2931.
Gap junctions between electronically coupled cells in tissue culture and brown fat.
- RICHARDSON, K.C., JARETT, L. and FINKE, E.H.
1960 Stain Technol. 35, 313-323
Embedding in epoxyresins for ultrathin sectioning in electron microscopy.
- RUUSUVAARA, P. and PALKAMA, A.
1974 Acta Ophthalmol. 52, 41-46.
Effect of short-term increased intraocular pressure on the fine structure of the retina.
- SHAKIB, M. and ASHTON, N.
1966 Brit. J. Ophthalmol. 50, 325-382
Ultrastructural changes in focal retinal ischaemia.
- SIPPERLEY, J., ANDERSON, D.R. and HAMASAKI, D.I.
1973 Arch. Ophthalmol. 90, 358-360.
The short-term effect of intraocular pressure elevation on the human electroretinogram.

SJOSTRAND, F.S. and NILSSON, S.E.

1964 In "The rabbit in eye research" ed. J.H. Prince
Thomas Springfield III

SMITH, G.G. and BAIRD, C.D.

1952 Am. J. Ophthal. 35, 133-136

Survival time of retinal cells when deprived of their blood supply by
increased intraocular pressure.

SPITZNAS, M. and HOGAN, M.J.

1970 Arch. Ophthal. 84, 810-819

Outer segments and photoreceptors and the retinal pigment epithelium.

STEINBERG, R.H., SCHMIDT, R. and BROWN, K.T.

1970 Nature 227, 728-730

Intracellular responses to light from cat pigment epithelium: origin of the
electroretinogram c-wave.

STERN, W.H. and ERNEST, J.T.

1974 Am. J. Ophthal. 78, 438-448

Microsphere occlusion of the choriocapillaris in rhesus monkeys.

STONE, J.

1969 Vision Res. 9, 351-356

Structure of the cats' retina after occlusion of the retinal circulation.

SULKIN, N.M. and SULKIN, D.F.

1965 Lab. Invest. 8, 1523-1546

An electron microscopic study of the effects of chronic hypoxia on cardiac
muscle, hepatic and autonomic ganglion cells.

TOYODA, J.I., NOSAKI, H., and TOMITA, T.

1969 Vision Res. 9, 453-463

Light-induced resistance changes in single photoreceptors of Necturus and
Gekko.

TRIPATHI, B. and ASHTON, N.

1971 Brit. J. Ophthal. 55, 1-11

Vaso-glial connections in the rabbit retina.

TRUMP, B.F., GOLDBLATT, P.J., and STOWELL, R.E.

1962 Lab. Invest. 11, 986-1015

An electron microscopic study of early cytoplasmic alterations in hepatic
parenchymal cells of mouse liver during necrosis.

TSO, M.O.M.

1973 Invest. Ophthal. 12, 17-34

Photoc maculopathy in rhesus monkey. A light and electron microscopic study.

TSO, M.O.M., ALBERT, D. and ZIMMERMAN, I.E.

1973 Invest. Ophthal. 12, 554-566

Organ culture of human retinal pigment epithelium and choroid: a model for
the study of cytologic behaviour of retinal pigment epithelium in vitro.

TURNBULL, W.

1948 Trans. Canad. Ophthal. Soc. 1, 116-134

The effects of experimental retinal anaemia in rats.

UENOYAMA, K., McDONALD, J.S. and DRANCE, S.M.

1968 Canad. J. Ophthal. 3, 58-64

The effect of artificially elevated intraocular pressure on the electroretinogram of the rabbit.

UENOYAMA, K., McDONALD, J.S. and DRANCE, S.M.

1969 Canad. J. Ophthal. 4, 72-79

The effect of artificially elevated intraocular pressure on the electroretinogram and visually evoked cortical potential of the rabbit.

UENOYAMA, K., McDONALD, J.S. and DRANCE, S.M.

1969 Arch. Ophthal. 81, 722-729

The effect of intraocular pressure on visual electrical responses.

UENOYAMA, K., McDONALD, J.S. and DRANCE, S.M.

1968 Canad. J. Ophthal. 3, 154-158

The effect of artificially elevated intraocular pressure on the electroretinogram of the cat.

UGA, S. and SMELSER, G.

1973 Invest. Ophthal. 12, 434-448

Comparative study of the fine structure of retinal Müller cells in various vertebrates.

USAMI, E.

1965 Jap. J. Ophthal. 9, 108-115

The influence of the pressure on ERG of a rabbit especially on A-wave and oscillatory potential.

VANYSEK, J., HRACHOVINA, H., ANTON, M. and MOSTER, M.

1968 In "The clinical value of electroretinography" ed. J. Francois, S.

Karger, Basel and New York 312-330

The ERG in some circulatory and metabolic disturbances.

VASSILEVA, P.I. and DUBOU, S.B.

1976 In "Vision and circulation" ed. Cant J.S. H. Kimpton, London.

Changes in the glycogen content and the electroretinogram in retinal ischaemia experimentally induced in rabbits.

WAGENMAN, A.

1890 Arch. f. Ophth. 36 1

Experimentelle untersuchungen ueber den einfluss der circulation in den netzhaut und aderhautgefassen auf die ernahrung des auges, insbesondere der retina und ueber folgen der schnervendurchscheirdung.

WALLER, A.D.

1909 Quart. J. Exp. Physiol. 2, 169-185

On the Double nature of the photoelectrical response of the frogs' retina.

WALLOW, I.H.L. and TSO, M.O.M.

1973 Amer. J. Ophthalm. 75, 610-626

Repair after Xenon arc photocoagulation. II. A clinical and light microscopic study of the evolution of retinal lesions in the rhesus monkey.

WARD, B.

1967 Am. J. Optom. 44, 183-191

Some effects of short-term pressure increases in the cat eye.

WEBSTER, H. and AMES, A.

1965 J. Cell Biol. 26, 885-908

Reversible and irreversible changes in the fine structure of nervous tissue during oxygen and glucose deprivation.

WEISS, H.

1972 Ophthalm. Res. 3, 360-371

The carbohydrate reserve in the vitreous body and retina of the rabbits eye during and after pressure ischaemia and insulin hypoglycaemia.

WERBLIN, F.S. and DOWLING, J.F.

1969 J. Neurophysiol. 32, 339-355

Organisation of retina of mud puppy, Necturus maculosus. II. Intracellular recording.

WILKUS, R.J., CHATRIAN, G.E. and LETTICH, E.

1971 Electroenceph. Clin. Neurophysiol. 31, 537-546

The electroretinogram during terminal anoxia in humans.

WINKELSTEIN, J., MENEFEE, M., GAND, M. and BELL, A.

1963 Stain Techn. 38, 202, 204.

Basic fuchsin as a stain for osmium fixed epon-embedded tissue.

WINKLER, B.S.

1972 Exp. Eye Res. 13, 227-235

Analysis of the rabbits' electroretinogram following unilateral transection of the optic nerve.

WISE, G.N., DOLLERY, C.T. and HENKIND, P.

1971 "The Retinal Circulation".

Harper Row - New York and London.

YOUNG, R.W.

1967 J. Cell Biol. 33, 61-73

The renewal of photoreceptor cell outer segments.

